CATENA

AN INTERDISCIPLINARY JOURNAL OF

SOIL SCIENCE -
HYDROLOGY - GEOMORPHOLOGY

FOCUSING ON

GEOECOLOGY AND LANDSCAPE EVOLUTION

founded by H. Rohdenburg

IUSS-UISS-IBU

A Cooperating Journal of the International Society of Soil Science

---

Special Issue

The Significance of Soil, Water and Landscape Processes in Banded Vegetation Patterning

C. Valentin and J. Poesen (Editors)

CATENA

Scope of the Journal

Catena publishes papers describing original field and laboratory investigations and reviews on geo-ecology and landscape evolution with emphasis on interdisciplinary aspects of soil, hydrology and geomorphology. It aims to disseminate new knowledge and foster better understanding of the physical environment, of evolutionary sequences that have resulted in past and current landscapes, and of the natural processes that are likely to determine the fate of our terrestrial environment.

Papers within any one of the above topics are welcome provided they are of sufficiently wide interest and relevance.

CATENA

VOLUME 37 (1999)

THE SIGNIFICANCE OF SOIL, WATER AND LANDSCAPE PROCESSES IN BANDED VEGETATION PATTERNING

Edited by

C. Valentin and J. Poesen

CONTENTS

Soil and water components of banded vegetation patterns

C. Valentin [a,*], J.M. d'Herbès [b], J. Poesen [c]

[a] IRD, 210, rue La Fayette, 75480 Paris cedex 10, France
[b] IRD, B P. 5045, 34032 Montpellier, France
[c] Fund for Scientific Research Flanders, Laboratory for Experimental Geomorphology, Katholieke Universiteit Leuven, Redingenstraat 16, B-3000 Leuven, Belgium

Abstract

Banded landscapes are comprised of alternating bands of vegetation and bare ground aligned along the contours in arid and semi-arid regions (50–750 mm rainfall), on very gentle and uniform slopes (0.2–2%). Vegetated bands can be perpendicular to the direction of the dominant wind, or more frequently of the slope. Under given climatic conditions, slope gradient is the controlling factor of the type of pattern ('spotted', 'broadly' or 'typically' banded). For a given slope gradient, mean annual rainfall determines the contrast between the vegetated and bare phase, as well as the band length and the interband width:band width ratio. A typical transect through such two-phase mosaic includes a dynamic succession of surface crusts which generates a run-off–run-on system. This favours the capture of limited water resources and thus a biomass production greater for banded patterns than spotted patterns or uniformly scattered vegetation. Moreover, vegetated bands act as natural bench structures that greatly limit soil erosion. As suggested by modelling, banded vegetation patterns can equally be derived from nearly bare areas or from dense vegetation patterns. Because banded vegetation patterns have often been considered as a form of degradation of previous continuous vegetation cover, many attempts have been made by foresters to restore this initial cover by reforestation of the bare interbands. However the numerous failures of reforestation of the bare interbands illustrate the key role of these mosaic components in the maintenance of the tiger bush ecosystem. Banded vegetation patterns are more resilient to climate change than to human disturbances. The loss of landscape patchiness due to the clearing of the bands either for fuelwood or for ephemeral cropping induces a rapid decline in soil fertility and water infiltration potential. Long-term monitoring shows that the interband width:band width ratio adapts to rainfall variations that are intrinsic of semi-arid zones. Moreover, climatic changes might

---

* Corresponding author.

also induce a change in the type of patterning, suggesting that banded vegetation patterns are highly self-sustainable. The ecological differences between the pioneer and the decaying edges of the vegetated bands, the temporal/spatial succession of soil crusts, as well as other indices such as the spatial distribution of soil organic matter and termite nests suggest the upslope migration of the bands. Nevertheless field evidence of such a shift remains scarce. Profound lessons can be learnt from the study of banded landscapes in terms of ecosystems functions. When designing water-harvesting systems, or restoring degraded arid and semi-arid land, banded vegetation patterns should be imitated to optimize biomass production and limit land degradation. © 1999 Elsevier Science B.V. All rights reserved.

Keywords: Landscape patchiness; Banded vegetation pattern; Soil crusting; Water-harvesting, Semi-arid zone

---

1. Introduction

Studies of soil erosion, both theoretical and field oriented, have usually focused on agricultural plots. Much research has been therefore experimental and small scale in character. Integrating it into larger-scale models requires substantial progress in accounting for processes in real landscapes at the appropriate spatial and temporal scales. This raises questions about major controls on erosional process variations within a landscape (e.g., soil, topography, and land use). However, important effects of landscapes on run-off production and erosion also depend on the ways in which different sites interact with one another. Moreover, the effects of erosional processes across an entire landscape are often different from their effects within a small area (e.g., Poesen et al., 1996). In recent years, erosion modellers have become increasingly aware of the need to incorporate landscape patchiness and interactions.

This special issue of Catena does not claim to address all these complex issues. It aims to provide insights on the interactions between soil, water and vegetation in a peculiar type of ecosystem that occurs in arid and semi-arid zones. In these regions landscapes are commonly organized in a two-phase mosaic including vegetated and bare components. Among these communities, two main types have been often distinguished. The most common consists of spotted patches more or less circular (e.g., Puigdefabregas and Sanchez, 1996; Lavee et al., 1998), the second of banded patches (Fig. 1). This paper, as well as the series of papers of this special issue will refer to this latter type.

Banded vegetation patterns encompass densely vegetated stripes (bands) alternating regularly with bare areas of soil (interbands). Such patterns have drawn a growing attention among the scientific community over the last decades not only because they pose intriguing questions on (i) their forming processes (e.g., Thiéry et al., 1995), (ii) the interactions between patterns and functions (e.g., Boaler and Hodge, 1964; Noy-Meir, 1973; Ludwig and Tongway, 1995), (iii) their sensibility to climatic changes (e.g., Boudet, 1972; Couteron, 1997), but also (iv) because of their economical importance in terms of fuel and fodder production (e.g., d'Herbès et al., 1997a,b).

The most characteristic form of banded vegetation has been first recognized from aerial photographs and called 'tiger bush' in Niger (Clos-Arceduc, 1956) and the Sudan (Worral, 1960). Among clearly banded patterns, great similarities can be observed between aerial-photos from many parts of the world. However, ground truth may differ
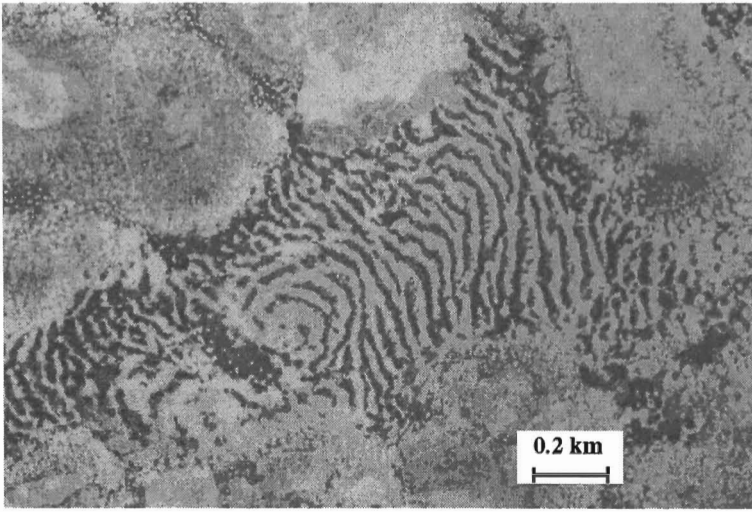
a
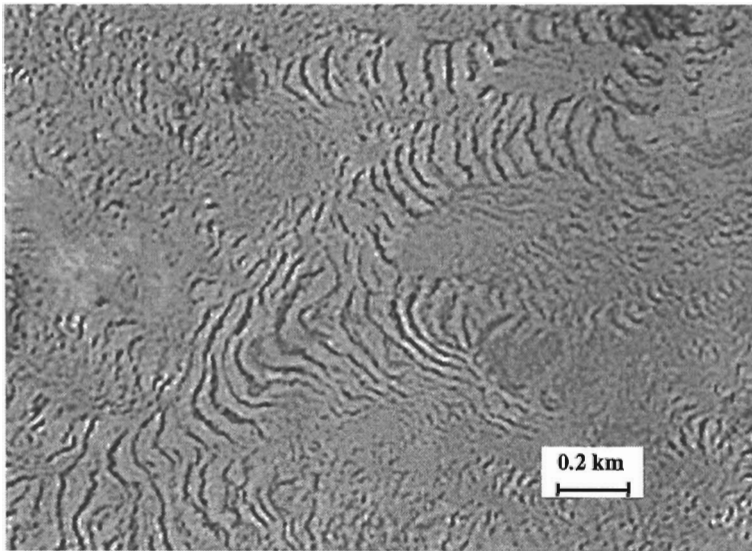
b

Fig. 1. Typical type of banded vegetation pattern (a) in Niger (13°40′N, 2°40′E, 80 km East of Niamey, Institut Géographique National aerial photograph, AOF 1950) and (b) Somalia (9°31′N; 49°11′E, in the vicinity of Qardho, SPOT XS image of 30 May 1988, KJ 159/331).

widely since banded vegetation can consist either of grass (Worral, 1959), trees (Worral, 1960), shrubs (MacDonald et al., 1999), or trees and grass (Slatyer, 1961).

altitude (m)
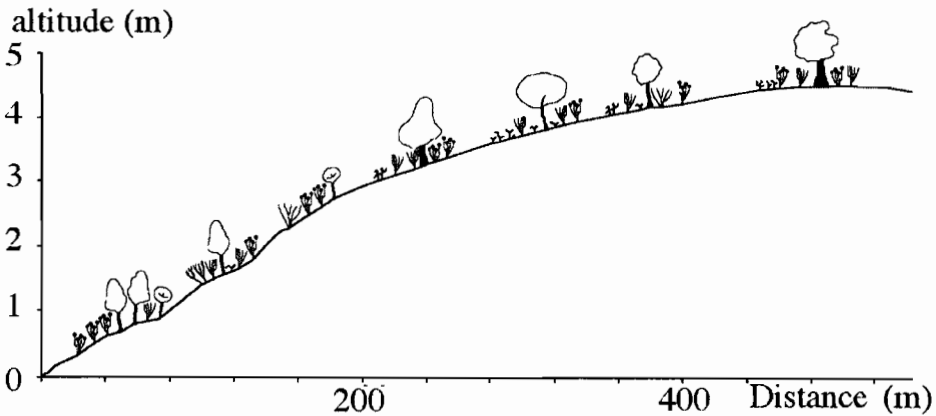
Fig. 2. Transect through a typical banded vegetation pattern in Niger (adapted from Ambouta, 1997)

Most studies have focused on one single or a series of successions of vegetated bands and bare interbands. Such periods, or cycle of banding, have been frequently sampled in the field along a transect perpendicular to the contour (Fig. 2). More seldom have been the authors who have combined local sampling to a regional survey, based either on aerial-photograph examinations (Leprun, 1999; Zonneveld, 1999), or on satellite image studies (Mougenot and Hamani, 1997). Only a few studies on banded mosaics have been developed across a wide range of climatic gradients (Bergkamp et al., 1999; Leprun, 1999; Valentin and d'Herbès, 1999).

A wealth of hypotheses have been put forward about the processes that enable the formation and maintenance of these ecosystems. For example, some authors postulated the impact of contrasting soils (Wickens and Collier, 1971; Mabbut and Fanning, 1987). A few advocated the role of wind (Ives, 1946; White, 1969; Leprun, 1992). More numerous were those who hypothesised the impact of overland flow (e.g., Boaler and Hodge, 1964; White, 1971; Cornet et al., 1988; Dunkerley and Brown, 1995).

The objective of this paper is to review some of the major findings pertaining to soil and water components of banded vegetation patterns.

2. Global distribution of the banded vegetation patterning

Many authors after White (1971) have reported that vegetation banding occurs wherever annual rainfall is low (50–750 mm), irrespective of soils and parent materials. It is also widely accepted that banding vegetation can develop only where overland flow cannot concentrate, namely on very gentle and uniform slopes (0.2–2%, Bromley et al., 1997). However in southeastern Spain, banded vegetation has been observed on steeper slopes of 10–30° (Puigdefabregas and Sanchez, 1996) and 6–20° (Bergkamp et al., 1999).

Bromley et al. (1997) noted also that patterned vegetation types share other characteristics as a homogeneous, horizontal isotropic substrate and a tendency to develop low permeability surface crusts.

Table 1
Main references on banded vegetation patterns

Ref.	Region	Authors and date	Ref.	Region	Authors and date
A	Australia	Dunkerley and Brown, 1995	Me	Mexico	Janeau et al., 1999
A	Australia	Dunkerley and Brown, 1999	Me	Mexico	Mauchamp, 1992
A	Australia	Greene, 1992	Me	Mexico	Mauchamp et al., 1994
A	Australia	Greene et al., 1994	Me	Mexico	Mauchamp and Janeau, 1993
A	Australia	Greig-Smith, 1979	Me	Mexico	Montaña, 1992
A	Australia	Litchfield and Mabbut, 1962	Me	Mexico	Montaña et al., 1990
A	Australia	Ludwig and Tongway, 1995	N	Niger	Ambouta, 1984
A	Australia	Ludwig et al., 1994	N	Niger	Ambouta, 1997
A	Australia	Ludwig et al., 1999	N	Niger	Chappel et al., 1999
A	Australia	Mabbut and Fanning, 1987	N	Niger	Chase and Boudouresque, 1987
A	Australia	MacDonald et al., 1999	N	Niger	Bromley et al., 1997
A	Australia	Slatyer, 1961	N	Niger	d'Herbès et al., 1997b
A	Australia	Tongway and Ludwig, 1989	N	Niger	d'Herbès et al., 1997a
A	Australia	Tongway and Ludwig, 1990	N	Niger	Galle et al., 1997
A	Australia	Tongway and Ludwig, 1994	N	Niger	Galle et al., 1999
Ar	Saudi Arabia	Vesey-Fitzgerald, 1957	N	Niger	Guillaume et al., in press a
Af	South Africa	MacDonald, 1978	N	Niger	Guillaume et al., in press b
Af	South Africa	Van der Meulen and Morris, 1979	N	Niger	Ichaou and d'Herbès, 1997
B	Burkina Faso	Couteron, 1997	N	Niger	Malam Issa et al., 1999
B	Burkina Faso	Couteron and Kokou, 1997	N	Niger	Mougenot and Hamani, 1997
B	Burkina Faso	Couteron et al., 1996	N	Niger	Orr, 1995
B	Burkina Faso	Ouédraogo and Lepage, 1997	N	Niger	Peltier et al., 1994a,b
B	Burkina Faso	Serpantié et al., 1992	N	Niger	Seghieri et al., 1996
E	East Africa	Belski, 1990	N	Niger	Vandervaere et al., 1997
E	East Africa	Boaler and Hodge, 1962	N	Niger	Wallace and Holwill, 1997
E	East Africa	Gilliland, 1952	N	Niger	White, 1970
E	East Africa	Greenwood, 1957	N	Niger	White, 1971
E	East Africa	Hemming, 1965	N	Niger/ global	Thiéry et al., 1995
E	East Africa	MacFayden, 1950	N	Niger/ global	Thiéry et al., 1996
E/J/S	East Africa/ Jordan/Syria	Boaler and Hodge, 1964	N	Niger/ global	Valentin and d'Herbès, 1999
J	Jordan	White, 1969	Ni	Nigeria	Clayton, 1966
M	Mali	Boudet, 1972	Ni	Nigeria	Grove, 1957
M	Mali	Hiernaux and Gérard, in press	Ni	Nigeria	Zonneveld, 1999
M/B	Mali/ Burkina Faso	Leprun, 1992	Su	Sudan	Morrison et al., 1948
M/B	Mali/ Burkina Faso	Leprun, 1999	Su	Sudan	Ruxton and Berry, 1960
M/N	Mali/Niger	Clos-Arceduc, 1956	Su	Sudan	Warren, 1973
Ma	Mauritania	Audry and Rossetti, 1962	Su	Sudan	Wickens and Collier, 1971
Me	Mexico	Cornet, 1992	Su	Sudan	Worral, 1959
Me	Mexico	Cornet et al., 1988	Su	Sudan	Worral, 1960
Me	Mexico	Cornet et al., 1992	(U)	USA	Ives, 1946
Me	Mexico	Delhoume, 1995	(U)	USA	MacMahon and Shimpf, 1981
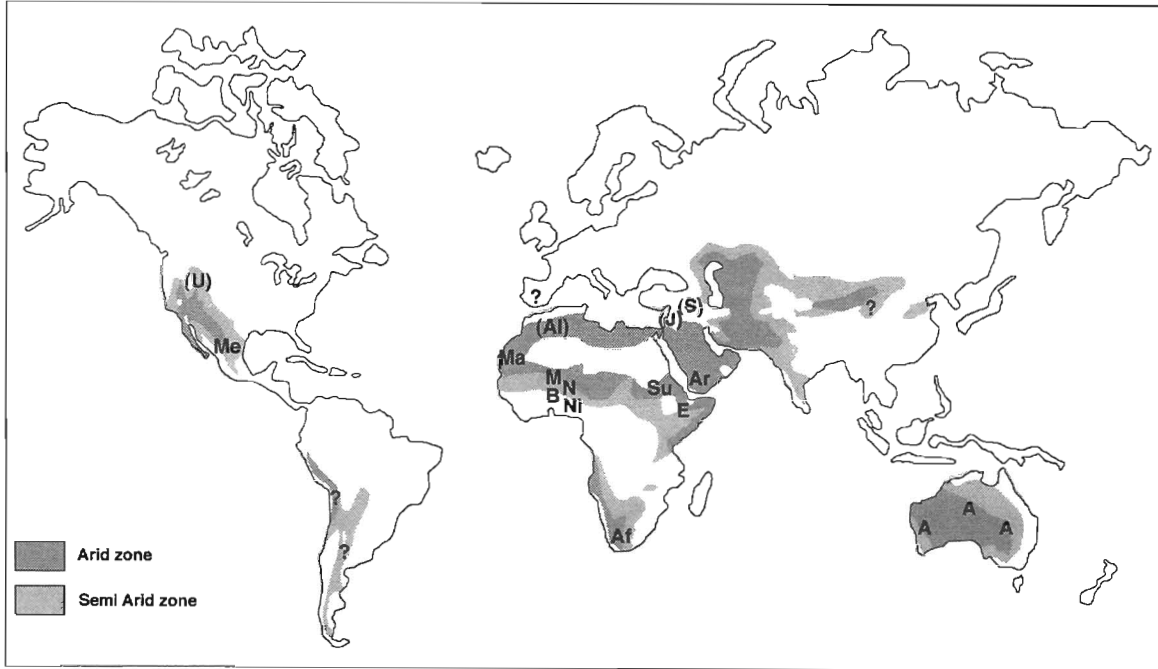
Fig. 3. Global distribution of banded vegetation pattern as indicated by available literature. For symbols see Table 1.

The domain of occurrence of the banded vegetation patterns as indicated by available literature (Table 1, Fig. 3) has certainly been biased by the number of studies conducted in Africa and in Australia compared to other continents. Banded vegetation is thus likely to cover larger areas in South America and in Asia but systematic surveys still have to be conducted at the global scale.

3. Types of banded vegetation patterns and associated factors

Comparisons among the literature data are rendered difficult because most authors have focused on only one aspect of banded vegetation patterns without referring to a minimum set of data necessary to define clearly the patterns and their associated components. Often, key data are lacking, e.g., mean annual rainfall (MAR), slope gradient (SL), wavelength (WL; i.e., the length of a cycle including a band and an interband), vegetation and soil types. Even more critical is the common absence of a clear sketch or aerial-photo to depict the two-phase mosaic. Therefore, it is unclear whether the authors referred to the same type of patterns. Referring to a typical banded pattern (for example, the tiger bush in Niger, Table 2), several variants can be observed in the same region or in other parts of the world, depending on the degree of banding, the contrast and the dimensions of the two-phase mosaic elements (Fig. 4).

Table 2
Main characteristics of banded vegetation patterns as indicated in the literature

Source	Country	MAR (mm)	MSG (%)	VW (m)	BW (m)	WL (m)	Band type
White, 1969	Jordan	75	NA	5	63	68	Shrubs/grass
Hemming, 1965	Somalia	150	0.602	NA	NA	NA	Perennial grass
Dunkerley and Brown, 1995	Australia	190	1.833	20	25	45	Chenopod schrub
Leprun, 1999	Mali	200	2.100	NA	NA	60	Trees/grass
Boaler and Hodge, 1964	Somalia	213	0.222	NA	NA	133	Grass, woodland
Mabbut and Fanning, 1987	Australia	225	0.350	40	40	80	Trees/shrubs
Dunkerley and Brown, 1999	Australia	240	0.400	12	9	20	Perennial grass/shrubs
Dunkerley and Brown, 1999	Australia	240	1.320	27	11	38	Perennial grass/shrubs
Slatyer, 1961	Australia	250	0.200	28	133	160	Trees/grass
Worral, 1960	Sudan	250	0.123	48	185	233	Tree
Audry and Rossetti, 1962	Mauritania	250	0.300	NA	NA	94	Perennial grass
Worral, 1959	Sudan	250	0.357	10	22	32	Grass
Montaña et al., 1990	Mexico	260	0.372	NA	NA	120	Shrubs
Valentin and d'Herbès, 1999	Niger	310	0.400	17	39	55	Trees/grass
Wickens and Collier, 1971	Sudan	350	0.500	NA	NA	NA	NA
Wickens and Collier, 1971	Sudan	450	0.500	NA	NA	90	Trees
Leprun, 1999	Mali	550	1.300	NA	NA	250	Trees/grass
Thiéry et al., 1995	Niger	560	0.524	39	35	74	Trees/grass
Valentin and d'Herbès, 1999	Niger	641	0.480	35	20	55	Trees/grass

MAR: mean annual rainfall, MSG: mean slope gradient, VW: wavelength (WL = VW + BW).
NA: not available.
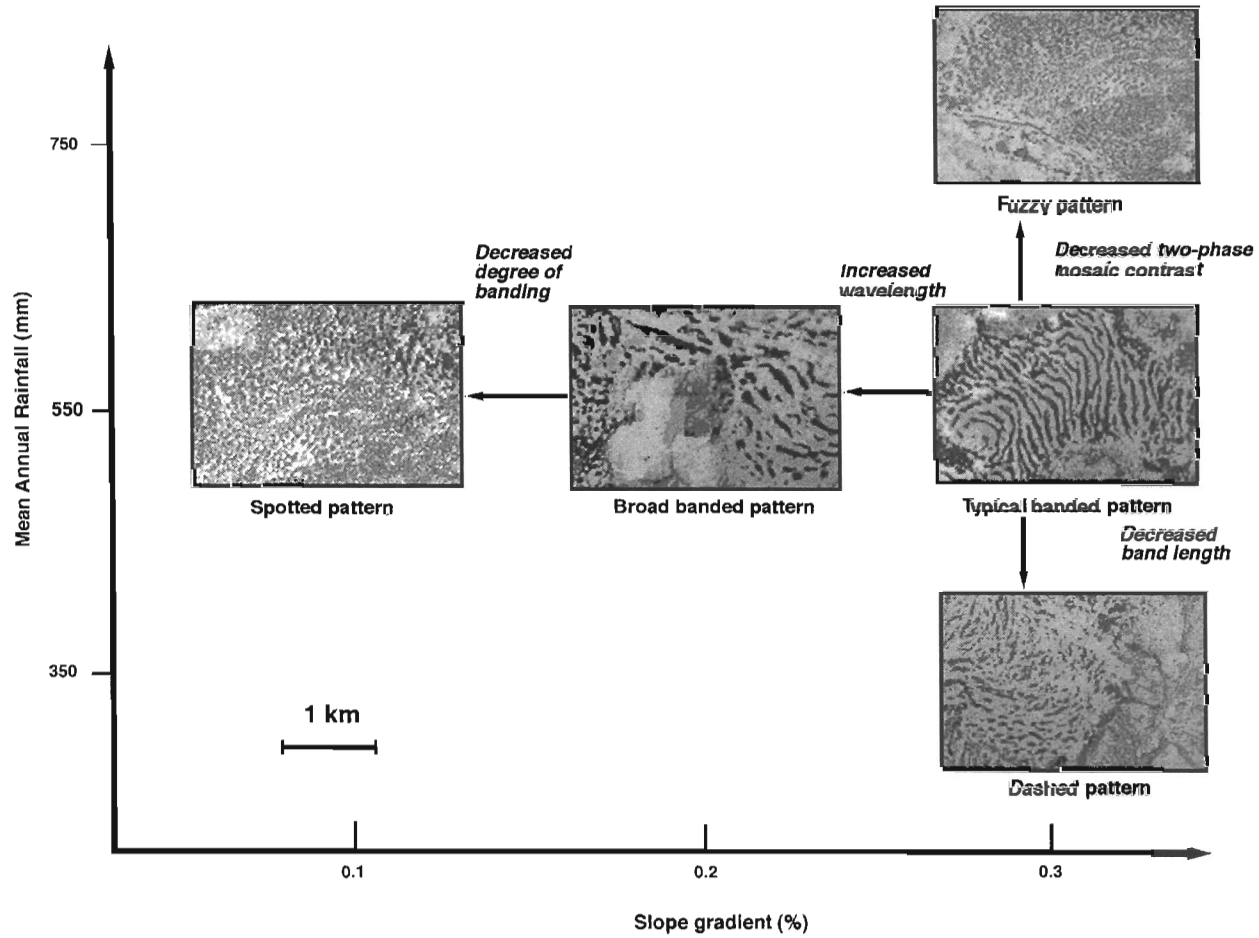
Fig. 4. Typical type of banding vegetation patterns and possible variants (examples from Niger).

3.1. Degree of banding

Before the current use of aerial-photos, the existence of banded vegetation had been overlooked. Identifying patterns unequivocally in the field remains very difficult. Sampling may be thus corrupted owing to possible confusion between clearly banded patterns and other patterns. Intergrades between banded and spotted patterns can occur along a single transect even over a short distance (Fig. 5). Even on aerial-photos, pattern categorization can be subjective. To establish an objective typology of vegetation patterns, a simple method was proposed by d'Herbès et al. (1997a,b). It was based on an index of diversity DI adapted from Hill (1973):

$$DI = 1/\sum p_i^2$$

with $p_i = l_i/L$, and L = total length of one transect and l_i = length of each transect component. The components were defined as homogeneous zones according to surface features and vegetation structure (Degraded, Run-off, Sedimentation, Pioneer, Central; Thiéry et al., 1995; see Fig. 7).

This index was systematically computed for transects of 50 m long, established parallel to the contour in the middle of the bare interbands (Run-off zone R) of 22 vegetation mosaics in southeastern Niger (d'Herbès et al., 1997a,b).
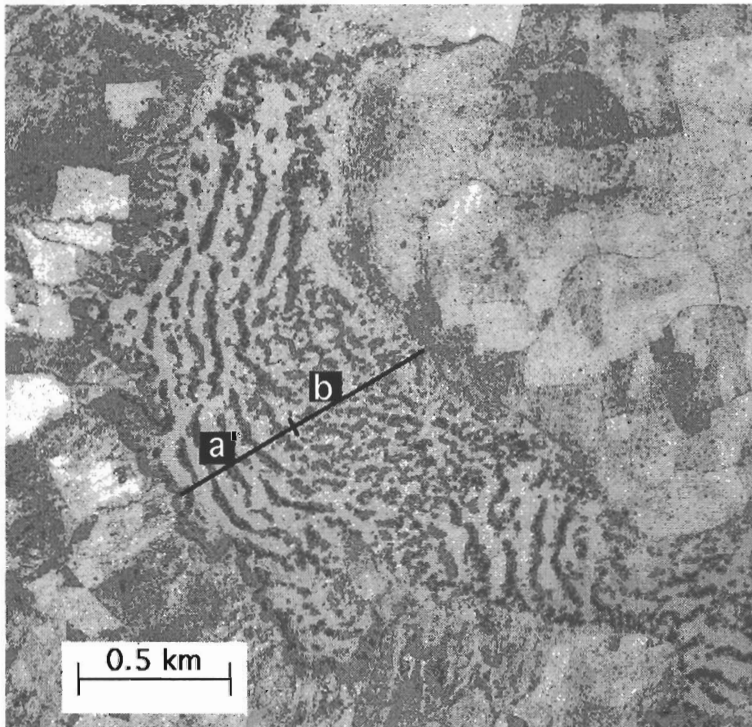
Fig. 5. Example of variations of vegetation patterns on a plateau in Niger. Mean annual rainfall: 550 mm. (a) Typical banded pattern, slope gradient 0.41%; (b) Spotted pattern, slope gradient 0.09%).

Clearly banded patterns were found for DI < 1.23. This limit was associated with a slope gradient threshold (SG > 0.2%), below which DI increased sharply as the patterns were no longer banded but spotted.

Under given semi-arid climatic conditions, SG is therefore the controlling factor of the occurrence of banded vegetation pattern (Fig. 4). This may be related to the topographic threshold critical to promote a clear anisotropic overland flow.

3.2. Contrast between the two-phase mosaic elements

This slope gradient threshold tends to increase with mean annual rainfall MAR (Fig. 6). In other words, for a given slope gradient, vegetation pattern is more likely to be banded under dry than under wetter conditions. This has been observed along a 200 km long transect across plateaux in southeastern Niger (Valentin and d'Herbès, 1999). With a similar mean slope gradient ranging from 0.2 to 0.7%, plateaux are mainly covered with banded vegetation in the areas receiving less than 550 mm annual rainfall and with less contrasted ('fuzzy') vegetation patterns in the wetter zones. In the latter region, banded vegetation is restricted to the edges of the plateaux with slightly steeper slopes.

3.3. Dimensions of the two-phase mosaic elements

3.3.1. Width

Several distinctions have been proposed among the clearly banded patterns based on the length and the width of the bands. In contrast with the typical Niger tiger bush that occurs in the centre of the Niamey area, Ambouta (1997) distinguished a 'dashed pattern' consisting of short and narrow thickets, separated by wide bare interbands in the
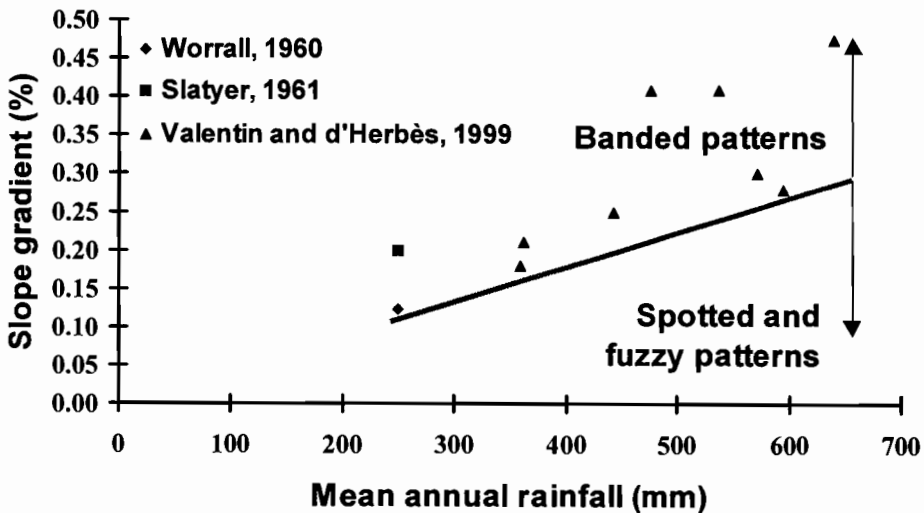
Fig. 6. Impact of mean annual rainfall on the critical slope gradient value for the occurrence of banding pattern (after the data of Worral, 1960; Slatyer, 1961; d'Herbès et al., 1997a,b).

drier zone. Similarly, Ludwig et al. (1999) distinguished in Australia stripes (short bands similar to the above 'dashes') and strands (long bands, analogous to the typical tiger bush).

3.3.2. Wavelength

Either in Niger (Ambouta, 1984; d'Herbès et al., 1997a,b), or in Australia (Mabbut and Fanning, 1987; Dunkerley and Brown, 1995) distinctive banded patterns have been recognized consisting of broad bands of thickets alternating with broad and bare interbands. They are usually referred to as 'broad-banded patterns'. The occurrence of typical- and broad-banded patterns nearly on the same locations have been explained by slight difference in slope gradient values. Several authors (d'Herbès et al., 1997a,b; Eddy et al., 1999) have reported that WL increases when SG decreases. However, as mentioned earlier there is a minimum value of SG below which vegetation is no longer banded but spotted. Near this critical limit of SG (0.2% in Niger), bands and interbands tend to reach a maximum width just before being disorganized. Typical-banded, broad-banded and no banded vegetation can therefore be adjacent as a result of slight differences in SG (0.25%, 0.20%, 0.15% respectively; d'Herbès et al., 1997a,b).

4. Soil components of banded patterns

4.1. Soil properties

One of the most crucial conditions to the development of banded vegetation patterns is the low infiltrability of soils and thus their ability to produce overland flow. For example, where aeolian sands cover the soil uniformly, no vegetation banding occurs on the Niger plateaux (d'Herbès and Valentin, 1997).

Although the greater depth of interband soils is reported from banding of *Terminalia brownii* savannah in the Sudan (Wickens and Collier, 1971), most observers (e.g., Ambouta, 1984; Bromley et al., 1997) agree that there is little difference between the soils of band and interband, besides the one directly induced by positive feedbacks from vegetation, faunal and hydrological differences. For example, MacDonald et al. (1999) reported that the cations were concentrated within the bare areas of a chenopod shrubland in South East Australia. The sodium concentration decreased towards the centre of the vegetation arcs. The authors observed that such distribution is not responsible for banding pattern but conversely is chiefly influenced by differences in soil moisture resulting from the accumulation of run-on vegetation depression and run-off from bare and impermeable gilgaï mounds.

The contrast in the soils which support banded vegetation patterns is thus mainly in the surface and subsoil features.

4.2. Surface features

Most authors have noted the very smooth surface of interbands, which efficiently generates run-off generation, compared to the rougher surfaces of the band more

favourable to infiltration and sediment trapping (e.g., Dunkerley and Brown, 1999; Janeau et al., 1999). The occurrence of crusted surfaces in the interbands have been noted in most studies (e.g., Boaler and Hodge, 1962; White, 1971, Mabbut and Fanning, 1987; Tongway and Ludwig, 1990; Greene, 1992; Leprun, 1992). Differences between the bare interbands and the vegetated bands can be induced by slight difference in silt content between the two zones. In northern Nigeria, Zonneveld (1999) ascribed such difference to former early Holocene to late Pleistocene dunes levelled by pediplanisation (sheet erosion) separated by filled-in valleys. Recent studies in Niger (e.g., Thiéry et al., 1995; Bromley et al., 1997; Malam Issa et al., 1999; Valentin and d'Herbès, 1999) have characterized the types of surface crust across the five typical zones forming banded vegetation patterns using the crust typology proposed by Valentin and Bresson (1992).

From a run-off generation point of view, the successive steps of crusting process can be considered from the lower edge of the vegetated band to the destruction of the crust within the core of the next lower vegetated band (Fig. 7).

(1) The degraded zone (D). Structural crusts (of the sieving type) tend to develop as a result of vegetation decays consecutive to insufficient water supply. These crusts consist of three well-sorted layers. The uppermost layer is composed of loose, coarse sand, the middle consists of fine, densely packed grains with vesicular pores, and the lower layer shows a higher content of fine particles with considerably reduced porosity. This latter layer is responsible for the very low infiltrability of the crust (Casenave and Valentin, 1992).

(2) The run-off zone (R). In the upper and middle part of the bare interband, a more or less clear succession of crusts is commonly observed (Valentin and d'Herbès, 1999). Erosion crusts develop out of sieving crusts from which the loose sandy layers have been removed by overland flow and/or by wind. They are built up with one smooth, impervious and hard layer made of compacted thin particles. These crusts which are often red in the upper parts of the bare areas cannot be colonized by aerial vegetation (because of their resistance to seedling emergence) but by microphytes (e.g., cyanobacteria of the species *Chroococus limnecus* Näg.; Malam Issa et al., 1999) which produce a darker colour. The microphytic erosion crusts occur downslope of the red erosion crusts. The distribution of the patches with coarse pavement crust is more erratic due to the irregularity of the depth of the gravelly layers. These coarse pavements crusts embed coarse fragments in a crust the microstructure of which is very similar to the sieving crust. Vesicular porosity is very pronounced especially below the coarse fragments. Such crusts have very low infiltrability (Valentin and Casenave, 1992). Because these coarse pavement crusts armour the soil underneath, they tend to protrude slightly from the adjacent erosion crusts. Such coarse pavement crusts are also very common in the bare interbands of banding patterns in northern Mexico (Janeau et al., 1999) and Australia (Dunkerley and Brown, 1999; MacDonald et al., 1999). Erosion crusts and coarse pavement crusts promote run-off, which is reflected in the occurrence of run-off crusts. These are built up with interbedding of sandy layers and seals of finer particles. They also contain vesicular pores.

(3) The sedimentation zone (S). Small depressions where water may ephemerally pond are observed at the lower edges of the bare zone. Erosion crusts, coarse pavement crusts and run-off crusts are covered with sedimentation crusts. They consist of densely
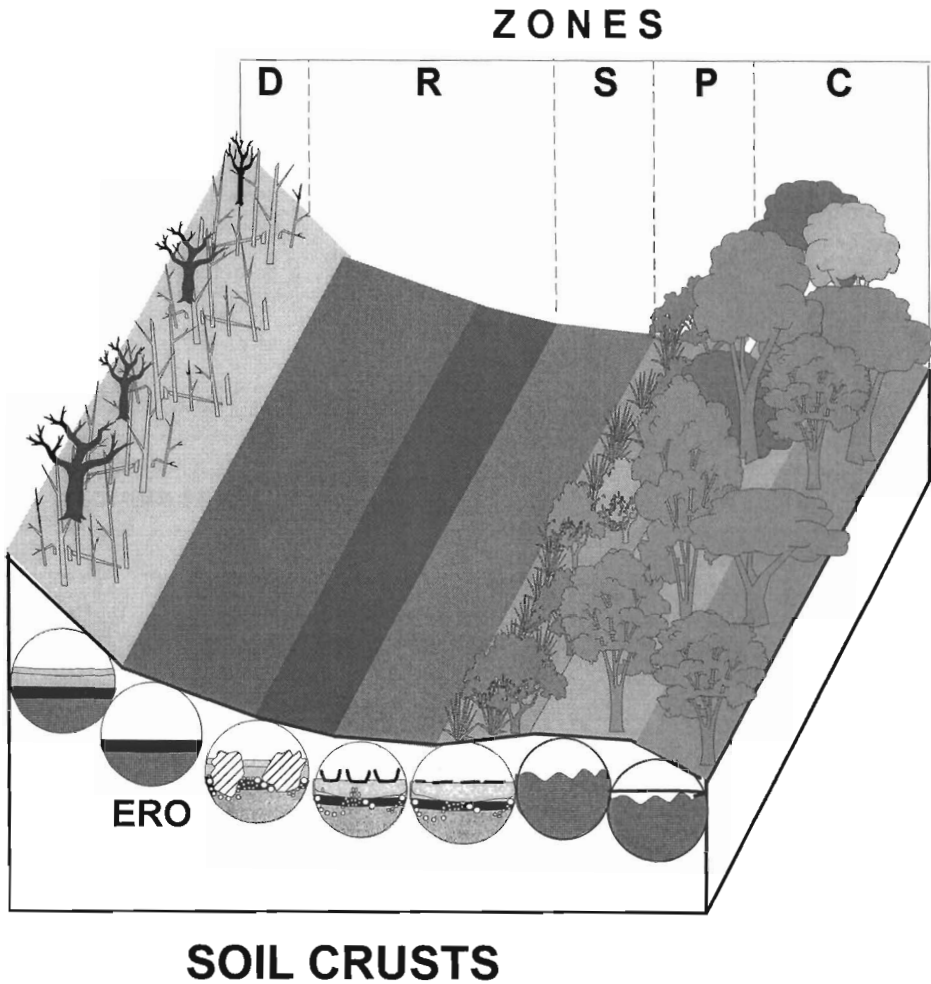
ZONES

SOIL CRUSTS

Fig. 7. Typical succession of surface conditions across a banded vegetation pattern in Niger. *Zones*: D: degraded, R: run-off, S: sedimentation, P: pioneer, C: central. *Soil crusts*: ST3: sieving structural crust with three micro-layers, ERO: erosion crust, G: gravel crust, SED: sedimentation crust, MSED: microphytic sedimentation crust, BIO: bioturbated surface, ST1: structural crust with one microlayer.

packed and well-sorted particles, the size of which gradually increases with depth. When dry, these crusts often break up into curled-up plates due to shrinking.

(4) The pioneer front zone (P). Cracks of sedimentation crusts favour the colonization by pioneer grassy vegetation. Once colonized, these sedimentation crusts often become more platy in structure, do not curl up and are more colonized by algae (microphytic sedimentation crusts, or microbiotic crusts; Eldridge and Greene, 1994; Malam Issa et al., 1999). Their porosity includes abundant biopores due to termite activity. The vegetation accelerates sediment trapping. The gradual accumulation of material in the
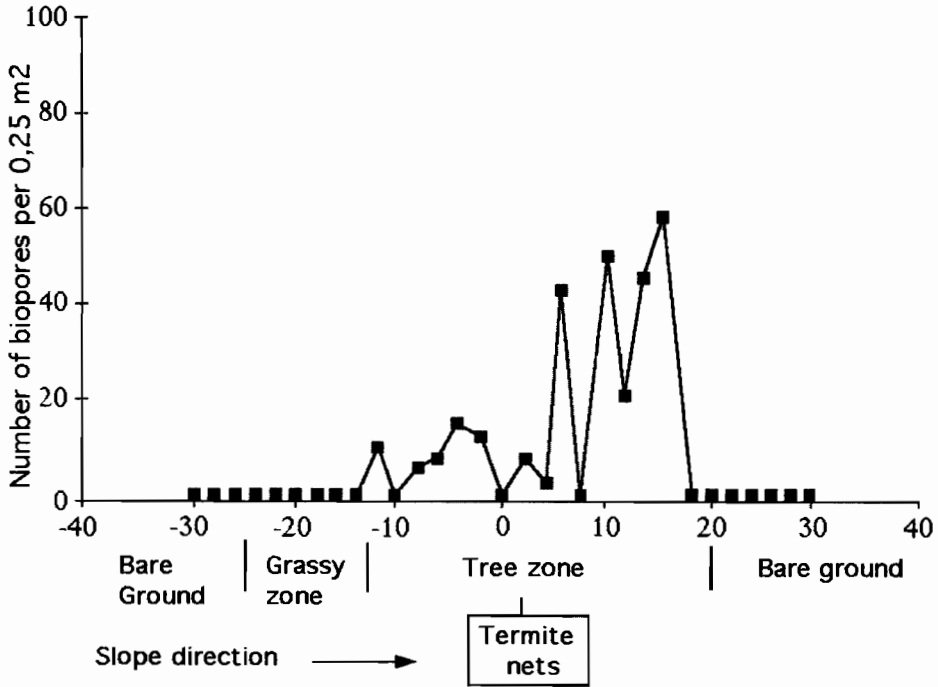
Fig. 8. Distribution of the density of biopores created by termites along a banded vegetation pattern in northern Burkina Faso (after Ouédraogo and Lepage, 1997).

depressions has been considered as one of the driving force of the gradual upslope encroachment of the vegetated band (d'Herbès et al., 1997a,b). Irregularities in the degree of silting up of these depressions might be responsible for the existence of salients (or 'capes' and 'bays') in the upslope band edge (Thiéry et al., 1995).

(5) The central zone (C). In the core of the vegetated bands, thick and permanent litter protects the soil surface from rainfall impact and favours termite activity causing bioturbation of the upper few centimetres and the destruction of the crust (Ouédraogo and Lepage, 1997; Fig. 8). However, this central zone is most commonly restricted to a very narrow belt of few meters (Valentin and d'Herbès, 1999). Furthermore, the litter and the termite activity do not affect the whole surface so that the previously formed crust can be locally maintained and some new structural crusts can even develop.

5. Aeolian and hydrological processes

5.1. Wind

Topsoil in the vegetated bands is generally slightly more sandy than in the bare interbands (e.g., Ambouta, 1984). This textural difference has been frequently ascribed

to sand trapping by the vegetation (e.g., White, 1971). In Mali, Leprun (1992, 1999) observed micro-dunes upslope of the bare interbands and vegetated bands perpendicular to the direction of the dominant wind. White (1969, 1971) suggested that in Jordan wind might be the initiating factor of banded patterns. The accumulation of wind-blown material around isolated plants might act as a nucleus for the development of vegetation arcs. In northern Nigeria, banded vegetation patterns associated with former levelled dunes are also orientated perpendicular to the prevailing wind direction during the period of dune formation (Clayton, 1966, 1969; Zonneveld, 1999).

5.2. Overland flow

Although the impact of hydrological processes on the development and maintenance of banded vegetation patterns has been postulated in earlier studies (e.g., Boaler and Hodge, 1964; White, 1971), the first measurements of soil moisture across the banded patterns are relatively recent (Ambouta, 1984; Cornet et al., 1988). Infiltration and run-off studies have required various equipments such as disk permeameters (Greene, 1992; Greene et al., 1994; Vandervaere et al., 1997), tension infiltrometers (Bromley et al., 1997), run-off plots (Galle et al., 1999), and rainfall simulators (Tongway and Ludwig, 1990; Greene and Sawtell, 1992; Bergkamp et al., 1999; Janeau et al., 1999). Field data confirmed what was expected from the surface conditions. Highly contrasted run-off coefficients (Table 3), minimal infiltration rates (Table 4) and soil water content profiles (Galle et al., 1999) were obtained in the different zones of the banded vegetation pattern.

These data corroborate the theory of Noy-Meir (1973) that many run-off–run-on systems of the semi-arid and arid regions function as source–sink systems. In the case of the banded vegetation patterns, water is shed from the bare zones to accumulate in the bands. More specifically, as shown in Niger (Valentin and d'Herbès, 1999), all the mosaic components can be considered as the source and the narrow central part of the vegetated band as the sink. Therefore, the amount of water received and infiltrated into

Table 3
Run-off coefficients (volume of total run-off/volume of total rainfall; %) in the various zones across banded vegetated patterns

Country	Zone					Source
	D	R	S	P	C	
Mexico[a]	34	75	71	NA	31	Janeau et al., 1999
Australia	NA	55	NA	NA	0	Greene, 1993
Niger[b]	18	54	NA	2	0	Galle et al., 1999
Spain[c]	NA	23	NA	NA	0	Bergkamp et al., 1999

D: degraded zone, R: run-off zone, S: sedimentation zone, P: pioneer zone, C: central zone. For location of zones see Fig. 7.
[a]Average from 10 simulated rainfall runs under various rainfall intensity and soil moisture conditions.
[b]Over a period of 4 years, only rains exceeding 5 mm were considered.
[c]Average from 11 rainfall simulation plots.
NA: not available.

Table 4
Minimum infiltration rate (mm h^{-1}) in the various zones across banded vegetated patterns

Country	Zone					Source
	D	R	S	P	C	
Mexico	8	3	1	NA	16	Janeau et al., 1999
Australia	NA	4	NA	NA	> 30	Greene and Sawtell, 1992
Australia	NA	10	NA	NA	60	Greene, 1992
Australia	NA	7	NA	NA	> 22	Greene, 1993
Niger	9	14	NA	7	37	Bromley et al., 1997
Niger	3	NA	2	NA	NA	Vandervaere et al., 1997
Spain	NA	24	NA	NA	51	Bergkamp et al., 1999

D: degraded zone, R run-off zone, S: sedimentation zone, P: pioneer zone, C: central zone. For location of zones see Fig. 7
NA: not available.

this central zone can be much higher than precipitation. The available values of the concentration ratio between infiltrated water amount and rainwater amount, vary from 2 in Australia (Tongway and Ludwig, 1990), and 3.5 in northern Mexico (Cornet et al., 1992), to approximately 4 near Niamey in Niger (Bromley et al., 1997; Galle et al., 1999). A simulation model based upon hydrologic parameters of the surface conditions across the banded patterns in Niger showed that this concentration ratio decreased linearly with increasing annual rainfall (Valentin and d'Herbès, 1999). Another model (Ludwig et al., 1999) indicated that under Australian conditions, the loss of run-off was about 30% greater from landscapes with no banded/bare patches than for those with patches. This was associated with a difference of 45% in net primary production. The banded vegetation systems were about 8% more efficient in capturing run-off than the spotted pattern, which was reflected in a 10% higher net primary production. Similar observations were made in West Africa where the woody biomass of unpatterned vegetation remains about 50% of the tiger bush (Ichaou and d'Herbès, 1997; Valentin and d'Herbès, 1999). The impact of overland flow on the maintenance of the banded vegetation pattern was also clearly demonstrated by building a wall to seclude the pioneer and the central zones from any run-on. This experiment clearly decreased plant productivity (Galle et al., 1997).

5.3. Erosion

Data on compressive strength of the topsoil across two banded mosaics in western New South Wales, Australia, suggested that little sediment transport was possible across the patterns (Dunkerley and Brown, 1999). This is supported by the fact that banded patterns commonly act as closed hydrological systems, with no or exceptional outflow (e.g., Galle et al., 1999; Valentin and d'Herbès, 1999). Since the most common topographic profile across banded vegetation consists of a gently sloping run-off zone leading downslope onto a flatter interception zone, it favours soil conservation as would do a bench structure.

Recent laboratory rainfall and run-on experiments suggested that sequential scour/deposition features could favour the development of small-scale vegetation bands as observed in the field in semi-arid northern Kenya (Bryan and Brun, 1999).

Using ^{137}Cs techniques to measure erosion and deposition rates in Niger tiger bush, Chappell (1995) found a net soil loss of 3 t ha^{-1} yr^{-1} in the interbands and a net soil gain of 4 t ha^{-1} yr^{-1} in the bands. These results suggest that soil gain is not only due to the accumulation of sediment redistributed by surface wash but also by wind deposition. In the region, Drees et al. (1993) monitored a mean dust deposition rate of 2 t ha^{-1} yr^{-1} over 8 years.

6. Genesis and dynamics

6.1. Genesis

The intriguing question of how banded vegetation patterns originate has not yet been elucidated. In particular, the possible temporal succession between unpatterned and patterned vegetation have not been clearly documented. Two main alternative hypotheses have been advocated, either the gradual degradation of an originally uniform plant cover due to climatic or human disturbances (White, 1971), or conversely the colonization of previously degraded bare areas under improving climatic or land use conditions (Boudet, 1972; Bryan and Brun, 1999). Banded patterns were observed for example where vegetation recovered from wildfire in Spain (Cammeraat and Imeson, 1999).

To compensate the absence of long-term monitoring experiments, Thiéry et al. (1995) elaborated a simple model to simulate the development of banded vegetation patterns. This landscape model was based on cellular automata, i.e., fixed arrays in which each cell represents an area of the land surface. Only two hypotheses were required: the establishment, growth and survival of a given plant is (1) negatively affected by the influence of plants situated upslope (competition) and (2) positively by lateral and downslope plants (synergy). To represent time, the model updated the state of all cells in the grid iteratively. On a practical level, it was compatible with aerial photos so that results could be compared with real patterns as observed on the Niger plateaux. By varying only the two parameters a (upslope resource competition) and b (lateral synergies) and the number of iterations, the model could generate almost all the patterns observed on aerial photos. Because these results were independent of the initial tree density, they suggest that banded vegetation patterns could equally be derived from nearly bare areas or from dense vegetation patterns. Current studies aim at providing ecological meaning to the coefficients a and b and to specify time spans.

A similar model was developed by Puigdefabregas et al. (in press) to elucidate the development of banded patterns in a primeval forest of Tierra del Fuego island (Argentina), with tree stripes perpendicular to the prevailing wind direction. The climate was cold oceanic, with 5°C annual temperature and 600 mm annual rainfall. Older and dying trees occurred in the windward edge of each band and seedling regrowth in the lee side. The authors hypothesised that (1) vulnerability of trees to wind damage increased with age, (2) clusters of older trees produced cone-shaped wind shadows that protected

larger clusters of younger trees leeward. Based on these hypotheses, banded patterns were simulated, the initial state being a heterogeneous forest with randomly distributed tree ages. The model showed that increasing tree growth rates led to longer wavelengths and higher wave propagation rates, while increasing wind killing capacity led to shorter wavelengths and lower propagation rates. Similar wind-induced and moving cyclic waves of death, regeneration and maturation have also been observed in other 'wave regenerating forests' in the northeastern United States (Sprugel, 1976; Sprugel and Bormann, 1981) and in central Japan (Kohyama, 1988; Sato and Iwasa, 1993).

6.2. Responses to human disturbances

Because banded vegetation patterns have often been considered as a form of degradation of previous continuous vegetation cover, many attempts have been made by foresters to restore this initial cover by reforestation of the bare interbands. Adapting their model (Thiéry et al., 1995) to such tree planting, Thiéry et al. (1996) showed that planted trees disappear after only two iterations, suggesting a rapid failure of these plantations. Even more important to note was the resulting thinning of the downslope natural vegetation band. The model results were corroborated by the numerous failures of reforestation of the bare interbands in the tiger bush region (d'Herbès et al., 1997a,b). This illustrates the key role of these mosaic components in the maintenance of the tiger bush ecosystem.

The loss of landscape patchiness is associated with a rapid decline in soil fertility and water infiltration potential (Ludwig et al., 1999). The most serious degradation of the system results from the clearing of the bands either for fuelwood or for ephemeral cropping of sorghum and millet. This leads to degraded landscapes that are extremely costly and hazardous to reclaim (Torrekens et al., 1997).

6.3. Responses to climate change

Measuring the interband width:band width ratio (IRB) on sequential aerial photos from 1950 to 1992 along a 200 km transect in Niger, Valentin and d'Herbès (1999) established a clear correlation between this ratio and the mean annual rainfall averaged over the last 15 years (MAR_{15}). IRB increased dramatically from 1.1 to 2.3 when rainfall decreased from 426 mm to 315 mm in 1992. Such results illustrate the great adaptability of the banded vegetation pattern to rainfall variations that are intrinsic to arid and semi-arid zones.

Fig. 6 suggests that climatic changes might also induce a change in the type of patterning, especially between typical banded and fuzzy patterns. Such transition has been reported in northern Burkina Faso comparing aerial photos taken in 1952 and 1984 (Serpantié et al., 1992). Fuzzy patterns evolved into a typical banded pattern most likely as a response to the very severe droughts of 1971–1974 and 1983–1984. This increased contrast is related to a reduction of the vegetation cover from 50 to 33%. The fuzzy character of the older pattern in the 1950s was due to isolated shrubs and trees in the interbands which did resist the droughts of the 1970s and the 1980s (Couteron, 1997).

Nevertheless, evidences of transformation of vegetation patterns remain very rare because they can occur only when, for a given slope gradient, the mean annual rainfall

reaches a critical limit as illustrated in Fig. 6. This restricts the possible use of the banded patterns as indicators of climatic changes.

These ecosystems can clearly adapt to altering climatic inputs and can be thus considered as highly resilient.

6.4. Upslope migration of the vegetation bands

Many authors have inferred from their observations that the banded patterns should migrate upslope (e.g., Boudet, 1972; Cornet et al., 1988). The upslope edge consists of young and pioneer vegetation, the downslope edge of decayed plants. This hypothesis was supported by the model of Thiéry et al. (1995) which showed that competition for upslope resources implies upslope migration. Remnants of termite mounds of *Macrotermes subhyalinus* Rambur were commonly observed within the bare interbands (e.g., 18.3 nests ha^{-1}, in northern Burkina Faso) whereas habited nests occurred only in the bands (22.3 nests ha^{-1}; Ouédraogo and Lepage, 1997). Irrespective of biological considerations, uniform subsoil characteristics also tend to substantiate such shift. Stable bands should be associated with more contrasted subsoils between bands and interbands. At the soil surface, the spatial succession of genetically linked surface crusts suggests also a temporal succession. In particular, the distribution of erosion and sedimentation crusts reflects an upslope shift of the erosional and depositional fronts.

Despite these facts, evidences of upslope migration of banded patterns remain very scarce (Table 5). This is partly due to the small velocity which cannot be accurately assessed on sequential aerial photographs and satellite images. Due to climatic variations, the characteristics of banded vegetation patterns need to be monitored on the long run. Moreover, such monitoring has to be carried out at a great number of transects because of the frequent lateral irregularities of the pioneer front consisting of 'capes' and 'bays'. Indirect methods such as ^{137}Cs technique (Chappel et al., 1999), dendrochronology (Ichaou and d'Herbès, 1997), and measurement of δ^{13}C (Guillaume et al., in press a,Guillaume et al., in press b) support the hypothesis of upslope migration but remain tedious and costly.

As reported by few authors (White, 1969; Wickens and Collier, 1971), upslope migration of the banded pattern is sometimes not perceivable. Tongway and Ludwig

Table 5
Velocity of upslope migration of banded vegetation patterns

Country	Site	Method	MAR (mm)	MSG (%)	MAV (m yr^{-1})	Source
Niger	Banizoumbou	^{137}Cs techniques	495	0.27	0.19–0.27	Chappel et al , 1999
Niger	Sofiabangou	Dendrochronolgy	476	0 41	0.5	d'Herbès et al., 1997a,b
Sudan	Butana	Field monitoring	250	0.36	0.3–1 5	Worral, 1959
Mali	Hombori	Field monitoring (21 years)	450	0.9	0.75	Leprun, 1999
Mali	N'Daki	Field monitoring (21 years)	300	1.9	0.25	Leprun, 1999
Mali	Gossi	Field monitoring (4 years)	200	2 1	0 20	Leprun, 1999

MAR: mean annual rainfall. MSG: mean slope gradient. MAV: mean annual velocity.

(1990) anticipated upslope movement of the vegetation bands, but were unable to measure any change over 10 years (Tongway, personal communication). Mabbut and Fanning (1987) considered that upslope migration does not occur in the systems because of the hardpan location which was much deeper under the vegetation band than on the interband zone.

These results suggest that upslope migration cannot be therefore considered as invariable for all banded vegetation patterns. Further research is needed to document the factors controlling migration velocity.

7. Conclusions

Over the last years, a number of essential questions related to banded vegetation patterns have been unravelled at least partly. The types of patterns and of components, as the interband width:band width ratio, are controlled by topographic and to a lesser extent by climatic factors. Hydrological processes have also been substantially documented. Other issues such as the temporal dynamics of these ecosystems in terms of genesis and upslope migration should still be cleared up.

Among the most interesting results are the close relationships that have been established between patterns, ecological processes including hydrological and erosion processes and biomass production.

Profound lessons can be learnt from the study of banded landscapes in terms of ecosystems functions. A better understanding of these functions has influenced changes in management practices in Niger and Australia. In particular, decision-makers are now more aware of the invaluable role of banded vegetation patterns in terms of soil, water and nutrients conservation.

Robust and resilient to climatic change, and to moderate land use, this type of landscape patchiness offers a remarkable example of capture, concentration and storage of resources in dry and poor environments. Land managers should attempt to mimic such banded vegetation patterns when restoring degraded arid or semi-arid land and when designing water-harvesting systems.

References

Ambouta, K J.-M., 1984. Contribution à l'édaphologie de la brousse tigrée de l'Ouest nigérien Doctor-Engineer thesis, University of Nancy, 116 pp.

Ambouta, K J.-M , 1997. Définition et caractérisation au sol des différents types de végétation contractée au Niger. In d'Herbès, J.-M., Ambouta, J.-M.K., Peltier, R. (Eds.), Fonctionnement et Gestion des Écosystèmes Forestiers Contractés Sahéliens. John Libbey Eurotext, Paris, pp. 41–57.

Audry, P., Rossetti, C., 1962. Observation sur les sols et la végétation en Mauritanie du sud-est et sur la bordure adjacente du Mali (1959 et 1961). Prospection Ecologique en Afrique Occidentale, FAO, Rome, pp. 53–71.

Belski, A.J., 1990 Tree/grass ratios in east African savannas: a comparison of existing models Journal of Biogeography 17, 483–489.

Bergkamp, G., Cerda, A., Imeson, A.C., 1999. Magnitude–frequency analysis of water redistribution along a climate gradient in Spain. Catena, this issue.

Boaler, S.B., Hodge, C.A.H., 1962. Vegetation bands in Somaliland. Journal of Ecology 50, 465–524.

Boaler, S.B , Hodge, C.A.H., 1964. Observations on vegetation arcs in the northern region, Somalia Republic. Journal of Ecology 52, 511–544.

Boudet, G., 1972 Désertification de l'Afrique tropicale sèche. Adansonia 12 (4), 505–524, série 2.

Bromley, J., Brouwer, J., Barker, T., Gaze, S., Valentin, C., 1997. The role of surface water redistribution in an area of patterned vegetation in south west Niger. Journal of Hydrology 198, 1–29.

Bryan, R.B., Brun, S.E , 1999. Laboratory experiments on sequential scour/deposition and their application to the development of banded vegetation Catena, this issue.

Cammeraat, L.H., Imeson, A.C., 1999. The evolution and significance of soil–vegetation patterns following land abandonment and fire in Spain. Catena 37, 107–127.

Casenave, A., Valentin, C., 1992. A runoff capability classification system based on surface features criteria in semi-arid areas of Africa. Journal of Hydrology 130, 231–249.

Chappell, A., 1995. Geostatistical mapping and ordination analysed of ^{137}Cs-derived net soil flux in southwest Niger. Unpublished doctoral thesis, University of London.

Chappel, A., Valentin, C., Warren, A., Noon, P., Charlton, M., d'Herbès, J.M., 1999. Testing the validity of upslope migration in banded vegetation from southwest Niger. Catena 37, 217–229.

Chase, R.G., Boudouresque, E., 1987. Methods to stimulate plant regrowth on bare sahelian forest soils in the region of Niamey, Niger Agriculture, Ecosystems and Environment 18, 211–221.

Clayton, W.D., 1966. Vegetation ripples near Gummi, Nigeria. Journal of Ecology 54, 415–417.

Clayton, W.D., 1969. The vegetation of Katsina province, Nigeria. Journal of Ecology 57, 445–451.

Clos-Arceduc, M., 1956. Etude sur photographies aériennes d'une formation végétale sahélienne: la brousse tigrée. Bulletin de l'IFAN 7 (3), 677–684, série A.

Cornet, A., 1992. Relation entre la structure spatiale des peuplements végétaux et le bilan hydrique des sols de quelques phytocénoses en zone aride. In: Le Floc'h, E., Grouzis, M., Cornet, A., Bille, J.C. (Eds.), L'Aridité, une Contrainte au Développement. Editions de l'ORSTOM, Paris, pp. 245–265.

Cornet, A.F., Delhoume, J.P., Montaña, C., 1988 Dynamics of striped vegetation patterns and water balance in the Chihuahuan desert. In: During, H.J., Wergner, M.J.A., Willems, J.H. (Eds.), Diversity and Pattern in Land Communities SPB Academic Publishing, The Hague, Netherlands, pp. 221–231

Cornet, A.F , Montaña, C., Delhoume, J.P., Lopez-Portillo, J., 1992. Water flows and the dynamics of desert vegetation stripes. In: Hansen, A.J., Di Castri, F. (Eds.), Landscape Boundaries. Consequences for Biotic Diversity and Ecological Flows, Chap. 16. Ecological Studies 92. Springer-Verlag, New York, pp. 327–345.

Couteron, P., 1997. Sécheresse et hétérogénéité spatiale de paysages végétaux soudano-sahéliens: exemple au nord-ouest du Burkina Faso. In: d'Herbès, J.-M., Ambouta, J.-M.K., Peltier, R. (Eds.), Fonctionnement et Gestion des Écosystèmes Forestiers Contractés Sahéliens. John Libbey Eurotext, Paris, pp. 69–79.

Couteron, P., Kokou, K., 1997. Woody vegetation spatial patterns in a semi-arid savanna of Burkina Faso, west Africa. Plant Ecology 132, 211–227.

Couteron, P., Mahamane, A., Ouedraogo, P., 1996. Analyse de la structure de peuplements ligneux dans un 'fourré tigré' au nord Yatenga (Burkina Faso). Etat actuel et conséquences évolutives. Annales des Sciences Forestières 53, 867–884.

Delhoume, J.P , 1995. Fonctionnement hydro-pédologique d'une toposéquence de sols en milieu aride (Réserve de la Biosphère de Mapimi, Nord-Mexique). PhD Thesis, Université de Poitiers, France.

d'Herbès, J.M., Valentin, C., 1997. Land surface conditions of the Niamey region, Niger: ecological and hydrological implications. Journal of Hydrology 188 to 189, 18–42.

d'Herbès, J.M., Ambouta, J.M.K., Peltier, R. (Eds.), 1997. Fonctionnement et Gestion des Écosystèmes Forestiers Contractés Sahéliens. John Libbey Eurotext, Paris, 274 pp.

d'Herbès, J.M., Valentin, C., Thiéry, J., 1997. La brousse tigrée au Niger: synthèse des connaissances acquises. Hypothèses sur la genèse et les facteurs déterminant les différentes structures contractées. In: d'Herbès, J.M., Ambouta, J.M.K., Peltier, R. (Eds.), Fonctionnement et Gestion des Écosystèmes Forestiers Contractés Sahéliens. John Libbey Eurotext, Paris, pp. 120–131.

Drees, L.R., Manu, A., Wilding, L.P., 1993. Characteristics of aeolian dusts in Niger, West Africa. Geoderma 59, 213–233.

Dunkerley, D.L., Brown, K.J., 1995. Runoff and runon areas in a patterned chenopod shrubland, arid western New South Wales, Australia: characteristics and origin. Journal of Arid Environments 30, 41–55.

Dunkerley, D., Brown, K., 1999. Banded vegetation near Broken Hill, Australia: significance of surface roughness and soil physical properties. Catena 37, 75–88.

Eddy, J., Humphreys, G.S., Hart, D.M., Mitchell, P.B., Fanning, P.C., 1999. Vegetation arcs and litter dams: similarities and differences. Catena 37, 57–73.

Eldridge, D.J., Greene, R.S.B., 1994. Microbiotic soil crusts: a review of their roles in soil and ecological processes in the rangelands of Australia. Australian Journal of Soil.

Galle, S., Seghieri, J., Mounkaïla, H., 1997. Fonctionnement hydrique et biologique de la brousse tigrée nigérienne à l'échelle locale. In. d'Herbès, J.-M., Ambouta, J.-M.K., Peltier, R. (Eds.), Fonctionnement et Gestion des Écosystèmes Forestiers Contractés Sahéliens. John Libbey Eurotext, Paris, pp. 131–152.

Galle, S., Ehrmann, M., Peugeot, 1999. Water balance on a banded vegetation pattern. The case of the tiger bush in western Niger. Catena 37, 197–216.

Gilliland, H.B., 1952. The vegetation of eastern British Somaliland. Journal of Ecology 40, 91–124.

Greene, R.S.B., 1992. Soil physical properties of three geomorphic zones in a semi-arid mulga woodland. Australian Journal of Soil Research 30 (1), 55–69.

Greene, R.S.B., 1993. Infiltration measurements in the semi-arid woodland of eastern Australia—a comparison of methods. Proceedings of the XVII International Grassland Congress. Palmerston North, New Zealand, pp. 79–80.

Greene, R.S.B., Sawtell, G.R., 1992. A collection system for measuring runoff and soil erosion with a mobile rainfall simulator on crusted and stony red earth soils. Australian Journal of Soil Research 30, 457–463.

Greene, R.S.B., Kinnell, P.I.A., Wood, J.T., 1994. Role of plant cover and stock trampling on runoff and soil erosion from semi-arid wooded rangelands. Australian Journal of Soil Research 32, 953, 973.

Greenwood, J.E.G.W., 1957 The development of vegetation patterns in Somaliland Protectorate. Geographic Journal 123, 465–473.

Greig-Smith, P., 1979. Patterns in vegetation. Journal of Ecology 67, 755–779.

Grove, A.F., 1957. Patterned ground in northern Nigeria. Geographic Journal 123, 271–274.

Guillaume, K., Huard, M., Mariotti, A., Abbadie, L., in press a. ^{13}C natural abundance in plant and soil organic matter in tiger bush, Niamey, Niger. Ecology.

Guillaume, K., Abbadie, L., Mariotti, A., Nacro, H., in press b. Soil organic matter dynamics in tiger bush, Niamey, Niger. Acta Oecologica.

Hemming, C.F., 1965. Vegetation arcs in Somaliland. Journal of Ecology 53, 57–67.

Hiernaux, P., Gérard, B., in press. Does patchiness increase vegetation productivity, biodiversity and stability? The case of 'Brousse Tigrée' in the Sahel. Acta Oecologica.

Hill, M.O., 1973. Diversity and evenness: a unifying notation and its consequences. Ecology 54 (2), 427–432.

Ichaou, A., d'Herbès, J.-M., 1997. Productivité comparée des formations structurées et non structurées dans le Sahel nigérien: conséquences pour la gestion forestière. In: d'Herbès, J.-M., Ambouta, J.-M.K., Peltier, R. (Eds.), Fonctionnement et Gestion des Écosystèmes Forestiers Contractés Sahéliens. John Libbey Eurotext, Paris, pp. 119–130.

Ives, R., 1946 Desert riples. American Journal of Science 244, 492–501.

Janeau, J.L., Mauchamp, A., Tarin, G., 1999. The soil surface characteristics of vegetation stripes in Northern Mexico and their influences on the system hydrodynamics. Catena 37, 165–173.

Kohyama, T., 1988. Etiology of 'Shigamare' dieback and regeneration in subalpine Abies forests of Japan. GeoJournal 17, 201–209.

Lavee, H., Imeson, A.C., Sarah, P., 1998. The impact of climate change on geomorphology and desertification along a Mediterranean–arid transect. Land Degradation and Development 9, 407–422.

Leprun, J.-C., 1992. Etude de quelques brousses tigrées sahéliennes: structure, dynamique, Ecologie. In: Le Floc'h, E., Grouzis, M., Cornet, A., Bille, J.C. (Eds.), L'Aridité, une Contrainte au Développement. Editions de l'ORSTOM, Paris, pp. 221–244.

Leprun, J.-C., 1999. The influences of ecological factors on tiger bush and dotted bush patterns along a gradient from Mali to northern Burkina Faso. Catena 37, 25–44.

Litchfield, W.H., Mabbut, J A., 1962. Hardpan in soils of semi-arid western Australia. Journal of Soil Science 13, 148–159.

Ludwig, J.A., Tongway, D.J., 1995. Spatial organisation of landscapes and its function in semi-arid woodlands, Australia. Landscape Ecology 1, 209–215.

Ludwig, J.A., Tongway, D.J., Marsden, S.G., 1994. A flow–filter model for simulating the conservation of

limited resources in spatially heterogeneous semi-arid landscapes. Pacific Conservation Biology 1, 209–213.

Ludwig, J.A., Tongway, D.J., Mardsen, S.G., 1999. Stripes, strands or stipples: modelling the influence of three landscape banding patterns on resource capture and productivity in semi-arid woodlands. Australia. Catena 37, 257–273.

Mabbut, J.A., Fanning, P.C., 1987. Vegetation banding in arid western Australia. Journal of Arid Environments 12, 41–59.

Mac Donald, I.A.W., 1978. Pattern and process in semi-arid grassveld in Rhodesia. Proc. Grassland Soc. South Africa 13, 103–109.

MacDonald, B.C.T., Melville, M.D., White, I., 1999. The distribution of soluble cations within a patterned ground gilgai complex, western New South Wales. Australia. Catena 37, 89–105.

MacFayden, W.A., 1950. Vegetation patterns in British Somalilands. Nature 165, 121.

MacMahon, J.A., Shimpf, D.J, 1981. Water as a factor in the biology of North American desert plants. In: Evans, D.D., Thames, J.L. (Eds.), Water in Desert Ecosystems. IBP, 11, pp. 114–171.

Malam Issa, O., Trichet, J., Defarge, C., Couté, A., Valentin, C., 1999. Morphology and microstructure of soil microbiotic crusts on a tiger bush sequence Niger, Sahel. Catena 37, 175–196.

Mauchamp, A., 1992. L'hétérogénéité spatiale, sa dynamique et ses implications dans une mosaïque de végétation en zone aride. PhD Thesis, Univ. de Montpellier II, France.

Mauchamp, A., Janeau, J.L., 1993. Water funneling by the crown of Flourensia cernua, a Chihuahuan Desert shrub. Journal of Arid Environments 25, 299–306.

Mauchamp, A., Rambal, S., Lepart, J., 1994. Simulating the dynamics of a vegetation mosaic: a spatialized functional model. Ecological Modelling 71, 107–130.

Montaña, C., 1992. The colonization of bare areas in two-phase mosaics of an arid ecosystem. Journal of Ecology 80, 315–327.

Montaña, C., Lopez-Portillo, J., Mauchamp, A., 1990. The response of two woody species to the conditions created by a shifting ecotone in an arid ecosystem. Journal of Ecology 78, 789–798.

Morrison, C.G.T., Hoyle, A.C., Hope-Simpson, J.F., 1948. Tropical soil–vegetation catenas and mosaics: a study in the south western part of the Anglo-Egyptian Sudan. Journal of Ecology 36, 1–84.

Mougenot, B., Hamani, S., 1997. Les possibilités de classification des formations contractées à partir de la télédétection aérienne et satellitaire. Exemple dans l'ouest nigérien. In: d'Herbès, J.M., Ambouta, J.M.K., Peltier, R. (Eds.), Fonctionnement et Gestion des Écosystèmes Forestiers Contractés Sahéliens. John Libbey Eurotext, Paris, pp. 59–68.

Noy-Meir, I., 1973. Desert ecosystems: environment and producers. Annual Review of Ecology and Systematics 4, 25–51.

Orr, B., 1995. Natural forest management in Sahelian ecosystems of southern Niger. Journal of Arid Environments 30, 129–142.

Ouédraogo, P., Lepage, M., 1997. Rôle des termitières de Macrotermes subhyalinus Rambur dans une brousse tigrée (Yatenga, Burkina Faso). In: d'Herbès, J.-M., Ambouta, J.-M.K., Peltier, R. (Eds.), Fonctionnement et Gestion des Écosystèmes Forestiers Contractés Sahéliens. John Libbey Eurotext, Paris, pp. 81–94.

Peltier, R., Lawali, A.M., Montagne, P., 1994a. Aménagement villageois des brousses tachetées au Niger. Bois et Forêts des Tropiques 242, 59–76.

Peltier, R., Lawali, A.M., Montagne, P., 1994b. Aménagement villageois des brousses tachetées au Niger. Bois et Forêts des Tropiques 243, 5–24.

Poesen, J., Boardman, J., Wilcox, B., Valentin, C., 1996. Soil erosion monitoring and experimentation for global change studies. Journal of Soil and Water Conservation 51 (5), 386–390.

Puigdefabregas, J., Sanchez, G., 1996. Geomorphological implications of vegetation patchiness on semi-arid slopes. In: Anderson, M.G., Brooks, S.M. (Eds.), Advance in Hillslope Processes, Vol. 2 Wiley, Chichester, pp. 1027–1060.

Puigdefabregas, J., Gallart, F., Bianciotto, O., Allogia, M., del Barrio, G., in press. Banded vegetation patterning in a sub-Antarctic forest of Tierra del Fuego, as an outcome of the interaction between wind and tree growth. Acta Oecologica.

Ruxton, B.P., Berry, L., 1960. The Butana grass patterns. Journal of Soil Science 11, 61–62.

Sato, K., Iwasa, Y., 1993. Modeling of wave regeneration in subalpine Abies forests: population dynamics with spatial structure. Ecology 74 (5), 1538–1550.

Seghieri, J., Galle, S., Rajot, J.-L., Ehrmann, M., 1996. Relationships between the soil moisture regime and the growth of the herbaceous plants in a natural vegetation mosaic in Niger. Journal of Arid Environment 36, 87–102.

Serpantié, G., Tezenas du Montcel, L., Valentin, C., 1992. La dynamique des états de surface d'un territoire agro-pastoral soudano-sahélien. Conséquences et propositions. In: Le Floc'h, E., Grouzis, M., Cornet, A., Bille, J.C. (Eds.), L'Aridité, une Contrainte au Développement. Editions de l'ORSTOM, Paris, pp. 419–447.

Slatyer, R O., 1961. Methodology of a water balance study conducted on a desert woodland (*Acacia aneura* F. Muell.) community in central Australia. In Plant–Water Relationships in Arid and Semi-Arid Conditions. Proc. of the Madrid symposium, UNESCO Arid Zone Research, Vol. 16, pp. 15–25.

Sprugel, D.G., 1976. Dynamic structure of wave regenerated *Abies balsamea* forests in the northeastern United States. Journal of Ecology 64, 889–911.

Sprugel, D.G , Bormann, F.H., 1981. Natural disturbance and the steady state in high altitude balsam fir forests. Science 211, 390–393.

Thiéry, J., d'Herbès, J.-M., Valentin, C., 1995. A model for simulating the genesis of banded patterns in Niger. Journal of Ecology 83, 497–507.

Thiéry, J.-M., d'Herbès, J.-M., Valentin, C., 1996. Un modèle simplifié de gestion des écosystèmes forestiers contractés sahéliens. In: Blasco, F. (Ed), Tendances Nouvelles en Modélisation pour l'Environnement. Elsevier, Paris, pp. 111–116.

Tongway, D.J., Ludwig, J.A., 1989. Mulga log mounds: fertile patches in the semi-arid woodlands of eastern Australia. Australian Journal of Ecology 14, 263–268.

Tongway, D.J., Ludwig, J.A., 1990. Vegetation and soil patterning in semi-arid mulga lands of eastern Australia. Australian Journal of Ecology 15, 23–24.

Tongway, D.J., Ludwig, J.A., 1994. Small-scale resource heterogeneity in semi-arid landscapes. Pacific Conservation Biology 1, 201–208.

Torrekens, P . J. Brouwer, Hiernaux, P., 1997. Evolution de la végétation spontanée sur plateaux latéritiques traités par des travaux anti-érosifs dans le departement de Dosso, Niger. In: d'Herbès, J.-M., Ambouta, J.-M K., Peltier, R. (Eds.), Fonctionnement et Gestion des Écosystèmes Forestiers Contractés Sahéliens John Libbey Eurotext, Paris, pp. 235–246.

Valentin, C., Bresson, L.M., 1992. Morphology, genesis and classification of soil crusts in loamy and sandy soils. Geoderma 55, 225–245.

Valentin, C., Casenave, A., 1992. Infiltration into sealed soils as influenced by gravel cover. Soil Science Society of America Journal 56, 1167–1673.

Valentin, C., d'Herbès, J.M., 1999 Niger tiger bush as a natural water harvesting system. Catena 37, 231–256

Van der Meulen, F., Morris, J.W., 1979. Striped vegetation patterns in a transvaal savanna. Geo-Eco-Trop 3 (4), 253–266.

Vandervaere, J.-P., Peugeot, C., Angulo Jaramillo, R., Vauclin, M., Lebel, T., 1997. Estimating hydraulic conductivity of crusted soils by using disc infiltrometers and micro-tensiometers. Journal of Hydrology 188 to 189 (1 to 4), 203–223.

Vesey-Fitzgerald, D.F , 1957. The vegetation of the Red Sea coast north of Jedda, Saudi Arabia. Journal of Ecology 45, 547–562

Wallace, J.S., Holwill, C.J , 1997. Soil evaporation from tiger-bush in southwest Niger. Journal of Hydrology 188 to 189, 43–73

Warren, A., 1973. Some vegetation patterns in the Republic of the Sudan—a discussion. Geoderma 9, 75–78.

White, L.P., 1969. Vegetation arcs in Jordan. Journal of Ecology 57, 461–464.

White, L.P., 1970. Brousse tigrée patterns in southern Niger Journal of Ecology 58, 549–553.

White, L.P., 1971. Vegetation stripes on sheet wash surfaces. Journal of Ecology 59 (2), 615–622.

Wickens, G.E., Collier, F.W., 1971. Some vegetation patterns in the Republic of the Sudan. Geoderma 6, 43–59.

Worral, G.A., 1959. The Butana grass patterns. Journal of Soil Science 10, 34–53.

Worral, G.A., 1960. Patchiness in vegetation in the northern Sudan. Journal of Ecology 48, 107–117.

Zonneveld, I., 1999. A geomorphological based banded ('tiger') pattern related to former dune fields in Sokoto, northern Nigeria Catena 37, 45–56.

The influences of ecological factors on tiger bush and dotted bush patterns along a gradient from Mali to northern Burkina Faso

Jean Claude Leprun *

ORSTOM, BP 5045, 34032 Montpellier Cedex, France

Abstract

Seven catenas across contracted vegetation patterns, including tiger bush and dotted bush, were studied in the Gourma region in Mali and in northern Burkina Faso (mean annual rainfall 200–550 mm). The tiger bush encompasses an alternate succession of bands oriented nearly perpendicularly to the wind direction NE–SW: sandy grassy microdune, sloped band of bare crusted ground and woody depressive band. A similar succession, without wind orientation, is found for the dotted bush. In this region, tiger bush develops under specific conditions: (1) same orientation but opposite direction of wind and slope, (2) sedimentary and metamorphic rocks (sandstone and schist ironcrust), (3) shallow (< 1 m) and impervious soils. Under such circumstances, the dynamics of banded patterns result from alternate and successive action of water and wind erosion. Field evidences showed that vegetation bands migrate upwards with a velocity of 0.2–0.7 m yr^{-1}. © 1999 Elsevier Science B.V. All rights reserved.

Keywords: Vegetation pattern; Catena; Mali; Burkina Faso

1. Introduction

Clos-Arceduc (1956) called 'brousse tigrée' (in English—tiger bush) the banded vegetation patterns he observed in Sahelian areas because the alternation of dark wooded bands and bare light bands was similar on aerial photographs to the fur of a tiger. Since then, many other studies have been devoted to the tiger bush in Africa, including Clos-Arceduc (1956), Audry and Rosseti (1962), Boaler and Hodge (1962), Gallais

---

(1963), Boulet et al. (1964), Heming (1970), White (1970), Wickens and Collier (1971), Janke (1976), Leprun (1978, 1979, 1983), Ambouta (1984). Updates of a former research (Leprun, 1992), as well as recent field studies in Mauritania (Gravier, 1993), in Burkina Faso (Serpantié et al., 1992; Couteron and Serpantié, 1995), in Niger (Galle and Peugeot, 1993; Seghieri et al., 1994) reinvigorated the debate on the origin of these patterns (Thiéry et al., 1995) and their main driving forces. In particular, most of these studies emphasised the role of overland flow in the development and maintenance of vegetated bands perpendicular to the slope.

The objectives of this work were: (1) to estimate the respective impact of wind and topography upon the occurrence of tiger bush patterns, (2) to assess the upward migration of the vegetation bands.
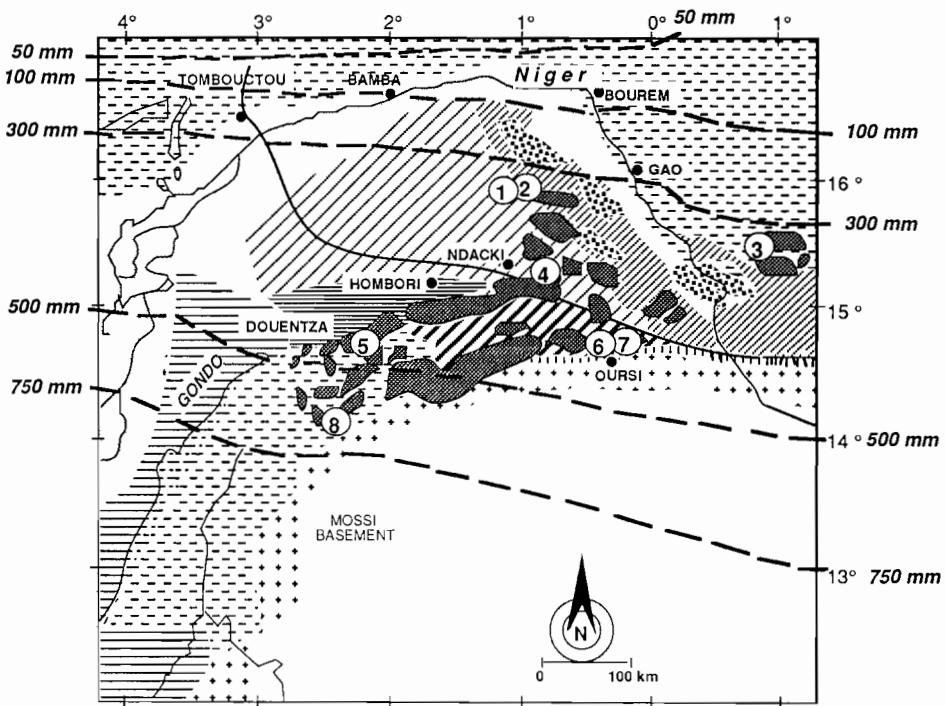
Fig 1. Location of the studied catenas and geological map. Precambrian: (1) basement; (2) Bourré granite Paleozoic: (3) Firgoun sandstone; (4) Labezanga series (shist); (5) Ydouban group (shist); (6) Hombori–Douentza formation (sandstone), (7) Bandiagara–Koutiala group (sandstone) Cenozoic: (8) Continental terminal (sandstone). Quaternary (9) fluvial deposits. (10) Tiger bush patterns. (11) Hombori–Goundam threshold; (12) isohyets, (13) studied catenas (1–2) GOSII and GOS III; (3) ANS; (4) NDA; (5) KER; (6–7) ZAM I and ZAM II; (8) TEN)

Table 1

Physicochemical characteristics of the surface layer of the soils of the studied catenas

	Clays (> 2 μm)	Silt (2–50 μm)	Sand (50–2000 μm)	pH	Organic matter (%)	N (%)	P (%)	S (m.e/100 g)	CEC (m.e/100 g)
Microdune									
GOS 20	1.4	2.4	96.1	6.8	0.1	0.18	0.16	0.86	0.10
GOS 34	2.7	4.0	92.3	7.6	0.2	0.22	0.27	1.52	1.73
ANS 4	5.1	3.6	90.7	7.8	1.0	0.33	0.20	2.59	9.70
NDA 3	12.4	21.3	67.8	6.5	0.7	0.56	0.22	3.33	6.61
KER 2	13.8	9.9	75.4	4.9	0.6	0.38	0.23	0.64	5.82
TEN 3	6.1	11.3	77.4	6.7	1.6	0.69	0.21	3.01	6.10
Bare ground band									
GOS 24	19.7	31.9	47.0	6.7	0.1	0.41	0.25	3.82	4 04
GOS 32	21.4	38.7	38.3	7.2	0.6	0.58	0.51	5.85	4.98
ANS 2	5.8	30.3	62.7	7.3	1.1	0.52	0.60	3.65	4.10
NDA 2	31.6	31.2	36.5	7.2	1.0	0.82	0.76	15.42	15.47
KER 3	23.5	13.4	63.2	5.0	0.5	0.39	0.31	1.63	6.92
ZAM 2	9.9	15.9	69.4	5.2	0.5	0.26	0.37	0.83	1.03
TEN 2	32.6	25.7	43.4	5.6	2.0	0.67	0.40	3.40	15.30
Wooded band									
GOS 29	34.5	40.7	21.7	6.2	1.1	1.25	0.47	4.45	8.82
GOS 36	21.3	18.7	59.0	6.1	3.0	1.61	0.66	7.28	15.30
ANS 3	8.6	20.1	71.9	7.6	1.5	0.60	0.51	4.75	7.60
NDA 1	23.3	29.2	46.4	7.6	2.9	1.88	0.60	14.93	16 62
KER 4	35.2	13.2	51.0	5.0	0.8	0.63	0.49	2.50	13 38
ZAM 4	23.5	18.1	55.1	6.9	1.2	0.82	0.60	4.00	8 16
TEN 1	24.3	30.0	32.4	5.5	4.8	1.77	0.52	5.01	13 3

Table 2
Main characteristics of the selected catenas

Name and location	Latitude/longitude[a]	MAR[b] (mm)	Bedrock	Direction[c]	Height (m) and slope (%)[d]	Distance[e] (m)	Pits[f]
GOS II 17.5 km from Gossi to Gao	15°49'00"N, 1°17'10"W	200	Precambrian argillaceous schist of Ydouban (Reichelt, 1972)	NE–SW	1.3 m, 2.1%	60	16
GOS III 2.6 km from Gossi to Hombori,	15°16'10"N, 1°10'40"W	200	Precambrian fine siliceous and ferruginous schist of Ydouban	NNE–SSW	4.05 m, 5.2%	78	10
ANS 110 km from Amsongo to Menaka	15°53'30"N, 1°35'15"W	225	ironcrust developed on Tertiary argillaceous sandstone formations of Continental terminal sandstone	NNW–SSE	2.25 m, 1 3%	171	4
NDA 43 km from Gossi, to N'Daki,	15°34'40"N, 1°05'00"W	300	Precambrian argillaceous schist of Ydouban	ENE–WSW	1.5 m, 1.9%	78	4
KER near Kerano, south of the Hombori–Douentza trail	14°58'40"N, 2°39'30"W	450	ironcrust on micaceous schist of Ydouban	NNE–SSW	1.65 m, 0.9%	185	4
ZAM I 11 km from Oursi	14°46'20"N, 0°30'10"W	450	ironcrust on Tertiary argillaceous sandstone of Continental terminal	NNE–SSW	0.6 m, 0.8%	70	4
ZAM II 11 km from Oursi	14°46'20"N, 0°30'10"W	450	ironcrust on Tertiary argillaceous sandstone of Continental terminal	NNE–SSW	0.85 m, 0.6%	140	5
TEN	15°25'30"N 2°36'00"W	550	iron-crusted CT sandstone	NNW–SSE	1.35 m, 1.3%	250	4

[a]Geographic coordinates, latitude and longitude.
[b]Mean annual rainfall.
[c]Direction of the catena.
[d]Height (m) and slope (%) between the highest and the lowest point of the catena.
[e]Distance between two successive wooded bands.
[f]Number of pedological pits.

2. Material and methods

2.1. The study area

The study area (Fig. 1) ranges from lat 16°N in the Gourma region in Mali with 200 mm annual rainfall, to lat 14°30′N with 500 mm in the north of Burkina Faso. Scarce but heavy showers occur from July to October. The average temperature is 28°C in the north and 31°C in the south, and the average minima are 12°C in the north and 17°C in the south. The bedrock in Burkina Faso consists of the granito-gneissic Precambrian shield in Burkina Faso, and shale and schist in the Gourma region. The shield is overlaid by tertiary argillaceaous sandstone formations referred to as Continental terminal and by a succession of sandy dunes, from 40 000 years BP (Inchirian and Ogolian) to nowadays.

2.2. Field studies and laboratory analyses

Eight catenas have been selected along the climatic gradient (Fig. 1). Their study included topographic measurements using a topometer (accuracy 1 mm), vegetation
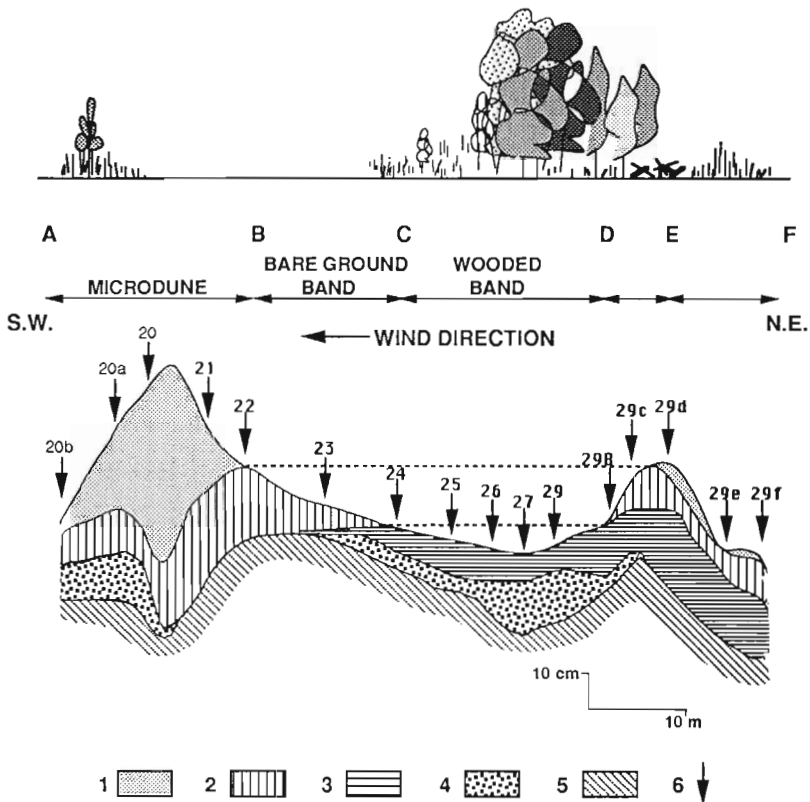
Fig. 2. Cross section of the catena GOS II. (1) Sand, (2) sandy loam, (3) silty clay, (4) ferruginous nodules, (5) schist, (6) soil profile.

(structure, species and sociability) and soil (description of profiles). Soil samples were collected to assess grain size distribution, pH, organic matter content, N, P, S and CEC (Table 1). Table 2 presents the main characters of the selected catenas.

To assess a possible migration of the bands, several cemented benchmarks with metallic axis deeply embedded in the soil have been installed along the catena GOS II and located with reference to fixed points (big trees, big termite mounds). The distance of these benchmarks to the vegetation limits was monitored over a period of 4 years. Moreover, migration of bands was also assessed as referred to two astronomical benchmarks of IGN (National Geographic Institute) in 1955 and 1996. One of these marks was located south of Hombori (14°59′N; 2°5′W), and the other one near the catena NDA. Moreover, local knowledge of the Touareg population was collected.

3. Results

3.1. Main characters of the selected catenas

3.1.1. The catena GOS II (Figs. 2 and 3)

The wooded bands were curved and approximately SE–NW oriented, 10 to 25 m wide and 100 to 600 m long, and usually broader in the middle than at the ends. The bare ground bands were 20 to 200 m wide.

The sequence could be divided into three parts (Figs. 2 and 3).

● *A sandy microdune AB* of 50 cm height, at the highest point of the catena, in discontinuity with a sandy loam layer, partially with fine gravel, and on a fine gravel layer with ferruginous nodules resulting from weathered schist, and on this schist

Fig. 3. Catena GOS II. (1) Woody band, (2) bare crusted ground of the gently sloping band, (3) sandy grassy microdune.

moderately weathered. The sandy loam layer included termite relictual features and root stumps of woody species. This microdune was densely colonised with psamiphilic graminae, green only during the rainy season, mainly *Schoenfeldia gracilis* and *Aristida mutabilis*, and also some rare, young *Acacia* trees 0.30 to 0.40 m.

● *A gently sloping bare ground BC* with structural and erosion crusts (after the classification of Casenave and Valentin, 1989), with a sandy loam to coarse sand texture with scattered ferruginous fine gravel. This bare crusted consisted of the outcropping sandy loam layer containing root stumps. Some eroded and abandoned termite mounds occurred on this section.

● *A lower, densely wooded band CD* with a loamy to clayey sand layer, lying directly on a ferruginous nodules layer derived from the schist. This wooded band consisted of: (1) An upper part or *front* with fine superficial crust of clay (sedimentation crust), colonised with a succession of stripes, few decimetres wide, and composed of hydrophilic graminae *Panicum laetum*, *S. gracilis*, *Eragrostis pilosa* and *Andropogon gayanus*, staying hardy long after the rainy season, and some young woody plants
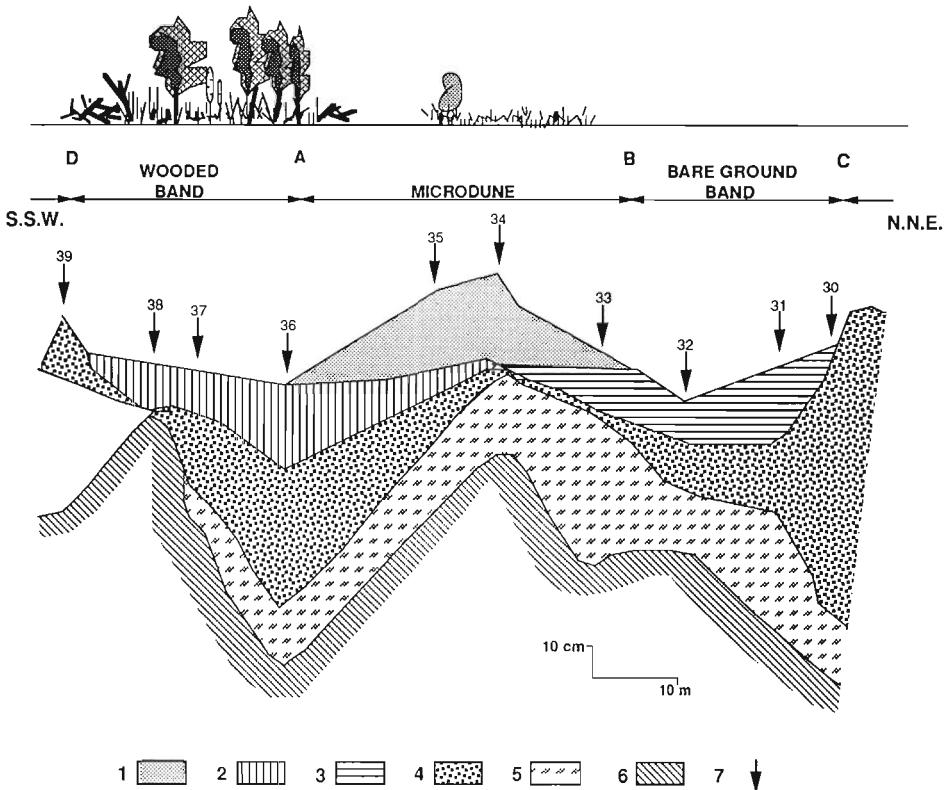
Fig. 4. Cross section of the catena GOS III. (1) Sand, (2) sandy loam, (3) silty clay, (4) ferruginous nodules, (5) weathered schist, (6) schist, (7) soil profile.

(*Acacia* and *Balanites*). (2) A central part DE, or *heart* densely wooded with active termite mounds, 2 to 5 m high *Acacia ehrenbergiana*, *Acacia ataxacantha*, *Acacia laeta* and *Acacia radiana*. The herbaceous layers was mainly composed of *And. gayanus* and a felting of *P. laetum* which was densely exploited by termite galleries. The most developed shrubs were located in the inner part of the heart, whereas the contact with the front was mainly composed of young acacias. (3) A rear part E or *tail* where the same layers as in CD were found except that a thin sandy layer appeared at surface, whereas the ferruginous nodules tended to disappear. This tail (EF) was characterized by a decrease in density and diversity of the woody and herbaceous species, and many dead shrubs and a 1.5 m high partially abandoned *Bellicositermes* termite mound.

During the first rains of the rainy season, violent and strong showers (38.3 mm followed by 68.4 mm the day after) infiltrated in the microdune, ran off the bare ground band and infiltrated very slowly (during 2 days in some locations) near the front where fine particles sedimented.

3.1.2. The catena GOS III (Fig. 4)

Located near GOS II, GOS III has been studied in detail (Leprun, 1992). Main differences with GOS II include the bed rock (siliceaous and ferruginous schist), a shift of the sequence toward the left (compare Figs. 2 and 4) and the invasion of the front of the wooded band AD by the sandy microdune. The wooded band was located in a depression of the bed rock. Nevertheless, the weathered schist layer with ferruginous nodules was exposed at the two extremities of the cross section (Fig. 4).
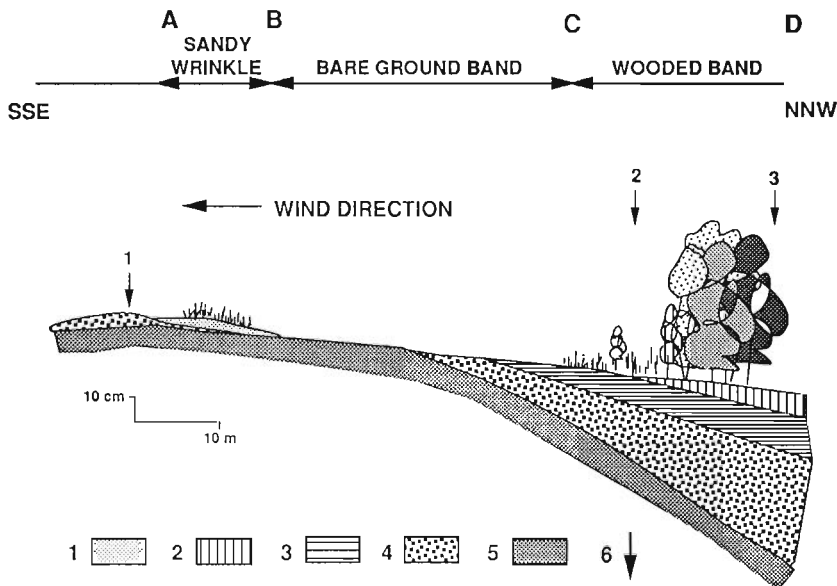
Fig. 5. Cross section of the catena ANS. (1) Sand, (2) sandy loam, (3) silty clay, (4) ferruginous nodules, (5) ironcrust, (6) soil profile.

3.1.3. The catena ANS (Fig. 5)

This was a dotted pattern with more or less annular structures. These wooded dots are located in the hollows and undulations of the clayey sandstone and often grouped around a larger depression, at the centre of which it is not uncommon to find a dried up pond in the middle of dismantled ironcrust blocks. Despite the highly sandy texture of the rock material, there are no microdunes. In the AB portion, only some sandy wrinkles (few centimetres thick) remained, without vegetation above the gravel layer originated from the underlying ironcrust. The bare ground band BC surrounding the wooded dot consisted of exposed iron pan on the upper spots and gravel in the lower patches. The front of the wooded island was colonised by the graminae *A. mutabilis* and *S. gracilis* and by young *Acacia senegalensis* and *Casia tora*, and surrounded by dead trees and scrubs. It encroached on a silty clay layer which thickened towards the centre of the depression, where it passed underneath the sandy loam layer. The densely wooded heart was primarily made up by tall *Commiphora africana*, *Aca. senegalensis*, *Boscia senegalensis*, and *Balanites aegyptica*. The herbaceous layer was dominated by hardy species among which certain are clearly hydrophilic: *Achyranthe aspera*, *Cyperus rotondus*, *P. laetum*, *Tribulus terrestris*, and *And. gayanus*. There were numerous inhabited termite mounds of *Belicositermes* and *Macrotermes*.

Compared to the banded tiger bush, this dotted bush included neither sandy microdune nor tail.

3.1.4. Catena NDA (Fig. 6)

The schist did not exhibit the succession of quartzous and micaceous layers. This bed rock was uniformly covered with a layer of ferruginous nodules which originated from a dismantled ironcrust and continuous parallel layers of fine material. The microdune
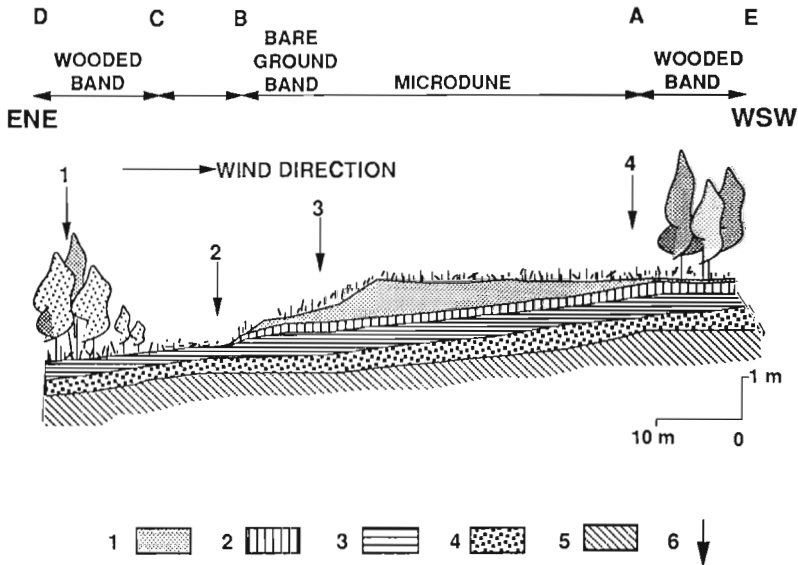
Fig. 6. Cross section of the catena NDA. (1) Sand, (2) sandy loam, (3) silty clay, (4) ferruginous nodules, (5) schist, (6) soil profile.
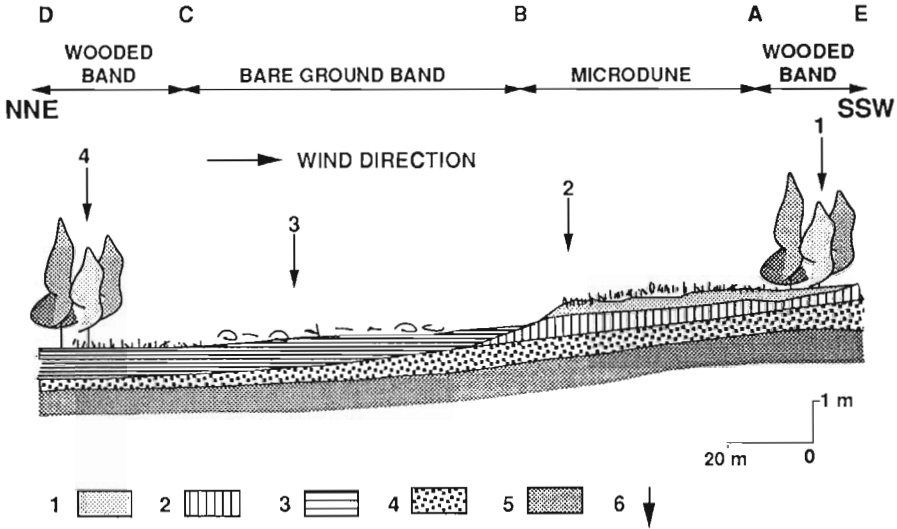
Fig. 7. Cross section of the catena KER. (1) Sand, (2) sandy loam, (3) silty clay, (4) ferruginous nodules, (5) ironcrust, (6) soil profile.

oriented perpendicularly to the dominating NE wind was several decametres long. A dead woody belt separated the narrow bare ground band from the wooded front. This crust of the bare band covered a loamy to silty clay layer, and a truncated sandy loam layer which also occurred under the microdune. The dominant woody species were *Grewia bicolor*, *Grevia flavescens* and *Dichrostachys cinerea*. The graminae colonising the front part of the wooded band were the same as for GOS II and III.
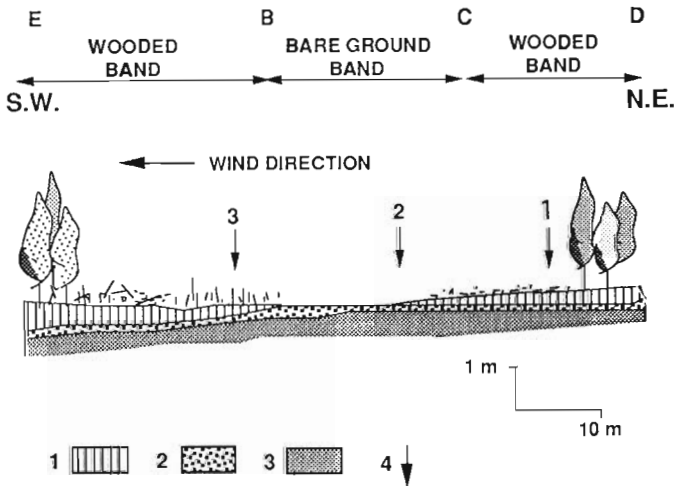
Fig. 8. Cross section of the catena ZAM I. (1) Sandy loam, (2) ferruginous nodules, (3) ironcrust, (6) soil profile.
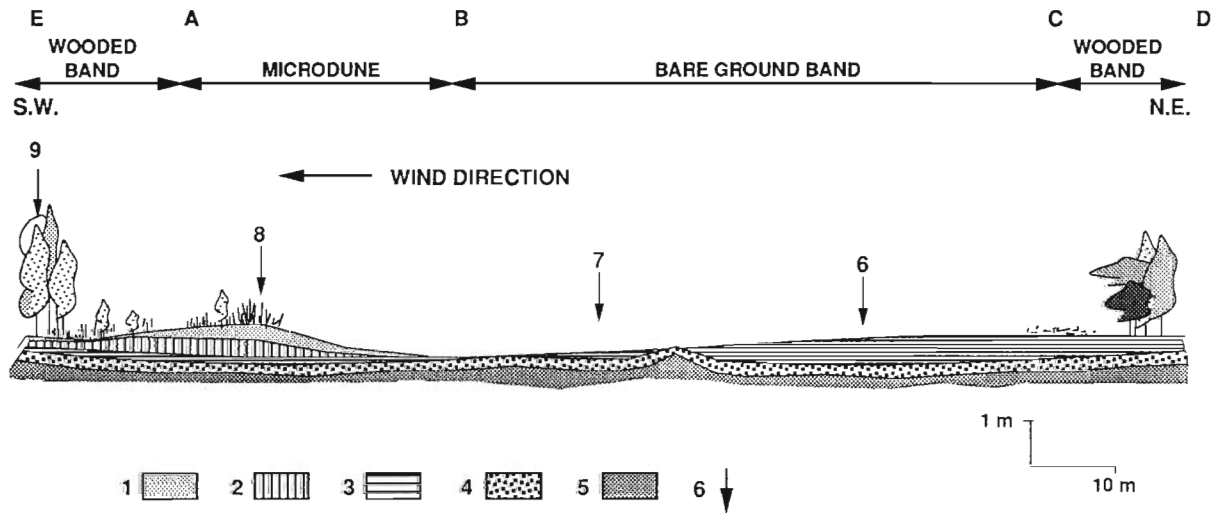
Fig. 9. Cross section of the catena ZAM II. (1) Sand, (2) sandy loam, (3) silty clay, (4) ferruginous nodules, (5) ironcrust, (6) soil profile.

3.1.5. Catena KER (Fig. 7)

The main differences with the previous catena consisted in a uniform development of ironcrust in the schist, a consistent increase in the bands width, and a vegetation dominated by *C. africana* and *Ptercocarpus lucens* for the woody species and *And. gayanus* and *Pennisetum pedicellatum* for the graminae species.

3.1.6. Catena ZAM I and II (Fig. 8 Fig. 9 Fig. 10)

These two catenas, a few hundred metres apart, laying on the same indurated sandstone showed some similarities including: a similar layer with ferruginous nodules overlaying the ironcrust, and a truncated sandy loam layer so that ferruginous nodules
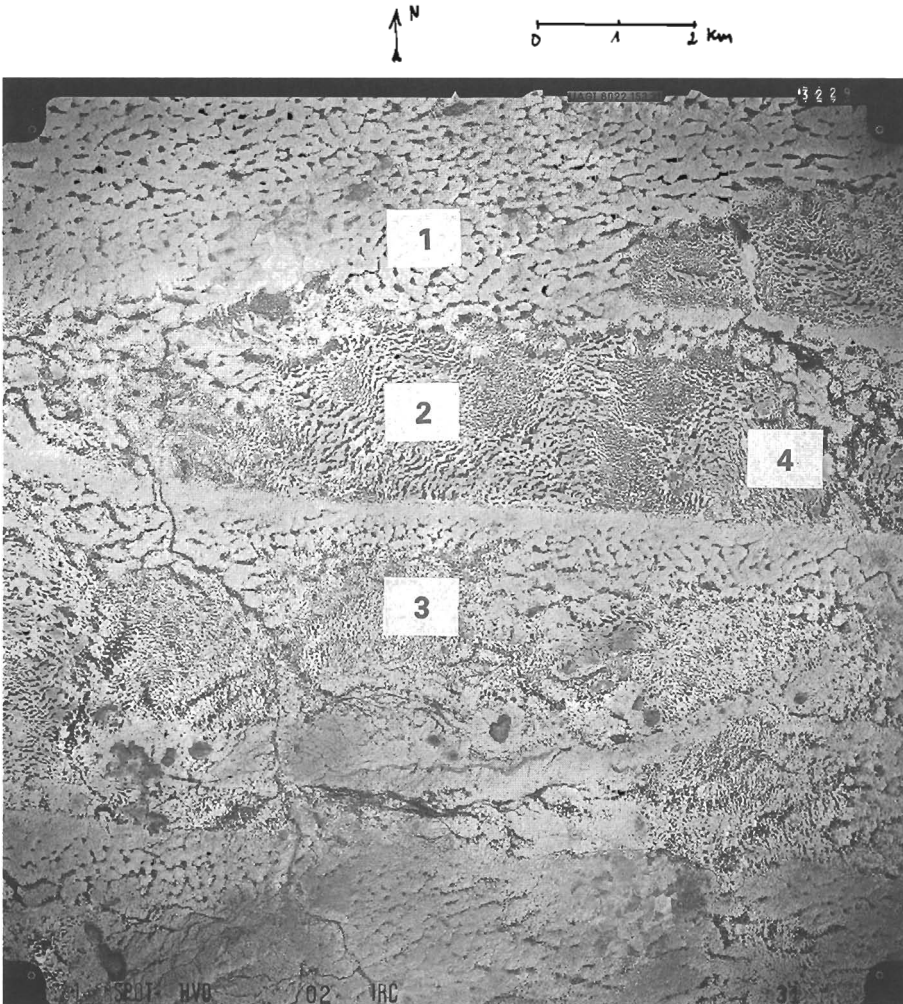
Fig. 10. (1) Dune fields, (2) tiger bush, (3) dotted bush, (4) location of the catenas Zam I and Zam II. SPOT mission, Africa, IGN/SAA, 1982, HVO.

were exposed in the bare ground band, same vegetation as for KER, but *Cenchrus biflorus* occurred in the graminae species, and *Combretum micranthum* in the woody species, and low termite mounds type *Macrotermes* and *Cubitermes*. Nevertheless, these two catenas showed some particularities. The bare ground band could be twice as wide from one to the other catena. The catena ZAM I had neither sandy microdune, nor truncated underlying sandy loam layer, but only a thin sandy wrinkle. The exposure of the nodular ferruginous layer was more important in ZAM I than in ZAM II.

3.1.7. Catena TEN (Fig. 11)

Similar to catena ANS, catena TEN was located in a dotted bush area, due to circular depressions in the Continental terminal sandstone which originated from the local break-downs of the ironcrust. It showed the same organisation as the catena ANS: broad bare ground concentric zones; densely wooded heart, located in the centre of the depression on a thick tropical ferruginous soil, poorly lixiviated and rich in organic matter which is well distributed throughout the profile; extremely small or absent front and tail zones; thin sandy wrinkles; broad bare ground zone located on the ironcrust or the ferruginous nodules. The vegetation was the same than for ZAM (*Com. micranthum* and *Pte. lucens*).

3.2. Migration of the banded patterns

The cemented landmarks with metallic axis indicated an average migration of the stripes of 0.80 m over 4 years. Such movement was more rapid near the microdune than
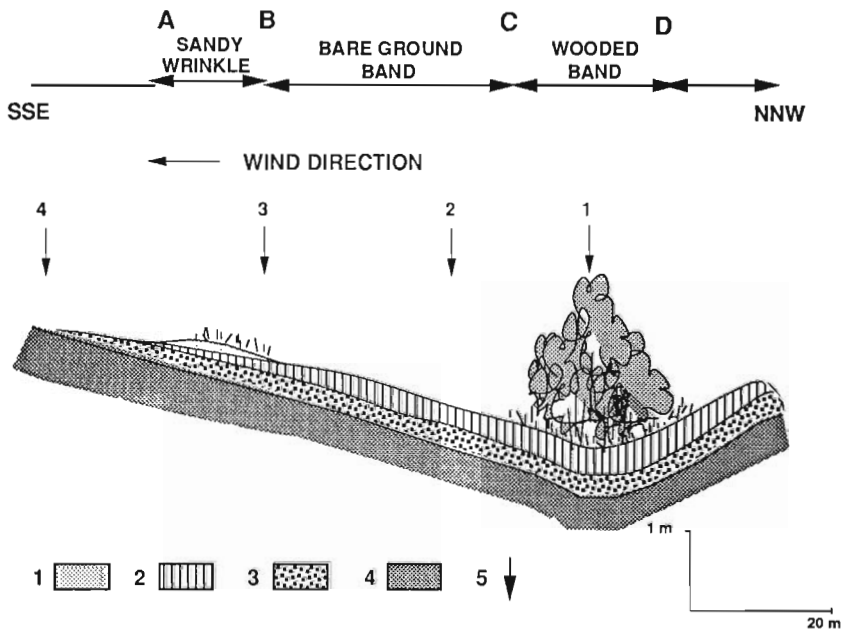
Fig. 11. Cross section of the catena TEN. (1) Sand, (2) sandy loam, (3) ferruginous nodules (5) ironcrust, (6) soil profile.

near the wooded front. It also varied with years, the average migration during a rainy year being two-fold than the one observed during dryer years.

Over a period of 21 years, the mean annual shift as referred to the geographical benchmarks was 0.75 m in the south of Hombori (Tega), and 0.25 m yr^{-1} have been measured near the catena NDA.

The enquiry among the Touareg population confirmed such shifts. Remnants of an ancient pastoral settlement near a termite mound in a wooded band 20 years ago, were now found in the middle of a bare stripe.

4. Discussion

4.1. Comparison of the different ecological factors and components of the contracted formations

4.1.1. Climate

The studied tiger bush, showed more or less the same succession of bare and wooded bands, oriented NE–SW, with annual rainfall ranging from 200 to 550 mm. The two examples of very similar dotted bush formation were located under very different rainfall conditions (ANS under 225 mm and TEN under 550 mm). The dominating wind from the NE was more constant and stronger in the North near Gao, than in the South near Oursi.

4.1.2. Bed-rocks

In most cases, they were more or less iron-crusted sedimentary or metamorphic rocks such as sandstones or schists. The lateritic ironcrust increased and generalised from north to south, as the relief became more tabular (sandstone of the Continental terminal or margin sandstone) or monoclinal (Precambrian schists). The same bed rocks, located under different rainfall conditions exhibited identical sequences of tiger bush (GOS III and KER on schist) or dotted bush (ANS and TEN on iron-crusted sandstone).

4.1.3. Slope gradient

Lithology controlled low slope gradient which decreased from north to south, from 5% on the schist to 0.6% on the iron-crusted sandstone in the case of banded tiger bush (Table 2). On a given bedrock (Continental terminal), higher slope gradient (1.3%, ANS and TEN) was found for dotted bush than for tiger bush (0.6 and 0.8% for Zam II and Zam I, respectively).

4.1.4. Hydrology

All the studied formations were located in endoreic zones where runoff water concentrated in the depressions or the lower points of the topography.

4.1.5. Soil

Because the layers, distinguishable mainly by their texture, were made of different deposited materials, most of the soils were thin, young and poorly differentiated. The soil was thicker only in the depressions (dotted bush ANS and TEN) where it exhibited

a slightly differentiated ferruginous facies or a sub-arid soil facies with gradual transition among some more pedologically differentiated layers. The layers of ferruginous nodules were ubiquitous. They originated from the dismantled ironcrust and were exposed where the overlying fine layers had been removed by erosion. The sandy microdune, always present at the north and the centre of the zone, decreased in the south. It overlaid invariably a sandy loam layer, truncated near the bare ground band or zone and changing to a more silty clay layer downwards. These layers often included decomposed woody roots and remnants of termite nests.

4.1.6. Floristic composition

Although many species were common to some formations, none of the studied formations had strictly the same floristic composition. *Acacia* woody species, *A. mutabilis* and *S. gracilis* dominated in the north, *Com. micranthum, Pte. lucens, And. gayanus, Pen. pedicellatum* and *Cen. biflorus* in the south. Many of the Sahelian species usually common under 500–600 mm rainfall, were found in the contracted formations under 200–300 mm rainfall, near their northern limit.

Interpretation of the catena GOS II.

The evidences of biological activity (termites, root stumps) under the microdune AB indicate that this depleted part of the bed rock had been occupied by a wooded band, probably similar to the one, now located in the CD depression.

This was similar to the mesofauna distribution: the active termite mounds were situated only in the centre of the wooded bands, whereas the big abandoned and dismantling termitarias were in the tail and in some of the widest bare ground bands.

4.2. Dynamic of the studied contracted patterns

The dynamic of the northern tiger bush is suggested by the detailed study of the catena GOS II. During the rainy season, the sheet water erosion which is the most efficient on the BC slope (Fig. 2), removes the superficial material and truncates the sandy loam and partially, the nodular underlying layers. The raindrop impact sorts out the textural fractions of this layer. While the coarser fraction (gravel and coarse sand) stay in place, the finer elements (clay and silt) are removed, transported by the overland flow and accumulated in CD, near the wooded band front. Water penetrates slowly towards the centre of the wooded stripe. During the dry season, the wind from NE removes the sand splashed by the water drops in the bare ground band (structural crust). This sand accumulates in AB, forming a sandy ridge or microdune. During the rainy season, the seeds trapped in the microdune germinate because of the readily infiltrated water into the sand. The graminae and woody seeds, stocked in the finer sediments, near the wooded front, emerge also during the rainy season. Because such processes are repeated every year, more or less intensively, the erosive truncation of the bare ground band moves in the SW direction, following the progression of the microdune. This microdune then invades the tail of the next wooded zone, covering and destroying the woody species (GOS II, in EF Fig. 2 and GOS III in A Fig. 4). The finer elements accumulated downslope of BC fill partially the depression CD. Benefiting from sediments and run-on, the colonisation of the wooded band near the CD front by graminae

and woody seeds, leads to a general shift of the wooded band in the SW direction. As a result of the gradual decrease of the water intake in the centre and peculiarly near the tail, the most hydrophilic species die. This hydrological dynamic explains, thus, the typical dissymmetrical pattern of the tiger bush: including young woody and hydrophilic graminae in the front, mature woody adult plants in the centre and decaying plants in the tail. Such simultaneous migration of the soils due to both water and wind erosion results in a lateral sorting of the textural fractions with sand accumulation in SW and sedimentation of the finer fraction in NE. Ferruginous nodules are not removed and accumulate in the hollows of the bed rock. This may explain why the partially nodular, sandy loam layer that outcrops in CD (upper dotted line from profile 22 to profile 29c, and lower dotted line from profile 24 to profile 29b Fig. 2) is changed into a nodule-free fine silty loam layer. This layer is also partially eroded (partial incisions between profile 24 and 29b IG. 2). As the wooded band migrates, the root stumps of the dead woody and the termite mounds DE are left behind, and gradually invaded by the sand EF of the next advancing bush. The lack of soil moisture, nutrients and shade of the wooded stripe, causes the abandonment of the nest and its gradual collapse due to erosion. Its materials, mainly clay and loam, slakes and forms bare and crusted concentric circles, before being structured again during the next cycle.

In GOS II, the erosion does not reach the nodular layer and the underlying schist, whereas in GOS III the erosion removed this layer in CE and gets near it in BC (profile 32, Fig. 4).

Where the bedrock is the iron-crusted sandstone of Continental terminal (like in ANS or TEN), the nodular layer and ironcrust are often exposed due to water erosion. The finer fraction originated from the dismantled ironcrust sediments in circular lower zones (CD). However, this process is limited due to the low quantity of silt and clay in BC. Similarly, the supply of sand from BC is not sufficient for the microdune to be formed. Because of the predominance of nodules and ironpan, and the subsequent lack of clay, silt and loam which are the agents of the migration, the motor being the water and the wind, the dynamic of the system is stopped. The woody and herbaceous vegetation, and the termite mounds stay in the centre of the depression, and develop in equilibrium. The surrounding front of this vegetation remains steady and exhibits a combination of sprouting, growing plants and decaying plants. The tiger bush with bands submitted to a continuous migration of the soil-vegetation couple is then turned into a fixed dotted bush.

On the iron-crusted schist, under 250 to 450 mm annual rainfall (NDA and KER), similar organisation to the tiger bush in GOS II and III was observed. The layers above the nodular ferruginous layer and the ironcrust are thick enough to prevent the exposure of these lower layers.

Further south, under 450 to 500 mm rainfall, on the iron-crusted sandstone of Continental terminal, the tiger bush still evolves as a result of the progression of the microdune and regression of fine materials where superficial layers are thick enough (ZAM II), but tends to stop where the ironcrust is exposed in the bare ground band BC. Nevertheless, erosion is already reaching the highest points of the bed rock, bringing the ferruginous nodule to out crop in BC (ZAM I). In this case, the sandy microdune is replaced by a sandy film, only colonised by graminae.

The evolution is completely stopped in ANS (Fig. 5) and in TEN (Fig. 11). The iron-crusted sandstone of Continental terminal formation is undulating and dotted with circular depressions, denoting the presence of weak zones where the ironcrust has been dismantled into big blocks, and where water accumulates. Water erosion is limited to the banks of the depressions where sediments accumulate, resulting in a fixed dotted bush.

4.3. Evidences and assessment of the migration of the tiger bush

Two observations suggest the migration bands in the tiger bush.

(1) The occurrence of poorly decomposed plant residues, root stumps and termite nests under the present bare ground bands, where neither living vegetation nor inhabited termite mounds were found. Under Saharo-Sahelian conditions (annual rainfall 200–300 mm), the occurrence of high inhabited termite mounds (*Bellicotermes*) which are common in the southern Sahelian and Sudanian zones, is restricted to the centre of the wooded bands of the tiger bush or in the dotted where sufficient water, shade and food are available for their development and survival. The abandoned and collapsed termite mound of the bare stripes can be therefore considered as remnants of ancient wooded stripes. In the catena GOS II (DE, Fig. 2), one of the termite mounds has been abandoned and eroded owing to the migration of wooded bands to SW and the sandy invasion from the NE.

(2) The absence in the soils of the tiger bush of any typical layers of the adjacent Sahelian soils. The succession of parallel layers made of recent deposits are very different from those of soils formed over long periods. The only pedogenically evolved layers with a vertical and isohumic distribution of soil organic matter occurred in the dotted bush where the absence of migration enabled pedogenic processes (Table 1, ANS and TEN,).

The presumed shift was substantiated by field assessment using landmarks, with a velocity ranging from 0.20 to 0.70 m yr^{-1}. The rate of migration seems to depend more on edaphic conditions than on rainfall since tiger bush patterns occur between 200 and 550 mm in the studied area, and up to 750 mm in Niger. Velocity is reduced in the southern tiger bush to zero where the topography and the exposed nodular layer and the ironpan favour dotted bush.

4.4. Hypothesis on the formation of the tiger bush

Many authors have proposed hypotheses on the formation of the contracted Sahelian formations. Various factors have been put forward including termite activity (Clos-Arceduc, 1956), overgrazing (Boudet, 1972), or a combination of edaphic and climatic factors (Janke, 1976). This last hypothesis, established from observations near Niamey in Niger, is the most complete, and in closest agreement with ours.

A long drought period, as the Sahel suffered in the 70s, may have destroyed most of the vegetation. On the sandy loam substrata, originated from more or less iron-crusted sedimentary or schistose rocks, with a gentle slope due to the monoclinal structure oriented NE–SW (like many geological formations in this area), the thin soils are very prone to erosion. Water erosion affects the bare crusted slopes and sorts out the eroded

particles into textural fractions. The sandy sediments are removed by the wind from NE during the dry season (harmattan) and deposited upslope. A part of the finer particles clogs the pores, seals the surface and hence, decreases infiltration, whilst the other part is removed downslope by overland flow until it reaches a depression, due to the ripples related to the schistosity or the stratification of the bed rock. The accumulation of fine particles and water, in this succession of depressions foster their subsequent colonisation by the vegetation and the soil fauna, especially the termites, and promotes the formation of parallel wooded and bare ground bands. An annual cycle includes a phase of regressive water erosion and downslope sedimentation during the rainy season and a phases of deflation and upslope aeolian deposits during the dry season. This repeated cycle results in an upslope migration of the sandy materials along the slope and favour a constant progress of associated vegetation and fauna. Such dynamic is stopped where the bed rock or the topography of the ironcrust changes (flat thick ergs—sandy surfaces—or regs-pebbly surfaces—in the north, and granitic shield with chaotic relief, and circular depressions in the iron-crusted sandstone of the Continental terminal, in the South), or where the fine overlying materials have been completely eroded leading to the exposure of the ironcrust. The tiger bush is first changed into dotted bush and further into a poor steppic formation, typical of this area.

5. Conclusions

(1) Contracted vegetation patterns in the Sahel, tiger bush and dotted bush, studied along eight detailed catenas are made of the cyclic successions of bands going downslope: (a) a sandy grassy microdune; (b) a bare ground sandy loam crusted gently sloping surface; (c) a densely wooded loam clay sand depression. These bands are submitted to a rapid and continuous shifting dynamic from NE to SW. This is the direction of the dominant wind (harmattan), the orientation of the sandstone, the schist and of the steepest slope.

(2) On the bare ground crusted band, the eroded and sorted out soil particles experience two different processes. The finer, clay and loam, are removed downslope by the overland flow and accumulate in the depressions to form the wooded band where vegetation and fauna subsequently concentrate. The sandy particles are shifted by aeolian deflation and deposited upslope forming a microdune.

(3) The migration velocity varies from 0.20 to 0.75 m yr^{-1}. Further south (annual rainfall > 500 mm), the change in lithology and in surface runoff patterns (from sheet to linear flow) tend to stop the migration of the tiger bush, and to alter it into a dotted bush.

(4) The observations suggest that the formation, development and evolution of these formations result from an the combination of an array of factors: (a) an aggressive contrasted tropical climate, semi-arid Sahelian type, with a permanent wind blowing from NE (harmattan), and an average annual rainfall ranging from 200 to 500 mm, and more (750 mm in Niger); (b) a rocky substratum with a sedimentary or metamorphic petrography (more or less iron-crusted sandstone and clayey schist), with a monoclinal lithology, oriented NE–SW, giving to the bed rock a low and constant slope $< 5\%$; (c) the presence of thin (< 1 m), continuous and fragile soil layers without or with poor pedogenic features; (d) local and regional endoreism.

(5) Petrography seems to be the main limiting factor (Fig. 1) due to: (a) a gently sloping monoclinal lithology oriented NE–SW; (b) to the stratification and the small undulation of the bed rock, that enable water to accumulate in the depressions. The sedimentary origin of the bed rock controls the sandy loamy clay texture of the original weathered materials. In particular, the stratification, oriented perpendicularly to the dominant wind direction and its slope facing the wind control, the process and the direction of the stripe migration.

(6) Under 200 mm, water erosion and runoff are insufficient for the processes to occur. Over 800 mm, the upper limit of the Sahelian climate, superficial flow tends to become linear, hence suppressing the hydrodynamic influence of the bands. Also, despite not being necessary to the formation of the contracted bush, the action of the wind is necessary for its migration.

(7) Even though the tiger bush patterns are natural formations corresponding to Sahelian ecological niches, with bioceonosis of a more humid environment, in a semi-arid environment, they are very fragile ecosystems and their survival depends closely on climatic crises, and on their human corollaries of over-use and destruction.

Acknowledgements

References

Ambouta, K., 1984. Contribution à l'édaphologie de la brousse tigrée de l'ouest Nigérien. Thèse docteur-ingénieur, Univ. Nancy I, 116 pp.

Audry, P., Rosseti, Ch., 1962. Observations sur les sols et la végétation en Mauritanie du sud-est et dur la bordure adjancente du Mali, 1959–1961. FAO, 24067/F/1, Rome.

Boaler, S.B., Hodge, C.A.H., 1962. Vegetation stripes in Somaliland. J. Ecol. 50, 465–474.

Boudet, G., 1972. Désertification de l'Afrique tropicale sèche. Adansonia, sér. 2 12, 505–524.

Boulet, R., Gavaud, M., Bocquier, G., 1964. Etude pédologique du Niger Central. ORSTOM, Dakar, 211 pp

Casenave, A., Valentin, C., 1989. Les états de surface de la zone sahélienne. Influence sur l'infiltration Didactiques ORSTOM, 229 pp.

Clos-Arceduc, M., 1956. Etude sur photographies aériennes d'une formation végétale Sahélienne: la brousse tigrée. Bull IFAN, sér. A 7 (3), 677–684.

Couteron, P., Serpantié, G , 1995. Cartographie d'un couvert végétal Soudano-Sahélien à partir d'images Spot XS. Exemple du Nord-Yatenga (Burkina Faso). Photo-Interprétation 1, 19–24.

Gallais, J., 1963. Pasteurs et paysans du Gourma. La condition Sahélienne. Mém. Centre Et. Géogr. Trop. CNRS, Paris, 239 pp.

Galle, S., Peugeot, C., 1993. Soil water spatial distribution of tiger bush in Niger. AGU meeting, San Fancisco, USA, 6–10 Dec. 1993.

Gravier, M., 1993. Le Tagant entre Sahel et Sahara (Mauritanie). Thèse géographie, Univ. Aix-Marseille, 304 pp.

Heming, C.F., 1970. Vegetation arcs in Somaliland. J. Ecol. 53, 57–67.

Janke, B., 1976. Zum problem der vegetationstreifen (Brousse tigrée) im semiariden Afrika. Geokologische untersuchungen in West-Niger. Die Erde 107, 31–46.

Leprun, J.C , 1978 Etude de l'évolution d'un système d'exploitation sahélien au Mali. Compte rendu de fin
     d'études sur les sols et leur susceptibilité à l'érosion, les terres de cures salées, les formations de 'brousse
     tigrée' dans le Gourma ORSTOM-DGRST, Dakar, 51 pp.

Leprun, J.C., 1979. Rapport scientifique complémentaire de l'A.C C LAT Etude de l'évolution d'un système
     d'exploitation sahélien au Mali. Volet pédologie. ORSTOM-DGRST, Dakar, 27 pp.

Leprun, J.C., 1983. Les sols. Les relations sols-végétation. In. Etude des potentialités pastorales et de leur
     évolution en milieu sahélien au Mali. A.C.C.-G.R I.Z.A.-L A.T., Groupe de Recherches Interdisciplinaires
     en zones arides et Minist. Dével. Rural, Rép. du Mali pp. 19–30, 43–56.

Leprun, J.C , 1992. Les brousses tigrées: structure, dynamique, écologie (Mali et Burkina Faso). In: L'aridité·
     une contrainte au développement. Caractérisation-réponses biologiques-stratégies des sociétés. Didactiques
     ORSTOM, Paris, pp. 221-244.

Reichelt, R., 1972. Géologie du Gourma (Afrique occidentale). Un seuil et bassin du précambrien supérieur, 1
     map 1:500000, Mém. BRGM, 53, 213 pp.

Seghieri, J., Galle, S , Rajot, J L., 1994 La brousse tigrée dans la Sahel Nigérien: étude de la confluctuation
     du stock hydrique et de la végétation annuelle. Journées hydrologiques de l'ORSTOM, 13–14 Sept. 1994,
     in press.

Serpantié, G., Tezenas De Montcel, L., Valentin, C., 1992. La dynamique des états de surface d'un territoire
     agro-pastoral soudano-sahélien In: L'aridité, une contrainte au développement. Didactiques, ORSTOM,
     pp. 419–447.

Thiéry, J.M., D'Herbès, J.-M., Valentin, C., 1995. A model simulating the genesis of banded vegetation
     patterns in Niger. J. Ecol. 83, 497–507.

White, H., 1970. Brousse tigrée patterns in Southern Niger. J. Soil Sci. 58, 549–553.

Wickens, C.E., Collier, F.W., 1971. Some vegetation patterns in the Republic of Sudan Geoderma 6, 43–59.

A geomorphological based banded ('tiger') vegetation pattern related to former dune fields in Sokoto (Northern Nigeria)

Isaak S. Zonneveld [a,b,] *

[a] *Agricultural University Wageningen, Wageningen, Netherlands*
[b] *International Institute for Aerospace Surveys and Earth Sciences, ITC, P.O. Box 6, Enschede 7500 AA, Netherlands*

Abstract

A banded vegetation pattern has been observed on aerial photographs of Sokoto province in Northern Nigeria. It was successfully used as a land mapping characteristic in the soil and vegetation (land unit) reconnaissance survey see FAO (1969) [FAO, 1969. Soils Survey and Land Classification, Soils and Water Resources Survey of the Sokoto Valley (Nigeria). Final report Vol. V, FAO/SF:67/Nr3.], Zonneveld et al. (1971) [Zonneveld, I.S., de Leeuw, P.N., Sombroek, W.G., 1971. An ecological interpretation of aerial photographs in a savanna region in northern Nigeria. Publication of the International Institute for Aerial Survey and Earth Sciences (ITC) Enschede, The Netherlands, 41 pp.]. The banded pattern is visible through vegetation density related to differences in surface hydrology. The latter are caused by variation in soil sealing that is connected with a by sheet erosion (pediplanisation) levelled former early Holocene to late Pleistocene dune landscape (Sangiwa coversand landscape). The difference in sealing is related to a (very small) difference in silt content between the levelled former dunes and the filled in valleys in combination with extreme low organic matter content. The lower silt content in the valley filling is connected with the re-sedimentation process, a feature well known in coversand formation. The sealing is a present day process. Fresh loosened soil material (by ploughing and soil pit digging) is after one rain shower already covered with a sealed crust of several millimetres through which no water penetrates. The orientation of the bands (about NNW–SSE) is perpendicular to the prevailing wind direction (ENE–WSW) during the period of formation of the former dunes. The genesis of this pattern of regional scale appears to be quite different from local scale banded patterns known to us in dry zones in Africa and Asia and described, in the same period of

---

* Corresponding author. Vaarwerkhorst 63, 7531 HL Enschede, Netherlands. Tel.: +31-53-4353-890

our study as 'Brousse tigrée', being moving vegetation arcs related to sheet runoff and by consequence oriented perpendicular to that water flow. © 1999 Elsevier Science B.V. All rights reserved.

1. Introduction

The description and explanation of a banded vegetation pattern that are hereby presented are not the result of a special directed study as an aim in itself, but a byproduct of a large area (reconnaissance) soil and vegetation survey. The latter measures in total about 100 000 km^2 and had to be mapped on scale 1:200 000 by three soil scientists in a little more than 1 year, see FAO (1969), Sombroek and Zonneveld (1971). The 'set up' and argumentation may therefore differ from an independent problem-oriented study. A disadvantage of such a survey-connected study may be that surveys of this kind are strongly directed by time schedules. It is not always possible to investigate any interesting detail beyond the strict required knowledge of the terrain within the aim of the survey. An advantage of being part of such a survey, however, is that besides budgetary aspects, the problem is placed in a clear wide land(scape) ecological context and the description and understanding of it make use of, in fact codevelope, with the findings of geomorphological, geological vegetation, ecological and pedological study in the context of the survey; compare Zonneveld (1995). Airphoto interpretation is, for a main part, posing hypothesis about the character including the genesis of patterns and the field work supplies (beyond the overall landscape ecological evidence provided by the pattern) indispensable extra data to verify or falsify these hypothesis. Interpreting aerial photographs, one uses, besides general landscape ecological knowledge (especially geomorphology and vegetation), essentially the principle of convergence of evidence of image properties. The field work is done on sample sites which are chosen randomly, stratified, on the base of the pattern, as in this case the elements of the described banded and 'supposed' aeolic, fluviatile features. The next data are used for discussing the genesis of the banded pattern. (1) The photo interpretation (done essentially by the surveyors themselves) of the whole area on photographs 1:40 000, (compare Fig. 1). (2) Field data on vegetation and relief collected at several hundreds of stratified random selected sample sites in that part of the area where the banded pattern occurs. Soil descriptions and laboratory analyses from profile pits in approximately 20% of these sites. The others were described by auger sampling only. Laboratory analysis of 83 soil samples were used from the pattern at stake and 151 from related land units required for comparison (see Fig. 2). (3) These data could be compared with descriptions of more than a thousand sample sites in the rest of the 100 000 km^2 area, that all were used for the final soil and vegetation and land(scape) classification. See Zonneveld (1995), also Zonneveld (1988), for the basic aspects of the methodology. For further details about the methods of survey and analysis, refer to FAO (1969) and Sombroek and Zonneveld (1971).
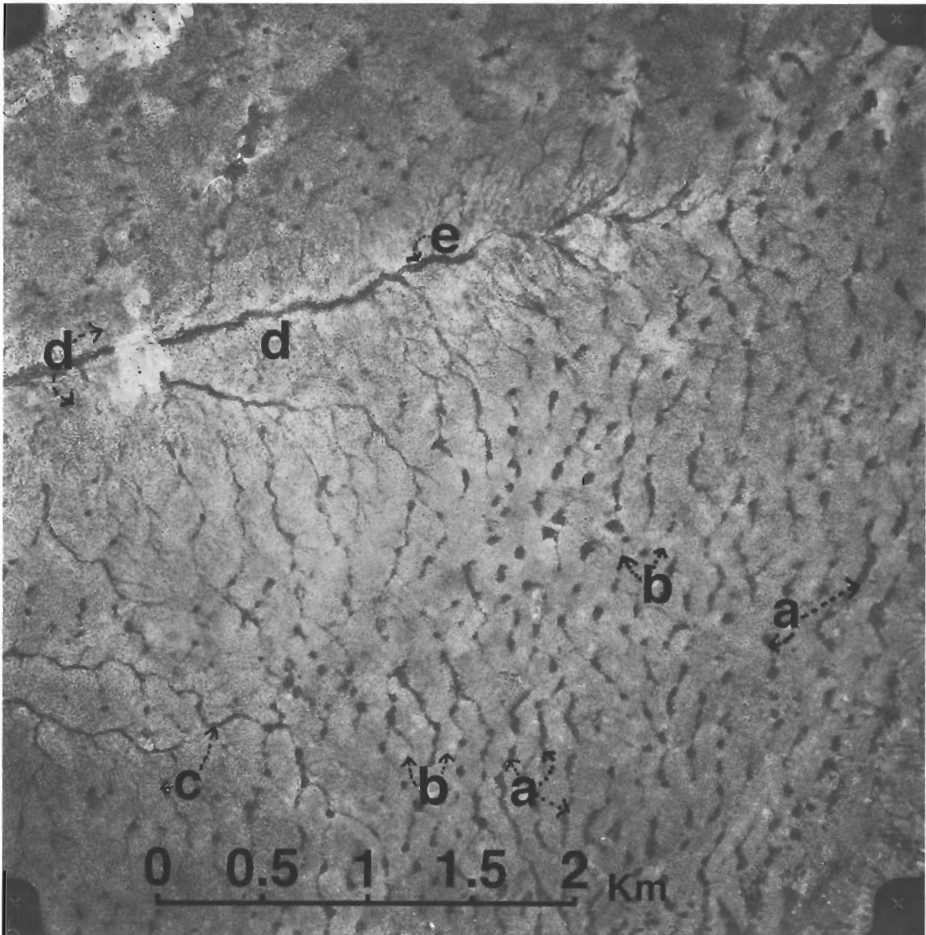
Fig. 1. Aerial photograph of an area in Sokoto province, Northern Nigeria, showing geomorphological induced vegetation patterns on Sangiwa coversand and Turetata washplain deposits. (Reproduction scale somewhat reduced).

Besides the scientific importance of the described and explained phenomena, this study may serve as an example of how patterns on aerial photographs may be used in interpretation of soil and vegetation features and geomorphological processes.

The described banded vegetation pattern was observed on aerial photographs (and could later also be recognized on satellite images) of the Northern part of Sokoto province in Northern Nigeria (see Fig. 1). Because of the obvious resemblance, we called it after the discovery around 1963/1964 'Tiger pattern' (FAO, 1969; Sombroek and Zonneveld, 1971; Zonneveld et al., 1971).

At first glance on the photographs, before the field visit took place, there was no doubt about the aeolic origin as dune fields. Although in those days the geologist who had previously studied the areas (globally and without aerial photographs) had not yet

COMPARISON OF GRAINSIZE DISTRIBUTION
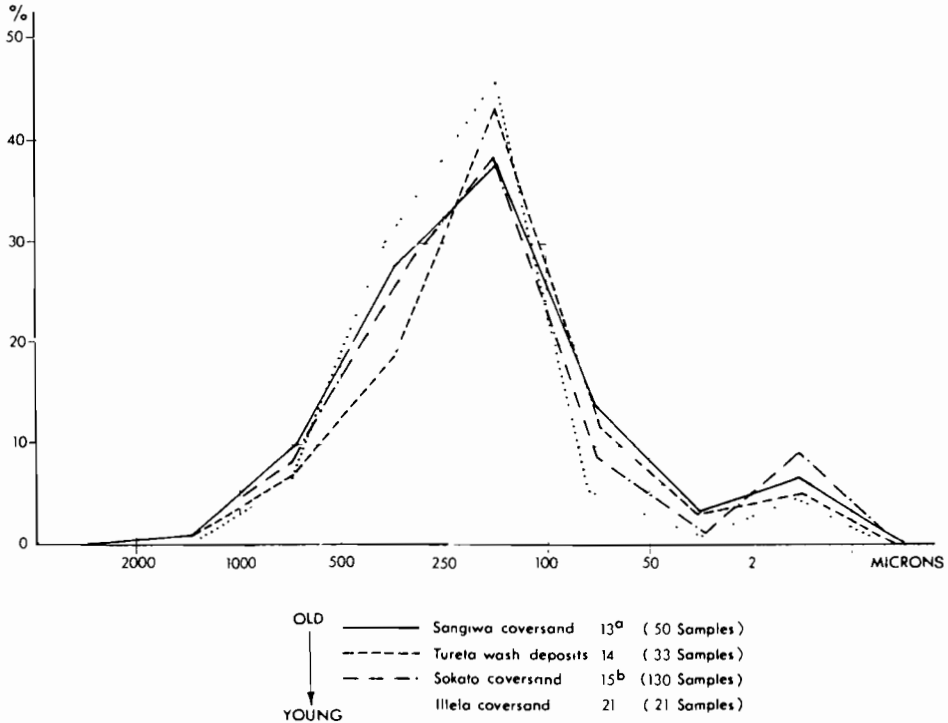
Fig. 2. Grain size distribution of Sangiwa coversand, Tureta wash, Sokoto coversand and Illela coversand deposits.

recognized these sandy formation as (aeolic) coversands. However, the lack of stereo depth later confirmed lack of considerable (even absence of) relief in the field and demanded for more explanation and more close observation.

2. The area

The location of the area is the Sokoto-Rima basin in Northern Nigeria between 4° and 8°E and 11° and 14°N and is land(scape) ecologically, usually indicated as 'Sudan zone.'

The climate is characterized by a severe dry season with dry eastern winds ('Harmattan') from October to May and an intensive wet season from May to September, with an average rainfall of about 400 mm in the North to 600 in the southern part. The vegetation has been described as a grazed and periodically burned *Combretum nigricans* 'Sudan' savanna, see FAO (1969), Sombroek and Zonneveld (1971).

The geological formation at the place of the banded pattern are described as aeolic 'Sangiwa' coversands of several metres (up to 15 m) over late Cretaceous kaolinitic 'Gundumi' or Tertiary 'Gwandu' deposits, usually bordering 'Rima' sandstone of

Cretaceous age (Sombroek and Zonneveld, 1971). The coversands are most probably formed in the late Pleistocene as the first of a series of aeolic desert deposits later followed by somewhat better sorted 'Sokoto' coversands locally reworked to still coarser 'Illela' coversands. The texture can be described as poorly to relatively well-sorted fine sand (see Fig. 2 for details). The mineralogical composition is mainly *quartz*, locally with considerable additions of *epidote, hornblende* and *andalusite*. The soils are classified as 'Red Acid Sands' or *Quarzipsamment* (see USDA, 1960; Dudal, 1968; FAO, 1969; Sombroek and Zonneveld, 1971). Some transitions may occur to *Red or yellowish brown leached kaolinitic soils (Normustult)* where the coversand is very shallow.

3. The pattern

3.1. Shape and size of pattern elements

The configuration of the pattern elements as reflected in the grey tone on the photographs (see Fig. 1) equals in form and scale mainly a ripple mark feature clearly suggesting an aeolic genesis. So this became the leading hypothesis of the photo interpretation and hence for the explanation of the pattern. Towards the sides where the coversand is thinner and overlying kaolinitic late Cretaceous 'Gundumi' deposits, also more dendritic figures exist pointing to some fluviatile influences (see Fig. 1). Neither the 'dune' shape nor the 'river' landform are however within the study area, reflected in the vertical dimension. Between the two elements of the ripple figures, in the largest part of the survey area, differences in height exist of hardly 1 m and usually even less, with slope of approximately 1% or slightly more, just enough to encourage surface flow (sheet erosion) towards the dark coloured 'depression'(the supposed former dune slacks). Towards the North (North of 13°30′N), a very gradual transition to a real in the field recognizable dune landscape is apparent with, outside the survey area, differences between dune slacks and ridges up to about 10 m. This fact, together with the size, shape and arrangements of the pattern elements is a strong argument for the hypothesis of the aeolic character of the deposit.

A similar sheet erosion process may have reduced the relief in the fluviatile forms, even the larger 'river' elements, except sometime for the most 'down stream' 'gully' that indeed may show a slight lower, even discontinuously bordered 'bed'. The larger areas belonging to this fluviatile patters are indicated as (*Tureta*) 'Sandy washplain' (Sombroek and Zonneveld, 1971). From geomorphological evidence, it is however clear that the 'fill' of the dune valleys is identical to the washplain sediment, so consequently have similar properties in relation to soil formation and ecological processes.

4. The vegetation

(The names of the mentioned species are in accordance with Blair Rains, 1968 and Geerling, 1982).

Combined study on the photographs and in the field reveals that the gray tone mainly reflects vegetation density(cover). In the dark patches on the photograph (element a), we found approximately 10-m-high trees of the species *C. nigricans, Balanitis aegyptiaca* and rarely *Sclerocarya birrea* and *Anogeissus leiocarpus*. Common shrubs are *Piliostigma reticulatum, Guiera senegalensis* and *C. glutinosum*, also *Acacia ataxacantha, A. pennata* are often found. The dominant grass is usually *Loudetia togoensis*; other common grasses are *Andropogon pseudapricus* and *Aristida kerstingii*. In the most dense (most shaded) places, occasionally *Pennisetum pedicellatum* may be present. Rarely, the grasses mentioned for element d (see below) may occur in low cover.

At the light-coloured places (element b of Fig. 1), we find an open vegetation of shrubs not exceeding 3 m height, with *G. senegalensis*, some *C. glutinosum* and *C. nigricans*. We find an open cover of the, for the former element first mentioned grasses but never *Pennisetum* and never the grasses common in element d.

The element d on the photograph (Fig. 1) belongs to a fluviatile-shaped pattern. The vegetation appears to be a rather devastated open woodland with trees over 10 m high with *C. nigricans, A. leiocarpus, Prosopis africana, Butyrospermum parkii. Entada africana, Sclerocarya birrea, Balanites aegyptiaca* and in the southern part of the area also *Bombax costatum*. Among the shrubs we found also *C. glutinosum, P. reticulata, A. pennata, A. ataxacantha, Dichrostachys glomerata* and *Cochlospermum tinctorium*. A dominant grass may be *Diheteropogon hagerupii*; other grasses and herbs are *Digitaria gayana, Hyparrhenia bagirmica, L. annua* and *Borreria radiata*. At shaded places, we find *P. pedicellatum*. Various shrubs remain rather long green into the dry season at these places, at least the dead leafs remain long at the branches.

At the central very lowest places of the gully like pattern elements, we may find *Terminalia* and *Ficus* spp. (see e of Fig. 1, c at the same photograph is transitional to element a). At various places, clear recent cuttings of trees can be observed. Locally trials to cultivation are present (see the white spot at Fig. 1 between the two letters d), these appeared to have at the clear banded pattern no result in contrast to the larger dark areas of the fluviatile pattern, where also range land conditions are more favourable. Hence, the composition of the vegetation reflects clearly a sequence in more favourable hydrological conditions from the light coloured pattern elements toward the darker ones, with an optimal condition in the (darkest) lower part of the Tureta washplain 'drainage' channels.

5. The soils

The soils could be classified in all pattern elements just as a *Quarzipsamment*, 'Red acid sand'. They only show a faint thin A horizon with a very low organic matter content. No striking differences could be observed in terms of characteristics used in any soil classification system also not at family levels.

A visit during the rainy season brought the solution. During the heavy rain shower, the water penetrated at the, as dark elements on the photographs appearing places directly into the soil. At the light places, however, it remained at the soil surface, slowly running off into the direction of the dark elements. It appeared that a thin sealed layer of

Table 1

Micromorphological features of coversand and washplain soils (thin sections made by the Netherlands Soil Survey Institute, Wageningen)

Deposit and profile no.	Depth (cm)	Plate no.	Clay bridges	Clay coatings	Variation in grain sizes	Dominant grain size	Open space %	Plant tissues	Iron concr	Stratification
Sangiwa coversand	0–4	3	(+)	+ +	+ +	+	15	+ +	−	+ + +
	4–8	4	+ +	+ +	+	+	20	+ +	+	+ +
E5/1	26–30	5	−	+	+	+ +	80	+ +	+	−
	60–63	8	+ + +	+ + +	+ +	+	35	+ +	+	−
	100–103	6	+ +	+ + +	+	+ +	30	+ +	+	−
	158–162	2	−	−	+ +	+ +	40	−	−	−
Tureta washplain dep.	0–3	2	−	−	−	+ +	80	+ +	−	+
	60–61	9	+ + +	+ + +	+	+ +	30	+ +	+	−
E5/16	164–168	10	+ + +	+ + +	(·)	+ +	40	+	+	−
Sokoto coversand	0–7	7	+ +	+ +	+	+	50	+ + +	+	(+)
	20–27	10	+ +(+)	+ +	+	+	50	+ + +	+ +	−
D4/36	82–86	12	+ + +	+ + +	+	+	50	+ + +	+ +	−
Illela coversand	0–4	1	−	−	−	+ +	40	+ + +	+	+
	4–15	3	+ +	+ +	−	+(+)	40	+ + +	+ +	+
F4/38	31–51	4	+ +	+ +	+	+ +	40	+ +	+ + +	−

Explanation of symbols.

Clay bridges and coatings: − = none, + = few, + + = common, + + + = many.

Variation in grain sizes· − = little, + = moderate, + + = strong.

Dominant grain size (in part of microscope image taken up): + ≤ 1/10, + + = 1/10–1/2, + + + ≥ 1/2 of image.

Open spaces (in % of microscope image): approximate estimations.

Plant tissues: − = absent, + = few, + + = common, + + + = many.

Stratification in grain sizes: − = absent, + = weak, + + = broken-up, + + + = clear.

several millimetres only caused this superficial runoff. Even after a relatively long shower, the soil remained dust dry below that thin crust. The freshly ploughed soil appeared to seal instantly after one shower. The soil removed from our soil pits appeared to be fully sealed and still dust dry after inspection a few weeks later.

Micromorphological study by thin sections was executed (by the Netherlands Soils survey institute Wageningen) on samples taken in profiles with and without a clearly sealed layer. The results are given in Table 1, derived from Sombroek and Zonneveld (1971), p. 38.

6. Discussion

The composition of the vegetation, as well as the described soil condition (permeability) and the observed behaviour of the surface water during a rain shower, points to an eco-hydrological more favourable situation in the darker patches compared with the lighter patches. As there is no evidence that other factors (like fertility, human or animal interference) could be a main cause of such a type of pattern, the main factor determining the difference in site quality apparently is the water regime, as influenced by the combination of relief and sealing both in connection with sheet erosion processes.

Arguments for the obvious hypothesis of an aeolic origin have been mentioned already. The description of the influence of gradual climate changes as can be derived from river deposit patterns and other landforms by Michel (1969a,b), Michel (1970a,b) and Sombroek and Zonneveld (1971) supports this hypothesis strongly.

The most probable genesis of the pattern can be portrayed as in Fig. 3.

The following factors play a role:

(i) the climate bound process of sheet erosion,

(ii) a (slight) silt content of the sediment,

(iii) the lack of biological induced soil structure (lack of organic matter due to an unfavourable climate for organic matter preservation aggravated by frequent fires).

The original aeolic and fluviatile-generated relief apparently has been levelled by a process of sheet erosion. The latter is the common erosion process in the semi arid zone with summer rains and a long dry winter season; compare also Poesen (1992). The whole area shows the dominance of this process during at least a large part of the Holocene. The main result is the pediplanisation, since the beginning of the Holocene. Evidences of the pediplanization process are the special landform of the sedimentary rocks (due to the escarpment-wise retreating erosion) as well as the round shaped 'inselbergs' on the neighbouring igneous rocks of the (precambian) 'basement complex' (Sombroek and Zonneveld, 1971).

This sheet erosion of the coversand area started gradually at the transition in time from a pure desert climate, when the Sahara had a much more southerly border, to a more humid period.

Although trials to exactly date the deposition of the Sangiwa sands and later erosion processes failed so far, one may, by estimation, suppose the deposition to have taken place during the last interpluvial (in the order of some 10 a 20000 years ago). The
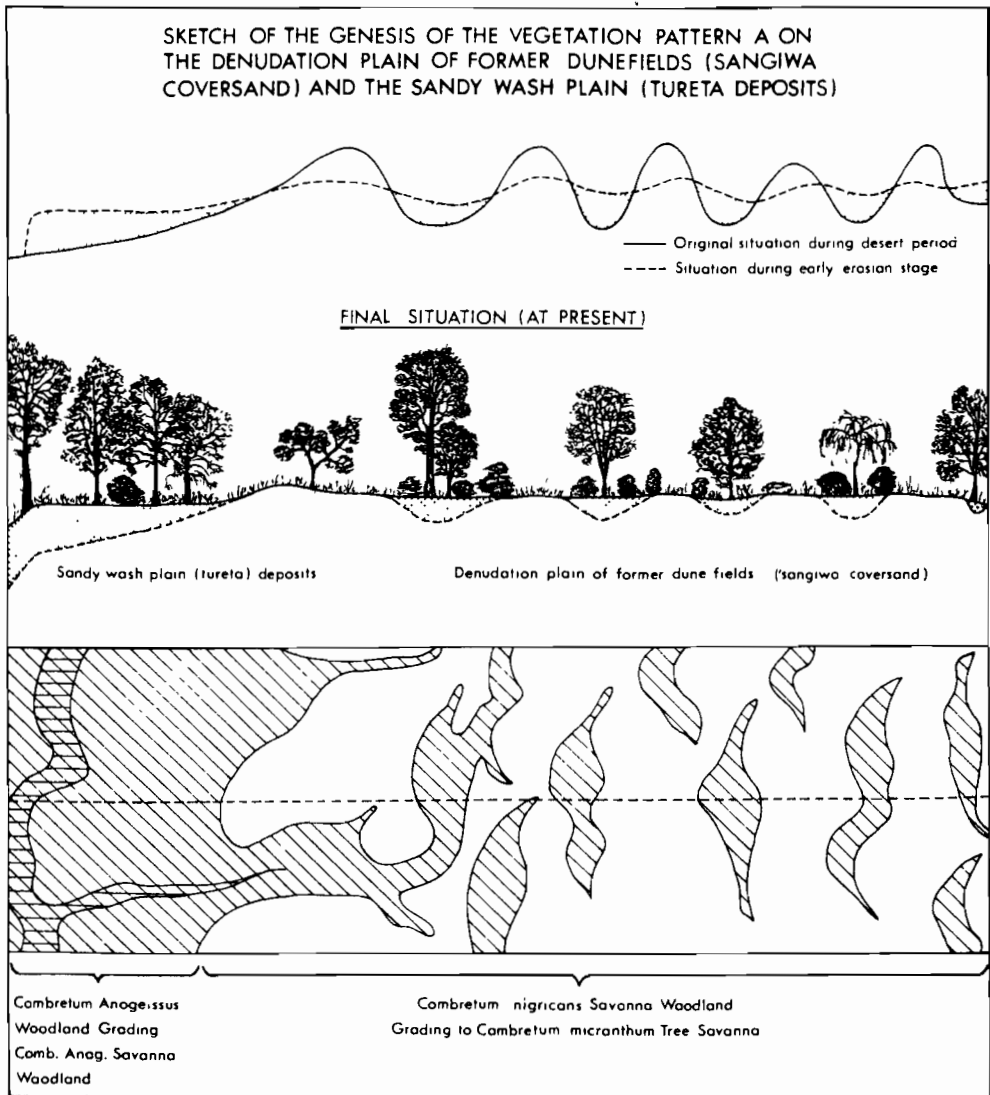
Fig. 3. Sketch of the genesis of the vegetation pattern on the denudation plain of former dune fields (Sangiwa coversand) and the sandy washplain (Tureta deposits) (from Zonneveld et al., 1971).

sheet erosion that still continues may have occurred also at the transitions towards the wet period as well as after the decline of the pluvial up to now. Geomorphological history of the large river flood planes and archaeological evidences deep into the Sahara and the above-mentioned erosion of termitaria show evidence that the latter erosion order may have occurred during a period of an order of magnitude of several thousands of years. (Sombroek and Zonneveld (1971)

The transition from dry to humid can also be observed spatially as the relief decreases from north to south where the erosion process started earlier. Sheet erosion requires however a nonpermeable surface in order to maintain an overland flow. At first glance, 'psamments' may not be the most likely base for surface sealing. However, Fig. 2 shows the differences in texture between the various patches of the pattern. The original *Sangiwa* sands appears to have just enough silt to form a crust (see Fig. 2).

The silt content in the less or not sealed sediments appear to be lower. The reason of this can be found in the resedimentation process which often results in a loss of the finest fractions either by fluviatile or aeolic processes. For example, the Pleistocene cold desert fringe coversands from the last glaciation in the Netherlands show also a similar decrease in fine fraction after resedimentation. The dune valleys, in contrast to the washplain, have no outlet. So even in case of some sealing, the water eventually has more time to penetrate the top layer.

The dominant role of sheet erosion, as main geomorphological process in (sub) recent periods, is also reflected in the interesting dotted pattern caused by levelling of former (fossil) termitaria at more loamy deposits in the neighbourhood of the banded pattern as described by Sombroek and Zonneveld (1971) and Zonneveld et al. (1971).

Sealing could be counteracted by soil structure formation under biological influence (fresh organic matter). The extremely long dry periods in combination with anthro-pogenic generated fires, counteract this certainly on those places were the vegetation is less dense. So one can expect a tendency, as an example of a negative feedback system increasing stability, that once the vegetation has reacted on a slightly more favourable hydrological situation, the organic matter production of the vegetation it self helps in maintaining the favourable permeability. Under these circumstances, rain-fed agriculture appears to be disastrous and therefore virtually impossible, as the first shower after ploughing causes sealing. Theoretically, the creation of more permanent humidity that allows some formation of stabile structure improving humus is a prerequisite for agriculture at these soils. Under the present conditions, any form of irrigation seems, however, in the study area to be excluded.

The banded *Sangiwa* pattern so serves as a clear indication of a special landscape ecological situation connected with a special geomorphological history, resulting in a special texture which still indirectly is related to climatic factors.

It is an example how vegetation features instead of actual physical landform like this could be used as land unit mapping characteristics, compare Zonneveld (1995). But the image as shown by the vegetation as such could be recognized because its geomorpho-logical (aeolic and fluviatile) shape features.

7. Comparison with other banded patterns

So far, we found in literature only one description of similar banded patterns like ours conducted by Clayton (1966, 1969). It refers apparently also to Sangiwa sands in the neighbouring areas in Nigeria.

Not any dune pattern needs to be banded. One can well imagine that a certain not banded relief in sandy deposits after levelling by sheet erosion may result in a dot

pattern with similar properties of the elements in relation to surface hydrology. Also at Fig. 3, one may observe transitions from bands to dots. So Sombroek et al. (1976, and oral communication) described in local soil survey reports in Kenya similar, be it more 'panther'- than 'tiger'-like, patterns related to the more static Sangiwa fossil dune pattern.

Most publications, from the same period as our study and later, about banded patterns, deal with quite deviating phenomena, be it under a similar name: 'Brousse tigrée'. So did White (1969, 1970, 1971) for Republique Nigère. Greenwood (1957) described similar features as 'Vegetation arcs' in Somalia. Thiéry et al. (1995) summarize the genesis as moving vegetation arcs under influence of sheet-run-off. See, e.g., Bergkamp et al. (1996), Chappel et al. (1996), Galle et al. (1996) and others in this issue. These patterns have a very much different genesis. Also here runoff water is a cause but they have a much more dynamic character. The orientation of the bands irrespective the compass direction is determined by the terrain slope and are perpendicular to the water flow (not the wind). These vegetated arcs are not necessarily the lowest parts, provided they receive and hold surface water. It are the places were sediment (and organic matter) accumulate, in contrast with the strongly sealed parts of the surface mosaic, that serves as runoff bed. Stronger then in our static bands, here a clear dynamic equilibrium exist between mutual influence of vegetation, sedimentation, structure building (by organic matter).

We observed similar 'brouse tigrée' patterns at different scales in the field and by air in wadies in the Syrian and other deserts. These arcs may generate, collapse and move in time and space, depending on the balance between runoff and intrinsic vegetation growth factors.

For more details, especially also about the termite related dot patterns mentioned earlier, may be referred to Sombroek and Zonneveld (1971), Zonneveld et al. (1971), Zonneveld (1975).

References

Blair Rains, A., 1968. A field key to the commoner genera of Nigerian grasses. Samaru Miscellaneous Paper No. 7. Inst. for Agricultural Research, Amadu Bello University, Samaru, Zaria, Nigeria.

Bergkamp, G., Cerda, A., Imeson, A., Jongejans, J., 1996. The importance of surface water redistribution for the ware budget of banded vegetation structures. This publication.

Chappel, A., Valentin, C., Peugeot, C., Warren, A., 1996. Impact of water harvesting variations along a climactic transect in Niger upon productivity and pattern in Niger. This publication.

Clayton, W.D., 1966. Vegetation ripples near Gummi, Nigeria. J. Ecol. 54, 415–417.

Clayton, W.D., 1969. The vegetation of Katsina province, Nigeria. J. Ecol. 57, 445–451.

Dudal, R., 1968. Definition of soil units for the soil map of the world. FAO/UNESCO World Soil Resources Report 33, Rome.

FAO, 1969. Soils Survey and Land Classification, Soils and Water resources Survey of the Sokoto Valley (Nigeria) Final report Vol. V FAO/SF:67/Nr3.

Galle, Ehrmann, M., Peugeot, C., 1996. Water balance in banded vegetation pattern: the case of the Tiger bush in West Niger. This publication.

Geerling, Ch., 1982. Guide de terrain des ligneux Sahéliens et Soudano-Guinéens. Mededelingen Land-

bouwhogeschool Wageningen, Nederland 82-3, 340 pp.(See also Flora of West Tropical Africa, 2nd edn. Millbank London)

Greenwood, J.E.G., 1957 The development of vegetation patterns in Somaliland protectorate. The Geograph. J 123, 465–473.

Michel, P., 1969a. Les Grandes étappes de la morphogénèse dans les bassin des fleuve Senegal en Gambie pendant le Quaternaire. Bull. Inst. Afr. Noir A. 31 (2), 293–324.

Michel, P., 1969b. Les depôts du Quaternair de la vallée interieur du Niger, d'après H. Busier. Bull. ASEQUA 21, 55–57.

Michel, P., 1970a. Chronologie du Quaternair des bassin des fleuves Sénégal et Gambie, Essai de synthès. Bull. ASEQUA 25, 53–64.

Michel, P , 1970b. Chronologie du Quaternair des bassin des fleuves Sénégal et Gambie, Essai de synthès. Bull ASEQUA 26.

Poesen, J.A W., 1992. Mechanisms of overland-flow generation and sediment production on loamy and sandy soils with and without rock fragments. In: Parsons, A.J., Abrams, A.D. (Eds.), Overland Flow. Hydraulics and Erosion Mechanics. UCL Press, London, pp. 275–305.

Sombroek, W.G , Zonneveld, I.S., 1971 Ancient dune fields and fluviatile deposits in the Rima-Sokoto River basin (N.W. Nigeria) Soil Survey Papers No. 5. Netherlands Soils Survey Institute, Wageningen. Colour printed map, 107 pp

Sombroek, W.G., Mbuvi, J.P., Okwaro, H.W., 1976. Soils of the semi-arid Savanna zone of North-Eastern Kenya. Kenya Soils Survey. Miscellaneous Soil Paper M2, 14 pp.

Thiéry, J.M., d'Herbès, J M., Valentin, C., 1995. A model simulating the genesis of banded vegetation paterns in Niger. J. Ecol. 83, 497–507.

USDA, 1960. Soil survey staff. Soil classification, a comprehensive system.

White, L.P., 1969. Vegetation arcs in Jordan. J. Ecol. 57, 5461–5464.

White, L.P., 1970. 'Brousse tigrée' patterns in souther Niger 54. J. Ecol. 58, 549–553

White, L.P , 1971. Vegetation stripes on sheet wash surfaces. J. Ecol. 59, 615–622.

Zonneveld, I.S , 1975. Der Zusammenhang zwischen dem Horizontal-gefüge der Vegetation und dem Edaphischen Zustand in einem Savannegebiet Nord-Nigerias Vegetation und Substrat, Berichte der Int Symp. der Internat. Verein. f. Vegetationskunde, (Rinteln 1969). Cramer in A R. Gantner Verlag, Fl 9094 VADUZ, 1975, pp. 511–527

Zonneveld, I.S, 1988. Vegetation mapping. In: Küchler, Zonneveld (Eds.), Handbook of Vegetation Science 10, Chaps. 4, 11a, 17, 20, and especially 29. Kluwer Ac. Pub. Dordrecht, Boston, London, 635 pp.

Zonneveld, I.S., 1995. Land Ecology, an Introduction to Landscape Ecology as a Base for Land Evaluation, Land Management and Conservation SPB Acad. Publ., Amsterdam, 199 pp.

Zonneveld, I.S , de Leeuw, P.N., Sombroek, W.G , 1971. An ecological interpretation of Aerial photographs in a savanna region in northern Nigeria. Publication of the International Institute for Aerial Survey and Earth sciences (ITC) Enschede, The Netherlands, 41 pp.

Vegetation arcs and litter dams: similarities and differences

J. Eddy [a], G.S. Humphreys [a,*], D.M. Hart [a], P.B. Mitchell [a], P.C. Fanning [b]

[a] *School of Earth Sciences, Macquarie University, Macquarie 2109, Australia*
[b] *Graduate School of the Environment, Macquarie University, Macquarie 2109, Australia*

Abstract

Vegetation arcs are near parallel bands of denser vegetation aligned perpendicular to slope and separated by barer inter-arc zones. These patterns occur in arid and semi-arid areas of gentle to very gentle gradient. Similar, but much smaller scale patterns, here referred to as 'litter dams and microterraces', occur in a variety of climatic regions, from tropical to temperate to arid, on steeper slopes, as well as on very gentle slopes. We describe similarities between arcs and dams in attributes such as shape, orientation, cross-sectional profile, spatial organisation, and surface features (arrangement of plants, surface crusts). Differences are in spatial and temporal scale. Range of wavelengths, or spacing between bands, is 25–300 m for arcs and 0.1–2 m for dams. With regard to time, arcs may be stable for tens to a hundred or more years while dams may be ephemeral or remain stable for more than a decade. Overland flow involving the transport of organic material (leaves, charcoal, faecal pellets) as floating load over comparatively bare surfaces is an important factor in the maintenance of vegetation arcs and formation of and maintenance of litter dams. Recognising the importance of gradient to transport by overland flow a preliminary investigation of the relationship between wavelength and gradient was conducted. A combined analysis of a limited set of arc and dam data describes parallel lines which may indicate that similar processes are operating at the two scales. This would allow the convenience of process studies on dams as an aid in understanding the origin of arcs. However, the difference in the

---

* Corresponding author

intercept of the two lines with the ln(wavelength) axis may indicate changes in process that preclude extrapolations from one spatio-temporal scale to the other. © 1999 Elsevier Science B.V. All rights reserved.

1. Introduction

Several types of banded vegetation patterns are described in the literature. Those referred to in this paper as 'vegetation arcs' are near parallel bands (spacing 25–300 m) of denser vegetation aligned approximately perpendicular to slope and are known in arid and semi-arid areas on gentle slopes in Africa (e.g., Macfadyen, 1950a,b; Boaler and Hodge, 1964; Greenwood, 1957; White, 1970; Worrall, 1959, 1960), Australia (e.g., Mabbutt and Fanning, 1987; Greene, 1992; Ludwig et al., 1994; Dunkerley and Brown, 1995), Mexico, (Montaña et al., 1990) and the Middle East (White, 1969, 1971). Despite a low and erratic rainfall, mostly between 150–450 mm, the arcs support distinctive communities of grasses, shrubs and trees.

Litter dams and microterraces are similar to vegetation arcs in shape and orientation but they are considerably smaller (spacing 0.1–2 m). They are common in sub-humid to humid bushfire prone parts of Australia on gentle hillslopes subject to rainwash (Mitchell and Humphreys, 1987). The convex downslope dams consist of floating load material: ash, fragments of charcoal and acicular debris. Trailing edges of litter dams often merge with others forming an interconnected network over the hillslope in a similar way to vegetation arcs. The litter dam is the site of regeneration of fire-tolerant species, perennial grasses, stoloniferous rushes and sedges, seedlings of herbs and fire dependent obligate seeding shrubs. Downslope of the dam is a steeper scarp or erosion zone. Upslope of the dam a microterrace forms as bedload mineral material, composed mainly of sand-sized quartz grains, is deposited in the ponded zone created by the litter dam. Within the microterrace a variety of crusts form during the post-fire period as the microterrace is stabilised by algal and root mats, but it remains largely devoid of higher plants. In this sense microterraces resemble the vegetation deficient intergrove of vegetation arcs. The pattern of these microrelief forms has been observed to persist for longer than a decade between major fires. Similar features have been described in other settings (Paton et al., 1995) and under a variety of names, such as debris bars, floating load/bedload dams, barrier dams, listed in Mitchell and Humphreys (1987) who chose the term 'litter dam and microterrace' to describe both the material and the microrelief form.

The origin of vegetation arcs has not been fully established. Mechanisms that may contribute to their formation include the effect of prevailing winds (White, 1971) and entrapment of wind-blown sand behind barriers (Worrall, 1959), though it is apparent to many authors that sheetwash is an important contributing factor. With the much smaller litter dams rainwash, i.e., a combination of rainsplash, slopewash and sediment rafting (cf. Paton et al., 1995; van Zon, 1980) remain the most important factors providing that a suitable supply of organic debris is available. In both situations a form of overland flow is implicated. It is possible that a better understanding of litter dams may assist in

determining the origin of vegetation arcs. However, this approach by analogy works best only if similarities can be demonstrated. As a contribution towards this objective it is necessary to evaluate the similarities and differences between vegetation arcs and litter dams, and this is the purpose of the paper.

2. Materials and methods

Apart from observations at Fowlers Gap in semi-arid Australia we have relied on published accounts for information on vegetation arcs. In contrast, details on litter dams are largely from our own observations. Accordingly, the description of field sites and methods refers to litter dams only.

2.1. Field sites

Detailed observations of litter dams and related features have been made at two locations in eastern Australia: the Sydney Basin and the Pilliga State Forests (Fig. 1). Unqualified observations have extended from semi-arid New South Wales to the wet/dry tropics of the Northern Territory and the wet tropics of Papua New Guinea.

2.1.1. Sydney Basin

The study plots in the Sydney Basin (at Cherrybrook, Ku-ring-gai and Oxford Falls) were in natural bushland reserves on 2°–10° slopes on which 1–2 m high benches of quartzose Hawkesbury Sandstone outcrop. Texture contrast soils (Haplohumults, Soil Survey Staff, 1992; Yellow Podzolics, Stace et al., 1968) and shallow earthy sands (Quartzipsamments, Soil Survey Staff, 1992; Earthy sands/Lithosols, Stace et al., 1968) comprise an apedal loamy sand to fine sandy loam topsoil overlying clayey or loamy subsoils respectively. The vegetation is a woodland or open forest (after Specht, 1970) dominated by *Eucalyptus* spp. A shrub understorey is dominated by species of *Banksia*, *Hakea*, *Casuarina* and *Grevillea*. Patchy groundcover consists of perennial tussock grasses and stoloniferous rushes such as *Lomandra* spp. Average yearly rainfall is about 1200 mm falling to less than 1000 mm in drier years and exceeding 1900 mm in wetter years. Most rainfall occurs in storm events in autumn and summer.

2.1.2. Pilliga

In the Pilliga State Forests a mosaic of vegetation is supported on a variety of soils formed mainly from sediments derived from Jurassic Pilliga Sandstone. The vegetation communities referred to in this study occur on slopes up to 2°–4° and consist of an open woodland of *Eucalyptus viridis* growing in multi-stemmed habit referred to as 'mallee' and a forest of *Allocasuarina cristata* or 'belah'. The mallee-soils are texture contrast soils comprising sandy loam to sandy clay loam over a sandy clay with columnar structure (Natrustalf, Soil Survey Staff, 1992; Solodized Solonetz, Stace et al., 1968). The belah soil is a Vertisol (Soil Survey Staff, 1992); gilgaied Grey Clay (Stace et al., 1968). Average annual rainfall is about 600 mm, much of which falls during summer storms, though extremes of both drought and wet periods are common. The last major fire in the area was 45 years ago, with patchy minor fires occurring 30 years ago.
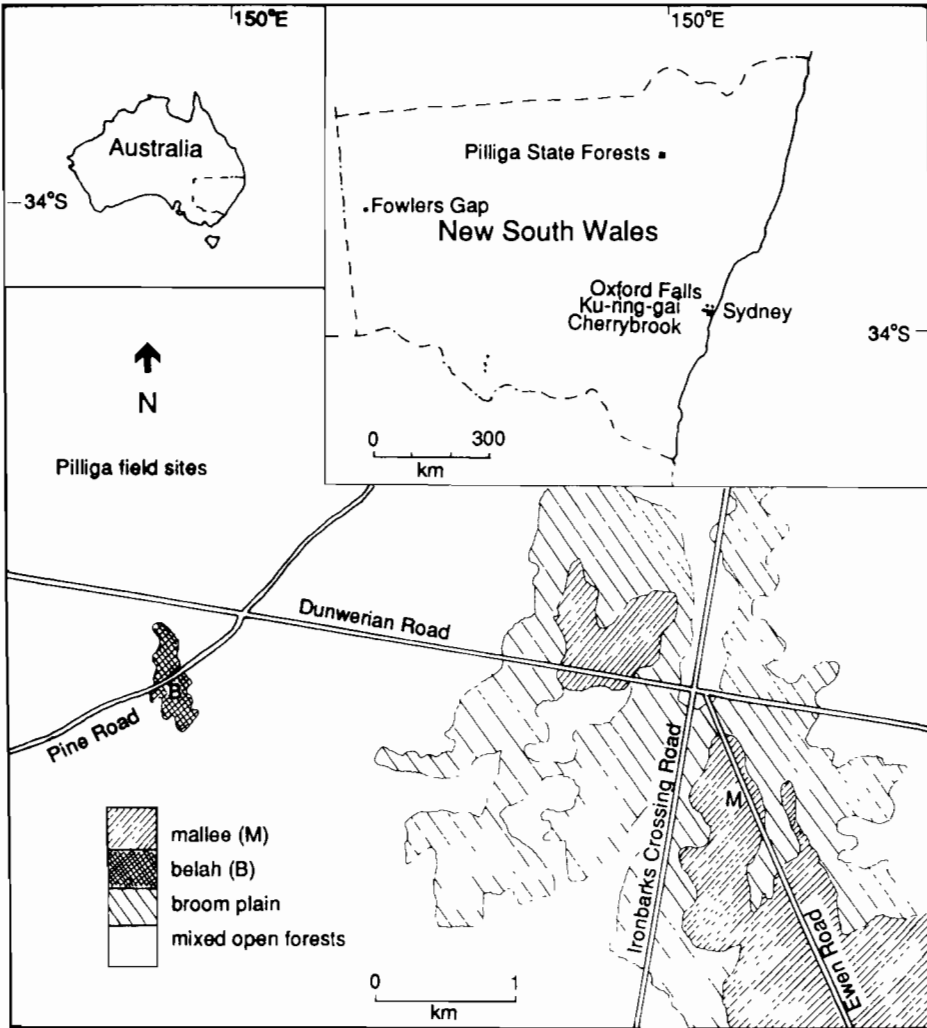
Fig. 1. Location of study sites.

2.2. Methods

A plan view of the distribution of surface litter in each vegetation community was mapped, over an area chosen so as to be large enough to illustrate the typical arrangement (plot size of 5 m × 5 m to 6 m × 7 m). Attention was paid to the identification of firmly compacted litter dams as distinct from under-canopy litter and loose, more easily transportable litter in canopy gaps. Measurements were made at 10 cm × 10 cm grid intervals from a levelled 1 m × 1 m or 1 m × 2 m frame to enable mapping of microrelief typical of each area.

Surface features (e.g., microbiotic or mineral crusts, presence and arrangement of herbs, forbs or cryptogams, type and compactness of litter) characteristic of each microtopographical zone were noted. Undisturbed soil samples, 0–5 cm depth, were collected from each zone for preparation of thin sections for micromorphological examination.

In the mallee community the vegetation was recorded along two intersecting transects; one along the maximum gradient (a gradsect, cf. Gillison and Brewer, 1985) and a transect along the contour, each 50 m long and one metre wide. These patterns were checked against aerial photographs of the site.

3. Results

3.1. Arcs and dams in plan

From aerial photographs in arid areas vegetation arcs appear as regularly spaced bands which, together with intervening bare or less densely vegetated areas, form a distinctive pattern (Fig. 2a) often covering many square kilometres. Bands on low slopes are typically convex downslope, orthogonal to the direction of sheet flow though convex upslope patterns have been observed along shallow water ways and on the side slopes of spurs (Mabbutt and Fanning, 1987). The plan view map of litter dams in the Pilliga State Forests also shows a pattern of convex downslope arcuate bands, parallel to contours (Fig. 2b) that is very similar to vegetation arcs. Furthermore, the trailing edges of dams merge with others to form an interconnected network over the hillslope, similar to the reticulate patterning of 'master groves' and 'minor groves' reported by Mabbutt and Fanning (1987).

3.2. Topographic profile
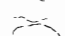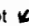
Although the earliest investigations did not elaborate on a topographic variation across vegetation bands/interbands it nevertheless became apparent that differences existed. For example Worrall (1960) reported that tree bands formed gentle risers and White (1969) noted that a slight rise was created by sand blown against the bases of shrubs in the vegetation band. Terminology used for different topographical zones varies from author to author. Some refer to the difference in vegetation cover (vegetation band/bare area), others to hydrological processes or resource availability (runoff/interception zones, fertile patch) and still others to ecological succession (pioneer zone). Taken together these illustrate the growing understanding of interactions of process and function in banded landscapes. In this section and in Fig. 3, referred to in (a) and (b) below, the original terminology of authors whose diagrams have been used is therefore retained, while some attempt has been made to integrate concepts by doubling up on labels for particular parts of the one diagram.

From published information, two types of topographic profile are distinguishable.

(a) The vegetated arc is supported on the 'riser' (Fig. 3a).

Slatyer (1961) noted from observations of water movement that the intergrove area was flatter just upslope of the tree band. About two-thirds of the vegetated band and the adjacent downslope intergrove area were on a greater than average slope forming a

(a)

1 Km

(b)
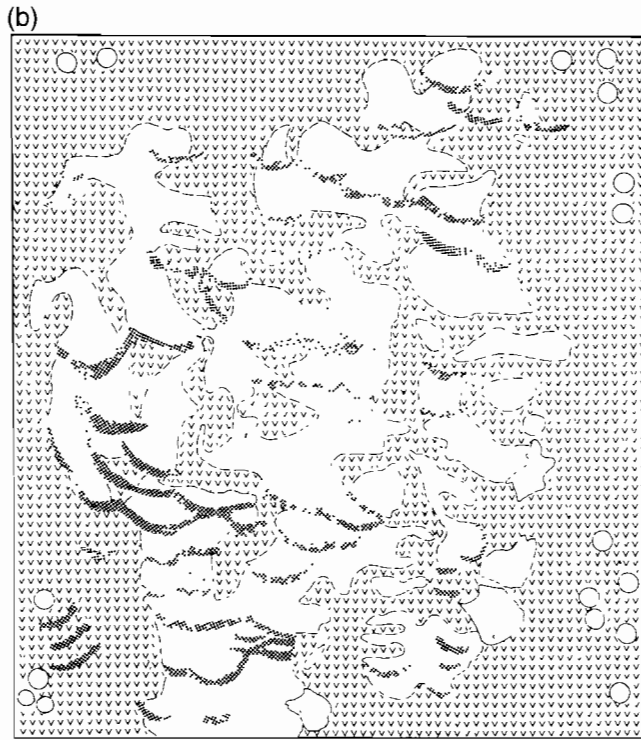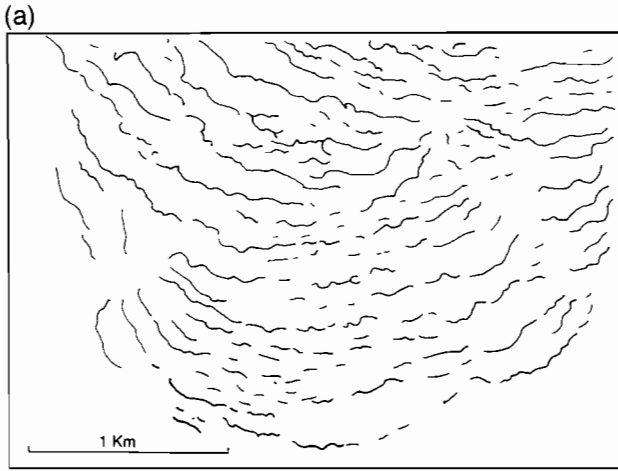
	litter dams		slope of plot ↙
	litter on tree mounds		
	or in diffuse litter trains		North ↓
	tree		
	rock		0 1 m
	runoff zone and microterrace with		
	microbiotic and mineral crusts		

convex-up (i.e., in a vertical sense) profile. Boaler and Hodge (1964) indicated in their Fig. 3 and Fig. 5 that the arc 'front' (the furthest upslope edge of the vegetation band) often occurred on a slight ridge while the 'body' of the arc occurred on the riser downslope from this. Thus the whole arc is on the convex-up part of the slope while the bare area often has a concave-up profile. A similar relationship between slope segments and pattern components is described by Mabbutt and Fanning (1987); see Fig. 3a(i)) and Dunkerley and Brown (1995). Litter dams of this type also occur (Fig. 3a(ii)). In the Sydney Basin vegetation consisting of tussocky perennial grasses, sedges and rushes grow along the crest of the litter dam and down the riser or scarp ending in a section of bare ground on a gentler slope which leads onto the flat depositional zone or microterrace proper.

(b) The vegetated arc is supported on the 'step-tread' (Fig. 3b).

Examples of this type in Australia are illustrated by Tongway (1994); see Fig. 3b(i)). The more steeply sloping runoff zone is sparsely vegetated and leads downslope onto a flatter interception zone. The arc of dominant trees or shrubs on the flat is often associated with a slight ridge before a bare steepened section leading to the next erosion zone. Montaña et al. (1990, Montaña (1992) report this type of topographical profile within the Chihuahuan Desert. Examples of litter dams in the Pilliga State Forest are analogous to these type (b) arcs (Fig. 3b(ii)). A slight ridge of mineral material forms under litter accumulations as soil material is introduced into the dam by termites engaged in the construction of gallery sheeting. In addition some soil is trapped within the litter during episodic rainwash events. These litter dams are sharply cut away on the downslope side to expose an almost vertical narrow strip of underlying bare soil. The runoff zone is the next steepest section while the interception area flattens out towards the next litter dam with its rather sparse tussocky grasses positioned along the next step edge.

3.3. Vegetation and surface features

In some banded landscapes the interband area is devoid of vegetation and forms an erosion zone that grades onto a sandy deposit or stony ground such as gibbers (Dunkerley and Brown, 1995) positioned upslope of the tree or shrub band along the convex-up break in slope. These are analogous to litter dams seen in the Sydney Basin where sand is deposited in a succession of thin layers bound by algae resulting in a multi-layered crust on the microterrace (Humphreys, 1994; Eddy et al., 1996a).

In other landscapes there is a succession of plant forms where a crusted runoff or erosion zone slopes down to a less steep interception zone or pioneer zone (Tongway, 1994). Mineral and organic grains are trapped amongst grasses and smaller shrubs on the upslope side of the slightly mounded tree / shrub band itself. This is analogous to litter

Fig. 2. (a) Plan view of vegetation arcs after Macfadyen (1950a). (b) Plan view of distribution of litter in canopy gap between mallee and cypress trees in Pilliga State Forest, N S.W. Note the relationship of the arcuate form to the local slope and the continuity of the densely compacted dam material with more diffuse litter trains thus forming a network over the area.

a(i) vegetation
      arc

shrubs

20 cm

gibbers   crusted
             ponded zone

vegetation band   bare interband area
on riser

0 m   100 m

a(ii) litter
      dam

litter

5C mm

sand deposits
crusts

grasses and root mats
stabilise slope
on riser
                                    microterrace

0 m   1 m

b(i) vegetation
      arc

vegetation band

50 cm

grasses

step-tread   runoff zone   interception zone fertile patch

0 m   100 m

b(ii) litter
      dam

40 mm

microbiotic mat,   moss mat,
structural/erosion crust   depositional crusts

step-tread   run-off /   microterrace
                 erosion zone

0 m   1 m

Fig. 3. Topographic profile of vegetation arcs and litter dams. (a) Example of (i) vegetation arc (Western Australia, after Mabbutt and Fanning, 1987) compared with (ii) litter dam (Sydney Basin). (b) Example of (i) vegetation arc (Western N.S.W., after Tongway, 1994) compared with (ii) litter dam (Pilliga, belah). Note horizontal and vertical scales. Vegetation not to scale.

dams and microterraces observed in the Pilliga State Forests. In the belah, for example, the erosion zone has a biotic crust of blue-green algae and ground-hugging cryptogams

dominated by the liverwort *Riccia limbata*. On the microterrace a dense mat of moss, dominated by *Barbula calycina*, acts as an interception zone that traps sand and silt particles. Sparse perennial grasses occur usually in the litter dam.

3.4. Surface condition

Micromorphological examination of surface soil in banded mulga vegetation (Greene, 1992) showed that porosity differs between three geomorphic zones (cf. runoff and interception zones and fertile patch (Tongway, 1994; Fig. 3b(i)). In the runoff zone a smooth discontinuous surface seal overlay dense soil consisting of tightly packed sand and silt grains. Large pores were absent as was organic debris and the surface soil was devoid of biological activity. The surface of the interception zone was smooth but more porous, with some aggregation of particles of sand, silt and clay. Rootlets and organic debris were present in the topsoil and cracks, 1–2 mm wide, extended into the subsoil. The soil adjacent to the cracks was highly bioturbated. The soil of the grove zone contained abundant organic matter and was much more bioturbated. Bioturbation continued along the cracks, similar in size and penetration depth to those in the interception zone, but the biopores were much larger (up to 10 mm). Another example, from West Africa, describing this type of variation in the surface condition is provided by Thiéry et al. (1995).

Preliminary micromorphological studies of soil sampled from the three zones of litter dams and microterraces from the Sydney Basin and the Pilliga State Forests illustrate a similar regular succession of porosity and crusts (Eddy et al., 1996a,b). On the runoff zone, often underlying a micobiotic mat consisting mainly of blue-green and green algae, structural slaking crusts, sometimes modified to erosion crusts, overlie a dense fabric with minimal bioturbation. In the interception zone, where ponding and deposition occur, complex multi-generational sedimentation crusts are found. Here bioturbation becomes evident and in clayey soils cracks extend to the subsoil. Within and under the litter dam bioturbation is at a maximum and this activity disrupts a multi-layered fabric similar to that in the interception zone.

3.5. Infiltration

Both arcs and dams act as efficient natural water harvesting systems. Worrall (1959) observed ponding upslope of grass arcs as did Boaler and Hodge (1964), who attributed runoff collection to 'the effect of the grass plants and their associated debris on water movement' (Boaler and Hodge, 1964, p. 535). Litter dams serve the same purpose as surface water detention occurs on microterraces. Under these conditions it might be expected that infiltration is greatest where ponding occurs. Indeed, in the case of litter dams we have observed a higher rate of infiltration into the soil in the ponded area than into soil beneath vegetated dams. This is particularly noticeable in the Sydney Basin, where slow wetting under the dam correlates with a higher degree of water repellence in the localised patch of underlying soil (Eddy et al., 1996b). The situation appears to be more complicated for vegetation arc complexes as Slatyer (1961) and Boaler and Hodge (1964) report greater depth of infiltration within the arcs than in the ponded zone. This

was attributed, in light rain, to leaf catchment and stem flow or, during heavy rainfall, to inflow from the bare ground outside the vegetated band (Boaler and Hodge, 1964).

3.6. Slope relationship

It is widely accepted that overland flow can be a major driving force behind the formation of vegetation arcs and an equivalent mechanism produces litter dams (Mitchell and Humphreys, 1987). Given the role of flowing water it is expected that some of the features of arcs and dams are strongly influenced by the gradient over which the water travels. From hydrological and sedimentological viewpoints these arcs may be interpreted as bedforms such as ripples and transverse ribs (e.g., Allen, 1982). In this case the two parameters most likely to be influenced are the wavelength or spacing between arcs/dams perpendicular to the flow direction and amplitude or height of the arc/dam above the natural gradient. To test this idea relevant information was sought from appropriate literature. An array of data on wavelength exists but little for amplitude and hence this latter parameter is not considered further. However, the existing data on wavelength and gradient are of variable quality and range from single averaged values for one or both parameters, for which no sense of sample size or variation is known, to more complete data sets. Therefore we have used only that information, presented in text, table or diagram, where data is given or could be calculated as wavelength against overall slope for each transect (Appendix A).

Because of the variable quality of these data we adopted, initially, a simple least squares regression. This produced a strong inverse ln, ln relationship between wavelength and gradient ($r^2 = 90.3\%$). However, the residual model diagnostics and scattergram plot (Fig. 4) indicate two non-overlapping subsets of arcs and dams, separately
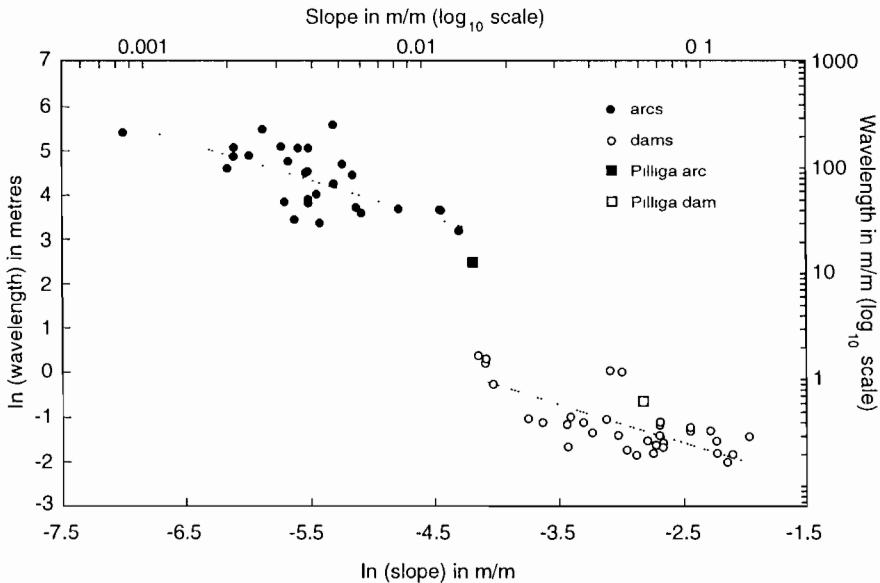
Fig. 4. ln, ln plot between wavelength and landsurface gradient for vegetation arcs and litter dams.

plotting on near parallel lines. We therefore sought to test whether or not the relationship between wavelength and gradient is different between the subsets using the following model: $\ln(\text{wavelength}) = \beta_0 + \beta_1 \ln(\text{gradient}) + \beta_2 S + \beta_3 S \cdot \ln(\text{gradient}) + \varepsilon$ where ln = natural logarithm S = an indicator variable ($S = 0$ for arcs, $S = 1$ for dams) $\varepsilon \cap N(0, \sigma^2)$

This showed that the β_3 coefficient was not statistically different from zero (p-value 0.542). Letting $\beta_3 = 0$ simplifies the model and yielded a least-squares multiple regression equation of $\ln(\text{wavelength}) = -0.351 - 0.855 \ln(\text{gradient}) - 3.325$ ($F = 905.83$, $df(2,60)$, $p < 0.0001$, $r^2 = 96.8\%$)—reasonable residual model diagnostics. From this the estimated equation for arcs is $\ln(\text{wavelength}) = -0.35 - 0.855 \ln(\text{gradient})$ and for dams is $\ln(\text{wavelength}) = -3.67 - 0.855 \ln(\text{gradient})$.

We conclude from this that the two data sets, arcs and dams, fit parallel lines (with slope of -0.855) but with different intercepts on the $\ln(\text{wavelength})$ axis.

4. Discussion

The comparison of vegetation arcs and litter dams describes many similarities. In areal plan arcuate bands of arcs and dams are arranged orthogonal to slope, often with trailing edges that interconnect to form a network. Two types of topographic profile are defined by the positioning of the vegetation on riser or step-tread. Runoff zones, interception zones and fertile patches exhibit a distinct sequence of vegetation and surface features, e.g., biotic and mineral crusts. Micromorphological examination shows a similar spatial arrangement of dense crusted and porous bioturbated near-surface soil materials. Both arcs and dams function as water harvesting systems and as traps for water- and wind-transported organic matter, thus concentrating resources in the landscape.

The main differences are in the spatial and temporal scales of the features and the slopes on which they occur. Wavelengths of arcs, which occur on very gentle slopes, are two to three orders of magnitude greater than wavelengths of dams, which occur on steeper slopes. The life-span of arcs may be over a hundred years, while dams may be ephemeral or persist for over a decade.

The statistical analysis also suggests that arcs and dams have a similar ln,ln relationship of wavelength to gradient indicated by their same slope value, although the intercepts with the ln(wavelength) axis for the two data sets are different (Fig. 4). From these results it appears that gradient is a major determinant in controlling spacing between both arcs and dams. However, the role of gradient in explaining spacing between arcs or dams as shown in this paper requires further comment.

First the data set is of limited quality and unevenly weighted with varying numbers of observations per study site. There is no overlap in values between the two sets for wavelength nor gradient, and, with the exception of one arc and dam data pair (Pilliga), there is no overlap in location, either. Additionally, only two sites provide litter dam data and one of these (Allen, 1982) is consistently underestimated by the fitted model. Although the present data set suggests parallel lines, it remains possible that future research may reveal other relationships.

Second, it is known that various banding patterns can be generated in simulation models in which other parameters are used (e.g., Thiéry et al., 1995; Lefever and Lejeune, 1997). Nevertheless, it remains true that whenever a gradient parameter is included (e.g., Gallart et al., 1993; Lefever and Lejeune, 1997) a banding pattern emerges that conforms to the vegetation arcs and litter dams described. Furthermore, two types of topographic profile occur in both vegetation arcs and litter dams, and it remains uncertain how these differences develop. Other parameters that could be important include the type of vegetation, the particle size of the soil over which runoff occurs, soil type and its possible effects on seepage into the riser, as well as the balance of processes leading to the maintenance or degradation of the arcs and dams. Regardless of morphological type, however, the relationship between wavelength and gradient remains.

Third, the range of slopes considered in our data is from 0.0009 to 0.142 m/m, with no overlap of the two data sub-sets. Several authors have noted that vegetation arcs rarely occur on gradients < 0.001 presumably because the flow is poorly organised given the surface roughness conditions on very low slopes. Vegetation arc wavelength would necessarily have a lower limit dependent on the canopy size of trees or shrubs. We do not know the minimum spacing of litter dams but note that on steeper slopes (gradient approx. 0.5 m/m) microterracettes (2–5 mm high, 2–3 cm spacing) occur in which the feature has a lobate form composed of mineral material and organics. Similarly we are uncertain as to the maximum spacing of litter dams and/or the minimum slopes on which they occur. Our measurements to date, however, conform with the general limits indicated in Fig. 4. In the Pilliga mallee, for example, both arcs and dams occur. The dominant mallee vegetation is organised into bands with an average wavelength of 12 m with interconnecting narrower bands, about 8 m apart, aligned parallel to the slope so that a lattice pattern occurs. Within the canopy gaps of this lattice litter dams occur. This juxtaposition may be explained by the relationships portrayed in Fig. 4, as the smaller scale dams are found on a slope segment which has a steeper gradient than the overall gradient encompassing the larger scale arc pattern. However, we have observed, on quite gentle slopes litter dams of greater wavelength and Ludwig and Tongway (1995) have noted fertile patches at a variety of scales, including litter trains (i.e., litter dams), that occur within vegetation arc complexes. It remains to be tested, whether these widely spaced litter dams conform to the relationship with gradient presented here.

Fourth, the disjunction between the two parallel lines in Fig. 4 requires an explanation. We remain unsure as to the real meaning of this but note that the type and size of particles transported during arc/dam initiation may be important. For example, in transverse ribs (i.e., regularly spaced gravel bands aligned normal to flow), wavelength is inversely proportional to gradient but proportional to maximum grain size (gravel) transported (Koster, 1978; Allen, 1982). Any sheetflood event producing vegetation arcs might be expected to be capable of transporting gravel bedload as well as litter (floating load). Wells and Dohrenwend (1985) report on arcuate sheetflood bedforms on unchannelled alluvial fan surfaces that contain fine gravel. Thus particle size and particle density (lower density litter compared to higher density mineral and rock fragments) may also prove to be important parameters in predicting wavelength.

The development of litter dams occurs during runoff events of small to moderate magnitude (Mitchell and Humphreys, 1987) and this development can be observed in real time. It has been suggested that sheet wash is also important in the development of vegetation arcs (Boaler and Hodge, 1964; White, 1971). However, the arid to semi-arid environments where vegetation arcs are commonly found are affected also by high magnitude runoff events. Do vegetation arcs form by gradual accumulation or are they a product of rare but large magnitude sheet flood events? Patton et al. (1993) describe vegetation arc-like features along the Ross River in Central Australia as large, low-relief transverse bedforms. They interpret these bedforms as products of a high magnitude paleo-flood event. However, the organic debris that contributes to these bedforms presumably was transported as floating load. Consequently, their bedforms may have developed gradually. The gradual accumulation of material is not unexpected as the organic debris provides seeds and added nutrients, and the resulting vegetation improves sediment trapping efficiency whether or not subsequent transport is via fluvial or aeolian processes. Nevertheless, this does not negate the possibility of an extreme event establishing an initial pattern that is subsequently modified over time via geomorphic processes in conjunction with ecological mechanisms.

5. Conclusion

This paper seeks to assess the appropriateness of using litter dams as an analogy to vegetation arcs. Vegetation arcs, although two to three orders of magnitude larger in wavelength, are similar to much smaller litter dams in terms of shape, orientation, cross-sectional profiles and in the types of surface features encountered. Analysis of wavelength and slope data for arcs and dams shows that spacing between arcs and dams is strongly associated with slope of the land-surface, possibly reflecting the relative importance of runoff as a major factor in determining wavelength of both arcs and dams Furthermore, both data sets have regression equations with the same slope value of -0.855. We suggest that this reflects similarities in mechanisms of formation of arcs and dams. However, arcs and dams plot as separate populations and this implies an important difference between them. Whether the difference in intercepts with the ln(wavelength) axis is merely a reflection of the difference in scale, with or without change(s) in operation of a similar slope-related mechanism, or, alternatively, indicates that a quite separate set of mechanisms is involved, awaits future research.

The formation of litter dams is readily observable and appears to be dependent entirely on rainwash moving particles downslope during a single rainfall event. The question of origin of arcs, however, may be difficult to resolve. We have seen at Fowlers Gap that vegetation arcs are a focal point of relatively intense bioturbation. If this is also true of other locations, the evidence needed to evaluate their origin may have been severely disturbed. We suggest that future research incorporate detailed stratigraphic, sedimentological, pedological and chronological based studies with an evaluation of past and present geomorphic and ecological processes if the question of origin is to be resolved. An essential part of this will be to seek an explanation of mechanisms which may operate at different spatial and temporal scales from the patterns themselves, either

Appendix A

ARCS-data source	Gradient (m/m)	Wave-length (m)	Band type	DAMS-data source	Gradient (m/m)	Wave-length (m)	Band type
Patton et al., 1993	0.0034	119	bedform	Eddy et al., 1996a,b	0.060	0.5	litter dam
Boaler and Hodge, 1964	0.0049	68.6[a]	Chrysopogon grass arcs in woodland	Mitchell and Humphreys, 1987	0.017	1.26	litter dams in dry sclerophyll woodland
	0.0049	256			0.047	1.07	
	0.0040	48.8			0.052	1.035	
	0.0039	94.5	Chrysopogon arcs in grass plain		0.070	0.235	
	0.0040	152.4			0.070	0.29	
	0.0040	45.7			0.070	0.315	
	0.0040	91.5			0.089	0.255	
	0.0022	132.6			0.089	0 285	
	0.0022	161.5			0.105	0.26	
	0.0037	159	Andropogon grass plain		0.125	0.16	
	0.0053	103.6			0.142	0.23	
Macfadyen, 1950a	0.0025	137	Acacia trees	Allen, 1982	0.016	1.45	debris bars; pine needles

Worrall, 1959	0.0036	32	Butana grass		0 017	1.38
	0.0083	38			0.018	0.78
	0.0044	28			0.024	0.35
	0.0043	54			0.027	0.33
	0.0059	40			0 033	0.19
	0.0062	35			0.033	0.32
Worrall, 1960	0.0028	249	tree bands		0.034	0.37
	0.0021	101			0.038	0.34
	0.0009	233			0.041	0.26
Mabbutt and Fanning, 1987	0.0119	37	mulga trees		0.046	0.35
	0.0033	48			0.050	0.25
	0.0058	83.5			0.054	0.18
Dunkerley and Brown, 1995	0.0117	37.5	saltbush		0.058	0.15
	0 0137	24			0.063	0.21
Ludwig and Tongway, 1995	0.0032	167	mulga trees		0.066	0.16
Eddy et al., 1996a,b	0.015	12	mallee		0.068	0.19
					0.072	0.20
					0.072	0.18
					0.110	0.21
					0.110	0.16
					0.120	0.13

[a]Measurements (Boaler and Hodge, 1964) to first decimal place result from conversion from feet to metres, rather than a higher degree of accuracy than other data.

as broader scale constraints or as the combined effect of smaller components of the system (Levin, 1992). Certainly temporal scale variations need to be considered. Arcs may persist for tens to a hundreds of years, while dams, though often ephemeral may remain stable for a few years (observed up to 14 years: Paton et al., 1995). Individual plant and plant community life cycles need to be considered in this context as well as spatial variation that these cycles may impose.

Acknowledgements

References

Allen, J.R.L., 1982. Sedimentary Structures, Their Character and Physical Basis, Vol. II. Elsevier, Amsterdam, 663 pp.

Boaler, S B., Hodge, C.A.H., 1964. Observations on vegetation arcs in the northern region, Somali Republic. J. Ecol. 52, 511–544.

Dunkerley, D.L., Brown, K.J., 1995. Runoff and runon areas in a patterned chenopod shrubland, arid western New South Wales, Australia. characteristics and origin. J. Arid Environ. 30, 41–55.

Eddy, J., Hart, D.M., Humphreys, G.S., 1996a. Spatial sequence of soil crusts within litter dams and microterraces in the Pilliga State Forests, N.S.W. Australian and New Zealand National Soils Conference 1996, Vol. 3: pp. 67–68.

Eddy, J. Humphreys, G.S., Mitchell, P.B , 1996b. Litter dams and microterraces—an overview. Australian and New Zealand National Soils Conference 1996, Vol 2: pp 67–68.

Gallart, F., Puigdefábregas, J., del Barrio, G., 1993. Computer simulation of high mountain terracettes as interaction between vegetation growth and sediment movement. Catena 20, 529–542.

Gillison, A.N., Brewer, K.R.W., 1985 The use of gradient directed transects or gradsects in natural resource surveys. J. Environ. Manage. 20, 103–127.

Greene, R.S.B., 1992. Soil physical properties of three geomorphic zones in a semi-arid mulga woodland Aust. J. Soil Res. 30, 55–69.

Greenwood, J.E G W., 1957. The development of vegetation patterns in Somaliland Protectorate. Geograph. J. 123, 465–473.

Humphreys, G.S., 1994. Bowl structures: a composite depositional crust. In: Ringrose-Voase, A J., Humphreys G.S. (Eds.), Soil Micromorphology: Studies in Management and Genesis. Proc. IX Int. Working Meeting on Soil Micromorphology, Townsville, Australia, July, 1992 Developments in Soil Science 22, Elsevier, Amsterdam, pp 787–798.

Koster, E.H., 1978. Transverse ribs: their characteristics, origin and paleohydraulic significance. In: Miall, A D (Ed.), Fluvial Sedimentology Can Soc Petrol. Geol. Memoir No. 5, pp 161–186.

Lefever, R., Lejeune, O., 1997. On the origin of Tiger Bush. Bull. Math. Biol. 59 (2), 263–294

Levin, S.A., 1992 The problem of pattern and scale in ecology. Ecology 73 (6), 1943–1967.

Ludwig, J.A., Tongway, D.J , Marsden, S.G., 1994. A flow-filter model for simulating the conservation of limited resources in spatially heterogeneous, semi-arid landscapes Pacific Conservation Biol. 1, 209–213

Ludwig, J A., Tongway, D.J., 1995. Spatial organisation of landscapes and its function in semi-arid woodlands, Australia. Landscape Ecol 10, 51–63.

Mabbutt, J.A., Fanning, P.C., 1987. Vegetation banding in arid Western Australia. J. Arid Environ. 12, 41–59.

Macfadyen, W.A., 1950a Soil and vegetation in British Somaliland. Nature 165, 121.

Macfadyen, W.A., 1950b. Vegetation patterns in the semi-desert plains of British Somaliland. Geograph. J. 116, 199–211

Mitchell, P.B., Humphreys, G.S., 1987. Litter dams and microterraces formed on hillslopes subject to rainwash in the Sydney Basin, Australia. Geoderma 39, 331–357.

Montaña, C., Lopez-Portillo, J., Mauchamp, A., 1990. The response of two woody species to the conditions created by a shifting ecotone in an arid ecosystem J. Ecol. 78, 789–798.

Montaña, C., 1992. The colonization of bare areas in two-phase mosaics of an arid system J. Ecol. 80, 315–327.

Paton, T.R., Humphreys, G.S., Mitchell, P.B., 1995. Soils: a new global view. UCL Press, London, 213 pp.

Patton, P.C., Pickup, G., Price, D.M., 1993. Holocene paleofloods of the Ross River, Central Australia. Quaternary Res. 40, 1–11.

Slatyer, R.O., 1961. Methodology of a water balance study conducted on a desert woodland (*Acacia aneura* F Muell.) community in Central Australia. Arid Zone Res. 16, 15–26.

Specht, R.L , 1970. Vegetation. In: Leeper, G.W. (Ed.), The Australian Environment, 4th ed., CSIRO and Melbourne Univ. Press, pp. 44–67.

Stace, H.C.T., Hubble, G.D., Brewer, R., Northcote, K.H., Sleeman, J.R., Mulcahy, M.J., Hallsworth, E.G., 1968. A Handbook of Australian Soils. Rellim, Adelaide, Australia.

Soil Survey Staff, 1992. Keys to Soil Taxonomy, 5th edn., SMSS Technical Monograph No. 19.

Thiéry, J.M., D'Herbès, J.-M., Valentin, C., 1995. A model simulating the genesis of banded vegetation patterns in Niger. J. Ecol. 83, 497–507.

Tongway, D., 1994. Rangeland Soil Condition Assessment Manual. Division of Wildlife and Ecology, CSIRO, Australia.

van Zon, H.J M., 1980 The transport of leaves and sediment over a forest floor. A case study in the Grand Duchy of Luxembourg. Catena 7, 97–110.

Wells, S.G., Dohrenwend, J C., 1985. Relict sheetflood bed forms on late Quaternary alluvial-fan surfaces in the southwestern United States. Geology 13, 512–516.

White, L.P., 1969. Vegetation arcs in Jordan. J. Ecol 57, 461–464.

White, L.P., 1970. Brousse Tigree patterns in southern Niger. J. Ecol. 58, 549–553.

White, L.P., 1971. Vegetation stripes on sheet wash surfaces. J. Ecol. 59, 615–622.

Worrall, G.A., 1959. The Butana grass patterns. J. Soil Sci. 10 (1), 34–53.

Worrall, G A , 1960 Tree patterns in the Sudan. J. Soil Sci. 11 (1), 63–67.

Banded vegetation near Broken Hill, Australia: significance of surface roughness and soil physical properties

D.L. Dunkerley [*], K.J. Brown

Department of Geography and Environmental Science, Monash University, Clayton, Victoria, Australia

Abstract

Selected physical properties of the soils developed within a strongly-banded grassland in arid New South Wales were investigated to reveal their possible significance for the hydrologic and erosional behaviour of the mosaic landscape. Detailed surface microtopography, surface roughness, soil bulk density and the unconfined compressive strength of the soils were determined using linear transects across the banded mosaic. The landscape is shown to consist of a tier of concave-upward microtopographic elements. Results indicate that the cross-pattern (downslope) variation in the soil parameters is systematically related to position within a particular component (grove, intergrove, etc.) of the mosaic. Compressive strength and bulk density increase downslope across intergroves, peaking at very high levels within the zone of forbs, while groves display lower but more uniform values. Surface roughness increases downslope through the intergrove and the zone of forbs at the upslope margin of a grove, reaching its maximum within the grove. Mosaic components thus cannot be treated as uniform in their soil properties, and single samples from within a component are shown in general to be inadequate. The mapped pattern of soil properties implies a very stable configuration for banded mosaics. Surface runoff is increasingly hindered during flow from the intergrove onto the grove. At the same time, soil resistance to entrainment increases in opposition to the shear forces generated by the runoff. In concert, these tendencies imply that little sediment transport is possible across the mosaic. The resulting landscape stability appears to confer robustness to the mosaic in the face of stresses such as drought and pastoralism, when plant cover may be temporarily thinned or absent. After drought, for example, water ponding would again begin at the downslope margin of the concave

---

[*] Corresponding author

topographic elements, fostering re-establishment of the groves. © 1999 Elsevier Science B.V. All rights reserved.

Keywords: Concave-upward element; Runon/runoff patterns; Mosaic landscape

1. Introduction

Relatively little is known about the extent of pattern-related variation in the physical properties of soils within the banded mosaic landscapes of dry regions. Most published data (e.g., Cornet et al., 1988) deal with distributions of moisture and plant nutrients. However, the most fundamental property of banded mosaics is the pattern of runoff and runon that sustains them. This is dominated by differences in the physical properties of the soils among mosaic components, notably their infiltration properties and their erosional behaviour. Many authors (e.g., Mabbutt and Fanning, 1987; Tongway and Ludwig, 1990) have drawn attention to the subdued microtopography associated with vegetation banding. This is evidently the result of differential erosion and deposition, together with shrink–swell phenomena. Given that surface sediment transport processes are size-selective, it seems reasonable to suppose that the microtopography, and the changing surface gradient associated with it, is associated with physical differences in the near-surface regolith. Some parameters, such as soil strength, are clearly relevant to the detachment of grains by splash or surface runoff. Others, including primarily the surface roughness, are important in the behaviour of the runoff that carries sediment following detachment. On a given gradient, flow speeds and shear stresses are inversely proportional to the roughness. The opportunity time for infiltration is promoted by surface roughness acting to retard flow, and at the same time, since flow speeds are lowered, surface scour must be restricted. Two simple parameters, unconfined compressive strength (UCS) and bulk density (ρ_b), were adopted in the present work as two soil properties relevant to these various processes.

The goal of the work was to investigate the variation in these soil properties and in soil surface roughness within a strongly-banded vegetation community. Data on the variation in these properties allows the development of hypotheses about the processes that take place during the infrequent episodes of surface runoff that are more difficult to observe directly.

Most field observations were replicated at two adjacent sites, less than 0.5 km apart, that display clear contrasts in band width. The goal of examining these two sites was to evaluate the possible role of soil factors in influencing the contrasting mosaic geometries. Since the sites were adjacent, other potentially influential factors such as rainfall environment, evaporative water losses and grazing pressure, could be excluded from consideration.

2. The field study area

The study site was located within a broad area of banded shrublands and grasslands in the Broken Hill region of western New South Wales. Mosaic landscapes also extend

into nearby areas of South Australia. The observations reported here were obtained at a site about 40 km SE of Broken Hill, in a mixed shrubland–grassland community (see Fig. 1). We refer to the two adjacent sites examined here as Menindee sites 1 and 2.

The climate of the region is arid, with an annual rainfall of approximately 240 mm. Summers are hot and dry, while winters are mild. The mean maximum temperatures for January and July are 33°C and 16°C, respectively, while the mean minimum temperatures are 19°C and 5°C. Rainfall through the region is sporadic and unreliable, with a coefficient of variability of approximately 50%. On the average, rain falls on about 44 days per year (Bureau of Meteorology, 1988).

Vegetation at site 1 consists almost entirely of tussock grasses of the species *Astrebla pectinata* (Barley Mitchell grass) though some shrubs, such as copperburr (*Bassia ventricosa*) and saltbush (*Atriplex vesicaria*), are present on the downslope section of individual bands. Such shrubs are more abundant than grasses at site 2. On the upslope edge of each vegetated band, ephemerals appear rapidly after rain. The bare bands are completely devoid of vegetation over large areas, though occasional ephemerals are present.

The rainfall regime of SE Australia is influenced by the El Niño-Southern Oscillation (ENSO) phenomena, and the study site undoubtedly experiences periodic droughts of 1–2 years, followed by similar periods of above average rainfall (Nicholls, 1991).

Low-intensity sheep grazing has been practiced in the area for more than 100 years, the entire landscape being partitioned into pastoral properties. We therefore infer that the mosaic patterning is sufficiently robust to survive both drought and prolonged grazing.
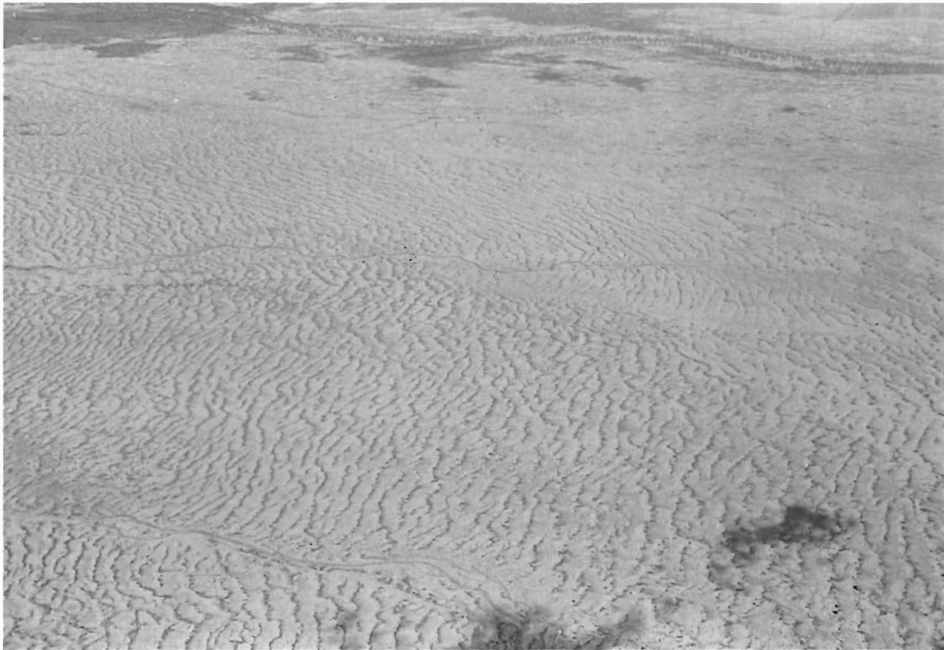
Fig. 1. Aerial photograph of typical banded mosaic landscape in the study area.

Undoubtedly, however, variations in landscape condition do occur. A 1995 field inspection of a South Australian site that displayed strikingly regular banding on aerial photographs taken in 1968 revealed only a rather diffuse vegetation zonation. However, the site did display very strongly-developed microrelief associated with the banding, similar to but considerably more pronounced than that revealed in the detailed surveys made at the Menindee sites. We are as yet unable to place the Menindee sites in the continuum of site condition, though certainly the vegetation banding in 1995, when our fieldwork was conducted, was strikingly regular and sharply defined, and though dry, vegetation cover in the groves was extensive.

3. Field methods

Transects spanning multiple wavelengths of the banded grassland were set out with markers. Detailed topographic profiles along these transects were derived from careful survey with a digital electronic distance measuring theodolite. Surveys of band margins were also made to assess the degree of contour-parallelism of the banding. The theodolite target, equipped with a broad supportive baseplate, was positioned gently to avoid disturbing the soil surface elevation across soils of varying mechanical properties.

Unconfined compressive strength of the uppermost 1–3 cm of regolith was measured at 1-m intervals along the transects with a hand-operated penetrometer equipped with interchangeable domed tips. Bulk density was evaluated from small cores extracted at points adjacent to the strength measurement sites. Since the site was under intense summer sun, with strong hot winds, no air drying of samples was performed. A 54-mm i.d. corer yielding 100-cm^3 samples was pushed into the soil and carefully removed by excavating around it. The samples were weighed in the field on a battery-powered balance accurate to 1%. To yield a larger sample volume, at each meter along the transects two cores were extracted and the mean value of ρ_b recorded.

Surface roughness was assessed in two ways. Within intergroves and the zone of small forbs which lies just upslope of groves, an $x–y$ profilemeter was used. This consisted of a 1 m $\times$ 1 m frame set on short legs. A travelling gantry mounted on this frame carried a rod which could be lowered vertically to touch the surface. The standard deviation of 100 point elevations measured to the nearest 1 mm on a 10-cm grid was used to quantify surface roughness. Within groves, measurements of this kind were not possible because of the dense tussocks and the greater surface roughness arising from crabhole collapse pipes. A survey of 60 points on a 1-m grid was therefore carried out for each grove with the digital theodolite. Elevations were again recorded with a precision of 1 mm and the standard deviation of the elevations calculated.

Plant canopy cover and surface stone cover were estimated from vertically-oriented photographs taken with a remotely-triggered camera held 2.5 m above the ground on a boom. Coloured slides were later projected onto a grid having 100 nodes and cover fraction estimated by counting occurrences on this grid. Photographs were taken at roughly the mid-point of each grove and intergrove along the study transects. The data from a transect were pooled and mean values for grove and intergrove sites along that transect recorded.

4. Results

The dimensions of the bands and the slopes and surface cover of the various mosaic components are set out in Table 1. Fig. 2 shows the topographic profiles of two study transects. Both show repeated cycles of the microtopography associated with the vegetation banding, though this is more regular in form at site 2. Site 1 lies on a gentler overall gradient than site 2 and it displays wider bands and interbands. However, the ratio of grove width:intergrove width also varies. At site 1, groves are on average 2.3 times wider than intergroves; at site 2, the factor is only 1.3. Thus, it would appear that a unit area of vegetation at site 1 requires less runoff-contributing area than that at site 2. Likewise, at site 1, the groves are on average 3.1 times steeper than the intergroves, while at site 2, the factor is only 2.3 times steeper.

Contour parallelism of the banding was confirmed. A 100-m segment of a typical upslope grove border showed a mean departure from the average elevation of only 2.3 cm. In contrast, the typical elevation change across a 25-m wide grove in this area (i.e., through only a quarter of the distance) is 20 cm. Thus, the upslope margins of the groves do indeed quite closely follow a constant elevation. This is especially noteworthy as these margins lie adjacent to the steepest and gentlest gradients in the landscape, so that any lack of contour-parallelism could result in significant elevation changes along the boundary.

The form of microtopography in the longitudinal profiles is very similar to that reported in a shrubland 150 km distant by Dunkerley and Brown (1995). The surface consists of a series of concave-upward elements. Each element begins with the relatively steep zone of grasses. The gradient then declines smoothly and steadily through the grove and the intergrove, ending, at site 1, at the zone of forbs, which sits on a very slight depositional ridge. At site 2, this feature was not recorded. The next grove is marked by another increase in gradient. There is no break of slope within these elements, but rather a smooth decline in gradient; the sharp breaks of slope evident in the profiles are the borders of successive microtopographic elements.

Were it not for the evident integrity of these elements, it would be intuitively reasonable to think of the mosaic as being made up of runoff source areas bordered downslope by a runon zone supporting plants. However, the repeating microtopographic

Table 1
Summary data for Menindee sites 1 and 2

Parameter	Menindee site 1	Menindee site 2
Mean grove width (m)	26.9	11 7
Mean intergrove width (m)	11.4	8 7
Mean grove relief (m)	0.14	0 2
Mean intergrove relief (m)	0.02	0.06
Overall mean hillslope gradient (°)	0.23	0.76
Mean grove gradient (°)	0.31	0.88
Mean intergrove gradient (°)	0.10	0.39
Mean plant canopy cover in groves (%)	35.5	33.5
Mean surface stone cover in intergroves (%)	6.7	6.3
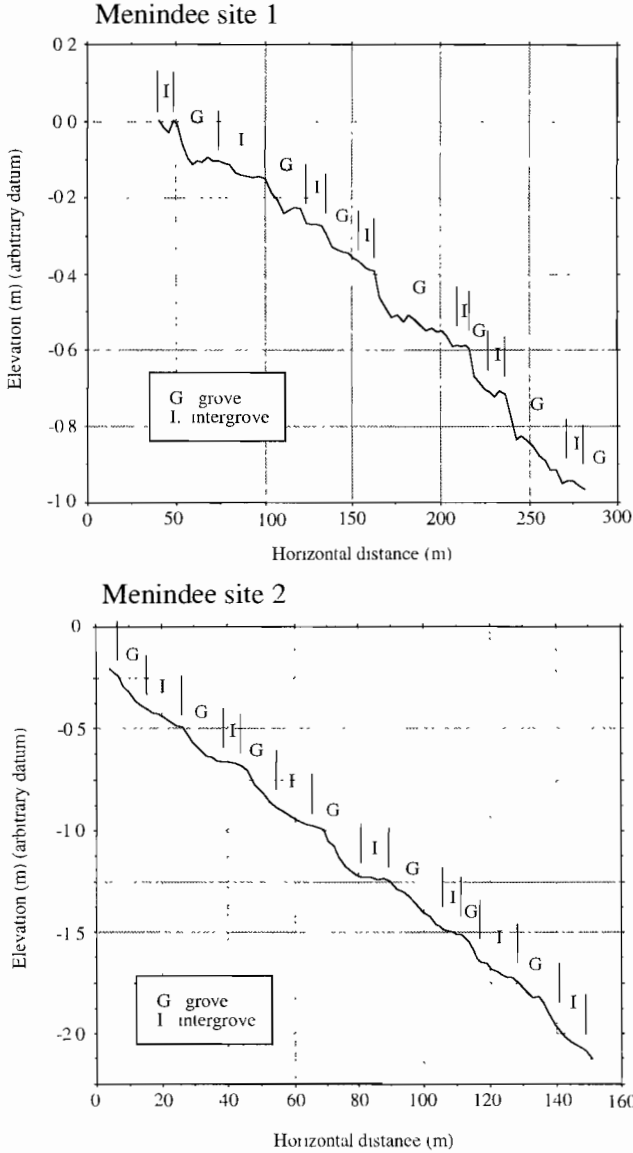
Fig. 2. Topographic profiles of Menindee sites 1 and 2. (Note scale differences between plots.)

elements just described have the runon zone upslope and the runoff zone below. Therefore, the elements appear to function as follows: plants colonise an area which receives sufficient runoff water from upslope. Water retention occurs very strongly among the plants, so that less is passed on to plants successively further downslope. After a distance set by water balance and plant requirements, insufficient water remains available, and the grove dies out, giving way to an intergrove. Runoff volume increases
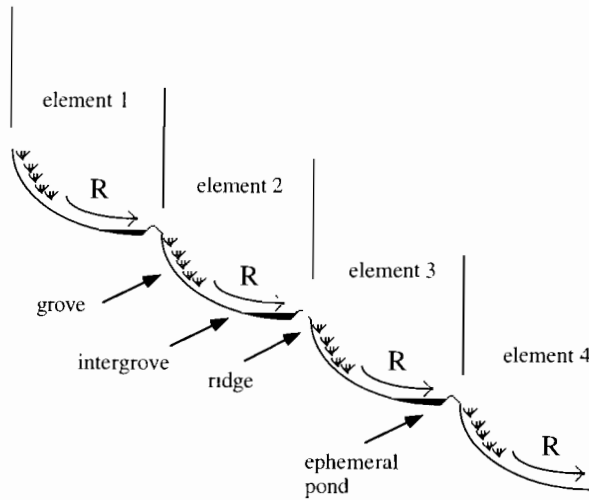
Fig. 3 Schematic diagram of the microtopographic framework adopted for the description of banded mosaic characteristics.

progressively here, and, when sufficient is available, another grove of plants can be supported by trapping the runoff. The concave-upward element can thus be accepted as a functional entity within banded mosaics of the kind studied here. Development of banded mosaics using this conception has successfully been simulated in a model presented by Dunkerley (1997a,b). The underlying functioning of the elements is schematised in Fig. 3.

This shows that the upslope, steepest part of the element loses little runoff water downslope. It follows that only restricted loss of nutrients or sediments can occur in runoff from this zone. However, as the grove gives way to the following intergrove, increasing amounts of these materials could in principle be removed in the runoff water. But once the threshold of adequate water availability is reached, a new grove develops and the mobile materials are trapped. Ponding of water and sediment deposition occur at the upslope margin of the grove. Forbs there colonise a small ridge which acts to promote laterally extensive ponding, and the distribution of available water among many plants along the border of the grove.

The remaining data will be presented in the context of this repeating concave-upward microtopographic element.

5. Unconfined compressive strength of mosaic soils

The unconfined compressive strength (UCS) data are consistent with the interpretation of mosaic behaviour just sketched. Profiles of UCS, together with the boundaries of the mosaic components, are shown in Fig. 4 and summary UCS and bulk density data are included in Table 2.

Menindee site 1
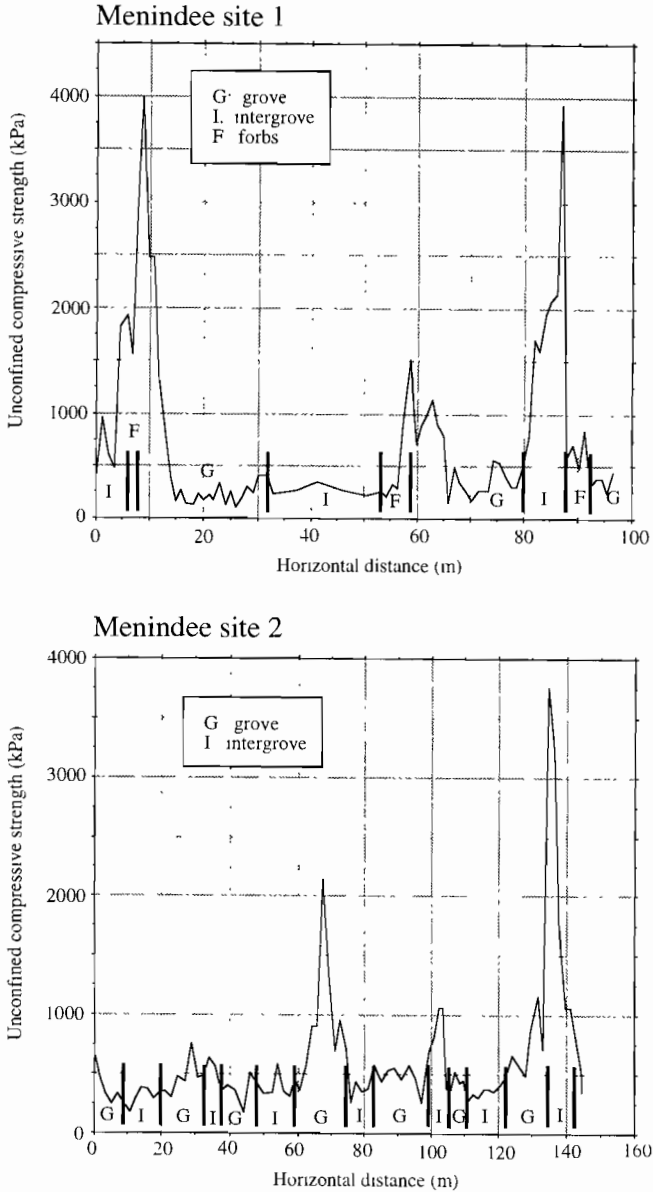
Menindee site 2

Fig. 4. Profiles of UCS across Menindee sites 1 and 2.

The patterns of UCS are not entirely regular. However, profiles at both sites display values that generally remain below 500 kPa. Periodically, the values climb over slope distances of 10–20 m to peaks in excess of 2000–3000 kPa. These peaks were very evident in the field, requiring that a smaller size of interchangeable tip be fitted to the penetrometer so that the soil strength could be overcome. At site 1, the three prominent

Table 2
Summary soil strength data for Menindee sites 1 and 2

Location	Menindee site 1				Menindee site 2			
Parameter	UCS (kPa)		ρ_b (g/cc)		UCS (kPa)		ρ_b (g/cc)	
Mosaic element	Mean	Standard deviation	Mean	Standard deviation	Mean	Standard deviation	Mean	Standard deviation
Inter-grove	1086	987	1.37	0.15	388	130	1.39	0.11
Forbs	1001	839	1.48	0.10	n/a	n/a	n/a	n/a
Grove	582	720	1.33	0.11	415	145	1.41	0.15

n/a: data not available.

peaks in the UCS data are associated with the zone of forbs, two lying at the forbs–grove boundary. At site 2, two of the UCS peaks occur within the intergroves, while one lies within a grove. The demarcation of the boundaries of mosaic elements in the field involves the exercise of judgement and has some uncertainty attached to it, and not all cycles of the banding are associated with peaks in soil UCS. However, since five of the six peaks in UCS are located in intergroves, especially the lowermost parts of intergroves, it seems reasonable to infer that soil UCS tends to be highest there. Formal statistical testing of differences among the zones is made difficult by their variability. A *t*-test for differences in the mean values of UCS and ρ_b (Freund, 1974, p. 281) at site 1, where our sample size is largest, showed that groves were significantly different in both characters (0.05 level) from both intergroves and the zone of forbs. No significant difference could however be established between the intergroves and the zone of forbs in either property. We have collected no data which isolate the mechanisms responsible for the strength fluctuations. There may be greater amounts of cementing agents such as carbonates or clays delivered from upslope. Better-developed surface rainbeat crusting might also contribute to soil strength. Though chemical and micromorphologic studies will be required to investigate this pattern more fully, the trends noted accord well with the idea of increasing deposition of binding agents of some kind within the lower parts of the microtopographic elements. The absence of peaks in soil UCS associated with some bands may reflect inadequacy of our sampling scheme, which was restricted to a single-line transect at each site, or lateral variations in the efficiency with which cementing agents are deposited or retained, perhaps in relation to patchiness in the surface roughness or plant cover, or the locations of ephemeral ponds.

6. Bulk density of mosaic soils

Trends in our bulk density data are less clear than those displayed by UCS. Nonetheless, ρ_b appears to reach its highest levels at the downslope border of the microtopographic elements. At site 1, prominent peaks in ρ_b were recorded at or near the zone of forbs. Within the groves, ρ_b fluctuates irregularly and tends to be lower than in intergroves. This is perhaps to be expected given that grove soils undergo extensive cracking and shrink–swell phenomena. The soils in groves are thus a patchwork of

recently-compressed and recently-dilated zones. Once again, though, the explanation of the absolute values of ρ_b encountered has not been elucidated. The patterns recorded seem consistent with the idea that clays or cementing agents are carried to the lower parts of the microtopographic elements by runoff water, as noted earlier in the discussion of UCS, partially filling void spaces within the soils and increasing the bulk density. The data are also consistent with relatively more frequent dilation of soils within the groves and with their more abundant organic matter, and hence with a more porous, open and friable soil structure. This was confirmed during excavations made at the field sites. However, bulk density data spanning more cycles of the banding are required for a fuller analysis of spatial variation in this parameter.

7. Surface roughness within the mosaic components

Finally, we turn to the surface roughness data, presented in Table 3. Data are only available for site 1.

The data, which are means of two analyses for each mosaic component, show highest roughness within the upslope parts of the microtopographic elements (the groves). This gives way to very low roughness in the intergrove below. Finally, within the zone of forbs, at the flat downslope margin of the elements, roughness increases slightly. In the field, reasons for the observed values could clearly be noted. Within the groves, the soil surface roughness is great because of disruption caused by shrink–swell phenomena. In the intergroves, the smooth surface, swept by surface runoff, owes its limited roughness primarily to a thin veneer of surface stones. These are often concentrated within the lower parts of the intergrove (see Fig. 5), where they have come to rest, with smaller stones lying in the zone of forbs.

The slightly-elevated roughness within the forbs reflects the presence of these small stones but more importantly, small mounds of material that appear to be depositional in origin. The mounds are localised and separated by swales through which ponded water trickles downslope onto the next element. Forbs colonise these mounds, which can thus be identified in the field even though their relief is really too small to be determined without exacting survey work. Field observation suggests that the intergrove is subdividable into a relatively stone-free (and smoother) upslope part and a stonier and rougher lower part. The lower intergrove, then, displays not only a declining topographic gradient, but also an increasing degree of surface roughness. Roughness within the

Table 3
Summary surface roughness data for Menindee site 1[a]

Mosaic component (Site 1)	Mean roughness (mm)
Grove	18.4
Intergrove	2.6
Zone of forbs	4 2

[a] Data are standard deviations of gridded elevation data; see text for explanation.
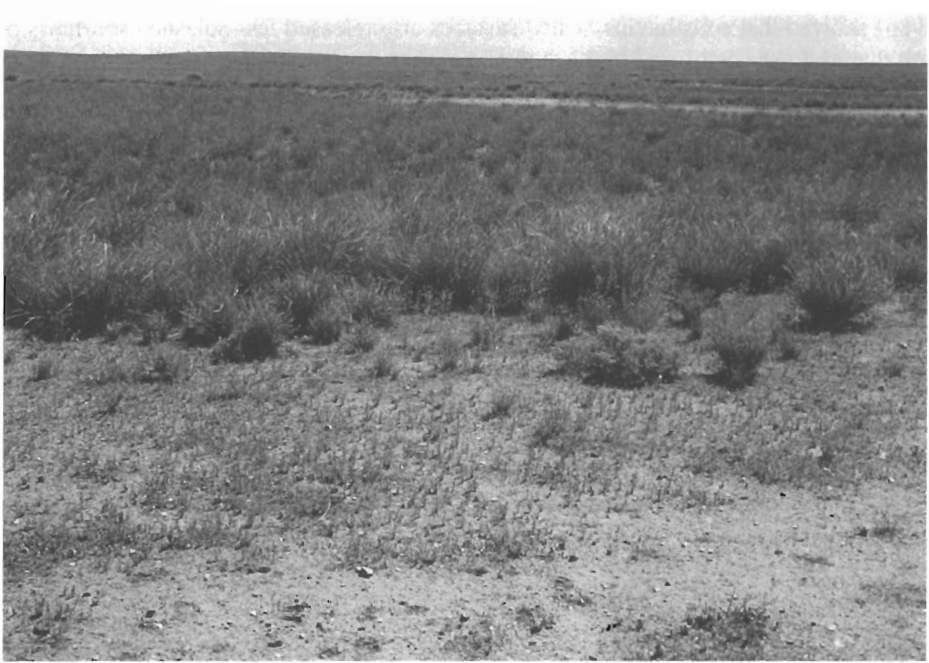
Fig. 5. View downslope over the lowermost part of a typical intergrove at Menindee site 1. The bare intergrove gives way to the zone of forbs in the foreground. Behind this, the upslope border of the grove is marked by a line of tussocks invigorated by recent rain. Subsequent intergroves are visible in the distance. Width of grove border in foreground is approximately 5 m.

groves appeared to be relatively uniform, with no or only negligible surface stone cover and shrink–swell features evident throughout.

8. Discussion

The landscape consists of shallow basins, which appear to conserve water and sediment on the hillslope with high efficiency. The soil physical properties assessed reveal that groves display the greatest internal uniformity, although the uppermost parts of groves may display elevated values of UCS akin to those of intergroves. Intergroves, and the zone of forbs bordering the groves, in contrast, display gradational changes. This variability means that soil properties cannot be assessed from point-samples. Rather, transect-samples are required in order to delimit the degree of variability within these components of the mosaic.

The great strength displayed by the soils of the downslope parts of intergroves and within the zones of forbs may be quite significant in the persistence of these mosaic landscapes. The mechanical strength limits grain dislodgment by raindrop splash despite the bareness of the intergroves. Al-Durrah and Bradford (1981) showed in single-drop experiments that the mass of splashed soil material diminished as soil shear strength and soil bulk density increased in uncrusted soils. From similar experiments, Bradford et al.

(1986) showed that soils having sealed surfaces also released less splashed soil mass per drop than did unsealed soils. In the study area, intergrove soils display high strength and bulk density and are also sealed, so that splash detachment must thus be restricted by all three characteristics. Though weaker, of lower bulk density and uncrusted, the soils of the groves are partially protected by the much more extensive plant canopy cover and leaf litter, so that there, too, splash detachment and transport is likely to be restricted. The same kinds of limitations apply to the entrainment of regolith particles by the shear forces developed in surface runoff. Within the groves, runoff must be extremely rare, so that little entrainment can occur there, while in the intergroves where runoff does occur, the soil surface displays very high strength. Thus, in the face of shear forces as well as raindrop impact, the surface appears to be extremely stable. The UCS data analysed here were derived under dry conditions, whereas the character of wet soils may be more important. Though we would expect the absolute values to change, the general trends in strength appear likely to persist.

Given its robustness, the microtopography created by erosion and deposition, as well as by shrink–swell, appears capable of enduring within the landscape even when the plant cover is altered by drought or grazing pressure. The microtopography may thus form a better framework for studying landscape hydrology and erosion than does the zonation of plants, which may be labile.

9. Grove and intergrove dimensions

Neither the plant canopy cover fraction within the groves nor the surface stone cover within the intergroves were significantly different between the two study sites. Nor were the soil properties examined able to distinguish between the sites. However, the grove and intergrove widths were significantly different (see Table 1), as were the grove width:intergrove width ratios. We conclude that the soil physical properties examined here, though clearly important in mosaic behaviour, are not those that control mosaic dimensions such as these.

Since the groves at site 1 were supported by a smaller area of intergrove but lie within the same external climatic environment, then either more runoff is generated from a unit area of intergrove at site 1 or the efficiency with which groves trap and hold water (including rain falling directly onto the grove) is greater there, or both.

Since the steeper intergroves at site 2 promote runoff, stronger grove water retention is required at site 1. The abundant leaf litter from the grasses at site 1 would provide additional protection of the soil surface against raindrop splash, as well as contributing to ephemeral litter barriers. These are associated with enhanced trapping of sediment and organic detritus and may trigger the accumulation of the low sediment ridge. During a field visit a few weeks after some rain had fallen, we observed abundant green leaves in the uppermost parts of the groves at site 1, but no such effect among the shrubs at site 2. Thus, rapidly-increased density of plant growth along the upslope grove border dynamically increases water trapping efficiency among the grasses, especially in sequences of rain events occurring over several weeks. The significance of the time sequence of rain events for grove hydrologic behaviour seems thus to be an important topic that we hope to address in later work.

10. Conclusions

There is clearly much to be learned about the study sites. However, several conclusions can be drawn from the work reported above.

(1) The stability and longevity of banded mosaic landscapes is enhanced by patterns of soil differentiation that evolve within the mosaic. In particular, the microtopographic elements that compose the mosaic are associated with spatial variations in soil strength and bulk density, as well as surface roughness, that oppose entrainment of materials by splash and surface runoff.

(2) The roughness data derived from site 1 show clearly that there are very significant variations in surface roughness among mosaic components. The great roughness of the groves reflects many small depressions where water may pond and slowly infiltrate. The very smooth intergroves, with hard rainbeat crusts, partially-swept free of stones, provide an efficient surface for runoff generation.

(3) Deposition at the gentle base of each concave element has resulted in the formation of a small ridge. This physical feature probably acts as a barrier to runoff and encourages laterally extensive water ponds. Since this behaviour would occur even in the absence of the plant cover, it provides a mechanism by which the water partitioning can persist in the face of drought or other pressure and the mosaic rapidly recover, upon the return of more favourable conditions. The extremely high soil strength displayed within the lowermost parts of the microtopographic elements would add to the robustness of the surface form even when unvegetated.

(4) The dimensions of mosaic elements are controlled by a complex set of influences. Water shedding and trapping efficiencies may vary with site characteristics such as the slope steepness, the abundance of litter and litter dams and the density and dimensions of plant stems or surface stones acting as surface roughness elements. Finally, it is clear that the rapidity of plant response to rain and the temporal distributions of rain events, may both be involved in a quite dynamic process of adjustment in grove water trapping efficiency. This is an important conclusion, since it suggests that in situ infiltration capacity data, taken under a limited set of field conditions, may not be sufficient to characterise site behaviour.

Acknowledgements

References

Al-Durrah, Bradford, 1981. New methods of studying soil detachment due to waterdrop impact. Soil Sci. Soc. Am. J. 45, 949–953.

Bradford, J.M., Remley, P.A., Ferris, J.E., Santini, J.B., 1986. Effect of soil surface sealing on splash from a single waterdrop. Soil Sci. Soc. Am. J. 50, 1547–1552.

Bureau of Meteorology, 1988. Climatic averages, Australia. Australian Government Publishing Service, Canberra, 532 pp.

Cornet A.F., Delhoume, J.P., Montana, C., 1988. Dynamics of striped vegetation patterns and water balance in the Chihuahuan Desert, pp 221–231. In: During, H.J., Werger, M.J.A., Willems, J.H (Eds.), Diversity and Pattern in Plant Communities. SPB Publishing, The Hague, 278 pp.

Dunkerley, D.L., 1997a. Banded vegetation. development under uniform rainfall from a simple cellular automaton model. Plant Ecology 129, 103–111.

Dunkerley, D.L., 1997b. Banded vegetation: survival under drought and grazing pressure from a simple cellular automaton model. J. Arid Environ. 35, 419–428.

Dunkerley, D.L., Brown, K.J., 1995. Runoff and runon areas in a patterned chenopod shrubland, arid western New South Wales, Australia. characteristics and origin. J. Arid Environ. 30, 41–55.

Freund, J.E., 1974. Modern Elementary Statistics, 4th edn. Prentice-Hall, London, 532 pp.

Mabbutt, J.A., Fanning, P C., 1987. Vegetation banding in arid Western Australia. J. Arid Environ. 12, 41–59.

Nicholls, N., 1991. The El Niño/Southern Oscillation and Australian vegetation. Vegetatio 91, 23–36.

Tongway, D J., Ludwig, J.A, 1990. Vegetation and soil patterning in semi-arid mulga lands of Eastern Australia. Aust. J. Ecol 15, 23–34.

The distribution of soluble cations within chenopod-patterned ground, arid western New South Wales, Australia

B.C.T. Macdonald [a,*], M.D. Melville [a], I. White [b]

[a] *School of Geography, University of New South Wales, Sydney, NSW, 2052, Australia*
[b] *Centre for Resource and Environmental Studies, Australian National University, Canberra, ACT, 0200, Australia*

Abstract

The soluble cation (Na, Mg, K, Ca) concentrations of the soils underlying different vegetated/soil surface units were measured within a chenopod-patterned ground complex. It was found that distribution of soil cations within the chenopod-patterned ground is not uniform across the landscape. The data shows that there are at least three chemically distinct zones: the bare, intermediate, and vegetated areas, within chenopod-patterned ground. The bare areas, which are considered salt dumps, are dominated by sodium and its concentration decreases towards the centre of the vegetated arcs. The magnesium and calcium ions have a similar pattern of distribution across vegetated–bare ground transects, but in the vegetated arcs they are relatively more concentrated than the sodium ions. The potassium ions are concentrated in the vegetated arcs and decrease in the bare ground. A model is proposed to explain how the spatial distribution of the soluble soil cations is maintained. © 1999 Elsevier Science B.V. All rights reserved.

Keywords: Soluble cation; Chenopod-patterned ground complex; Vegetated areas; Salt dumps; Gilgai phenomena

1. Introduction

1.1. Worldwide occurrence of patterned ground

Patterned ground is a landscape feature where the spatial variation of vegetated and bare areas are rhythmically repeated. The vegetation usually appears as arcs, stripes, or

---

* Corresponding author.

whorls (Wickens and Collier, 1971), with the main axis parallel to the contour (Montaña, 1992) and separated by bare areas. The vegetated arcs may form approximately continuous lines over a kilometre or more, and from the air, patterned ground looks like the stripes on a tiger skin (Macfayden, 1950) and is known as 'brousse tigrée' (White, 1970). Patterned ground has been reported in many localities around the world including Jordan (White, 1969), North America (White, 1971; Montaña, 1992), The Somali Republic (Macfayden, 1950; Greenwood, 1957; Boaler and Hodge, 1964; Hemming, 1965), and The Sudan (Worrall, 1959, 1960). In these areas it is usually developed in arid grassland and woodland.

Patterned ground also occurs in many parts of arid Australia which are dominated by mulga (*Acacia aneura*): in Western Australia (Litchfield and Mabbutt, 1962; Mabbutt and Fanning, 1987; Mott and McComb, 1979) and New South Wales (Tongway and Ludwig, 1990; Greene et al., 1992). Similar patterns are reported in Western Queensland (Boyland, 1973; Dawson and Ahern, 1973). Patterning has also been described in chenopod shrublands around the Barrier Ranges north of Broken Hill in semi-arid New South Wales (Mabbutt, 1973). Patterned ground as seen from the worldwide perspective occurs in many arid zone localities and is a response of the aridity (Goodspeed and Winkworth, 1978).

1.2. Chenopod-patterned ground

Chenopod-patterned ground of the Barrier Range is generally confined to foot-slopes, which are less than 5%. The microtopography of these slopes redistributes run-off through sheet flow, concentrating it in the vegetated arcs rather than it being uniformly distributed across the landscape (Dunkerly and Brown, 1995).

Mabbutt (1973) made the connection that microtopography of chenopod-patterned ground of the Barrier Range is generated by the 'gilgai phenomena' as a result of the differential wetting and swelling of the clayey subsoil of the vegetated arcs. Washburn (1956) describes a similar process occurring within polar, subpolar and alpine patterned ground which is caused by the freezing and thawing of the subsoil soil. The bare areas were considered the 'mounds', the vegetated areas the 'depressions' and the intermediate areas 'shelves' according to the gilgai descriptions of Hallsworth et al. (1955). The mound soils appear to be better structured than those of the shelf (Hallsworth et al., 1955). Despite the apparently more favourable soil physical properties of the mound, and the possibility of higher available soil water in the depressions or shelf, the differences in the vegetation between the areas are also due to different nutrient levels in the soils (Butler and Hubble, 1977).

The bare mounds and semi-bare shelves are considered run-off zones, while vegetated depressions are run-on zones. This hydrological system is common to all arid forms of patterned ground. The vegetated areas can receive in excess of 100% of total rainfall due to inputs of water from bare areas (Greene, 1992). Run-off water carries nutrients, sediments and seed, further benefiting the vegetated areas. 'Crabholes', which are small depressions averaging 50 cm in diameter and 30 cm in depth (Upton, 1983), are usually associated with the vegetated areas. Boaler and Hodge (1964) recognised that

holes, which are similar to crabholes, within vegetated areas promoted infiltration and acted as a sediment and seed trap. At a smaller scale the distribution of vegetation and soil surface (crusts, etc.) units are controlled by water redistribution within the vegetated area (Bromley et al., in press).

The soils of the bare and vegetated areas have different properties (Wilson and Liegh, 1964) and many writers (e.g., Greig-Smith, 1979; Charley, 1959) have attributed the differences to the presence of vegetation and differential penetration of water. However, the study of patterned ground has generally been confined to the relationship between the hydrological regime and its control and distribution of plant growth and soil crusts. Usually, only a secondary consideration has been given to the soil's chemical and physical properties and subsequently there is a failure to emphasise the spatial variation of soil properties in patterned ground. Studies do exist that have established patterns of association between vegetation distribution and soil properties that range in scale from that of the broad geological province (Noy-Meir, 1974) to that of soil changes around individual shrubs (Charley, 1972). However, there is a lack of data on the chemical properties at a scale underlying different vegetation/soil surface units within the patterned ground complex.

The aim of this paper is to investigate spatial variation of soil chemical properties at an intermediate scale between that Noy-Meir (1974) and that of Charley (1972). It is proposed that there is an association between the different vegetation and soil surface (soil and biotic crusts) units and the underlying soil chemical properties; that bare areas have a relatively larger soluble salt concentration compared to the vegetated areas. A model that explains this distribution, and incorporates vegetation, microtopographic and infiltration differences of a chenopod-patterned ground system will be discussed.

2. The study area

2.1. Environmental characteristics

The study site is located on the University of New South Wales Fowlers Gap Arid Zone Field Station, located approximately 110 km north of Broken Hill in western NSW, (Fig. 1). The stony chenopod-patterned ground site for detailed study is an enclosure, located in Airstrip Paddock, on the rolling stone country to the east of the Coko Ridge, in Nutherungie Landsystem, Unit 1 (Mabbutt et al., 1973).

2.2. The climate

The distribution of annual and seasonal rainfall is very variable for the region in both space and time. Most rainfall is probably delivered in 'wet spells' (Dunkerly and Brown, 1995) and when it does fall it tends to "consist of short bursts of high intensity rain lasting from a few minutes up to an hour" (Bell, 1973). Comparison of the mean potential evaporation (3613 mm Bell, 1973) and rainfall (237 mm Zhou, 1989) throughout the year at Fowlers Gap shows that monthly rainfall is never likely to exceed monthly evaporation. A complete climatic description can be found in Bell (1973).
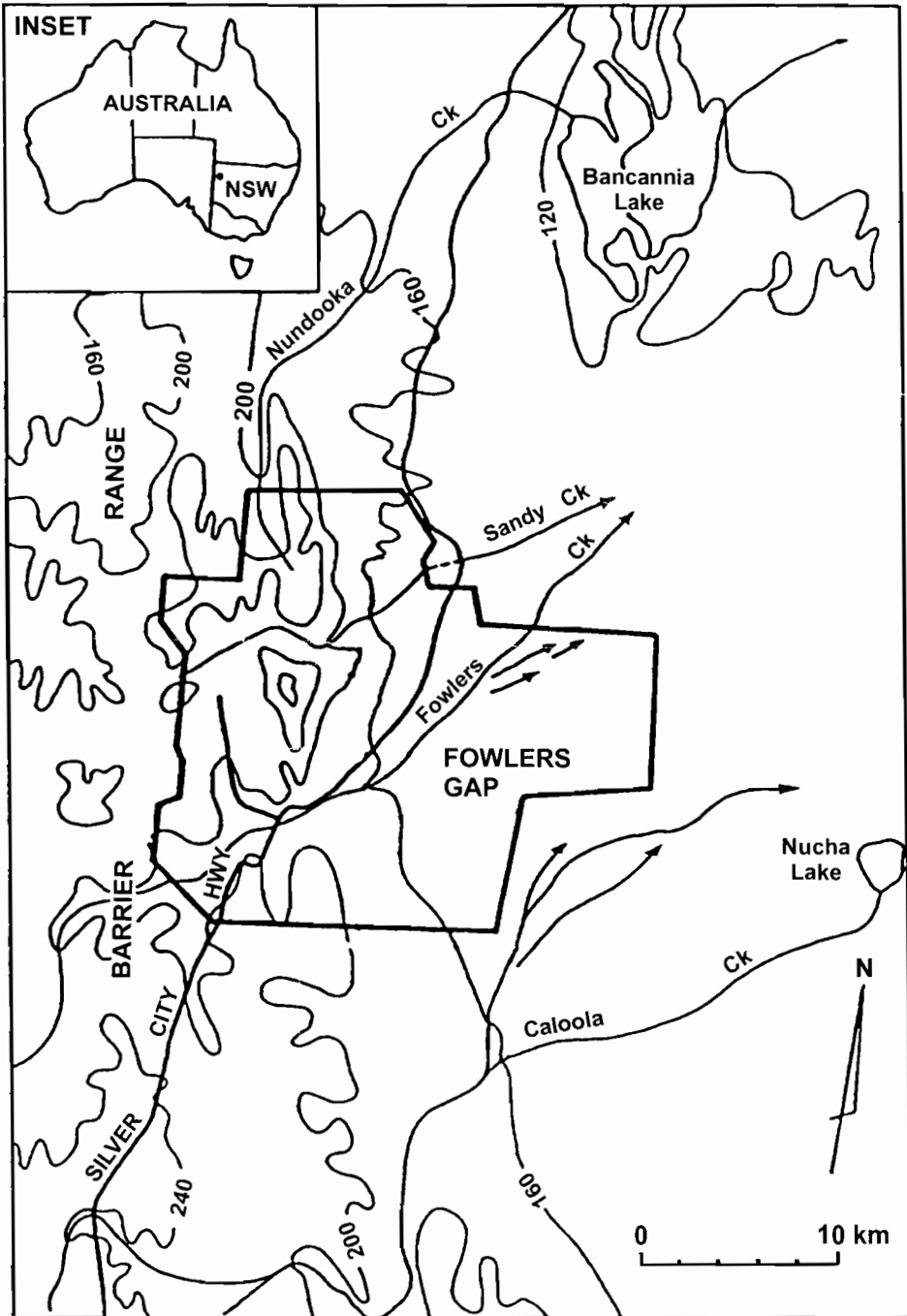
Fig. 1 Location map of Fowlers Gap Station (after Upton, 1983).

2.3. The soils

The soils of the hilly areas of Fowlers Gap, shown by Chartres (1982, 1983a,b) and Charley (1959), are morphologically similar, being three separated layers of aeolian and in situ weathered material. Each of these layers are best developed at a particular topographic position where they are not buried (Charley, 1959). This is similar to the evolutionary history of the rest of the south-eastern portion of the Australian arid zone as described by Jessup (1960a,b,c,d, 1961a,b,c).

2.4. The vegetation

High evaporation and low rainfall have resulted in low and open communities and in a perennial vegetation that is floristically poor (Burrell, 1973). Despite being protected by the enclosure (since 1968), the vegetation of the study site will not be truly representative of the original vegetation because the grazing which has occurred at the station has caused the replacement of the long-lived perennial chenopods by the semi-perennial chenopods or ephemeral species (Burrell, 1973).

3. Experimental procedures

3.1. Vegetation and soil surface analysis

Species distribution within the enclosure was mapped using the line–intercept method (Canfield, 1941). Transects were aligned downslope, spaced at 5 m intervals, and a marker was placed at each discernible change in the vegetation/soil surface on the basis of species cover and distribution. A vegetation/soil surface map was produced by visual interpolation between adjacent marking pins.

3.2. Topographic analysis

The elevations at 1 m intervals and each marking pin along the transects were surveyed using standard automatic levelling techniques to give 0.1 m contours reduced to an arbitrary local benchmark.

3.3. Soil sampling

Soil samples were taken at fixed depths (0–10, 10–50, 80–100, 150–200, 300–350 mm) from triplicate soil profiles from the approximate centre of representative sites of each unit in the enclosure. It is recognised that within the vegetated areas the salt distribution is at finer scale than that sampled. There will be differences in the salt concentration between *Atriplex vesicaria* and under *A. vesicaria* (Charley, 1959; Sharma and Tongway, 1973). However, the difference of the salt concentrations in this case is at a scale considerably less than between a bare area and a vegetated area within

a chenopod-patterned ground community. Thus, the within-variation of the vegetated area's soil salt distribution should not affect the overall outcome of the comparison of the different areas within chenopod-patterned ground. Samples were also taken in profiles from a 1 m deep and a 10 m long trench, which cut across 2 different units (Fig. 2) in the enclosure. The trench was placed on a typical area of patterned ground within the enclosure.

3.4. Chemical analysis

Chemical analyses were carried out on the triplicate soil samples by the following methods: (i) pH and electrical conductivity (EC)—1:5, soil:water suspensions with 20 min end-over-end shaking and centrifugation; (ii) soluble calcium, potassium, magnesium and sodium concentrations—were determined on appropriately diluted 1:5 soil-water extracts with $SrCl_2$ ionization suppressant at 1000 mg/l using an atomic absorption spectrophotometer (Baker and Suhr, 1982; Rhoades, 1982).
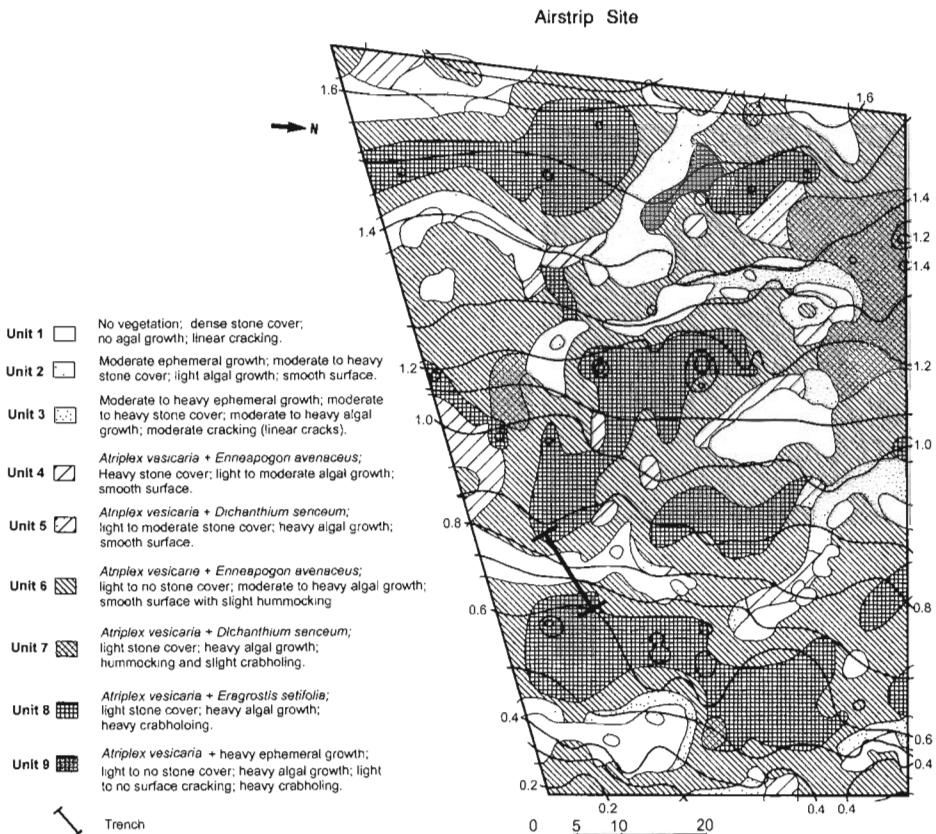
Fig. 2. Contour and vegetation map for the study site within Airstrip Paddock.

3.5. Surface infiltration

The infiltration rate of the surface soils were measured on representative surface types of patterned ground within the enclosure. Each of these measurements were replicated five times. The CSIRO Disc Permeameter was used to take the infiltration measurements, following the methodology of Perroux and White (1988), at supply potential $+10$ and -40 mm.

4. Results

4.1. Vegetation mapping and level surveying

The Airstrip enclosure is located 100 m downslope from an outcrop ridge of steeply dipping metaquartzite. The site therefore has a large amount of this material as rock fragments on the surface but including also a lot of iron stained vein quartz, probably sourced from the immediately underlying chloritic phyllite (Beavis and Beavis, 1984).

The litter is not uniform across the site but is concentrated into arcs, however, an amount of rock fragments occur in the vegetated areas between the stone arcs (Figs. 2 and 3). The Airstrip enclosure patterned ground is the sorted step type which is common
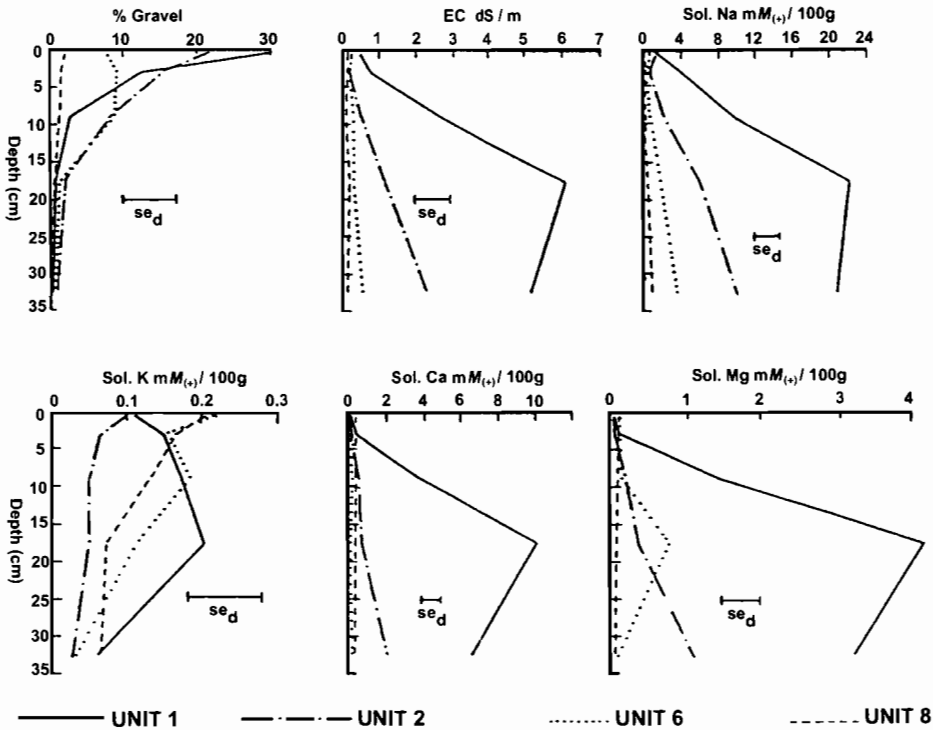
Fig. 3. The means and standard deviations of the triplicate samples from representative vegetation units for EC, gravel concentration, and soluble cations. Unit 1 is a bare area, 2 is a bare area, 6 is a vegetated area and 8 is a depression vegetated area.

on the Barrier Range foot-slopes (Mabbutt, 1979) and is characterised by discontinuous stony arcs. The vegetation analysis (including in-season ephemeral vegetation) and soil surface mapping determined nine different vegetation units ranging from completely bare stony ground to that dominated by *A. vesicaria* plus heavy ephemeral growth (Fig. 2). The contour map (Fig. 2) shows that the landscape has a weakly developed gilgai form, with crabholes concentrated in the vegetated depressions.

4.2. Soil chemical analysis

The results from the triplicate samples for EC and the soluble soil cation data (Fig. 3) for representative vegetation units show that the soils of the bare area (Unit 1) are significantly different from the rest of the intermediate and vegetated areas (Units 2, 6 and 8). The differences between the vegetated units (6 and 8) are not significant and on the basis of soil analysis, separation of those areas into discrete units is not possible. The distinction between Unit 1 and Unit 2 is possible on the basis of their soil properties. The terms bare areas (mounds) and vegetated (depressions) areas subsequently will be applied to Units 1 and 4–9, respectively, Units 2 and 3 being intermediate (shelves) between the two groups. The relative distribution of the soluble soil cations (Figs. 4 and 5) within the trench transect profiles can be assumed to be representative of chenopod-patterned ground at a similar topographic position.

The water soluble cation concentrations of the trench are illustrated in Figs. 4 and 5 by fitting isopleths to the concentrations in the measured soil profiles. These isopleth maps are representative of soluble cation distribution between vegetated and bare areas in the upper metre of soil profile within the enclosure site. The soils of both areas are dominated by soluble sodium throughout the majority of the profile. The largest concentrations of sodium were found in the top 70 cm of the bare area soils and they decreased rapidly from the centre of these arcs towards the vegetated areas (Fig. 4). The pattern of distribution for the soluble magnesium and calcium is similar to soluble sodium (Fig. 3). Figs. 3 and 4 show that there are great differences in the concentrations and the distribution of the soluble cations between the vegetated and bare areas.

The potassium distribution is concentrated towards the centre of the vegetated areas and decreases towards the centre of the bare areas (Fig. 5) because of this ion's role as an important plant nutrient that is relatively rapidly cycled by vegetation. It appears that the bare areas are salt dumps and the concentrations of the salts decline into the centre of the vegetation arcs.

4.3. Infiltration measurements

The surface soils of the bare stony ground have very small hydraulic conductivity values (Fig. 6) for both supply potentials. Infiltration measured with a positive supply potential ($+10$ mm) represents the contribution to flow from all pore sizes; that measured with a negative potential (-40 mm) excludes flow from the larger pores. The infiltration rate for the surface soils of the vegetated areas (Fig. 6) are greater when compared to the stony ground with Unit 8 having the greatest proportion of infiltration
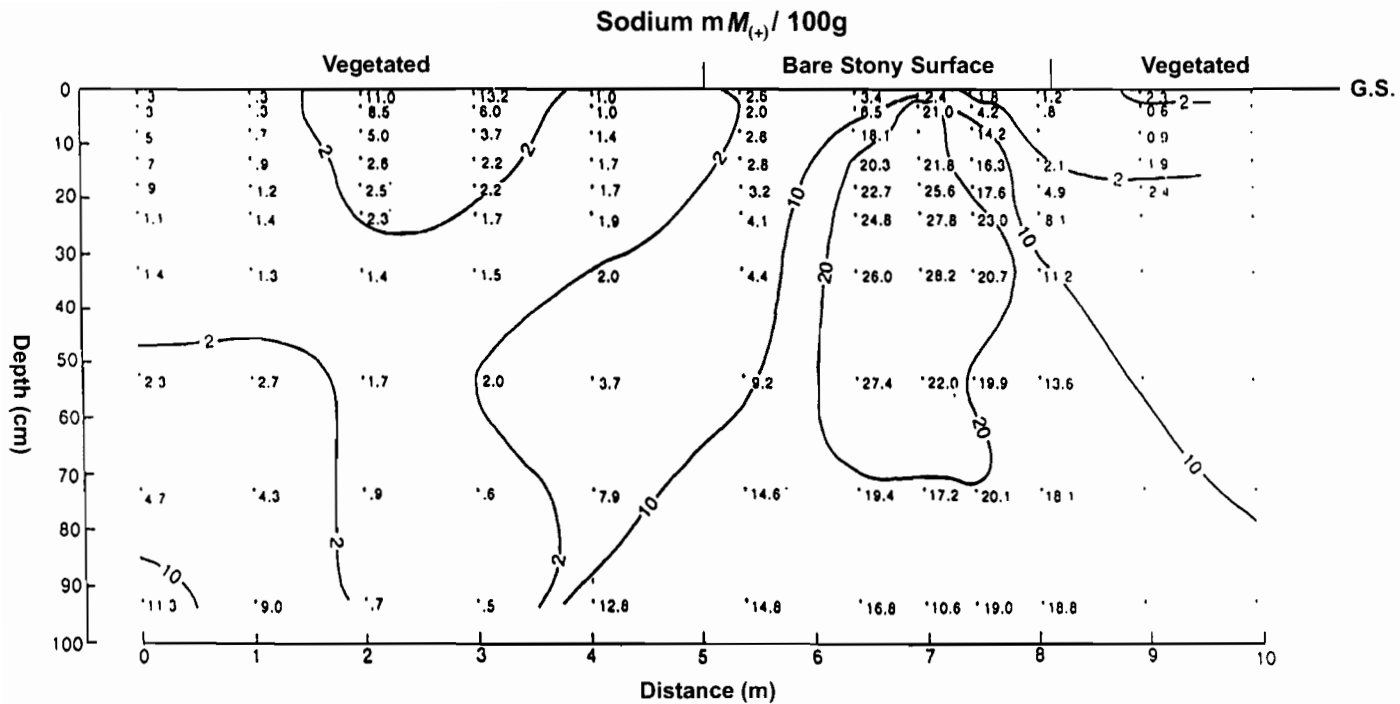
Fig. 4. The distribution of sodium (mM/100 g) within the trench profile.
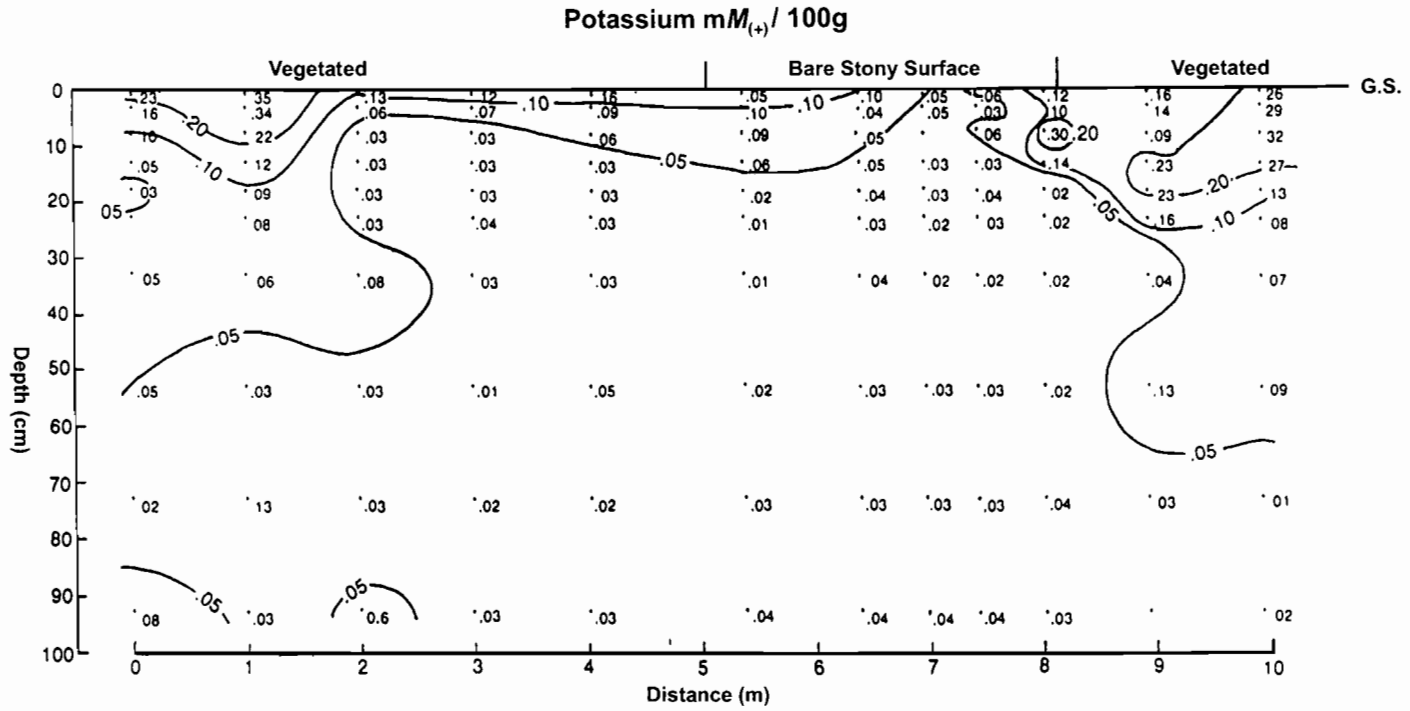
Fig. 5. The distribution of potassium (mM/100 g) within the trench profile.
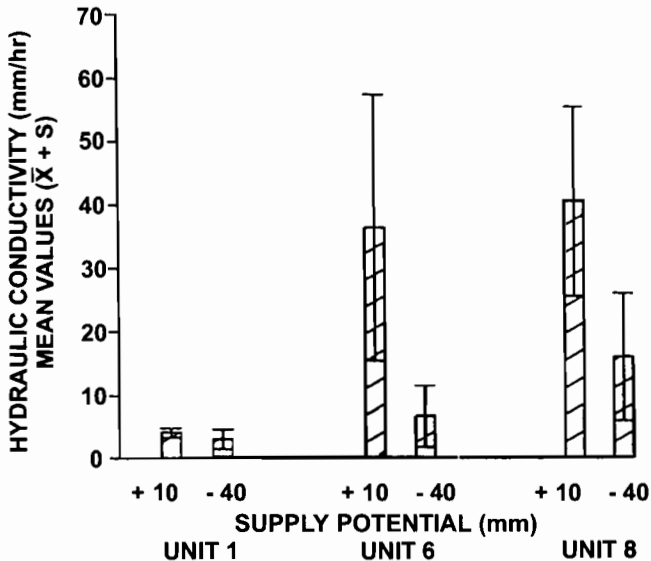
Fig. 6. The hydraulic conductivity (mm/h) of selected surface soils within Airstrip enclosure. Unit 1 is a bare stony area and Units 6 and 8 are vegetated areas.

through stable finer bio-pores. The soils of the vegetated ground (units 6 and 8) have stable macropores, indicated by the high values for +10 supply potential, which infiltrates much more water than the surface-sealed soils of the stony ground.

5. Discussion

The combination of the soil, topographic and vegetation analysis shows that chenopod-patterned ground contains three distinct zones. Namely, those areas lacking vegetation which in gilgai terminology are 'risers' (Unit 1), those with *A. vesicaria* and are called 'depressions' (Units 4–9), and the 'shelves' which grade between them containing only ephemeral growth and soil crusts (Fig. 2, Units 2–3).

The patterns of soluble salt distribution (Figs. 3–5) are a product of complex responses as the soils have adjusted to the preferential inputs of run-off water into the vegetated soil due to the gilgai complex. The bare areas are dominated by sodium because it is weakly bonded, highly soluble and easily redistributed by water movement (Troeh and Thompson, 1993; Rengasamany and Olsson, 1991). Teakle and Burvill (1938) found that soluble salts are highest in the surface soil when texture is heavy and leaching is ineffective. This is typical of the bare areas, which have low infiltration rates (Fig. 6). The distribution of sodium is concentrated in the bare ground to 70 cm and only at 80–90 cm do the vegetated areas have similar sodium salt concentration. Most probably, this is the limit of effective water penetration and subsequent redistribution of salts in the vegetated areas.

Fairly similar patterns occur for magnesium and calcium but they contain relatively higher concentrations than sodium in the vegetated areas due their greater bonding strengths with clays. The distribution of potassium within the whole system is controlled by vegetation-induced turnover. The vegetated areas have a greater absolute amount of potassium in the topsoil compared to the adjacent bare areas. The presence of potassium within the topsoil of the bare areas is probably due to the decomposition of organic matter present on the surface and the presence of microbiotic crusts.

There is a relatively slight increase in the concentration of sodium, calcium and magnesium within the topsoil of the vegetated areas. The increase of these soluble salts is because of the *A. vesicaria* salt cycling (Sharma and Tongway, 1973). Prior to grazing-induced land degradation the vegetation-induced salt turnover by the saltbushes (Charley and West, 1975) ensured that rainfall did not leach the depression sufficiently to allow competition by salt-intolerant species. The increase in soluble salts in the topsoil would lower the permanent wilting point (Charley, 1977), which would inhibit perennial establishment and growth. The saltbushes were, and in some cases still are, maintaining their own ecological niche within the system.

The present soluble salt distribution within the vegetated area is certainly influenced by *A. vesicaria*. However, it is unlikely that the redistribution of soluble salts from the vegetated soils was caused solely by *Atriplex* spp. salt cycling. The relative differences of the soluble salt concentrations between the soils of the vegetated and bare areas are too great.

5.1. Model of soluble salt distribution maintenance

The data supports the hypothesis that bare areas are salt dumps where salt is moved laterally from the vegetated areas over time. There is much evidence that the lateral movement of salts is possible provided the right conditions are established (Russell, 1966; Teakle and Burvill, 1938; Lawrie, 1978; Whittig and Janitzky, 1963). The establishment of the gilgai complex started the process by initialising the appropriate moisture gradients (Charley, 1959), which then would favour the movement of water, collected by the depressed vegetated areas, through the soil and under the bare areas (Fig. 7). This soil water would carry soluble salts, thus increasing salt concentration through time. The establishment of a favourable osmotic gradient would have taken place during this time due to inputs of soluble salts from the adjacent vegetation areas and from subsoil migration within the bare ground. This would further promote the movement of water in the soil, from the vegetated to the bare areas.

Daubenmire (1957) states that temperature gradients are important with plant ecology. Temperature of the soil affects soil water as it increases, by increasing the rate of moisture movement and the amount available to plants. Tongway and Ludwig (1996) found that within a degraded semi-arid *Aca. aneura* woodland, soil surfaces which were devoid of vegetation litter were be relatively warmer during the daytime than the soils whose surface was covered with litter and branches. A similar temperature gradient must occur between the bare and vegetated areas within chenopod-patterned ground. At nighttime, the bare soil surface cools more than that beneath the vegetated areas. This sets up a greater moisture potential gradient between the moister subsoil and the bare
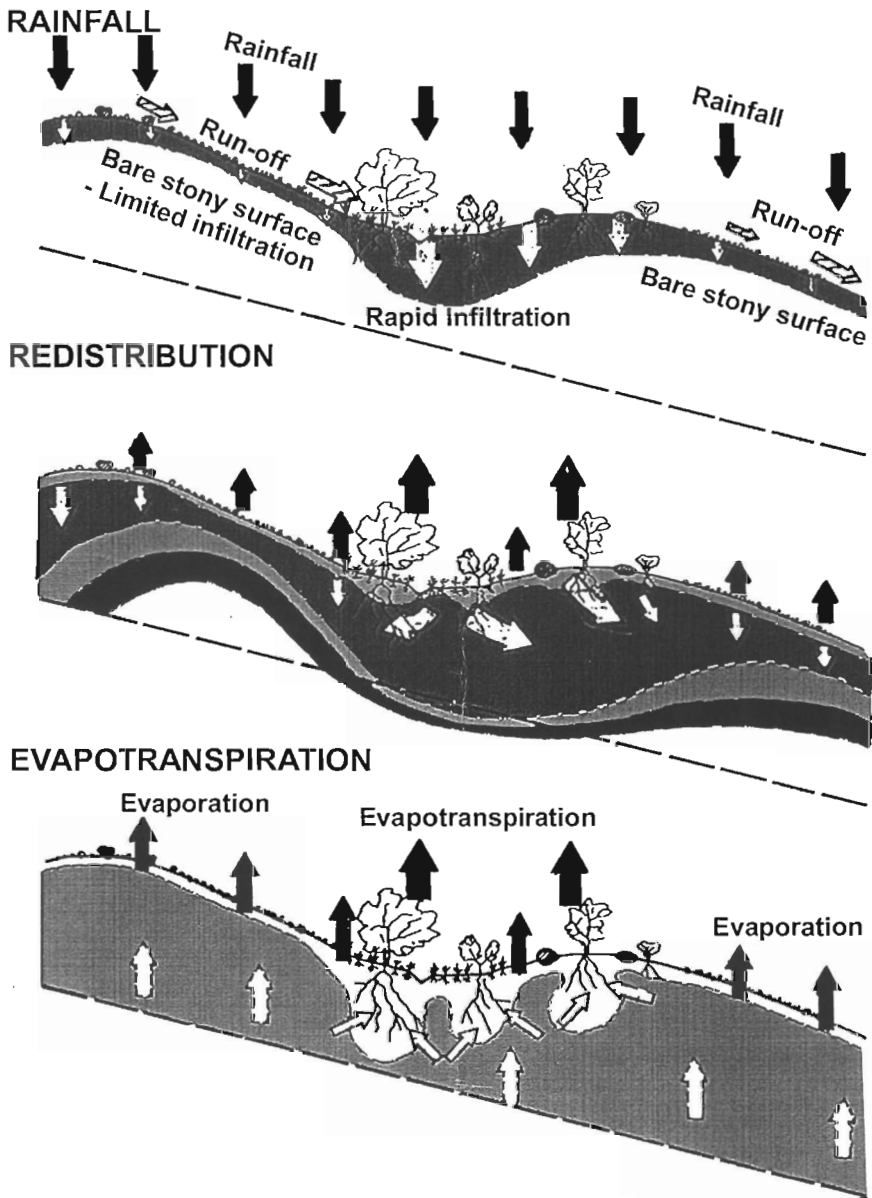
Fig. 7. A model showing the infiltration and redistribution of rainfall and soil water in a typical patterned ground complex. The black arrows represent atmospheric process and the white arrows represent terrestrial process. The moisture regions are represented by the darker shadings.

topsoil and preferentially moves water to that part of the complex. Both temperature and osmotic effects would enhance water movement from the subsoil of the bare areas and the adjacent vegetated areas.

It is hypothesised that the majority of the soil water in the bare ground is being evaporated from the soil's immediate subsurface. This would cause the migration of salts from the subsoil to the topsoil of the bare ground. Within the vegetated soils, salts are drawn from throughout the soil profile into the roots and through the transpiration stream. They are stored temporarily in/on the vegetation for re-cycling in litter fall to the soil surface and returned to the soil profile depth with infiltrating water (Sharma and Tongway, 1973). The gilgai complex has probably established a system where soil moisture and osmotic gradients all favour the flow of soil water (Fig. 7) carrying soluble salts from the vegetated areas and the bare area's subsoil, concentrating them into the bare area's upper subsoil.

The processes described in the above model would require long periods of soil stability. The soils present at the site have not been dated; however, a nearby area of patterned ground is Holocene in age (Dunkerly and Brown, 1995) and soil of the Mundi Mundi plain have been dated to 16,000 BP (Wasson, 1979). Thus, it is assumed that the soils of study area are similar in age and stability. There would of course have been additions and erosion of soil materials since this time. However, the landscape stability would have permitted the processes described in the model, sufficient time to modify the soil chemical landscape.

6. Conclusions

The vegetation pattern of the chenopod shrubland patterned ground described here, is chiefly due to differences in soil moisture, which arises largely through the run-off of rainwater from bare, impermeable gilgai mound to the vegetated depression. The hydrological and vegetational patterns in turn control the distribution of soil cations within patterned ground, but the large salt concentrations beneath the bare soil areas provide a feed-back mechanism to inhibit plant growth there. The pattern of salt redistribution is strengthened through time by positive feedback effects. The chemical and vegetational differences influence the soil's physical properties increasing the strength of the gilgai complex that further promotes the redistribution of run-off. This in turn would favour more salt transportation out of the vegetated areas because of the increased flow potential. At some point, the gilgai and patterned ground complex reaches a balance with the prevailing climatic conditions and the system would be maintained in a dynamic equilibrium. Mabbutt (1973) envisaged this dynamic equilibrium as the process, which controls the maintenance of the whole system. It represents the end point in the evolution of the landscape to the prevailing conditions such that the physical and chemical properties of the soil, and the amount and type of vegetation, remains relatively constant.

References

Baker, D.E., Suhr, N.H., 1982 Atomic absorption and flame emission spectrometry. In: Page, A.L., Miller, R.H., Keeney, D.R. (Eds.), Methods of Soil Analysis, Part 2; Chemical and Microbiological Properties, 2nd edn. American Society of Agronomy and Soil Science Society of America, Madison, WI, USA, pp. 13–28.

Bell, F.C., 1973. Climate of the Fowlers Gap Station. In: Mabbutt, J.A. (Ed.), Lands of the Fowlers Gap Station, New South Wales Fowlers Gap Arid Zone Research Station, Research Series No. 3. UNSW, pp. 123–149.

Beavis, F.G., Beavis, J.C., 1984. Geology, engineering geology and hydro-geology of Fowlers Gap Station. Fowlers Gap Arid Zone Research Station Series No. 6, UNSW.

Boaler, S.B., Hodge, C.A.H., 1964. Observation on vegetation arcs in the northern region, Somali Republic. J. Ecol. 52, 511–544

Boyland, E.E., 1973. Vegetation of the mulga lands with special reference to South Western Queensland. Trop. Grasslands 7, 23–34.

Bromley, J., Brouwer, J., Barker, A.P., Gaze, S.R., Valentin, C., in press. The role of surface water redistribution in an area of patterned vegetation in a semi-arid environment, south west Niger.

Burrell, J.P., 1973. Vegetation of the Fowlers Gap Station. In: Mabbutt, J.A. (Ed.), Lands of the Fowlers Gap Station, New South Wales. Fowlers Gap Arid Zone Research Station, Research Series No. 3., pp. 175–194.

Butler, B.E., Hubble, G.D., 1977. Morphologic properties. In: Russell, J.S., Greacen, E.L. (Eds.), Soil Factors in Crop Production in a Semi-arid Environment. Univ. Qld Press, St Lucia, pp. 9–33.

Canfield, R.H., 1941. Application of the line interception method in sampling range vegetation. J. For. 39, 388–394.

Charley, J.L., 1959. Soil salinity vegetation patterns in western New South Wales. PhD Thesis, University of New England, p. 274

Charley, J.L., 1972. The role of shrubs in nutrient cycling. In: Mckell, C.M., Blaisdell, J.P., Goodin, J.R. (Eds.), Wildland Shrubs—Their Biology and Utilisation. An International Symposium. Utah State Univ., Logan, UT, July 1971. USDA, pp. 182–204

Charley, J.L., 1977. Mineral cycling in rangeland ecosystems. In: Sosebee, R.E. (Ed.), Rangeland Plant Physiology. Rangeland Sci. Series, pp. 215–256.

Charley, J.L., West, N.E., 1975. Plant induced patterns in some shrub dominated semi-desert ecosystems of Utah. J. Ecol. 63, 945–964

Chartres, C.J., 1982. The pedogenesis of the desert loam soils in the Barrier Range, Western New South Wales: I. Soil parent materials. Aust. J. Soil Res. 20, 269–281.

Chartres, C.J., 1983a. The pedogenesis of the desert loam soils in the Barrier Range, Western New South Wales: II. Weathering and soil formation. Aust. J. Soil Res. 21, 1–13.

Chartres, C.J., 1983b. The micromorphology of desert loam soils and implications for quaternary studies in western New South Wales. In: Bullock, P., Murphy, C.P. (Eds.), Soil Micromorphology, Vol. I, Techniques and Applications. Academic Publishers, Berkhamsted, pp. 273–279.

Daubenmire, R., 1957. Influence of temperature upon soil moisture contents and its possible ecological significance. Ecology 38, 320–324.

Dawson, N.M., Ahern, C.R., 1973. Soils and landscapes of mulgalands with special reference to south western Queensland. Trop. Grasslands 7, 23–34.

Dunkerly, D.L., Brown, K.J., 1995. Runoff and runon areas in patterned chenopod shrubland, arid western New South Wales, Australia: characteristics and origins. J. Arid Environ. 30, 41–45.

Goodspeed, M.J., Winkworth, R.E., 1978. Fate and effect of runoff—with special reference to arid and semi-arid plain lands. In: Howes, K.M.W. (Ed.), Studies of the Australian Arid Zone: III. Water in Rangelands. Proceedings of the Symposium held at the Rangelands Research Unit, Alice Springs Field Centre, 15–18 October 1974, Melbourne. CSIRO Division of Land Resources Management, pp. 53–60.4

Greene, R.S.B., 1992. Soil physical properties of three geomorphic zones in semi-arid mulga woodland. Aust. J. Soil Res. 9, 157–164.

Greene, R.S.B., Kinnell, P.I.A., Wood, J.T., 1992. Role of plant cover in runoff and soil erosion from semi-arid wooded rangeland. Aust. J. Soil Res. 32 (5), 953–973.

Greenwood, J.E.G.W., 1957. The development of vegetation patterns in the Somaliland Protectorate. Geogr. J. 123, 465–473.

Greig-Smith, P., 1979. Pattern in vegetation. J. Ecol. 67, 755–779.

Hallsworth, E.G., Robertson, G.K., Gibbons, F.R., 1955. Studies in pedogenesis in New South Wales: VII. The gilgai soils. J. Soil Sci. 6 (1), 1–31.

Hemming, C.F., 1965. Vegetation arcs in Somaliland. J. Ecol. 53, 57–63

Jessup, R.W., 1960a. An introduction to the soils of the south-eastern portion of the Australian arid zone. J. Soil Sci. 11, 92–105

Jessup, R.W., 1960b. The lateritic soils of the south-eastern portion of the Australian arid zone. J. Soil Sci. 11 (1), 106–113.

Jessup, R.W., 1960c. The stony tableland soils of the south-eastern portion of the Australian arid zone. J. Soil. Sci. 11 (2), 188–197

Jessup, R.W., 1960d. Identification and significance of buried soils of quaternary age in the south-eastern portion of the Australian arid zone. J. Soil Sci. 11 (2), 197–205.

Jessup, R.W., 1961a. Evolution of the two youngest (Quaternary) soil layers on the south-eastern portion of the Australian arid zone: I. The paraklia layer. J. Soil Sci 12 (1), 52–63.

Jessup, R.W., 1961b. Evolution of the two youngest (Quaternary) soil layers on the south-eastern portion of the Australian arid zone: II. The bookaloo layer. J. Soil Sci. 12 (1), 64–72.

Jessup, R.W., 1961c. A Tertiary–Quaternary pedological chronology for the south-eastern portion of the Australian arid zone. J. Soil Sci 12 (2), 199–213.

Lawrie, J.W., 1978. Hardpans in western New South Wales. Proceedings of the First International Rangeland Congress, pp. 303–306.

Litchfield, W.H., Mabbutt, J.A., 1962. Hardpan in soils of the semi-arid Western Australia. J. Soil Sci. 13 (2), 149–159.

Mabbutt, J.A., 1973 Geomorphology of the Fowlers Gap Station. In: Mabbutt, J.A. (Ed.), Lands of the Fowlers Gap Station, New South Wales. Fowlers Gap Arid Zone Research Station. Research Series No. 3, pp. 67–83.

Mabbutt, J.A., 1979. Pavements and patterned ground in the Australian stony deserts. Stuttgartert Geogr. Studien 93, 107–123.

Mabbutt, J.A., Fanning, P.C., 1987. Vegetation banding in arid Western Australia. J. Arid Environ 12, 41–59.

Mabbutt, J.A., Burrell, J.P., Corbett, J.R., Sullivan, M.E., 1973. Landsystems of Fowlers Gap Station In: Mabbutt, J A. (Ed.), Lands of the Fowlers Gap Station, New South Wales. Fowlers Gap Arid Zone Research Station, Research Series No. 3, pp. 25–49.

Macfayden, W A., 1950. Vegetation patterns in the semi-desert plains of British Somaliland. Geogr. J. 116, 199–210.

Montaña, C., 1992. The colonisation of bare areas in two phase mosaics of an arid ecosystem. J. Ecol 80, 315–327.

Mott, J.A., McComb, A.J., 1979 Patterns in annual vegetation and soil microrelief in arid region of Western Australia. J. Ecol. 62, 115–126.

Noy-Meir, I., 1974. Multivariate analysis of the semiarid vegetation in south eastern Australia, Part II. Vegetation catenae and environment. Aust. J. Bot. 22, 154–155

Perroux, K.M., White, I., 1988 Designs for disc permeameters. Soil Sci. Soc. Am. J 52 (5), 1205–1215

Rengasamany, P., Olsson, K.A., 1991. Sodicitiy and soil structure. Aust. J. Soil. Res. 29, 935–952.

Rhoades, J.D., 1982. Soluble salts. In: Page, A.L., Miller, R.H., Keeney, D.R. (Eds.), Methods of Soil Analysis, Part 2; Chemical and Microbiological Properties, 2nd edn. American Society of Agronomy and Soil Science Society of America, Madison, WI, USA, pp. 167–180.

Russell, J.S., 1966. Changes in the properties of a deep gilgaied clay soil associated with the replacement of brigalow (Acacia harpophylla F. Muell) forest with grassland. Aust Soil. Conf., May, pp. 5–11.

Sharma, M.L., Tongway, D.J., 1973. Plant induced soil salinity patterns in two saltbush (Atriplex spp.) communities. Range Man. 26 (2), 121–125.

Teakle, L.J.H., Burvill, G.H., 1938. The movement of soluble salts in soils under light rainfall conditions. J. Dept. Agric. W. Aust. 15, 218–245.

Tongway, D.J., Ludwig, J.M., 1990. Vegetation and soil patterning in semi-arid mulga lands of eastern Australia. Aust. J. Ecol 15, 23–34.

Tongway, D.J., Ludwig, J.M., 1996. Rehabilitation of semiarid landscapes in Australia: I. Restoring productive soil patches. Restoration Ecol. 4 (4), 388–397.

Troeh, F.R., Thompson, L M., 1993. Soils and Soil Fertility, 4th edn. Oxford Univ. Press, Melbourne.

Upton, E., 1983. Genesis of crabhole microrelief at Fowlers Gap western New South Wales. Catena 10, 383–392.

Washburn, A L., 1956 A classification of patterned ground and review of suggested origins Bull Geol. Soc. Am 67, 823–866.

Wasson, R.J., 1979 Sedimentation history of the Mundi Mundi alluvial fans, Western NSW. Sed Geol. 22, 22–51

White, L.P , 1969. Vegetation arcs in Jordan. J. Ecol. 57, 461–464.

White, L.P., 1970. Brousse Tigrée patterns in southern Niger J. Ecol. 58, 549–553

White, L.P., 1971. Vegetation stripes on sheet wash surfaces. J. Ecol. 59, 615–622.

Whittig, L.D., Janitzky, P., 1963. Mechanisms of formation sodium carbonate in soils: I. Manifestations of biological conversions. J. Soil Sci. 14 (2), 322–333.

Wickens, G.E., Collier, F.W., 1971. Some vegetation patterns in the Republic of the Sudan. Geoderma 6, 43–59.

Wilson, J.W., Liegh, J.H., 1964. Vegetation patterns on an unusual gilgai soil in New South Wales. J Ecol 52, 379–389.

Worrall, G.A., 1959. The Butana grass patterns. J. Soil Sci. 10, 34–53.

Worrall, G.A., 1960. Tree patterns in The Sudan. J. Soil Sci. 11, 63–67.

Zhou, Q., 1989 The integration of remote sensing and geographical information systems for land resource management in the Australian arid zone. PhD Thesis, University of New South Wales.

The evolution and significance of soil–vegetation patterns following land abandonment and fire in Spain

L.H. Cammeraat *, A.C. Imeson

Landscape and Environmental Research Group, University of Amsterdam, Nieuwe Pinsengracht 130, 1018 VZ Amsterdam, Netherlands

Abstract

Examples are presented from two locations in SE and NE Spain where patterned or banded vegetation are found on semi-natural and abandoned land or where vegetation is recovering from wildfire. In both cases patterns are being investigated as process-pattern phenomena with the aim of understanding how different kinds of environmental gradients influence pattern evolution. On abandoned land, patterns occur at different scales. At the patch scale there are areas where *Plantago albicans* germinates in cracks and influences the accumulation of silty material. At the slope scale these form elongated steps that create a characteristic micro-topography. At the patch and slope scale *Stipa tenacissima* tussocks form an hexagonal pattern on level areas where water infiltrates in and around the tussocks. On sloping areas the *S. tenacissima* tussocks form parallel ovoid bands. They intercept fine and coarse material being eroded on the slopes by both overland flow and the hooves of sheep and goats. This also creates a distinctive micro-topography. Rainfall simulation experiments were undertaken in combination with monitoring activities in order to investigate the effects that key-processes of sediment and water movement have on the patterns. Other methods include controlled experiments and modelling. Biologically driven erosion processes are very important as key processes. Positive feedback mechanisms are important at various stages in the evolution of the pattern. The patterns studied play an important role in creating more favourable micro-environments where vegetation recovers first after disturbances. This is particularly the case following wildfire. The first post-fire rain produces patterns in ash and litter around sites, concentrating these at locations where shrubby vegetation subsequently resprouts or becomes

---

* Corresponding author

seeded. On abandoned land, the evolution of patterns reflects the parent material, grazing and the climate. © 1999 Elsevier Science B.V. All rights reserved.

1. Introduction

In Mediterranean areas semi-natural vegetation is often structured in a spotted or banded spatial configuration and these patterns are of importance for understanding runoff and erosion processes. The interaction between vegetation development, soil surface properties and water movement must be responsible for the patterns observed. The patterns found resemble features described for semi-arid regions such as in Australia (Tongway and Hindley, 1995), the Sahel zone of Africa (Thiéry et al., 1995), and the western USA (Pierson et al., 1994). Most of such patterns indicate a very sensitive relationship between the amount of available water and the vegetation. This invariably reflects positive feedback mechanisms between water movement and the vegetation (Imeson et al., 1995; Tongway and Hindley, 1995). The spatial patterning of the vegetation can used as an expression of soil properties important for water reallocation in and over the soil.

Under the plants often higher organic matter contents are found, favouring soil aggregation and soil faunal activity, both increasing macroporosity. A special micro-climate is present under plants and vegetated zones, with much smaller temperature amplitudes, more shading and often better soil moisture conditions than for bare soil conditions. This results in higher infiltration rates under the plants (runoff absorption) and lower infiltration rates on bare crusted soil surface (runoff generating areas). In water limited geo-ecological zones, such as the sub-humid and semi-arid Mediterranean areas, the spatial configuration of vegetated and bare areas is therefore very important and often indicates the spatial distribution of higher infiltration rates (Morin and Kosovsky, 1995).

Understanding the positive feed-back mechanisms that link water and vegetation has been an aim of recent research in Central and SE Spain undertaken on the context land degradation research (Imeson et al., 1995, 1996a; Bergkamp, 1996). This research has emphasised the importance of scale dependent linkages and has followed an hierarchical approach whereby processes at the fine scale are seen as important driving forces at the next hillslope level. Processes at this level operate under the constraints of the next higher level of scale (O'Neill et al., 1986). This means that the upscaling of small plots results, using for instance infiltration rates, cannot be done unless the spatial configuring of soil–plant phenomena is incorporated.

Land degradation and erosion processes are perceived to be important problems in many Mediterranean and semi-arid areas (Fantechi and Margaris, 1986; Thornes, 1995). In the northern Mediterranean much effort has been made to understand the effects of land use change and practices, fire and climatic change on land degradation. One of the most important aspects of this problem concerns the resilience of perturbed systems. The objective of this paper is to illustrate the potential significance of patterns in promoting

the resilience, stability and inertia of landscape systems subject to various stresses. One example is from a semi-arid area in SE Spain where matorral vegetation was taken into cultivation during the 1960s and subsequently abandoned in 1983. Under conditions of drought and grazing pressure, different process-pattern features have evolved at different scales when the area was colonised by vegetation. The second example from NE Spain describes the infiltration patterns that exist in forested areas and how, following fire, these and other patterns emerge to concentrate water resources for seedlings and resprouting trees. It is suggested that process-pattern phenomena can be used as indicators of ecosystem functioning.

2. The study areas

2.1. The Cañada Cazorla / Maestra Oliva site in SE Spain

The field location in SE Spain is located in the upper Guadalentín basin (Fig. 1) (37°50′00″NL; 1°48′40″WL). It is situated in the driest part of Europe, and has a semi-arid climate with an average precipitation of 277 mm yr^{-1} (Embalse de Puentes, 1951–1980). Precipitation falls mainly in autumn and spring and there is a high inter-annual variability. Average temperatures in the region range between 9.3 (January) and 26.0°C (July/August) with an average annual temperature of 16.8°C (Navarro-

Fig. 1. Location map indicating both research areas in Spain.

Hervás, 1991). The investigated site constitutes one of seven reference locations of the MEDALUS Project in the Upper Guadalentín region (MEDALUS, 1996; Imeson et al., 1996b). The field area has a flat to gentle rolling topography and is part of an almost flat planation surface, developed in horizontally bedded Pliocene marls, conglomerates and limestones. It consists of a plateau bounded in all directions by concave slopes on which erosion processes are active. On the lower gently sloping areas calcareous marls of Upper Cretaceous–Lower Tertiary age (I.G.M.E., 1981) are found. The large variation in soil types reflects a combination of lithological differences, topographic position and aspect. Some characteristics of the most frequently occurring soils are shown in Table 1.

The soils, with a silt loam texture, are shallow and highly calcareous with low to very low organic matter contents, depending on the vegetation cover. Under the plants, in semi-natural conditions, organic carbon levels are higher and soil aggregation is better. The bare areas between the plants are crusted and the soil aggregation is very weak. Both structural and depositional crusts are found (Valentin and Bresson, 1992), whereas under the plants the soil surface is more open due to soil aggregation and soil animal activity, permitting higher infiltration rates. Some aspects of microbial biomass and aggregate stability in relation to surface cover type or land use are discussed in Cerdà et al. (1994, 1995) and in Cammeraat and Imeson (1998).

Land use varies throughout the area and has changed considerably over the last 40 years. Only 37% of the land use is the same today (1995) as in 1957, as interpreted from aerial photography analysis. On the plateau, open semi-natural *Stipa tenacissima* L. (Esparto grass) matorral occurs as well as fallow agricultural lands, the latter being used for rain-fed cereal production. The steep upper and middle hillslopes are covered with open *S. tenacissima* matorral. The lower hillslope was abandoned in 1983 and shows bare and strongly crusted soils alternating with bands of *Plantago albicans*. However, one small area under *S. tenacissima* still remains on the foot slope. The valley bottom itself is still under cultivation, for growing rain fed cereals, and was tilled just before sampling. The talweg is terraced to reduce gully development and for water harvesting.

2.2. The Vilobí d'Onyar site in NE Spain

The field area is located in the Selva region near the village of Vilobí d'Onyar in the south of the Gerona Province, Catalonia (41°53′02″NL; 2°44′30″EL), which has a sub-humid Mediterranean climate receiving between 700 and 800 mm of rainfall and which is covered by extensive Mediterranean oak forests. It is located on sandy and gravely Pleistocene and Pliocene fan deposits that occupy a large roughly north–south running graben that separates two major parallel mountain ranges, with mainly acid igneous and metamorphic rocks. The mean summer and winter temperatures range from about 24°C in the summer to 8°C in the winter. Most of the precipitation falls in the spring and autumn. The research site forms one of the reference locations established to investigate relationships between soil characteristics, hydrology and forest fires (Sevink et al., 1989; Imeson et al., 1992). The morphology of the field site, located on a fan which slopes gently eastward, is rather simple reflecting the incision by shallow but rather steep sided valleys that also drain eastward. The maximum altitude difference is about 15 m. Basic information on soils and land use is given in Table 2. The soils at non

Table 1
Main surface characteristics of the soils of the Cañada Cazorla site

Position	Slope (°)	Soil type after F.A.O. (1989)	Horizon	Depth (cm)	Land use	Texture			Org. C (%)	CaCO$_3$ (%)
						Sand, %	Silt, %	Clay,%		
Plateau	0–1	Petric Calcisol	(crust)	0–3	Semi-nat.(St)	26.6	60.1	13.4	2.3	53.9
			(Ah)	3–18		27.0	68.0	5.0	2.9	59.7
Plateau	0–1	Petric Calcisol	(crust)	0–2	Fallow (C)	27.6	67.8	4.6	3.4	53.4
			(Ap1)	2–19		34.4	60.9	4.7	3.2	53.7
Upslope	12–25	Eutric Leptosol	(crust)	0–3	Semi-nat.(St)	36.7	51.7	11.0	1.8	78.4
			(Ah)	3–12		21.1	62.7	16.2	1.8	78.5
Mid slope	12–3	Eutric Leptosol	(crust)	0–3	Semi-nat.(St)	38.4	52.6	7.9	1.6	71.2
			(Ah)	3–9		32 4	55.2	10.3	2.0	68.8
Downslope	6–3	Haplic Calcisol	(crust)	0–2	Abandoned (Pl)	26.5	66.6	6.5	2.1	64.4
			(Ap1)	4–21		23.3	68.4	6.2	1.8	64.4
			(Bw)	21– > 40		14.9	64.5	9.6	1.2	52.6
Valley	3–0	Calcaric Regosol	(Ap1)	0–20	Fallow (C)	19.6	65.4	14.5	1.4	61.1
			(Ap2)	20–40		13.3	66.6	17.2	0.7	40.7

St: *S. tenacissima* dominated; Pl· *P. albicans* dominated; C. Rain fed cereals.

L.H. Cammeraat. A.C. Imeson / Catena 37 (1999) 107–127

111

Table 2
Main characteristics of the soils in the Vilobí d'Onyar region

Horizon	Depth (cm)	pH-CaCl$_2$	Org. C (%)	Sand (%)	Silt (%)	Clay (%)
Ah	0–5	4.8	2.4	61	29	10
E	5–20	4.5	0.4	60	32	8
Bt1	20–70	5.0	0.5	25	31	44
Bt2	70–120	5 4	0.2	32	33	35
BC	120–170	6.2	0	52	28	20

Slope segment soil surface characteristics

Position	Slope (°)	Soil surface type	Land-use	Vegetation	Cover (%)
Footslope	5	colluvium	burned	*Cistus* sp.	> 25
Midslope	30	Bt horizon	burned	no cover	0
Plateau	3	E horizon	burned	*Cistus* sp.	
Upperslope	20	E horizon	burned	*Cistus* sp	5

Soil profile characteristics (Albic Luvisol) after F.A.O. (1989).

eroded sites at the top of the fan consist of albic luvisols characterised by a strong texture contrast at the base of the albic horizon. On the slopes the underlying Bt and BC horizons are exposed on the surface according to the local incision and erosion. In most places a Bt horizon is only covered by a thin remnant of the E horizon. Large contrasts in the soil structure and hydrology occur according to the truncation. When the Bt horizon is exposed it is frequently subjected to rill erosion. The lower slope positions are characterised by accumulations of colluvium which was in places more than a metre deep. The field site was almost completely burnt in the summer of 1986, a small part of the forest being protected by a road. The forest is characterised by *Quercus suber*, *Arbutus unedo* and *Erica arborea*, as well as by pines that could not be identified after the fire. From 1987 until 1993, field investigations were undertaken to study the post fire evolution of infiltration and runoff patterns in relation to the recovery of the vegetation.

3. Methods

Soil description and classification were carried out following the guidelines for soil description (F.A.O., 1977; F.A.O., 1989). Laboratory analysis was carried out on samples taken from the soil of beneath the plant canopies and between the plants. Both the soil crust (if present), and the upper soil horizons were sampled, as described in Tables 1 and 2. Chemical analysis was carried out to determine pH, CaCO$_3$ (dissolution in HCl) and Organic Carbon (Allison method) using standard analytical techniques. Textural analysis was carried out by standard sieving procedure for the sand fractions and with a X-ray particle sizer (Microscan II) for the fractions smaller than 63 μm for the Guadalentín samples and with the pipette method for the other samples. Due to the very high CaCO$_3$ contents of the samples from the Guadalentín these were not decalcified before laboratory analysis. Rainfall simulations were carried out at two

scales: At the 0.5 m^2 plot scale, a portable dripping plate simulator (Bowyer-Bower and Burt, 1989) was used to apply three rainfall intensities. At the intermediate scale a large sprinkling rainfall simulator was used, covering 5 × 2.5 m^2 (SE Spain) or 10 × 2.5 m^2 (NE Spain). The experiments in SE Spain were designed in the following way: a rainfall intensity of 40 mm h^{-1} was applied for all experiments. An experiment of 2 days consisted of 5 consecutive storms, the first three of 10 min evenly spread over the first day of the experiment, and on the second day a storm of 10 min, after 1 h followed by a final storm of 30 min duration. In all cases demineralised water was used to prevent problems related to flocculation of suspended material and swelling of the topsoil, as these soils are very susceptible to dispersion. Time to ponding and overland flow was visually determined. Runoff was sampled at regular intervals and sediment load was determined by drying the runoff samples. The wetting front was studied by excavating a soil profile over 2 m width, after the experiments. The depth and lateral extension of the wetting front was recorded with measurement tapes and plotted on paper. Vegetation cover and structure were mapped in the field by using a grid counting method for small areas (< 1 m^2). Vegetation patterns on the hillslope scale were mapped at a scale of 1:100 or 1:50 using a grid system over 30 m length. Mapping also allowed for the identification of runoff, erosion, and deposition areas and patterns at the hillslope scale.

4. Results and analysis

4.1. Patterned phenomena in SE Spain

The plateau soil surface is flat and soil depth is delimited by a massive layered petrocalcic horizon to 18 cm depth. The soil surface under the *S. tenacissima* tussocks is slightly higher than the surrounding bare places and the soil surfaces can be distinguished into three main zones. The central zone of the living *S. tenacissima* tussock, has high porosity, high biological activity and an active root system. This part of the plant transmitted large amounts of rainfall directly to the soil via stem flow and root flow. After 10 min of rain at 40 mm h^{-1} (6.8 mm of rainfall) the wetting front protruded about 5–8 cm around the central rooting system into the soil matrix. The plant tussock is surrounded by a zone with some plant debris water repellent in nature, cryptogamic crusts and worm casts which are often colonised with lichen. This zone is overshadowed by dead standing litter at the sides of the *S. tenacissima* tussock with very high interception and storage capacities. Around this zone, a bare strongly crusted area with small embedded rock fragments is found. The 0.5–1 cm thick crust is underlain by a powdery layer, about 3 cm thick, with no soil structure at all. During rainfall simulations (intensity 40 mm h^{-1}) it was observed that the bare central areas were completely ponded and no overland flow occurred over the flat surfaces.

Rainfall simulations carried out on *S. tenacissima* tussocks clearly demonstrated the fast transmittance of soil water under living plants and the intercepting effect of the dead canopy. The wetting front under the plants showed clear quickly extending wet pockets around the central root system under the living central part of the plant. Under the dead standing part of the canopy no infiltration was observed, whereas in the surrounding

bare areas the wetting front moved more slowly but regularly with increasing rainfall depth. This can be explained by the following mechanisms: water intercepted in the living part of the canopy is partly transmitted as stemflow directly to the rooting zone, where water is transported by rootflow and along other preferential flowpaths of water in the partly water repellent subsoil. Some rain, falling through the canopy on the litter floor is also reallocated to the central part of the *S. tenacissima* tussock due to the water repellency of the litter material at the soil surface. Most water falling on the dead standing canopy is stored in the dead canopy or falls on the water repellent surface and is also redirected to the plant centre. After five successive short showers the importance of the stem-rootflow mechanism became clear, even under low amounts of precipitation.

The slopes have an open *S. tenacissima* vegetation cover (Fig. 2). The *S. tenacissima* plants are more widely distributed on the upper part of the slope, compared to the lower part of the slope, and also other species occur on the upper part of the slope such as rosemary bushes (*Rosmarinus officinalis*) and isolated pine trees (*Pinus halepensis*). Often the micro-topography of the slope surface shows miniature terracing, as a result of the accumulation of coarse and fine material in front of the *S. tenacissima* tussocks.

On the steeper parts of the slopes rock fragments are very common. They are derived from either limestone outcrops at the plateau rim, or are transported petrocalcic fragments. Most of them are not embedded in the soil crust and the amount of rock fragments decreases down slope as the gradient decreases.

During rainfall events which generate overland flow the water is transporting considerable amounts of sediment as could be derived from many traces on the soil surface. Fig. 2 illustrates the presence of overland flow pathways, visible as narrow channels of clean crusted surfaces, ending in sedimentation lobes, of gravel sized material near *S. tenacissima* tussocks. Some larger channels continue over much longer distances in between the widely distributed *S. tenacissima* tussocks, with deposition of gravel sized material along the channel sides as small natural levees of 5–10 cm width and 3–4 cm height. In larger complexes of *S. tenacissima* tussocks, complete infiltration may occur and no trace of overland flow was observed below these complex tussocks. In general the density and width of overland flow channels increases down slope, notwithstanding slope angle decrease.

In Fig. 3 the runoff characteristics are displayed obtained from experiments with the large sprinkler rainfall simulator. The sprinkled zone covered several connected open areas around isolated *S. tenacissima* tussocks. The experiment consisted of four 10-min and one 30-min shower carried out on two days. On a wetted surface and with rainfall durations longer than 10 min at an intensity of 40 mm h^{-1} runoff percentages reach over 60% at the plot scale. The soil moisture content at 5 cm depth under bare surface rose from an initial level of 0.06 cm^3 cm^{-3} to 0.17, 0.25 and 0.28 cm^3 cm^{-3} at the onset of the 2nd, 3rd, and 4th. event. The fifth event started with a level of 0.37 cm^3 cm^{-3}.

Fig. 2. Sketch map of the upper hillslope (22° to 12°) indicating relative dense arrangement of *S. tenacissima* tussocks and indicating the traces of overland flow as well as the places where sediment was deposited. Top of figure is the top of the hillslope.
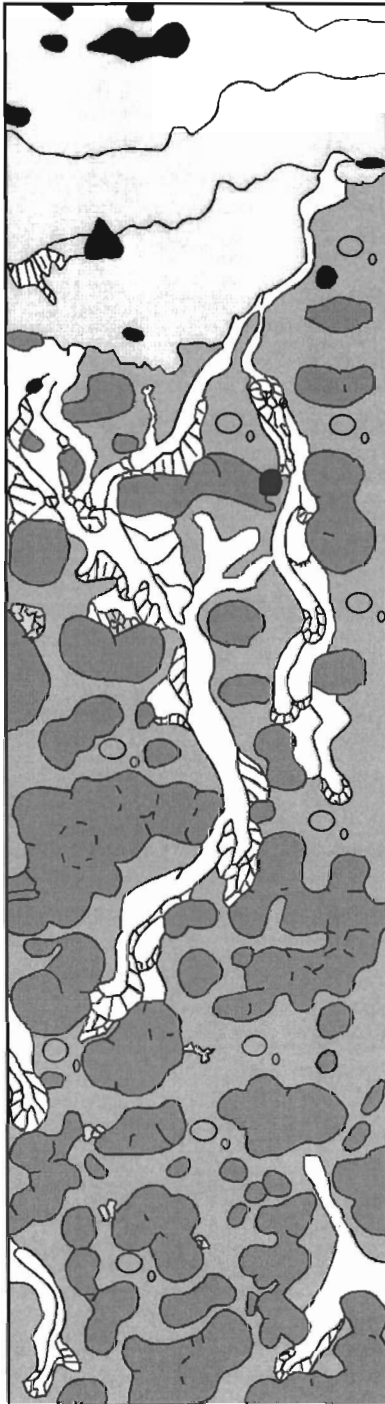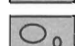
LEGEND

Vegetation

● Rosemary shrubs

⬤ Stipa tussocks
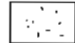
Stable surfaces

Bedrock (with step)

Crusted

Crusted with stones

Stone accumulation
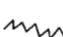
Surface processes

← Overland flow path

Active surfaces

Erosion surface

Lobeform deposition

Fanlike silt deposition

Coarse material

Micro-topography

Micro-step (1-2 cm)

Micro-step (2-4 cm)

Microstep (4-10 cm)

Scale (metres)

0   5
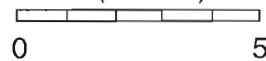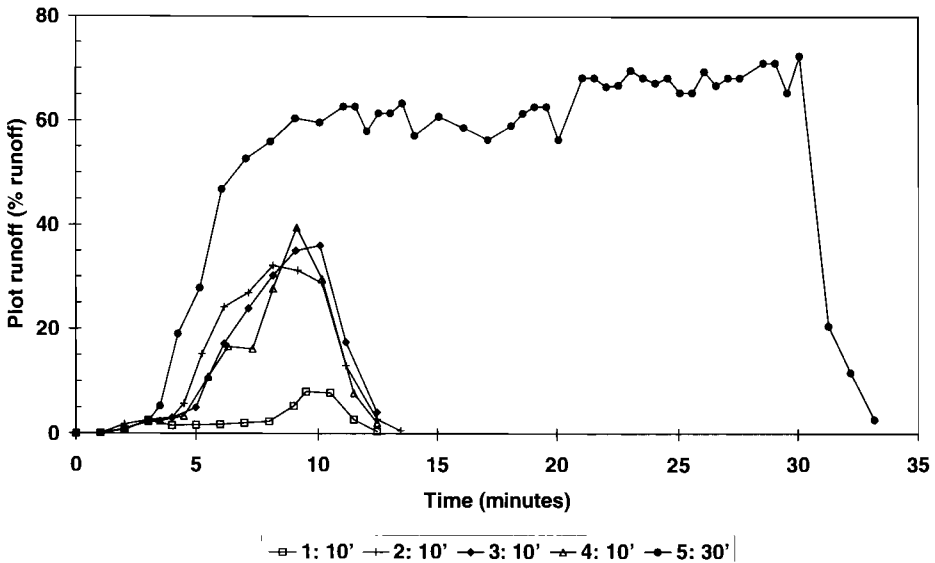
Fig. 3. Results of a rainfall simulation experiment on a sloping *S. tenacissima* covered area (2.5 × 5 m). Five small events of 40 mm h^{-1} are indicated, lasting 10 min except for the last one, which lasted 30 min. The events were divided over two days.

It is clear that the length and the frequency of relatively small rainfall events are very much determining the response of the soil. The first produced hardly any runoff, whereas the second to fourth shower gave similar results with respect to runoff with infiltration rates still decreasing during the storm. The fifth shower, carried out under wet initial conditions inherited from the previous showers, showed a strong increase in runoff levels and reached the final infiltration rate of this soil surface within 10 min after the start of the storm. Infiltration pattern showed similar subsurface distribution patterns as on the *S. tenacissima* covered plateau, with a larger infiltration depth in the upslope area of the plant tussock.

On the more gently sloping areas, two land-use types occurred (open *S. tenacissima* vegetation and sparsely vegetated abandoned fields). In both cases overland flow traces are still very common. This area is a remnant of a much larger area originally covered with *S. tenacissima* before it was brought into cultivation around the early 1960s and then successively abandoned in 1983. Aerial photographs of 1957 (M.A.P.A., 1957) reveal that the whole abandoned zone around the plateau was covered with semi-natural shrubland and that only the talwegs were being cultivated.

A part of the area presently covered with *S. tenacissima* is shown in Fig. 4, indicating its spatial distribution and the patterns of overland flow, deposition and erosion. The *S. tenacissima* tussock density is much less than on the steeper slope. Continuous flow paths of runoff were observed coalescing into larger pathways. Sediment deposition is not in the form of lobes of gravel sized material, but in accumulative sheets of fine (sand, silt and clay) material, selectively deposited in front of a *S. tenacissima* tussock,
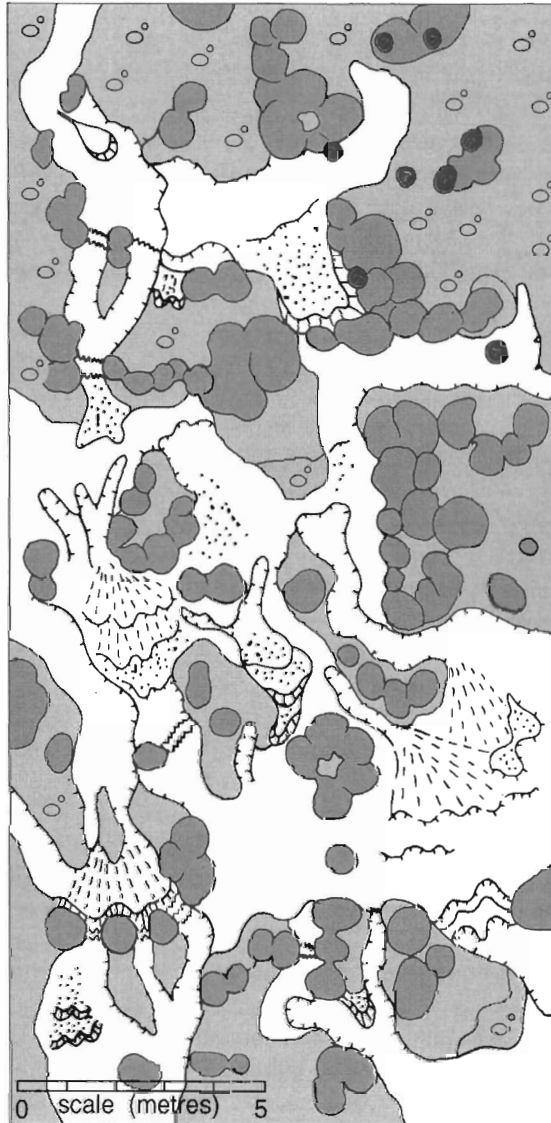
Fig. 4. Sketch map of the lower hillslope (8° to 2°) indicating a relative open arrangement of *S. tenacissima* tussocks with a clear presence of overland flow traces and sediment deposition. Legend as in Fig. 2.

forming small discontinuities in the micro-topography of the slope. In between bordering tussocks surface micro-steps occurred in the surface, which were being eroded upslope. The soil surface has strong depositional crust with a one grain thick coarse sand or fine gravel layer on top. The crust has a massive structure and is breaking into blocky elements, of about 3 cm thickness, at erosional micro-steps. These blocks disintegrate

into smaller parts, micro-aggregates and primary particles which are deposited lower on the slope.

The area where the *S. tenacissima* has been cleared for agricultural use, and which has been abandoned in 1983, a massive continuous bright crust is present, most probably formed by slaking and/or depositional processes. The silt loam material at the surface was found to be very sensitive to dispersion in relation to the electrical conductivity of the water. At very low electrolyte contents ($EC_{25} = 25$ μS cm^{-1}) material readily dispersed whereas at $CaCO_3$ dominated water ($EC_{25} = 800$ μS cm^{-1}) flocculation occurred much faster. Small desiccation cracks were found on the surface, rapidly disappearing upon wetting.

On this surface hardly any plants were present. This can be explained by a combination of several factors such as a hindered germination of seeds and very limited infiltration in the dense crust, the very low amounts of precipitation during recent years, the marly character of the soil with lower water retention capacities, and also grazing.

One of the dominant vegetation species is *P. albicans*, which is very small and adapted to trampling, and occurs in semi-linear bands or lines, developed in a direction parallel to the contours, at a more or less regular interval. Directly downslope of these plants micro-steps of a few (1–4) centimetres height have developed in the soil surface, due to the accumulation of mainly fine soil material and some organic debris.

It was also observed that at zones where more runoff is produced, especially in shallow depressions in the plateau slope, small rills and gullies have developed on the slope. They end shortly downslope of the break in the slope or piedmont junction in the footslope (Kirkby and Kirkby, 1974; Abrahams et al., 1994). Here they become transformed into blankets of silty sediments spreading out just below the slope transition, indicating a threshold in hydraulic conditions from sediment carrying overland flow and rill-flow towards a sedimentation dominated regime. This is also reflected by the effects of two short convective storms (approximately 30 mm within 30 min) in May and September, that produced overland flow in considerable amounts, resulting in the burying of the *P. albicans* plants under a silt blanket.

4.2. Patterned phenomena in burnt oak forests NE Spain

This section summarises the results of more than one hundred rainfall simulation experiments made on burnt areas in the vicinity of Vilobí and from studying runoff in natural storms. Measurements were first made at Vilobí one year after the fire. At other sites nearby, infiltration rates were measured directly following a fire and found to be relatively high. Due to wind, very intense thunderstorms and disturbance, the ash and burnt topsoil is redistributed and the surface attains patterned properties relatively quickly. In some cases this is enhanced by dead needles that drop from the trees killed by the fire.

At Vilobí, after one year micro steps, strips and polygonal patterns characterised the upper parts of the slope and the local terrace plateau. The polygons were formed by *Cistus* species. and other seedlings, and fine accumulating organic debris. About 80% of the area appeared as a bare sandy surface and the remainder appeared as vegetation covered areas. The vegetation covered areas consisted of the resprouting stems of plants

such as *A. unedo* and *E. arborea* around the bases of which organic rich debris and ash had accumulated. These areas formed bands along the slope. The bare areas were usually found where the organic top soil had been lost and thin layers of fine gravel and sand had accumulated. In places *Cistus* species. seedlings were present on the bare areas. On the steeper slopes clayey Bt horizons had been exposed on the surface.

Rainfall simulation experiments and laboratory investigations of samples from soils on the upper part of the slope where the Bt horizon was not on the surface, revealed that the soil below the bare surface was hydrophobic to a depth of 5 to 10 cm. The effects of the hydrophobicity were such that during rainfall simulation experiments the runoff would sometimes be high at the start of the storm, decrease during the experiment as the soil lost its water repellency and then increased again as the soil became wet. It was also apparent that not all of the area was hydrophobic. About 5% of the surface consisted of the openings of channels that contained organic rich soil or debris. These acted as conduits through the hydrophobic layer so that water by-passed the E horizon. Infiltration and runoff measurements were consequently highly variable as they reflected the interaction of three processes: the gradual decrease of the hydrophobic effect; the effect of soil moisture on sorptivity and the number of organically rich channels that were present to transmit by-pass flow.

Fig. 5 shows a number of successive rainfall simulation experiments made on a bare surface, two years after the fire. In order to emphasise the significance of hydrophobicity for low intensity storms results from a simulated intensity of 20 mm h^{-1} are shown. The measurements were made at 2 h intervals and the moisture content in the series shown
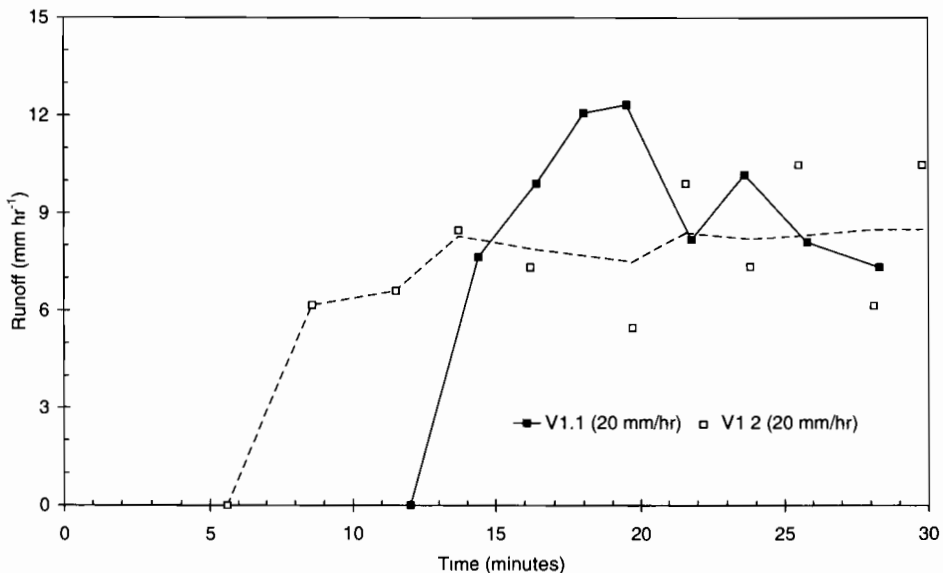
Fig. 5. Runoff curves from rainfall simulation experiments on burnt land at Vilobí (NE Spain), showing the effect of hydrophobicity. The line for V1.2 is interpolated between the observed points.

increased from 7 to 11 and 20%. During the first simulation event the loss of the hydrophobic effect can be seen in curve V1.1 after 20 min. The second curve shows a more regular infiltration behaviour after the loss of the water repellency effect upon wetting. At higher rainfall intensities it was found that the first events produced high rates of runoff and the second events very little or no runoff. In the winter, when soils are sometimes wet, this is not the case.

Fig. 6 illustrates the behaviour of the clayey soils during the summer. In these soils, there is no hydrophobic effect. A 30 min rainfall intensity of 20 mm h^{-1} produces no runoff so that data for higher intensities are shown to illustrate the behaviour. Runoff reaches a constant value that reflects the hydraulic conductivity of the horizon. In the summer this is quite high. The amount of runoff also reflects the rainfall intensity. At the forest site this ranged from 57 (V2.1) through 45 (V.2.2) to 31 (V2.3) mm h^{-1}. In the winter infiltration rates were found to be 20 to 40% lower than those in the summer and the clay soils always produced runoff within 5 min.

The rainfall simulation experiments described above showed that for bare areas runoff coefficients were often as high as 50%. These measurements were made on 1 m long plots. When the plot length was increased to 10 m on the bare soils with the AE horizon at the surface, it was found that very little or no runoff left the plots for 40 min storms with intensities of about 40 mm h^{-1}. What occurred was that the bare hydrophobic sand covered patches rapidly became ponded to a depth of several cm. Flow velocities were very low and it was apparent that the gravel and sand was a lag deposit. Although the material was moved by splash creep, the transport capacity of the runoff, calculated from measured values was too low to transport the sand and gravel. It was apparent in view of the ponding and lack of runoff that most of the infiltration was
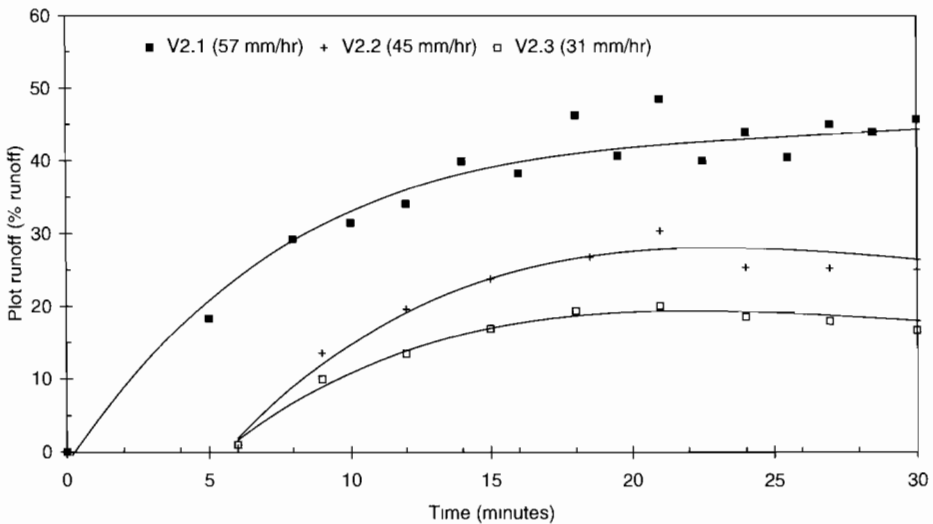
Fig. 6. Runoff curves from rainfall simulation experiments with different rainfall intensities under summer conditions on burnt land at Vilobí, (NE Spain).

taking place beneath the resprouting bands of shrubs. This was verified by excavating the sites after the rainfall simulation experiments.

5. Discussion

5.1. Patterned phenomena on S. tenacissima covered and abandoned land in SE Spain

In Fig. 7 the relation between rainfall intensity and time to ponding is given, indicating the differences in infiltration rates on bare areas at the different land use units discussed. It is very evident that the infiltration rates are lowest in the abandoned zone, due to the presence of the dense silty crust of the soil surface. It gives a result for the abandoned zone which can be used for upscaling, as the spatial heterogeneity is present at a much more detailed scale, falling within the spatial limits of the dripping plate simulator. The infiltration rates of the other land-use types are only reflecting the infiltration properties of the bare areas. Cerdà (1997) describes infiltration rates for small radial plots (50 cm diameter) for the bare, and vegetation covered sites in the area of study. He reports clear differences in infiltration rates for the different types of cover. However, these properties cannot directly be translated to larger areas, as the interaction between the different infiltration characteristics of the bare runoff and vegetated runon (water absorbing) areas are non-linear (Dunne et al., 1991; Bergkamp et al., 1996; Morin and Kosovsky, 1995). For this reason intermediate scale simulations were carried out,
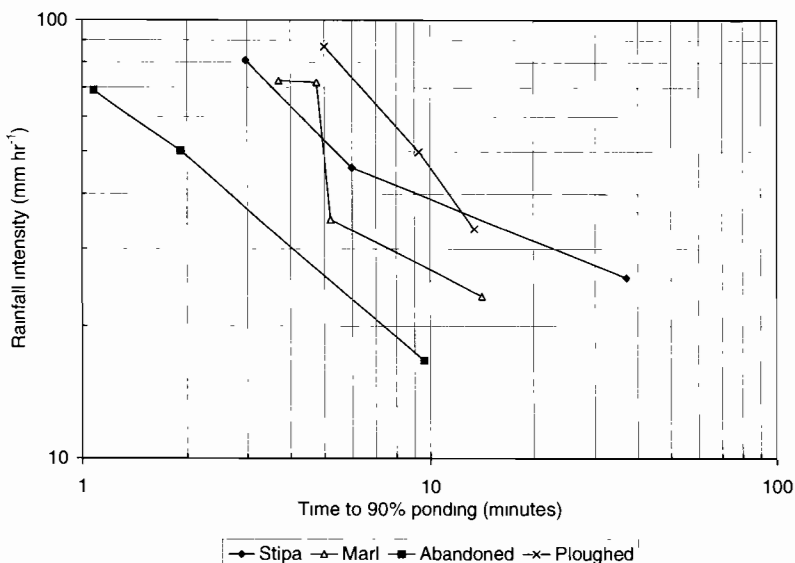
Fig. 7. Relation between rain fall intensity and time to ponding indicating the deterioration in infiltration after abandonment on strongly crusted and silty topsoils for the Cañada Cazorla region (SE Spain).

containing both vegetated, and bare areas to incorporate their mutual effect on infiltration and runoff production which were described before.

Under *S. tenacissima* tussocks infiltration was found to be greatly enhanced by an active stem-root flow system. This resulted in a deeper penetration of the wetting front under the living plant. It was not clear how much water was totally absorbed by the dead standing biomass and how much water was diverted towards the plant root system over the water repellent material on the soil surface. The bare area showed a slow regular increase in infiltration depth, and it might be suggested that two different rooting systems are active, one dealing with diverting water efficiently directly to the roots under small rainfall amounts and a second system, which is active under more wet conditions, when the wetting front under bare soil surfaces reaches deep enough to pass the surface crust and the dusty layer.

On the hillslope the *S. tenacissima* tussocks are situated at the downslope rim of small terracettes, built of accumulated sediment at the upslope side of the tussocks. This process of accumulation is described for mountain slopes in the Pyrenees (Gallart et al., 1993) and on metamorphic rocks (Sanchez and Puigdefabregas, 1994). Processes responsible for movement of slope material are wash and deposition by overland flow and rock fragments displaced by trampling, grazing animals. The downslope splash of soil material may also play a role.

On sloping areas the lateral redistribution of water over the surface becomes important and plant patterns develop over the slope. These become significant in determining whether overland flow is generated over longer distances or not. On more bare areas with less tussocks, more traces of overland flow and sediment deposition were found. The density of the *S. tenacissima* tussocks on the slopes studied showed a decrease with lower slope angles at lower slope position. On these slopes a decrease in rock fragment cover at the soil surface and a decreasing surface roughness are found in a downslope direction. Apparently, on these slopes so much water is produced that, with decreasing slope angles, more and more water is concentrated downslope. This conform with the results of the rainfall simulations, which indicate very high runoff figures for slopes with an open plant cover and for heavily crusted areas. Deposition of material increases with lower slope angles and the material is preferably deposited directly upslope of the *S. tenacissima* tussocks (see also Fig. 4). Puigdefabregas and Sanchez (1996) found that the sedimentation rate is a very important factor in the openness of the vegetation. It must be said, however, that the amount of rock fragments, which decreases downslope, certainly will influence infiltration properties and therefor also the transport capacity of overland flow (Poesen and Lavee, 1994). In other nearby areas where the banded nature of vegetation layout becomes prominent, virtually all water is absorbed in the plant tussocks and infiltrates into the soil. This was also found on thyme and rosemary type of matorral growing on an arch-form terracette micro-topography on limestone slopes in other areas in SE and Central Spain (Bergkamp et al., 1996). It is suggested that vegetation structure ranging from banded via arch formed and open polygon-like *S. tenacissima* structure towards a more spotted vegetation structure is leading towards an increasing amount of runoff concentration and sediment transport. This phenomenon is also described for semi-arid regions in Australia (Tongway and Hindley, 1995). Local factors related to this are also gradient and aspect, soil roughness

(rock fragment cover), soil surface conditions (crusting and infiltration capacity), sediment delivery, and cover percentages of vegetation. More regional factors affecting these processes are climatological conditions as well as geological properties.

The tussocks of the *S. tenacissima* plants act as important sinks for water, sediments and nutrients. The more continuous the vegetation structure is, the more effective it will be in capturing these important resources. The tussocks themselves also act as fertile islands on the slope, where organic matter and other nutrients are retained. They give shade and shelter to many soil animals which play an active role in bioturbation. This in turn positively affects infiltration and incorporation of organic matter in the soil which positively influences soil structure (Cammeraat and Imeson, 1998). This will favour the health of the plant and this whole cycle could be seen as a positive feed-back mechanism. In fact the presence of a (banded) vegetation structure could be used as an indicator of health of the ecosystem as also is proposed by Tongway and Hindley (1995) in Australian areas. The processes of sedimentation, erosion and water reallocation show a very dynamic interaction with vegetation. Sanchez and Puigdefabregas (1994) showed that the *S. tenacissima* tussocks have a radial growth pattern. Once the tussock becomes too large, it falls apart into a polygon of clumps of plants, each evolving into a separate new plant. This growth pattern is strongly influenced by gradient, sediment flux and water reallocation. The development of these vegetation structures is highly dynamic and different from the patterns as observed by Dunkerley and Brown (1995), who describe a type of vegetation banding as old stable features.

At much lower slope positions, at the slope break, deposition clearly becomes more and more important, and blankets of silt sized material are deposited, both in open *S. tenacissima* matorral and on abandoned fields. On this latter zone a thick silty crust is present, which micro-topographical steps are coinciding with bands of *P. albicans*. The vegetation bands have a wavelength with an average of 1.2 m. The general percentage cover of vegetation is very low, and this is apparently related to persistence of drought, presence of a heavy crust and grazing, although no actual traces of grazing were found. The small bands of plants act as a sediment trap during the scarce periods of overland flow, when silty sediments are transported downslope. Directly under the small steps erosion takes places during overland flow, creating small steep cuts in the surface with a height of about 2 cm, exposing coherent layered silts. Vegetation banding and the resultant stepped topography, are probably related to the dynamics of the erosion and sedimentation. A process is supposed where sediment is deposited in small lobes from concentrated flow lines. The sediments form a dense crust where germination is difficult and infiltration is reduced. Just downslope the micro-steps the new silt deposit and crust is less dense and infiltration and germination are expected to be favoured in this position. Hence the upslope part of the sedimentation lobe acts as a runoff producing area, whereas the lower rim of the sedimentation lobe acts as a water absorbing area (runon area). When several lobes of sediment grow laterally together over a longer period, and plants have established along its rim, this could result in a alternating banding of relative broad strongly crusted areas, and a narrow zone with plants. However, several other processes could also play a role, of which the formation of tracks by passing grazing flocks is one, as well as inheritance of micro-topography resulting from parallel contour ploughing.

5.2. The significance of patterned phenomena following fire (Vilobí area, NE Spain)

The results from Vilobí d'Onyar in NE Spain show that soil hydrophobicity plays an important role in concentrating infiltration beneath vegetation. The hydrophobic layer has a very positive effect as a rainwater harvesting mechanism. It does not seem to be produced as a result of the fire. Rainfall simulation experiments in undisturbed forests showed that as on the burnt land, the AE horizons were hydrophobic, except for both areas around the roots and in old root channels filled with organic matter. Low to moderate intensity summer rainfall is trapped by this mechanism and conserved in the BC horizons for use by shrubs and trees. It is a coincidence that just as is the case with the *S. tenacissima*, roots are concentrated probably in relation to different types of hydrological event and runoff generating mechanism. They are located both beneath the shrubs where runon water accumulates during periods that are antecedently dry but also in the BC horizon beneath the hydrophobic AE horizon. This area receives water through the by-pass channels during minor events that do not produce runon. In the winter during wet weather, completely different mechanisms sometimes exist when subsurface saturation overland flow can occur above the Bt horizon.

An important research question concerns the degree to which the resilience of the burnt area is affected by the runoff and infiltration patterns that are present prior to the fire. Patterns in soil structure and infiltration rates that have evolved under the forest over perhaps hundreds of years ensure that after a fire water is trapped and protected from evaporation by the hydrophobic effects. Observations and data suggest that soil erosion seldom occurs following a fire if the soil surface is left undisturbed. Management practices such as ploughing and terracing and post fire tree extraction destroy the natural runoff trapping mechanisms that are present. Perhaps a reason why post fire soil erosion is so high on plantations of exotic and other vegetation is that these do not have the facility to generate soil water harvesting strategies or that they cannot do so because of a lack of synergetic relationships with other ecosystem components.

6. Conclusions

From the study in SE Spain it is concluded that patterned phenomena are of great significance in explaining hillslope hydrology and patterns in soil erosion. These patterns form a potential key to understanding an important component of the resilience of the systems studied. The results also demonstrate that the non-random distributions of patterned phenomena on hillslopes need to be considered in up-scaling. The individual responses of bare and vegetated area to infiltration and overland flow cannot be understood without studying their spatial configuration. At the hillslope or basin scale, the spatial patterning of vegetation determines the flow concentration of overland flow as different bare areas may become connected if the infiltration rates of bares areas are exceeded by rainfall intensities and the absorption of water in the vegetated structures. The larger the upslope perimeter and perimeter/surface area ratio, and the larger the vegetation cover, the larger the capacity of infiltration will be. The semi-natural vegetation therefore is an important factor in reducing overland flow and land degrada-

tion. The disturbance of these areas by drought or overgrazing, or by removal of the vegetation will therefor decrease the ability to absorb the water at a local scale and increase the generation of runoff over larger areas. The natural revegetation was found to be very low indicating that these areas are vulnerable to land degradation after the destruction of the semi-natural *S. tenacissima* vegetation. Under these degraded circumstances the development of fine scale banded vegetation structures, dominated by *P. albicans* was observed, indicating a strong interrelationship with plant development, sedimentation and soil surface crusting.

Two conclusions from the study in NE Spain are emphasised. The first concerns the conclusion that hydrophobic effects are positive and not negative. There are two possible explanations. The first is that conditions in NE Spain are different from elsewhere. The second is that previous studies have considered infiltration and runoff rates measured from small scale experiments and scaled up to a hillslope or catchments scale using statistics. When larger scale measurements are used to establish how large scale slope sections generate runoff, it is clear that the system is behaving differently at this higher hierarchical level of scale. In other words when a hierarchical systems concept is applied to the interpretation of the data, it is evident that the small scale structures that have evolved create positive feedbacks at a higher scale that enable the vegetation to trap and conserve water and also to recover efficiently following a disturbance.

The second conclusion, which also applies to SE Spain is that patterns that take decades or hundreds of years to evolve are stabilising properties of ecosystems that help them to recover from disturbance or to resist stressors. Management should take this into account and follow strategies that enable these to be promoted or conserved. It seems that many attempts to restore land that has been burnt or abandoned are doomed to fail because they not only neglect the importance of water redistribution phenomenon, but actually promote their destruction.

References

Abrahams, A.D., Howard, A.D., Parsons, A.J., 1994. Rock-mantled slopes. In: Abrahams, A.D., Parsons, A.J. (Eds.), Geomorphology of Desert Environments. Chapman and Hall, London, pp. 173–212.

Bergkamp, G., 1996 Mediterranean geoecosystems: hierarchical organisation and degradation. PhD Thesis University of Amsterdam, 238 pp.

Bergkamp, G., Cammeraat, L.H., Martinez-Fernandez, J., 1996. Water movement and vegetation patterns on shrubland and an abandoned field in two desertification threatened areas in Spain. Earth Surface Processes and Landforms 21, 1073–1090.

Bowyer-Bower, T.A.S., Burt, T P., 1989. Rainfall simulators for investigating soil response to rainfall. Soil Technology 2, 1–16.

Cammeraat, L.H., Imeson, A.C., 1998. Deriving indicators of soil degradation from soil aggregation studies in SE Spain and S France. Geomorphology 23, 307–321.

Cerdà, A., García-Alvarez, A., Cammeraat, L.H., Imeson, A.C., 1994. In: García-Ruiz, J.H., Lasanta, T. (Eds.), Agregación del suelo en una catena afectada por el abandono del cultivo en la cuenca del Guadalentín (Murcia): I. Estabilidad y distribución de los agregados del suelo. Efectos Geomorfológicos del Abandono de Tierras. Sociedad Española de Geomorfología, Zaragoza, pp. 9–19.

Cerdà, A., García-Alvarez, A., Cammeraat, L.H., Imeson, A.C., 1995. Fluctuation estacional y dinámica microbiana en una catena afectada por el abandono del cultivo en la cuenca del Guadalentín (Murcia). Pirineos 145/146, 3–11.

Cerdà, A., 1997. The effect of patchy distribution of Stipa tenacissima L. on runoff and erosion. Journal of Arid Environments 36, 37–51.

Dunkerley, D.L., Brown, K.J., 1995. Runoff and runon areas in a patterned chenopod shrubland, arid western New South Wales, Australia: characteristics and origin. Journal of Arid Environments 30, 41–55.

Dunne, T., Zhang, W., Aubry, B.F., 1991. Effects of rainfall, vegetation, and microtopography on infiltration and runoff. Water Resources Research 27, 2271–2285.

F.A.O., 1977. Guidelines for soil profile description. Soil Survey and Fertility Branch. Land and Water Development Division, FAO, Roma, 150 pp.

F.A.O., 1989. FAO/Unesco Soil Map of the World, Revised Legend, World Resources Report 60, FAO, Rome. Reprinted as Technical Paper 20, ISRIC, Wageningen, 138 pp.

Fantechi, R., Margaris, N.S., 1986. Desertification in Europe. Reidel, Dordrecht, 229 pp.

Gallart, F., Puigdefabregas, J., Barrio, G.D., 1993. Computer simulation of high mountain terracettes as interaction between vegetation growth and sediment movement. Catena 20, 529–542.

I.G.M.E. (Instituto Geologico y Minero de España), 1981. Mapa Geologico de España, 1:50.000. Sheet Lorca (no. 953), Serv. Publ. Min. Industria, Madrid, 43 pp.

Imeson, A.C., Verstraten, J.M., Van Mulligen, E.J., Sevink, J., 1992. The effects of fire and water repellency on infiltration and runoff under Mediterranean type forest. Catena 19, 345–361.

Imeson, A.C., Cammeraat, L.H., Perez-Trejo, F., 1995. Desertification response units. In: Fantechi, R , Peter, D., Balabanis, P., Rubio, J.L. (Eds.), Desertification in a European Context: Physical and Socio-Economic Aspects. Office for Official Publications of the European Communities, Luxembourg, pp. 263–277.

Imeson, A.C., Perez-Trejo, F., Cammeraat, L.H., 1996a. The response of landscape-units to desertification. In: Brandt, J., Thornes, J B (Eds.), Mediterranean Desertification and Land-Use. Wiley, Chichester, pp. 447–469.

Imeson, A.C., Cammeraat, L.H., Prinsen, H.A.M., Cerdà, A., 1996b. Field site integration, data base management, desertification response units. In: MEDALUS II, Final Report Basic Field Programme. King's College, London, pp. 1–37.

Kirkby, A., Kirkby, M.J., 1974. Surface wash at the semi-arid break in slope. Z. Geomorph. N. F. Suppl. Bd. 21, 151–176.

M.A.P.A., 1957. Aerial photographs, Ministerio Agricultura Pesca y Alimentacion, Madrid.

MEDALUS, 1996. Research and policy interfacing in selected regions. MEDALUS II Final Report. Kings's College, London, 715 pp.

Morin, J., Kosovsky, A., 1995. The surface infiltration model. J. of Soil and Water Conservation 50, 470–476.

Navarro-Hervás, F., 1991. El sistema hidrográfico del Guadalentín. Consejeria de Politica Territorial, Obras Publicas y Medio Ambiente, Murcia, 256 pp.

O'Neill, R.V., DeAngelis, D.L., Waide, J.B., Allen, T.F.H., 1986. A Hierarchical Concept of Ecosystems. Princeton University Press, NJ, 253 pp.

Pierson, F.B., Van Vactor, S.S., Blackburn, W.H., Wood, J.C., 1994. Incorporating small scale spatial variability into predictions of hydrologic response on sagebrush rangelands. In: Blackburn, W.H., Schuman, G.E., Pierson, F B. (Eds.), Variability in Rangeland Water Erosion Processes. SSSA Special Publication 38. Soil Science Soc. of America, Madison, pp. 23–34.

Poesen, J., Lavee, H., 1994. Rock fragments in top soils: significance and processes. Catena 23, 1–28.

Puigdefabregas, J., Sanchez, G. 1996. Geomorphological implications of vegetation patchiness on semi-arid slopes. In: Anderson, M.G., Brooks, S.M. (Eds.), Advances in Hillslope Processes. Wiley, London, pp. 1027–1060.

Sanchez, G., Puigdefabregas, J., 1994. Interactions of plant growth and sediment on slopes in a semi-arid environment. Geomorphology 9, 243–260.

Sevink, J., Imeson, A.C., Verstraten, J.M., 1989. Humus form development and hillslope runoff, and the effect of fire and management under Mediterranean forest in NE-Spain. Catena 16, 461–475.

Thiéry, J.M., D'Herbes, J.-H., Valentin, C., 1995. A model simulating the genesis of banded vegetation patterns in Niger. Journal of Ecology 83, 497–507.

Thornes, J.B., 1995. Mediterranean desertification and the vegetation cover. In: Fantechi, R., Peter, D., Balabanis, P., Rubio, J.L. (Eds.), Desertification in a European Context: Physical and Socio-Economic Aspects. Office for Official Publications of the European Communities, Luxembourg, pp. 169–194.

Tongway, D., Hindley, N., 1995. Manual for assessment of soil condition tropical grassland. CSIRO, Division of Wildlife and Ecology, Canberra, 60 pp.

Valentin, C., Bresson, L.-M., 1992. Morphology, genesis and classification of surface crusts in loamy and sandy soils. Geoderma 55, 225–245.

ELSEVIER

Magnitude-frequency analysis of water redistribution along a climate gradient in Spain

G. Bergkamp [a,*], A. Cerdà [b], A.C. Imeson [a]

[a] *Ecosystem Management Group, IUCN, The World Conservation Union, Rue Mauverney 28, 1196 Gland Switzerland*
[b] *Departamento de Geografia Fisica, Universitat de València, 22060-46020, Valencia, Spain*

Abstract

Banded patterns in soils and vegetation form part of important discontinuities on semi-arid slopes in Spain. At fine scales (< 1 m) vegetation and well-structured soils are often located at the outer rim of small terracettes. Together they form banded patterns, distributed in a scattered way along contour lines. The objective of this study is to quantify the amount of surface water redistribution at fine spatial scales for three areas in Spain, having different rainfall regimes (290, 394 and 688 mm annual rainfall). Rainfall simulations experiments were carried out to determine runoff and infiltration characteristics of the bare and vegetated zones. The results of these experiments are combined with an analysis of the rainfall magnitude-frequency characteristics of the three area's. The combination of these two type of data has resulted in the calculations of a Redistribution Index (RI). The results showed a high variability in surface water redistribution from bare areas to banded vegetated zones. The combination of the infiltration characteristics at the different sites with the magnitude-frequency data of rainfall shows that most of the surface water redistribution originates from short storms with a duration of 10 min. The largest amount of redistribution during these events is found for areas having an intermediate rainfall regime with an annual rainfall of 394 mm. The Redistribution Index developed during this study provides a rapid methodology that can be used to evaluate differences in the importance of surface water redistribution in different banded vegetation structures at a regional scale. © 1999 Published by Elsevier Science B.V. All rights reserved.

Keywords: Water redistribution; Vegetation patterns; Climate gradient; Matorral; Runoff; Mediterranean

* Corresponding author. E-mail: gjb@hq.uiucn.org

1. Introduction

In many semi-arid environments, vegetation occurs in banded structures. Well known examples of banding at scales of hundreds of metres are described for the 'tiger bush' in the Sahel zone (Casenave and Valentine, 1989), banded patterns in the Mulga wood-lands in Australia (Ludwig and Tongway, 1995) and 'two-phase mosaics' in the Chihuahua Desert in Mexico (Montaña, 1992). In these environments, the movement of surface water from the less well vegetated bands forms an important input of water and nutrients into the vegetated bands. This redistribution of water affects dramatically the functioning of these ecosystems through, amongst other things, an increase in biomass production (Valentin and d'Herbes, this issue) and an increase in soil biological activity within the vegetated zones.

During investigations at several sites in Spain, it was observed that a banding of the semi-natural vegetation is present at a scale of metres. This banding is present in a scattered way along the contour lines and consists of small discontinuous stripes of vegetation located at the outer rims of small, stony terracettes, behind which mostly bare and often crusted surfaces are found. On the basis of these first observations, it was hypothesized that the hydrological functioning of these vegetated structures is strongly affected by surface water redistribution from the bare areas to the vegetated rims. This lead to the formulation of three main questions: (a) How much of the water input below the fine scale vegetation structures originates from surface water redistribution? (b) How does this amount of redistribution change with rainfall regime? and (c) How does the relative importance of redistribution depend on the time scale considered?

The amount of surface water redistribution, occurring under natural conditions, depends both on the infiltration characteristics of the bare and vegetated surfaces as well as the rainfall intensity, the storm duration and the recurrence intervals of specific events. For different locations within Spain these properties will be different. As both the infiltration characteristics and the rainfall intensity–return period relationships are highly non-linear, a comparison of the amount of surface water redistribution for different sites located in areas with different rainfall regimes will not be straightforward.

The objective of this paper is to quantify the amount of surface water redistribution in three areas in Spain having different climatological characteristics, for a fine spatial scale and temporal scales of 1 yr and 10 yr. The following approach focuses on: (a) the determination of runoff and infiltration characteristics by means of rainfall simulation experiments at a fine scale, (b) the analysis of meteorological data of the stations nearest to the field sites, and (c) the calculation of the amounts of surface water redistribution on the basis of the results of (a) and (b).

2. Research areas and sites

2.1. Research sites

The research was carried out in three areas in Spain, located along a climatological gradient. The first field site, Murcia, is located at 'El Ardal', in south east Spain near Murcia. The second site, Albacete, is located in central Spain in a less dryer area close to the city of Albacete. The third site is located near Valencia, near the Mediterranean
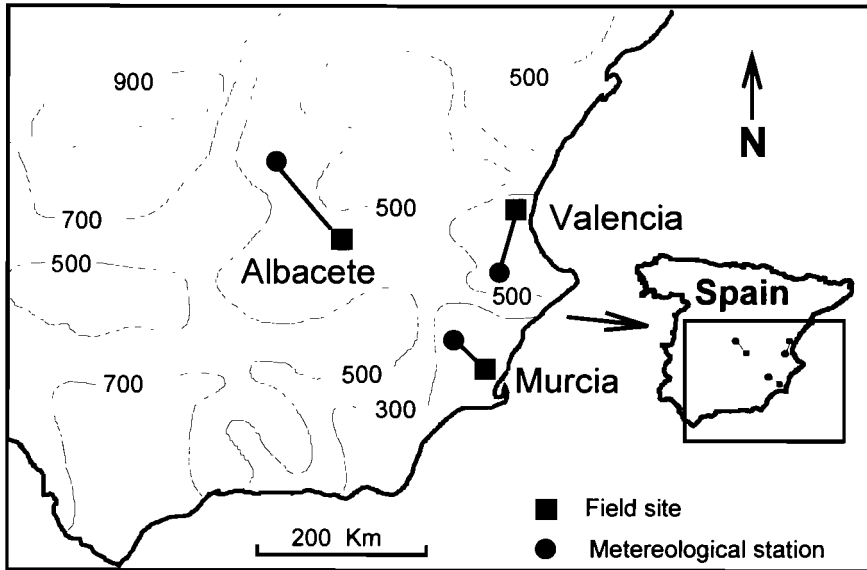
Fig. 1. Map of the south-east of Spain, indicating the location of the research sites and the meteorological stations used. Contour lines represent mean annual precipitation (mm).

coast (Fig. 1). The climatological characteristics of the three research locations show clear differences with respect to the amounts of total annual rainfall and the temperature

Table 1
Results of rainfall simulation experiments at the Murcia site

Plot no.	I, mm h^{-1}	Tcum, min	Pcum, mm	Roff, mm	Fcum, mm
M-1	56	5	5	0	5
		9	8	1	7
		17	16	5	11
		39	36	17	20
		47	44	18	26
M-2	42	3	2	0	2
		10	7	0	7
		20	14	0	14
		30	21	0	21
		40	28	0	28
		50	35	0	35
M-3	67	8	9	0	9
		18	20	0	20
		24	27	0	27
		30	34	0	34
		40	45	0	45
		50	56	0	56

I: mean rainfall intensity during experiment; Tcum: time from the start of the experiment; Pcum: total rainfall; Roff: runoff from the lower end of the plot; Fcum: cumulative infiltration.

regime (Table 1). The average yearly rainfall at the Valencia site is 688 mm. The Albacete site receives 394 mm and Murcia, 290 mm. All sites are underlain by limestone. The current land use at the Albacete and Murcia fieldsites is grazing by small herds of sheep and goats. The Valencia fieldsite is not grazed at present. The main effect of grazing is an unknown reduction of the vegetation biomass and a trampling of the soil surface around the plants, especially along grazing tracks.

The Murcia field site is located near Mula (Murcia Province) in the upper Mula basin (López-Bermúdez et al., 1991). This part of the Mula catchment is characterized by isolated hills of Eocene limestones reaching up to 600–1000 m.a.s.l. They are surrounded by gently undulating lower areas of Miocene marls and more recent colluvial material, with slopes between 6 and 15 degrees. The vegetation is characterised by a discontinuous scrub dominated by *Rosmarinus officinalis*, *Juniperus oxycedrus*, *Brachypodium retusum*, *Pinus halepensis*, *Thymus vulgaris* and *Cistus clusii*. These
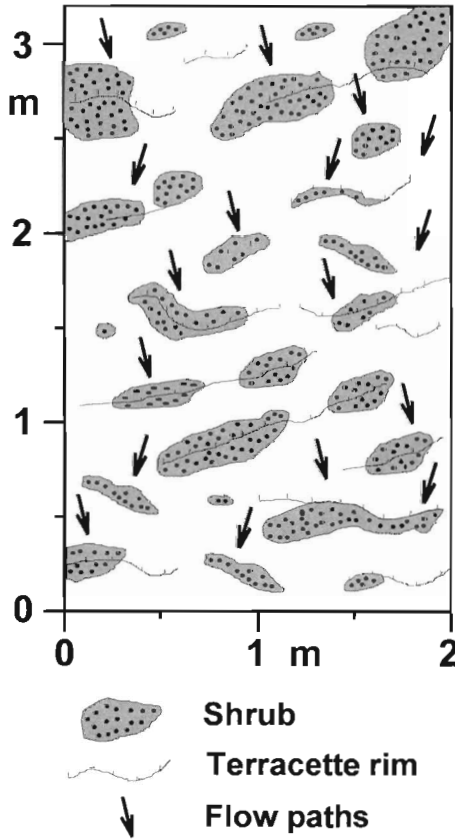
Fig. 2. Drawing of typical banded vegetation structure at fine scale observed at the Murcia and Albacete sites. At the Valencia site less elongated structures are present. Water is flowing from the top to the bottom of the figure.

plants are located mostly at the outer rim of terracettes (Fig. 2). In between these rims, bare areas are covered by stones and crusted surfaces. The stone fragments are of petrocalcic and limestone origin.

The Albacete field site corresponds to the EFEDA field-site 'Belmonte', located in the Záncara catchment (Cuenca Province). This field site is located approximately 100 km from the Albacete meteorological station. The area has a folded structure of Jurassic and Cretaceous marls, limestones and dolomites with major footslopes and higher valley terraces of Tertiary and Pliocene age. The Albacete field site is located on slopes of 13–20 degrees and is covered with a patchy, matorral vegetation, dominated by *T. vulgaris, B. retusum, Quercus rotundifolia* and *Quercus coccifera*. At a fine scale (< 2 m) the vegetation (*Thymus* spp. and *Brachypodium* spp.) is concentrated along the contour lines as indicated in Fig. 2. The soil surface is covered with limestone and dolomite rock fragments and partly crusted on the bare areas in between the terracette rims.

The Valencia field site is located near Genovés (La Costera, Valencia) at a height of 300–370 m and approximately 45 km from the Valencia meteorological station (Cerdà et al., 1995). The site is underlain by homogeneous limestone and covered by a matorral characterized by a patchy mosaic of shrubs (*Q. coccifera, Pistacia lentiscus, Chamaerops humilis, Rhamnus alaternus*) typical for the western part of the Mediterranean basin (Rivas Martínez, 1987). In between these shrubs banded patterns of perennials are present, such as *T. vulgaris, C. albidus, Globularia alypnum, R. officinalis, Fumana ericoides, Brachypodium retusum*. Banding in the vegetation is not developed as clearly as at the other two sites. More often vegetation is distributed in patches, varying in size between 2 and 5 m diameter.

3. Methodology

3.1. The approach

To determine the amount of surface water redistribution along the climatological gradient, the time to ponding of water on the soil surface for different rainfall intensities need to be known together with the long term data of the recurrence of storms with different rainfall intensities. In each climatic zone a research area was selected as described above. At all sites, rainfall simulation experiments were carried out to determine the infiltration characteristics and ponding curves. For the three sites, long term rainfall data from the nearest meteorological stations were derived from Elías and Ruiz (1979) and analyzed. The data comprise the interval 1940–1970. Although rainfall measurements were carried out at the research locations, data from the nearest meteorological stations were used as long-term rainfall data were needed for the analysis.

Based on selected ponding curves and the long term rainfall data, the amount of surface water redistribution for soil surfaces with different infiltration properties was calculated. Storms of 10 min and 60 min were used, to determine the way in which storm duration effects the amount of surface water redistribution along the climatological gradient. Ten minute and 60 min intervals were selected as data for these intervals are available from Elías and Ruiz (1979).

From these analyses a Redistribution Index (RI) is calculated, which equals the amount of redistribution relative to the total amount of rainfall minus plant interception for a 1 yr and 10 yr period. The RI provides a measure of the amount of redistributed rainfall relative to the amount of direct rainfall on the soil beneath the plant. The purpose of this index is to quantify the importance of redistribution relative to the amount of direct plant water input in a specific region. The RI can provide a quick methodology to be used to evaluate differences in the relative importance of surface water redistribution in different banded vegetation structures at a regional scale.

3.2. Field methods and experimental set-up

At the three selected research sites, rainfall simulation experiments were carried out. For the experiments at Albacete and Murcia a drip plate type of rainfall simulator was used. Rainfall was applied from a height of 1.5 m on plots of 1×0.75 m. During the experiments ponding was determined visually and the time to ponding recorded. During the experiments at the Murcia site, a rainfall intensity was used varying between 42 and 67 mm h^{-1} for 50 min (Table 1). Runoff and cumulative infiltration were measured using an experimental plot that included a bare area and a vegetated rim.

For the rainfall simulation experiments at Albacete, rainfall intensities of 20, 40, 60 and 80 mm h^{-1} were used during experiments performed on adjacent plots with a comparable cover and banded vegetation pattern. Measurements of soil moisture were carried using TDR. In total 21 rainfall simulations were carried out (Table 1).

During the rainfall simulation experiments carried out at Valencia, a sprinkler type rainfall simulator was used, described by Cerdà (1995). During these experiments, rainfall was applied from a height of 1.2 m at an intensity of 55 mm h^{-1} for 60 min over an area of 1 m^2. Runoff was measured from an area of 0.25 m^2, located in the middle of the wetted 1 m^2 area. During the experiments time to ponding and time to runoff were recorded. Before and after the experiments soil moisture was measured gravimetrically. The rainfall simulation experiments were performed on the bare areas behind the terracette rims as well as on the vegetated rims. On both of these surface types 11 experiments were carried out (Table 1).

3.3. Calculation of redistribution and the Redistribution Index (RI)

In calculating the amount of redistribution and the RI, attention was paid to the possible existing differences in redistribution for different storm durations. Therefore 10 min and 60 min duration storms were selected for the evaluation, as data was available for the return periods of storms with these durations at different rainfall intensities. To gain more insight into the dependency of calculated redistribution on the time scale of observation, return periods of 1 yr and 10 yr were selected for the calculations. No larger return periods were selected as storms with a longer return period occur so rarely that they are not likely to contribute significantly to the total amount of redistribution. Finally, the effect of soil type on redistribution was studied by selecting three types of ponding curves. The procedure used for calculating the amount of redistribution for return periods of 1 yr and 10 yr, based on three typical ponding curves and the rainfall data, consisted of four steps.

3.3.1. Step 1—Calculating of the number of events per intensity class

Firstly, the rainfall intensity data is grouped into classes of 10 mm h^{-1}. For each intensity class, the return periods are derived based on the medium value of each class. From these, the number of events during 1 yr and during 10 yr are calculated using, respectively:

$$N_1(I) = 365/\text{RT}(I) \tag{1}$$

$$N_{10}(I) = 3650/\text{RT}(I) \tag{2}$$

where N_1 (I): number of events with rainfall intensity (I) during 1 yr (365 days); N_{10} (I): number of events with rainfall intensity (I) during 10 yr (3650 days); I: rainfall intensity (mm h^{-1}); RT: return period of events with different rainfall intensities with 10 min or 60 min duration (days).

3.3.2. Step 2—Calculation of the duration of redistribution

Based on the field data three characteristic ponding curves are selected for the redistribution calculations. The three selected curves include: (1) a rapid ponding curve, (2) a moderate ponding curve, and (3) a slow ponding curve (see Section 4). For each of these ponding curves, the duration of redistribution at a given rainfall intensity and storm duration is calculated by subtracting the time to ponding for a given intensity from the duration of the storm event:

$$D_{x,I} = x - T_I \tag{3}$$

where $D_{x,I}$: duration of redistribution during storm with duration x and intensity I (min); x: duration of storm (10 or 60) (min); T_I: time to ponding (minutes) for rainfall intensity I.

3.3.3. Step 3—Calculation of the amount of redistribution

The total redistribution is calculated by multiplying the number of events during 1 or 10 yr with the duration of redistribution and the intensity per minute. Furthermore, the ratio of the surface of the contributing area relative to the surface of the vegetated area (5:1) is taken into account by multiplying the calculated amount of redistribution by 5. The ratio contributing receiving area is an average number derived from field observations. The amounts of redistribution per rainfall intensity interval are then summed (cf. Eqs. (4) and (5)). The rainfall intensity interval over which the summation is carried out equals the maximum range over which redistribution is important (see Section 4).

$$\sum_{I=0}^{I=165} R_{x,I} = N_1(I) \cdot D_{x,I} \cdot I/60 \cdot 5 \qquad \text{for: } x = 1 \tag{4}$$

$$\sum_{I=0}^{I=165} R_{x,I} = N_{10}(I) \cdot D_{x,I} \cdot I/60 \cdot 5 \qquad \text{for: } x = 10 \tag{5}$$

where R: surface water redistribution of bare area to vegetated area (mm).

3.3.4. Step 4—Calculation of RI

From the above calculated amount of redistribution and the data of mean annual rainfall and interception, RI is calculated (Eq. (6)). This index can be used as an indicator of the relative importance of the contribution of surface water redistribution for vegetated zones at fine scales. The index provides information on the amount of water input near plants derived from surface water redistribution relative to the amount of water input derived from rainfall reduced with the interception by the plant. The mean fraction of intercepted rain (0.28) was derived from Bergkamp (1996).

$$RI = R/(P - (P \cdot C)) \tag{6}$$

where RI: redistribution index; P: mean annual rainfall or 10 yr rainfall; C: mean annual interception fraction (0.28).

4. Results and discussion

4.1. Field measurements of runoff and infiltration

During the experiments carried out at the Murcia site, no runoff was measured at the lower side of the experimental plot (0.75 m^2), although ponding occurred rapidly on the bare areas in between the banded vegetation (Table 1). The water was observed to flow to these structures and to infiltrate there. During other experiments at the same site, with an intensity of 70 mm h^{-1}, this behaviour was also observed (Bergkamp et al., 1996).

At the Albacete site, ponding and movement of water over the soil surface in between the vegetated rims was observed to occur rapidly during the rainfall simulation experiments on all slope sections (Fig. 3). Despite this observed surface water movement no runoff was obtained at the lower edge of the plots. Water was observed to infiltrate rapidly near the vegetated rims as indicated by the arrows in Fig. 4. The variability of water movement on the surface and infiltration was however observed to be very high. Detailed TDR-measurements of changes in soil moisture contents at different depths during experiments showed these to change much more rapidly under the vegetated zones than under the bare areas (Bergkamp et al., 1996). Observation made by using dye tracers indicated that no exfiltration at the lower site of the vegetated rims occurred during the experiments.

The observation made during the experiments performed at the Valencia site, showed water to pond at the bare surface between 1 min, 37″ and 5 min, 30″ after the start of the experiments (Table 2). During 7 experiments located on vegetated zones no ponding occurred. Runoff coefficients for the bare surfaces varied between 9.5 to 47% while for the vegetated zones these were close to zero. The calculated averaged infiltration rates varied between 23 and 47 mm h^{-1} for the bare zones and were above 55 mm h^{-1} for most vegetated zones. Excavations carried out after each experiment showed that below the vegetation the soil was wetted in pockets, indicating that water had infiltrated non-uniformly along roots and macropores. This rapid infiltration caused the runoff from the bare zones to move only over small distances.
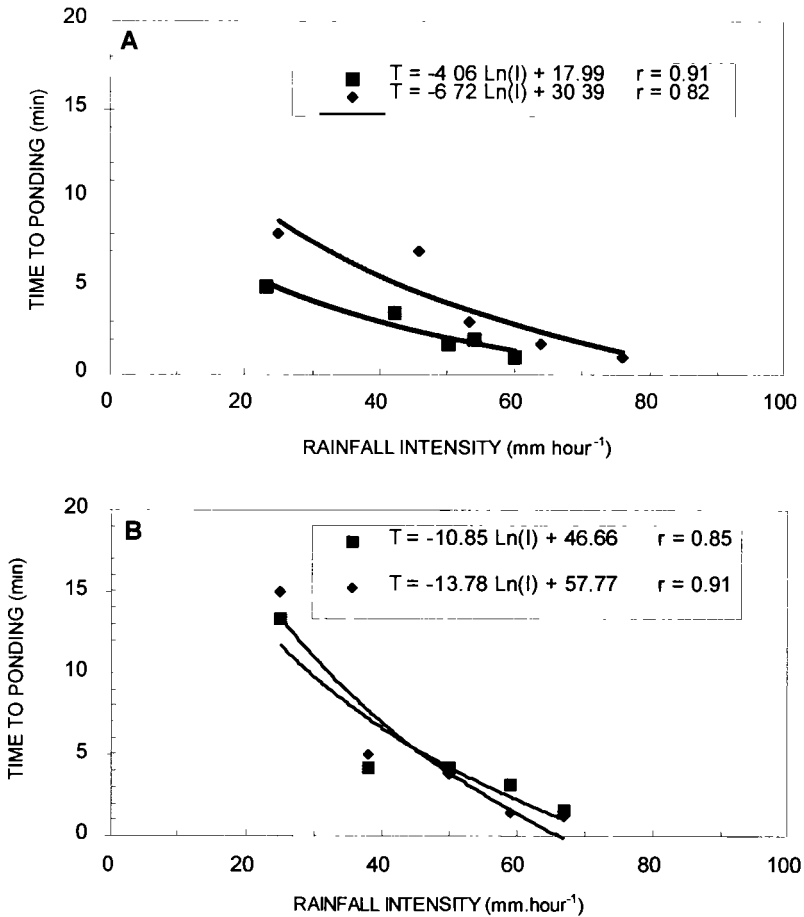
Fig. 3. Ponding curves derived from rainfall simulation experiments carried out at the Albacete field site. (A) Results of measurements on shrub covered slopes. (B) Results of measurements on more densely vegetated shrub covered slopes.

The results of the field experiments at the three sites confirmed the expectation that surface water redistribution originates from the bare surfaces behind the rims of the terracettes and that the generated runoff infiltrates rapidly in the vegetated zones. Furthermore, the results show that large differences exist at the sites. This means that the infiltration characteristics can vary significantly over short distances both between bare locations and vegetated parts of the banded structures and between different bare zones.

4.2. Characteristics of rainfall intensity-return periods

Return periods (RT) for different rainfall intensities (I) and durations of 10 min and 60 min were derived from Elías and Ruiz (1979). The data for the three meteorological stations nearest to the research sites were used, respectively Murcia, Albacete and
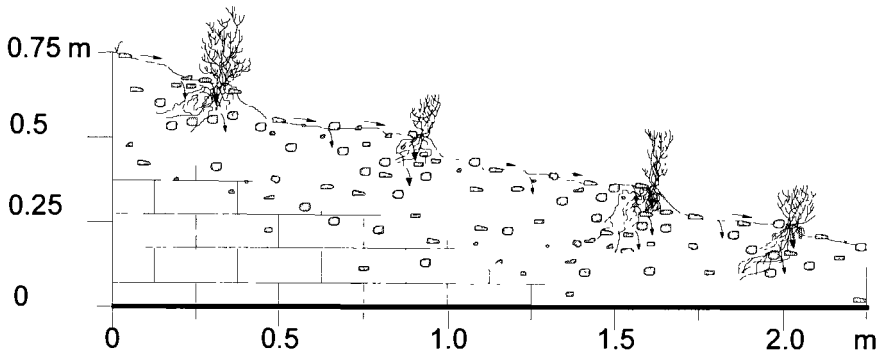
Fig. 4. Cross-section of terracettes with vegetation at the outer rims and bare, often crusted zones behind. Arrows indicate the locations where surface redistribution and infiltration is observed and measured. The size of the arrows is not indicative for the amount of flow.

Table 2
Valencia rainfall simulation data

Plot no.	Vc, %	SM0, %	SM4, %	Tp, min	Tr, min	Rc	Fc mmh⁻¹
Bare zones							
V-1	14	0.63	1.67	2'40"	3'30"	22.6	36.9
V-2	12	0.71	1.25	2'50"	3'15"	23.3	35.1
V-3	13	0.67	0.58	2'20"	2'45"	26	37.2
V-4	4	1.76	4.32	2'20"	1'34"	46.5	23.9
V-5	20	3.64	6.67	5'30"	8'45"	12	45.7
V-6	19	3.92	6.47	1'37"	6'49"	10.3	42.9
V-7	8	3.02	5.98	3'15"	3'50"	32.5	34.4
V-8	18	2.21	4.22	3'00"	4'03"	13.4	45 3
V-9	6	0.64	5.74	2'45"	2'57"	37.8	29.1
V-10	15	2.03	6.05	4'11"	4'33"	16.9	43 4
V-11	25	1.25	5.35	3'56"	4'27"	9.5	47.1
Vegetated zones							
V-1	85	2.14	4.87	np	nr	0	> 55
V-2	90	1.25	5.35	np	nr	0	> 55
V-3	94	2.14	4.12	np	nr	0	> 55
V-4	82	4.3	5.4	np	nr	0	> 55
V-5	94	3.13	4.37	np	nr	0	> 55
V-6	90	4.1	5.13	10'00"	nr	0	> 55
V-7	75	2.05	6.03	16'00"	19'00"	0.04	50.9
V-8	78	0.75	4.18	11'11"	11'50"	0.02	> 55
V-9	76	2.65	3.24	np	nr	0	> 55
V-10	75	3.21	4.56	12'43"	20'32"	0.03	52
V-11	86	1.98	3.76	np	nr	0	> 55

Vc: vegetation cover, SM0: soil moisture content at 0–2 cm depth at start of experiment, SM4: soil moisture content at 4–6 cm depth at start of experiment, Tp: time to ponding, Tr: time to runoff, Rc: runoff coefficient, Fc: steady-state infiltration rate, np: no ponding, nr: no runoff.

Valencia. On the basis of this data, regression lines were calculated for the three areas for, respectively, 10 min and 60 min storm duration (Figs. 5 and 6, Eqs. (7)–(12)).

$$RT = 0.67240 + 0.03710 \cdot I_{10 \text{ MURCIA}} \tag{7}$$

$$RT = 0.96116 + 0.07555 \cdot I_{60 \text{ MURCIA}} \tag{8}$$

$$RT = 1.2307 + 0.01956 \cdot I_{10.\text{ALBACETE}} \tag{9}$$

$$RT = 1.0957 + 0.07883 \cdot I_{60.\text{ALBACETE}} \tag{10}$$

$$RT = 1.7967 + 0.01269 \cdot I_{10.\text{VALENCIA}} \tag{11}$$

$$RT = 1.9122 + 0.02495 \cdot I_{60.\text{VALENCIA}}. \tag{12}$$

The rainfall intensity–return period relationship for 10 min storm data showed that for return periods larger than 1000 days, storms with the highest intensity occur at the Valencia station (Fig. 5). For return periods of less than 1000 days, 10 min duration storm intensity is highest at the Albacete area. The 10 min duration storm data from Murcia show much lower intensities than at Valencia. For example, a storm with a duration of 10 min and a return period of 10000 days has an intensity of 90 mm h^{-1} at Murcia and an intensity of 185 mm h^{-1} at Valencia.

The rainfall intensity data for the 60 min duration storms show a somewhat different picture (Fig. 6). The return period–rainfall intensity relationships for Albacete and Murcia are very similar and deviate markedly from the relationship derived for Valencia which is characterized by much higher intensities. These higher intensity storms with a longer duration originate from frontal storms that move inland from the Mediterranean sea during early autumn (Pérez Cueva, 1994). The station near Albacete, located approximately 140 km south east of Valencia, receives much less precipitation from these frontal storms. The rainfall at the station near Murcia is affected even less frequently by these frontal storms.

4.3. Surface water redistribution

During the field experiments it was observed that runoff generated on bare soil surfaces infiltrated rapidly near the banded soil and vegetation structures. Under natural
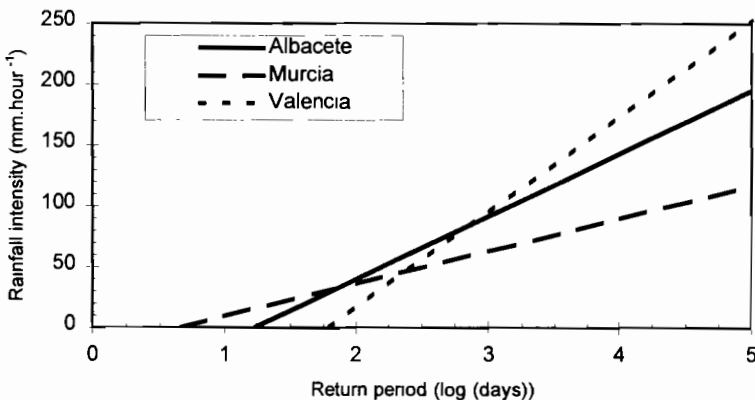
Fig. 5. Rainfall intensity–return periods (10 min duration) for the three areas. See also Eqs. (10), (12) and (14).
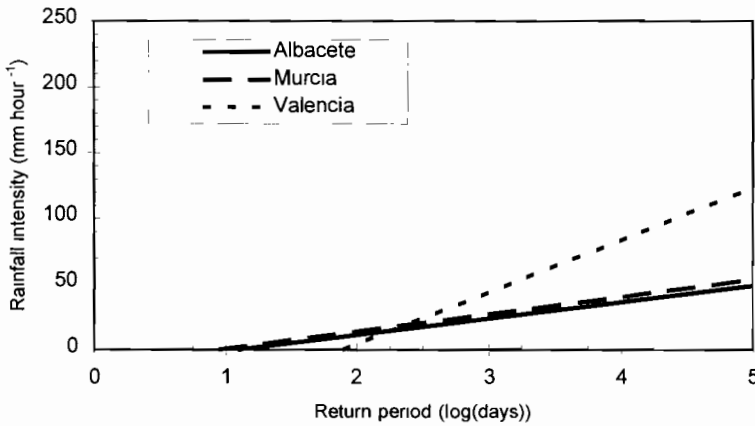
Fig. 6. Rainfall intensity–return periods (60 min duration) for the three areas. See also Eqs. (11), (13) and (15)

conditions, this could cause the structures to receive a supplement of water and dissolved nutrients. The supplement of water and nutrients could contribute to the development of the soil and vegetation at the vegetated zones through the local increase of resources and the improvement of the ability of these vegetated zones to capture water and nutrients. To understand whether surface water redistribution at the three research sites is important, the results of the field experiments need to be combined with those of the rainfall characteristics of the areas.

However, the data of the three sites are somewhat difficult to compare directly, due to the slightly different methods used and the differences in type of results. The data indicate that differences in runoff and infiltration characteristics at the sites are often larger than the differences between the sites. This hampers the analysis of the differences with respect to the differences in rainfall regimes between the three areas. To overcome this problem, three characteristic ponding curves, representative of a range of conditions present at all three sites, were used to calculate the fine scale surface water redistribution (Fig. 7, Eqs. (13)–(15)). Two of these (Curves 1 and 2) are derived from values of field experiments at Albacete. The third curve corresponds to a soil surface with a slow ponding.

$$\text{Curve } 1: T_I = -4\text{Ln}(I) + 19 \tag{13}$$

$$\text{Curve } 2: T_I = -13\text{Ln}(I) + 60 \tag{14}$$

$$\text{Curve } 3: T_I = -28\text{Ln}(I) + 130 \tag{15}$$

where T_I: time to ponding (minutes) for rainfall intensity I; I: rainfall intensity (mm h^{-1}).

4.4. Water redistribution—effects of storm duration and infiltration characteristics

The calculated amounts of surface water redistribution (R) (Eqs. (7) and (8)) vary greatly between storms of 10 min and 60 min duration and the three selected ponding
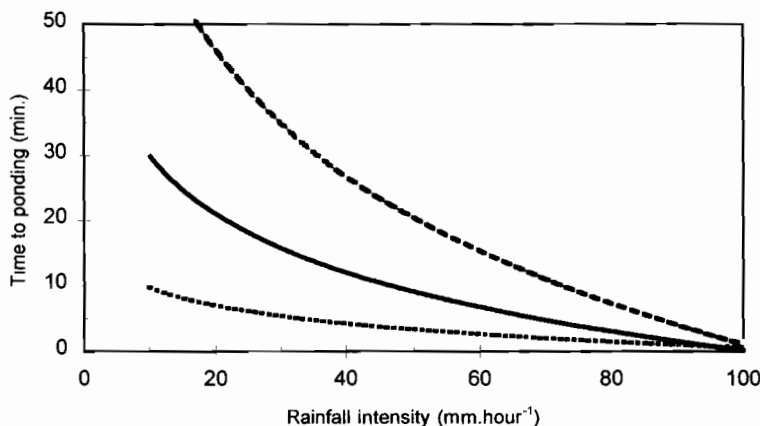
Fig. 7. The three selected ponding curves used for the redistribution calculations. Lower line: Curve 1; Middle line: Curve 2; Upper line: Curve 3 (see also Eqs. (3)–(5)).

curves (Table 3). Values of annual redistribution range from 388 mm to 7 mm depending on soil surface type and rainfall characteristics. Differences in redistribution between 10 min and 60 min storms for a recurrence of 1 yr are largest for Albacete—Curve 1 and for Murcia and Valencia—Curve 2. For a recurrence interval of 10 yr, differences between 10 min and 60 min storms are largest for Albecete—Curve 1, Murcia—Curve 2, and Valenencia—Curves 1 and 2. The total amounts of redistributed water are highest for 10 min events in Albacete and for 60 min events in Murcia and especially Valencia (Table 3).

Most redistribution is calculated for the type of soil surface on which ponding occurs most rapidly (Curve 1). Differences in total amount of redistribution between rapid ponding (Curve 1) and slow ponding (Curve 3) are largest at Albacete for storms of 10 min duration and a time scale of 10 yr (respectively 4503 and 780 mm). The smallest difference (7) is found for Murcia for storms of 10 min duration at a time scale of 1 yr (Table 3).

The above calculations are based on a general ratio of 5 to 1 between bare and receiving areas which occurred at all sites. This was irrespective of the size of the patches. If this calculation is used at sites where this ratio is different, this can be linearly corrected.

4.5. Water redistribution—effects of rainfall regime and time scale of observation

For storms with a duration of 10 min, the maximum amount of surface water redistribution was calculated for the area with an intermediate rainfall regime (Albacete) (Curve 1: 388 and 4503 mm for respectively 1 yr and 10 yr) (Table 3). For this area, most of the redistribution originates from storms with an intensity between 15 and 55 mm h^{-1}. For the driest area, Murcia, redistribution was found to be the least significant. Here redistribution occurs mainly during storms with an intensity less than 30 mm h^{-1}. The redistribution calculated for Valencia indicated important amounts of water to be

Table 3

Results of the calculations of redistribution and the three research sites for 1 yr and 10 yr recurrence intervals

	Units	1 Year recurrence						10 Year recurrence					
		10 min storm duration			60 min storm duration			10 min storm duration			60 min storm duration		
		Curve 1	Curve 2	Curve 3	Curve 1	Curve 2	Curve 3	Curve 1	Curve 2	Curve 3	Curve 1	Curve 2	Curve 3
Murcia													
I_{max}	mm h^{-1}	55	55	55	45	45	45	85	85	85	65	65	65
N at $I = 15$		22	22	22	3	3	3	215	215	215	29	29	29
N at $I = 35$		4	4	4	0	0	0	39	39	39	1	1	1
N at $I = 55$		1	1	1	0	0	0	7	7	7	0	0	0
P	mm	290	290	290	290	290	290	2900	2900	2900	2900	2900	2900
C	mm	81	81	81	81	81	81	812	812	812	812	812	812
R	mm	244	7	0	267	190	54	2669	216	24	2670	1902	537
Albacete													
I_{max}	mm h^{-1}	85	85	85	15	15	15	135	135	135	35	35	35
N at $I = 15$		11	11	11	2	2	2	109	109	109	19	19	19
N at $I = 35$		4	4	4	0	0	0	44	44	44	1	1	1
N at $I = 55$		2	2	2	0	0	0	18	18	18	0	0	0
P	mm	394	394	394	394	394	394	3940	3940	3940	3940	3940	3940
C	mm	110	110	110	110	110	110	1103	1103	1103	1103	1103	1103
R	mm	388	98	19	125	85	14	4503	1609	780	1680	1188	315
Valencia													
I_{max}	mm h^{-1}	85	85	85	35	35	35	165	165	165	75	75	75
N at $I = 15$		4	4	4	2	2	2	38	38	38	19	19	19
N at $I = 35$		2	2	2	1	1	1	21	21	21	6	6	6
N at $I = 55$		1	1	1	0	0	0	12	12	12	2	2	2
P	mm	688	688	688	688	688	688	6880	6880	6880	6880	6880	6880
C	mm	193	193	193	193	193	193	1926	1926	1926	1926	1926	1926
R	mm	238	83	19	338	256	110	3595	2058	1367	5137	4165	2390

I_{max}: maximum rainfall intensity contributing to redistribution; N: number of events; P: rainfall; C: interception; R: redistribution.

redistributed both during storm events of 10 and 60 min duration. This contrasts with the results for Albacete where redistribution during 60 min storms is found to be insignificant. Redistribution at Murcia is in between these two extremes.

These results show that for the study areas, important redistribution occurs during short storms of 10 min duration. This redistribution is highest within the area with an intermediate rainfall regime and an annual rainfall of 494 mm. For the sub-humid area, a shift towards redistribution occurring during longer storm events (60 min) can be seen. Within the semi-arid area having 290 mm annual rainfall, the redistribution is less in absolute sense. These results are in accordance with those of Yair and Lavee (1985), Yair (1986) and Lavee and Yair (1990) who found that the distance of surface water redistribution in arid areas is limited due to the short duration of the storm events.

Comparing the results of redistribution calculated for 1 and 10 yr, it can easily be seen that the amounts calculated for 10 yr are not the 10 fold of the amounts of 1 yr. At the time scale of 10 yr, storms with a return period of more than 1 yr and less than 10 yr affect the calculated amount of redistribution. This effect is smallest for the most arid location (Murcia) at which events with a higher intensity have return periods larger than 10 yr. For Valencia the differences are largest because at a time scale of 10 yr, storms having higher rainfall intensities occur and contribute significantly to redistribution. This can be seen from the data in Table 3, which show that for the Valencia area the number of storms of 60 min duration and intensities higher than 15 mm h^{-1} are much higher than for the other areas (values N at $I = 35$ and $I = 55$). Furthermore, the maximum intensity that contributes to redistribution is highest for the Valencia area ($I_{max} = 165$ mm h^{-1}). The data show that storms with a higher intensity and a duration of 60 min only occur at Valencia. Redistribution at Murcia originates mainly from very frequent short storms with a low intensity. The Albacete area forms an intermediate between these two extremes.

4.6. Redistribution Index (RI)—significance for regional scale analysis

For 10 min and 60 min events, RI was calculated (Eq. (6)). Values of RI greater than 1 indicate that more of the water input of the vegetated zones originates from surface water redistribution from the bare areas than from the amount input of rainfall reduced with the interception. RI-values close to zero indicate a negligible contribution of surface water redistribution to the water budget of vegetated zones.

Highest values for the RI were found for Albacete for 10 min storm events and ponding Curve 1 (1.59) (Fig. 8). As commented before, it is especially this area with an intermediate rainfall regime in which the redistribution is most significant. Values for 60 min events were much lower for all sites and all ponding curves, except for Valencia at a time scale of 10 yr for Curves 1 and 2. The values of RI were especially low for 60 min events at Murcia and Albacete indicating that in these areas most of the redistribution does not originate from the 60 min storm events but from short duration storms (10 min events).

The RI is well suited to indicate differences in the importance of fine scale surface water redistribution at a regional scale. The preliminary analysis performed indicates that it is a much more appropriate index to be used for this in semi-arid areas than other
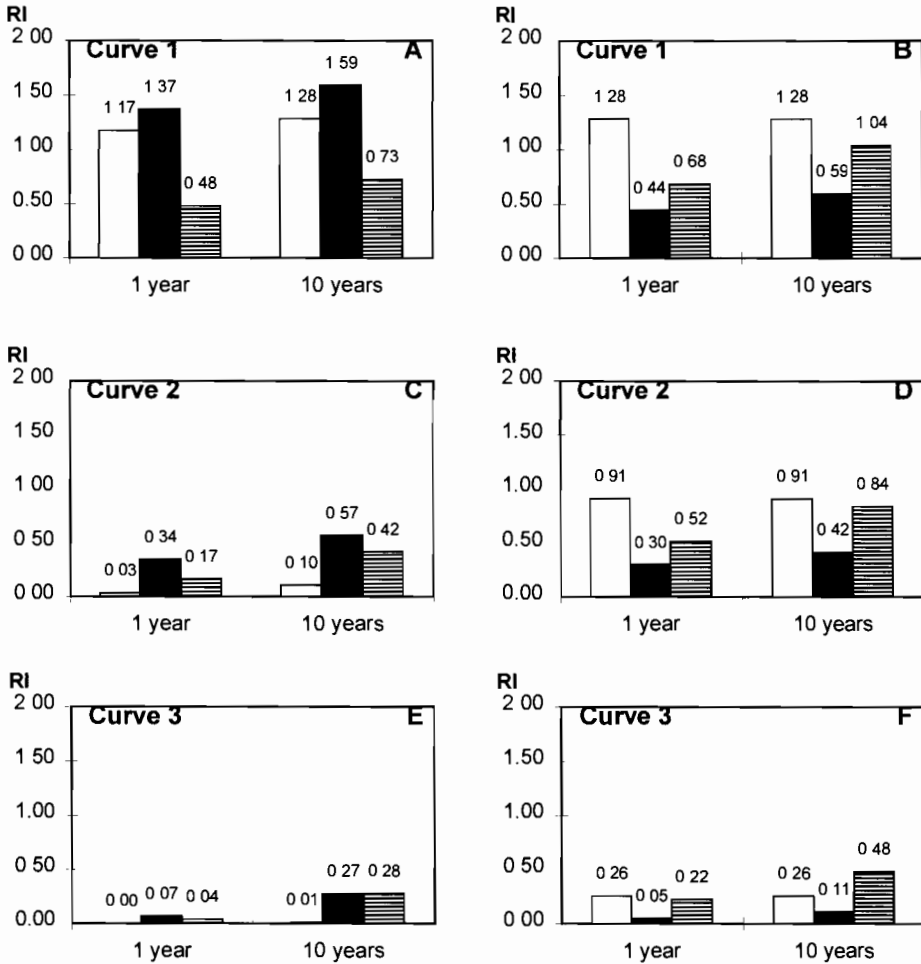
Fig. 8. Redistribution Index (RI) for storm events with a duration of 10 min (A, C, E) and 60 min (B, D, F). White: Murcia; Black: Albacete; Hatched: Valencia. Highest values are found for the intermediate rainfall regime area Albacete for short duration storms and for the Murcia area 60 min duration storms.

indices. These are often either difficult to calculate at a regional scale (e.g., RUSLE, or the climate erosion potential index—Kirkby and Cox, 1995) or are based upon only daily or hourly rainfall data (e.g., the Cumulative Erosion Potential—De Ploey et al., 1991). Within semi-arid areas, the importance of the 10 min storms should be included in any estimate of potential redistribution, as is shown for example by the differences in RI between 60 min and 10 min events for Albacete. Because the RI takes into account both the surface properties with respect to runoff generation and the short storm characteristics at different time scales, we think it is a most appropriate index to evaluate regional differences in redistribution occurring at fine spatial scales.

5. Conclusions

(1) At the investigated sites a high variability at fine scales in the contribution of surface water redistribution from bare areas to banded vegetated zones at scales of 1 m^2 were found. Differences in amount of redistribution between the ponding curves were largest for the intermediate rainfall regime.

(2) Within the semi-arid areas studied, the surface water redistribution originates mostly from short storms with a duration of 10 min. The largest amount of redistribution during these events for all ponding curves were found for the intermediate rainfall regime with an annual rainfall of 394 mm.

(3) Surface water redistribution was found to become more important at larger time scales as more extreme events are included in the observation series. This will especially be so on slowly ponding surfaces and areas with a rainfall regime as in Valencia.

(4) The relationship between redistribution and vegetation banding is most apparent for the semi-arid zone. Although redistribution is occurring at the sub-humid site, the banding at this site is much less clear. Probably vegetation at this site receives a sufficiently large water input from rainfall to maintain biomass production.

(5) The Redistribution Index developed during this study provides a quick methodology that can be used to evaluate differences in the importance of surface water redistribution in different banded vegetation structures at a regional scale.

Acknowledgements

References

Bergkamp, G., 1996. Mediterranean geoecosystems. Hierarchical organisation and degradation. PhD thesis, University of Amsterdam, 238 pp

Bergkamp, G., Cammeraat, L.H., Martinez Fernández, J., 1996. Water movement and vegetation patterns on shrubland and an abandoned field in two desertification threatened areas in Spain. Earth Surf. Proc. Landforms 21, 1073–1090.

Casenave, A., Valentine, C., 1989. Les états de surface de la zone sahélienne: influence sur l'infiltration. ORSTOM, Paris.

Cerdà, A., 1995. Factores y variaciones espacio–temporales de la infiltración en los ecosistemas mediterráneos. Geoforma Ediciones, Logrono, p. 151.

Cerdà, A., Imeson, A.C., Calvo, A., 1995. Fire and aspect induced differences on the erodibility and hydrology of soils at La Costera, Valencia, southeast Spain. Catena 24, 289–304.

De Ploey, J., Kirkby, M.J., Ahnert, F., 1991. Hillslope erosion by rainstorms—A magnitude-frequency analysis. Earth Surf. Proc. Landforms 16, 399–409.

Elías, J., Ruiz, J., 1979. Precipitaciones máximas en España. Ministerio de Agricultura, Madrid, 545 pp.

Kirkby, M.J., Cox, N.J., 1995. A climatic index for soil erosion potential (CSEP) including seasonal and vegetation factors. Catena 25, 333–352.

Lavee, H., Yair, A., 1990. Spatial variability of overland flow in a small arid basin. Int. Assoc. Hydrol. Sci. Publ. 189, 105–120.

López-Bermúdez, F., Roméro-Diaz, M.A., Martínez-Fernández, J., 1991. Soil erosion in a semi-arid mediterranean environment. El Ardal Experimental field (Murcia, Spain). In: Sala, M., Rubio, J.L., Garcia-Ruiz, J.M (Eds.), Soil Erosion Studies in Spain. Geoforma Ediciones, Longroño, Spain, pp. 137–152.

Ludwig, J.A., Tongway, D., 1995. Spatial organisation of landscapes and its function in semi-arid woodlands. Australia. Landscape Ecol. 10 (1), 51–63.

Montaña, C., 1992. The colonization of bare areas in two-phase mosaics of an arid ecosystem. J. Ecol. 80, 315–327.

Pérez Cueva, A., 1994. Atlas climático de la comunidad Valenciana. Comunidad Valenciana, Valencia, 205 pp

Rivas Martínez, S., 1987. Memoria del mapa de series de vegetacion de España, ICONA, Madrid, 357 pp.

Yair, A., Lavee, H., 1985. Runoff generation in arid and semi-arid zones. In: Anderson, M.G., Burt, T.P. (Eds.), Hydrological Forecasting, Wiley, Chichester, pp. 183–220.

Yair, 1986.

Laboratory experiments on sequential scour/deposition and their application to the development of banded vegetation

R.B. Bryan [*], S.E. Brun

Soil Erosion Laboratory, University of Toronto, Scarborough, Canada

Received 13 January 1998; accepted 18 February 1999

Abstract

Alternating bands of vegetation and bare soil, reported from many dryland regions, have been identified as indicators of rangeland deterioration triggered by overgrazing, cattle trampling or climatic change. Banded vegetation occurs at a range of scales and although it has been reported from a number of different environments, it is not characteristic of all degraded rangelands. It does appear particularly frequently on low angle, smooth slopes over soils of high erodibility but low permeability, where scant rainfall is sporadic or highly seasonal. It has been attributed both to wind and to water erosion, but few data on the processes active or their specific response to limiting environmental variables are available. Small-scale banded vegetation associated with small scour steps occurs on low angle alluvio-lacustrine flats surrounding Lake Baringo in semi-arid northern Kenya. In this area of strong moisture deficit, the dominant factor controlling the incidence of ground vegetation is variation in near-surface moisture storage. The regular spacing of the small-scale vegetation bands reflects preferential moisture storage in regularly-spaced sediment deposits. Field and laboratory runon and rainfall simulation experiments, previously reported, provided some data on the processes and conditions involved in formation of these deposits. This paper describes more closely-controlled laboratory rainfall simulation and runon experiments, carried out to identify the sequential scour and deposition processes involved, which are ultimately responsible for the regular variations in moisture storage capacity. These experiments, carried out in an 8.5 m long flume, show critical stream power (Ω) conditions in sheetwash and rain-impacted sheetflow required for sequential scour/deposition as 0.020–0.025 W m^{-2} and between 0.043 and 0.055 W m^{-2}, respectively. Experimental results indicate that vegetation bands at the scale observed at Baringo are consistent with development by sequential scour and deposition, caused by some combination of sheetwash, rainsplash and rainflow. The vegetation bands are composed primarily of unpalatable low herbaceous plants, dominated by

---

[*] Corresponding author. Tel.: + 1-416-978-5480; Fax: + 1-416-978-3834; E-mail: r.bryan@utoronto.ca

Trianthema triquetra. These plants colonize or survive better on deposition zones because of better soil moisture status. The vegetation bands can therefore indicate an initial stage in vegetation recovery rather than continuing rangeland deterioration, but at Baringo further development of vegetation appears to be restricted by high grazing intensities or by allelopathy. © 1999 Elsevier Science B.V. All rights reserved.

1. Introduction

Vegetation patterns in which more or less regularly spaced bands of vegetation alternate with zones of bare soil have been reported from many dryland regions (e.g., Litchfield and Mabbutt, 1962; Hemming, 1965; White, 1969, White, 1970, White, 1971; Mabbutt and Fanning, 1987; Cornet et al., 1988, Cornet et al., 1992; Thiery et al., 1995). These features, referred to as banded vegetation, vegetation arcs, vegetation stripes or brousse tigree, share superficial similarities, though there are considerable variations in detailed characteristics and relations to environmental controls. All reported occurrences are from dry regions, but these cover a range of annual precipitation conditions from 50–750 mm. The most critical feature appears to be sporadic or highly seasonal precipitation, so that vegetation is moisture-limited for all or part of the year.

Vegetation bands occur on smooth, gentle slopes between 0.13° and 1.2°, and are usually, though not invariably, perpendicular to the slope direction. Related soils vary but are typically shallow, rich in fine particles, highly erodible, and often have impermeable layers close to the surface. Detailed characteristics are extremely varied, with reported band spacing ranging from 3 to 300 m, band width from 1 to 70 m, and band length from 5 to 800 m. Vegetation is also diverse; bands are usually dominated by annual and perennial herbs and grasses, but large scale features can include low shrubs and trees as well. Good descriptions of the typical structure of larger bands from Mexico (Cornet et al., 1988) and Niger (Thiery et al., 1995) show a degraded downslope zone, a central closed bush/tree zone, and an upper pioneer zone. This structure markedly influences moisture fluxes (Cornet et al., 1992; Holwill, 1997); bare soil areas concentrate runoff which infiltrates in the adjacent downslope vegetated band. As the vegetation develops, progressively less water reaches the downslope edge of the band, which becomes desiccated and degraded. At the upper edge, pioneer plants slowly invade the bare soil zone, so that the vegetation bands tend to migrate slowly upslope (Worrall, 1959; Boaler and Hodge, 1964; Leprun, 1992).

Despite numerous good descriptions of the features, and several detailed studies of moisture dynamics, the processes involved in initiation of vegetation bands are still uncertain. Ives (1946) in the western United States, and Audrey and Rossetti (1962) in Mauretania attributed them to aeolian deposition, while Clos-Arceduc (1956) linked their formation in Niger to decay of termite mounds with increasing aridity. Most authors (e.g., White, 1971; Rapp, 1974), however, have linked vegetation bands to rangeland deterioration resulting from localized degradation of a vegetation cover by overgrazing, trampling or precipitation decline. Exposed or eroded soil, often crusted

and with reduced infiltration capacity, generates runoff which enhances moisture and vegetation growth in the adjacent downslope area. White (1971) and Cornet et al. (1992) have also suggested that in some cases banded vegetation may originate by colonization of patches of deposited sediment rather that degradation of existing vegetation.

The preceding review suggests that banded vegetation can arise from a range of processes at different locations, and perhaps at the same location. In the absence of observations, however, it is difficult to identify the precise processes involved, or to determine if the same controls operate at different scales. Moisture-stressed or damaged vegetation appears essential, but is clearly not sufficient, as degraded rangeland is much more widespread in occurrence than banded vegetation. One consistent feature, which is not specifically addressed in many papers, is the marked regularity of alternating vegetation and bare soil bands. This is significant, because the initial degradation of vegetation on rangelands is typically irregular and often more or less random. Some other process must therefore be involved which progressively leads to regular alternating bands. Aeolian sediment movement and deposition is one possibility, as noted by Ives (1946) and Audrey and Rossetti (1962). However, many vegetation bands occur in areas where water rather than wind erosion dominates, and it appears that in many cases, the process which produces regularly alternating bands is probably sequential scour and deposition by rainflow, sheetwash or rill erosion.

Bryan and Oostwoud Wijdenes (1992) described development of small-scale vegetation bands on low-angle alluvio-lacustrine flats surrounding Lake Baringo in the northern part of the Rift Valley, Kenya. The area is characterized by highly variable annual precipitation which averages 636 mm (Sutherland et al., 1991), and is concen-

Fig. 1. Sequential scour/deposition on lacustrine flats near Lake Baringo, Kenya, showing differential soil moisture conditions shortly after rainfall.

trated almost entirely in five months from April through August. The extensive flats which surround the lake are almost entirely devoid of ground vegetation for most of the year, though a scattered tree cover dominated by *Acacia*, *Terminalia* and *Balanites* species is found. Typical vegetation bands are found at many locations on the flats in association with low (2 to 5 cm high) scour steps which are spaced 3–20 m apart and extend for many metres in crenulate lines along contours. Each band consists of an upper bare, scoured 'micropediment' of compact, crusted soil, and a lower depositional zone, usually 2–3 m in width, immediately above the next scour step (Fig. 1). In depositional zones several centimetres of loose coarser soil are deposited on top of crusted, compact soil. These zones become conspicuous after rainstorms; scoured 'micropediments' dry out swiftly, but because of higher infiltration and moisture storage, depositional zones remain moist and support development of low ground vegetation. Several species are represented (Snelder, 1993) but the overwhelming dominant is *Trianthema triquetra* (Fig. 2), an unpalatable herbaceous annual or biennial herbaceous plant of the 'Aizoaceae' or 'carpet-weed family'. Other common species are *Portulaca oleracea* and *Gisekia pharnaceoides*, both of which are also herbaceous, *Portulaca* also having succulent leaves. Grass species are conspicuously infrequent throughout the area, but a number of species of *Eragrostis* are found in some of the vegetation bands.

Using field runon plots at Baringo, Bryan and Oostwoud Wijdenes (1992) identified the hydraulic characteristics associated with scour steps and depositional zones, and using simulated rainfall experiments in a laboratory flume in Toronto, Canada, showed
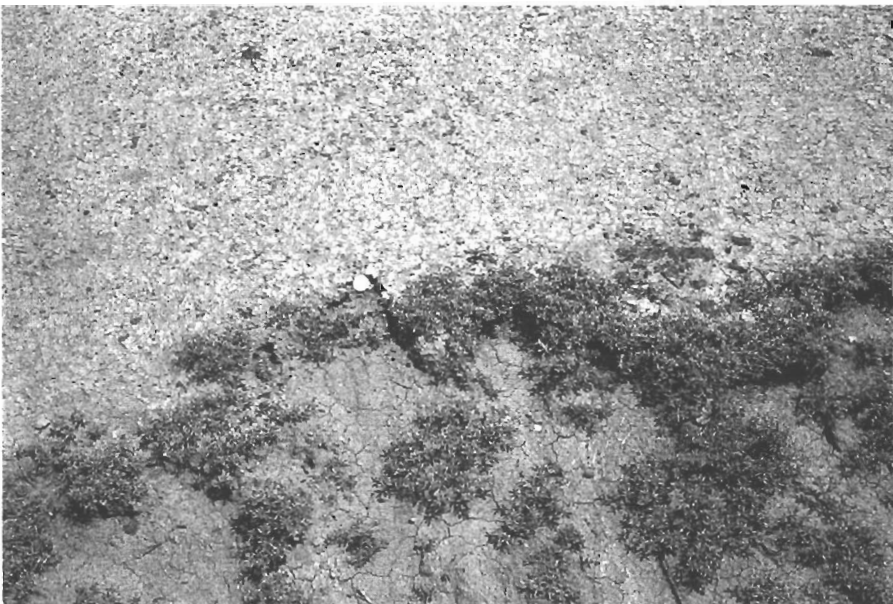
Fig. 2. Detail of species forming small-scale vegetation band, resulting from colonization of sediment deposition zones on flats near Lake Baringo, Kenya. Dominant species is *T. triquetra*.

that scour steps very similar in size to those at Baringo can form due to hydraulic conditions in sheetflow. On the 1.5° flume slope, critical threshold conditions for scour initiation were reached after flow lengths of approximately 10 m. Initial scour was followed sequentially by alternating zones of deposition and renewed scour. Although these experiments indicated linkage of sequential scour and deposition to hydraulic conditions, experimental controls were not sufficiently precise to permit clear definition of linkages between scour step spacing and local hydraulic conditions. The experiments described in the present paper were carried out under more closely controlled conditions to clarify these linkages and to provide a more precise understanding of the processes which control sequential scour and deposition and development of the small-scale vegetation bands at Baringo.

2. Experimental design

Experiments were carried out in the same 0.8 m wide laboratory flume used in the experiments of Bryan and Oostwoud Wijdenes (1992), but in this case length was restricted to 8.5 m, and the flume was set at a range of angles from 0.026 (1.5°) to 0.087 (5°). The initial intention was to generate runoff by simulated rainfall, as in the previous experiments. Three preliminary experiments with simulated rainfall did provide useful results, discussed below, but some difficulty was encountered in producing spatially homogeneous rainfall, and therefore in ensuring that scour location was not an artifact of rainfall patterns. Accordingly, it was decided to base subsequent experiments on runon generated by a constant head tank at the top of the flume. This produced controlled discharges from 1.0 to 3.0 l min^{-1}.

The soil used in the experiments was an artificial mixture of two natural soils from the vicinity of Toronto, the Pontypool fine loamy sand and the Peel clay, in a 4:1 ratio. This mixture was originally used by Bryan and Poesen (1989) in experiments on runoff and rill generation because of its sensitivity to surface sealing, and was also used for the original experiments by Bryan and Oostwoud Wijdenes (1992). The basic properties of the mixture are shown in Table 1, together with those of typical soils of the Njemps Flats at Baringo. The dispersed mixture is a fine sandy loam with 98% finer than 0.05 mm, but as used in the flume, it includes some stable aggregates, and has a bimodal

Table 1

Basic properties of artificial mixture of Ontario soils used in experiments compared with surface soil from Njemps Flats, Baringo, Kenya

	Pontypool loamy sand: peel clay mixture	Lameluk silt loam
Texture (USDA)	Sandy loam	Silt loam
Sand (%)	49.4	17.4
Silt (%)	32.5	66.1
Clay (%)	18.1	4.2
WSA > 0.5 (%)	34.0	1.4
Liquid limit (%)	17.1	35.0
pH	8.1	6 8

distribution with 43% between 0.106 and 0.5 mm and 34% between 0.5 and 4.0 mm in diameter. While the proportions of sand and silt in the two soils are clearly different, as most of the sand in the experimental mixture is very fine, the behavioural properties are rather similar. The soil was placed directly on the perspex base of the flume to a depth of 5 cm, and lightly compacted to a bulk density of 1.4 to 1.6 mg m^{-3}. It was then smoothed, shaped to produce a central thalweg with side slopes of 5°, and lightly raked before application of runon.

In addition to the three initial experiments with simulated rainfall, 12 experiments were completed with runon discharges of 1.0, 1.6, 2.2 and 3.0 l min^{-1} and flume slopes of 0.026, 0.061 and 0.087. Soil dried naturally between experiments, then was removed and resieved through a 4.00 mm square-hole sieve. Soil moisture was monitored with micro time domain reflectometer probes, linked through a Tektronix cable tester to a Campbell CR7 data logger. Most experiments started with antecedent soil moisture contents between air-dry and field capacity (Table 2). Each experiment was split into three 'sub-experiments' with brief intervals for measurement of surface microrelief, using a 'bedstead' with aluminum rods. Detailed cross and longitudinal profiles at intervals of 0.10 and 0.25 m, respectively, were measured to ±0.5 mm accuracy. These were used to produce precise maps of flume microtopography before and after each sub-experiment. Experiments were continued until runoff equilibrium or a close approximation was reached. During experiments, water and sediment discharge were measured

Table 2
Summary of experimental conditions and responses

Experiment number	Antecedent conditions		Slope $\sin(\theta)$	Water discharge (ℓ min^{-1})	Stream power (W m^{-2})	Average sediment discharge (g min^{-1})	Comment
	Soil moisture (ml ml^{-1})	Dry bulk density (mg m^3)					
P1[a]	0.12	1.28	0.087	2.9	0.043	52.7	S.S.
P2[a]	0.10	1.32	0.087	3.9	0.055	78.0	Rilling
P3[a]	0.09	1.25	0.087	4.1	0.058	75.0	Rilling
1	0.20	1.28	0.087	1.6	0.023	53.9	S.S
2	0.23	1.44	0.087	1.6	0.023	44.3	S.S
3	0.27	1.43	0.087	1.6	0.023	57.9	S.S.
4	0.17	1.39	0.087	1.6	0.023	30.9	S.S
5	0.22	1.37	0.087	1.6	0.023	44.8	S.S.
6	0.08	1.22	0.087	1.6	0.023	24.9	S.S.
7	0.12	1.27	0.087	1.0	0.014	9.9	No S.S.
8	0.11	1.31	0.061	2.2	0.022	19.3	No S.S.
9	0.13	1.32	0.061	1.6	0.016	7.1	No S.S.
10	0.17	1.22	0.061	1.0	0.010	3.8	No S.S.
11	0.06	1.20	0.026	3.0	0.013	2.6	No S.S.
12	0.07	1.13	0.061	2.2	0.022	19.6	S.S.

[a] Denotes simulated rainfall experiment.
Water discharge is final approximate equilibrium discharge for rainfall experiments or header-tank discharge for runon experiments.
SS: sequential scouring.
No SS: no sequential scouring.

every 6 min (approximately) at 0.5 m intervals between 3 and 5.5 m above the terminal weir. Onslope water and sediment discharge were measured using miniature, thin-walled (~ 100 μm) sampling cylinders (diameter: 4.2 cm; length 15 cm) with a single open end. Because of the thin cylinder walls, these could be used with minimal bed disturbance. Samplers were lowered manually into the flow at angles similar to the local bed slope, and allowed to fill until 5 cm from the cylinder opening. Samplers were sufficiently large to allow sampling times of 1–3.5 s, which were adjusted to discharge conditions. Measured filling time, water volume and sediment weight were used to calculate local water and sediment discharge rates for different points on the flume. As the samplers account only for a small proportion of total water and sediment discharge across the flow width, these calculated rates were calibrated against the total water and sediment discharges measured at the terminal weir. Flow velocities measured with dye tracers and flow width and depth measurements with thin rules were used to calculate standard hydraulic variables: total stream power (Ω); shear velocity (u^*), shear stress (τ), Froude Number (Fr), Reynolds Number (Re) and Darcy–Weisbach friction factor (ff) for each 0.25 m long slope segment.

3. Results

The basic conditions and results for each experiment are shown in Table 2. Localized erosion and deposition erosion and deposition occurred during all experiments producing a variety of topographic forms: braided washes, micro depositional fans and scour chutes and arcuate knickpoints. In some experiments occurrence was random and localized, but in most experiments (P1, experiments 1–6 and experiment 12), clear sequential scour and deposition patterns developed (see Fig. 3). In each case the pattern started with a narrow (5–10 cm wide), steep-walled scour chute, about 1 cm in depth and 0.25 m in length, from which large soil aggregates were conspicuously absent. These chutes were characterized by convergent flow averaging 3 mm in depth (range 1–10 mm) and 0.27 m s^{-1} in velocity. Each chute ended with a micro-depositional fan 20–50 mm in width, with a maximum accretion depth (in the thalweg) of 1–1.5 cm. Micro depositional fans were composed predominantly of coarse soil aggregates. Flow was divergent across the fans, with average velocity of 0.24 m s^{-1}. Depth was highly variable across the micro depositional fans, as flow typically separated into several small, shallow (1–2 mm deep) channels which oscillated to and fro across fan surfaces.

Observations during experiments show that the first stage in development of the typical scour/deposition sequence described above is selective transport of larger (1–4 mm diameter) aggregates. Even initial runoff with negligible flow velocity can move many of these aggregates, which protrude as individual particles above the general soil surface and the laminar sub-layer into higher-velocity surface flow layers. The bed shear stress exerted by initial runoff is certainly not adequate to cause aggregate suspension, but the flow velocity gradient does allow them to be rolled downflume as bedload. The step length of bedload movement varies as some aggregates become trapped in localized depressions, but most stop moving at about the same point where flow becomes
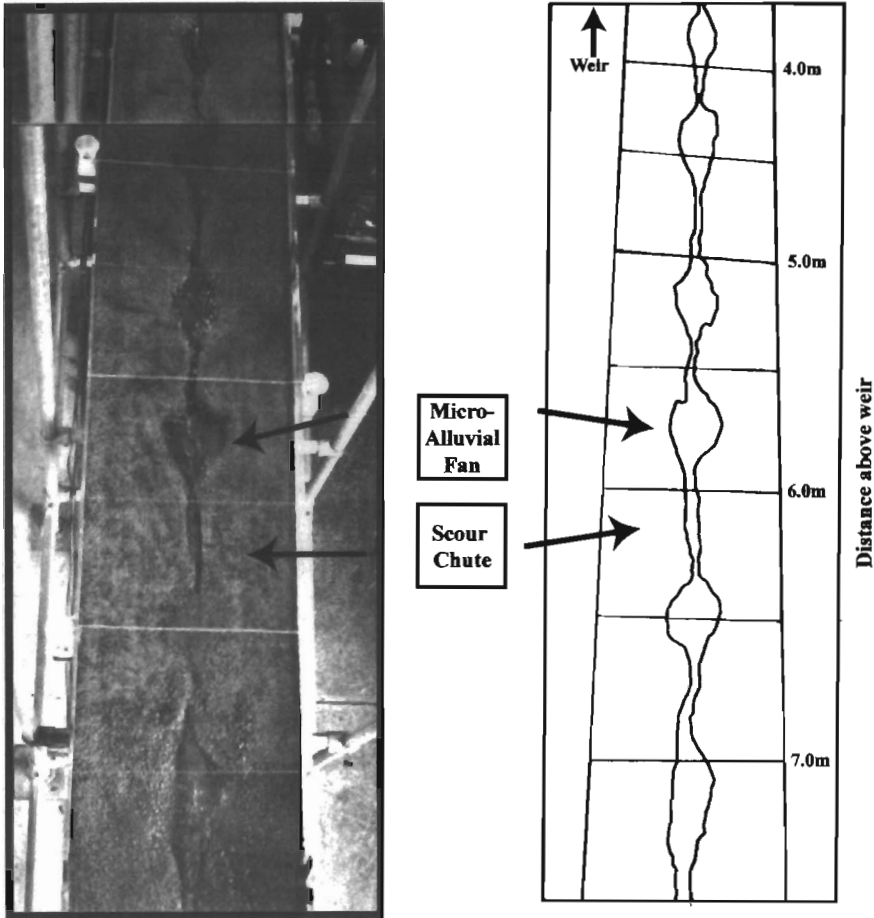
Fig. 3. Sequential scour/deposition formed under simulated rainfall in laboratory flume (Experiment P1).

shallower and diverges. This typically occurs as the flow passes over slight bed convexities. Many aggregates protrude above this shallower flow so the turning moment and tendency to roll downflume is reduced. The deposited aggregates increase surface roughness and hydraulic resistance, increasing the potential for cumulative deposition.

Once the basic pattern is established, flow progressively converges in the scour chute moving all aggregates to the adjacent downstream deposition zone. Progressive accretion increases flow divergence across the depositional fan, which then converges again on the downstream side. This converges establishes the necessary conditions for a second scour chute to develop downslope. The dimensions of individual chutes and fans, and the time required for sequential development vary considerable with precise local microtopography and soil surface conditions, but the pattern of evolution in experiment 1 (Fig. 4), with step lengths of approximately 2 m between each depositional zone, is rather typical.

Sub-Experiment A

Sub-Experiment B
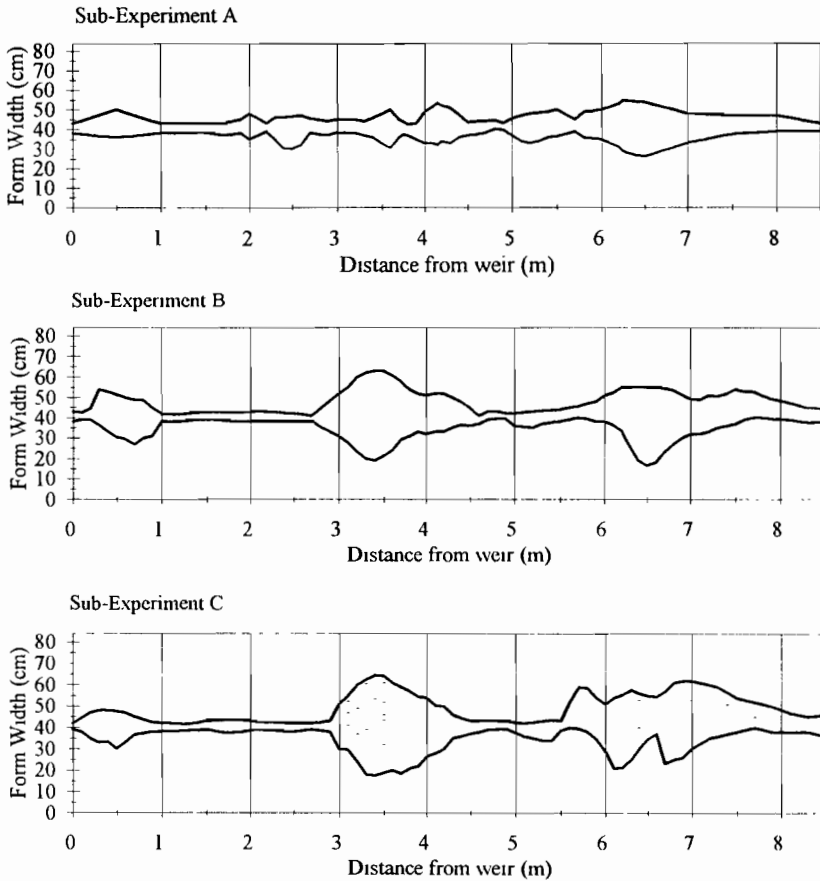
Sub-Experiment C

Fig. 4. Evolution of sequential scour/deposition in runon flume experiment, divided into three sub-experiments (Experiment 1).

If general conditions are suitable, the only apparent limit to the number of scour/chute sequences developed is the overall slope length. Fig. 5 shows numerous scour/deposition sequences developed on a 22.5 m long flume slope during another rainfall simulation experiment carried out on a 0.087 slope. In this case, the average step length was 0.5 m.

Each of the experiments in which sequential scour/deposition failed to develop behaved in different ways. In two of the initial rainfall simulation experiments (P2, P3), deeply incised rills developed over virtually the complete flume length, without significant deposition. In experiment 7 there was some initial aggregate displacement, but the surface stabilized rapidly and no significant scour developed. In experiments 8, 9 and 10, scouring only occurred in immediate proximity to the header tank, and was not selective. In each case, instead of a clear sequence of depositional fans, transported material was deposited over much of the flume surface as a thin braided wash or

Fig. 5. Multiple sequential scour/deposition cycles formed under simulated rainfall in 22.5 m long laboratory flume.

depositional crust of fine material. Virtually no material was mobilized on the flume during experiment 11.

4. Discussion

Collectively the experiments show that sequential scour and deposition depends on rather precise interaction of several factors. The essential requirement is selective

entrainment and transport of relatively large soil particles or aggregates over quite short distances. In theory the large particles could be sand grains, but in practice, cyclic scour and deposition is much more likely to occur when large aggregates are available, as aggregate densities are much lower than those of mineral particles (typically in the range $0.85–1.25$ g cm^3), and entrainment can therefore occur, even with the low bed shear stresses typical of sheetflow. Precise discharge, flow depth and hydraulic conditions are clearly critical. Critical threshold hydraulic conditions must be present before any material is mobilized. Thereafter development depends on flow transport capacity. If flow transport capacity is sufficient, sediment will be transported across the complete slope length without deposition. For sequential deposition patterns to form, therefore, fluctuations in local transport capacity must occur. For example, local variations in surface slope or variations in flow width can alter local water fluxes and sediment transport capacity. Localized patches of deposition will develop if the flux of sediment entering the site is greater than that leaving. Therefore, for sequential scour and deposition to occur, flow conditions must fluctuate between the entrainment threshold and the transport capacity.

Limited information is available on threshold hydraulic conditions in very thin flows, and most of this is related to the conditions necessary for rill incision. No hydraulic parameter is universally applicable, but stream power (w) (Rose, 1985), Froude Number (Fr) (Savat and De Ploey, 1982) and shear velocity (u^*) (Govers, 1985) have each proved useful, with threshold values of 0.5 W m^{-2}, $0.6–0.8$ and 0.035 m s^{-1}, respectively. As rill incision usually involves non-selective entrainment (Govers, 1985), these data are not directly applicable to the present situation. The few data available for the initial stages of microrill initiation (e.g., $w = 0.015$ W m^{-2}; $u^* = 0.023$ m s^{-1} (Bryan, 1990); Fr = 0.45 (Torri et al., 1987) are probably more directly relevant.

Amongst the hydraulic parameters cited, only overall stream power (Ω) shows a trend related to sequential scouring (Table 1). The values of stream power shown are mean values for the complete flume and experiment; actual on-slope hydraulic conditions at specific times and locations varied significantly due to local variations in flow width and slope and could not be used to determine the threshold conditions necessary for sequential scour development on the complete slope. In most of the experiments in which sequential scour/deposition developed, Ω was constant at 0.023 W m^{-2}, while for experiments in which no clear development was apparent, the mean Ω value was 0.015 W m^{-2}. The experiments which cannot be distinguished on the basis of Ω values are 8 and 12. In each of the initial simulated rainfall experiments, Ω was considerably higher, with mean values of 0.052 W m^{-2}, but the value for experiment P1 in which sequential scour/deposition did occur was 0.043 W m^{-2}. In Fig. 6, final equilibrium water discharge (Table 1) is plotted against overall flume slope for each experiment, with lines of equal stream power (Ω) superimposed. The figure also includes comparative data from the experiments of Bryan and Poesen (1989) and Bryan and Oostwoud Wijdenes (1992). Experiments in which sequential scour/deposition did not occur are associated with Ω values < 0.020 W m^{-2}, too low to promote significant scour. The exception is experiment 8 in which bed armouring developed. Stream power conditions were identical in experiment 12, in which sequential scour occurred, but soil bulk density was significantly lower.
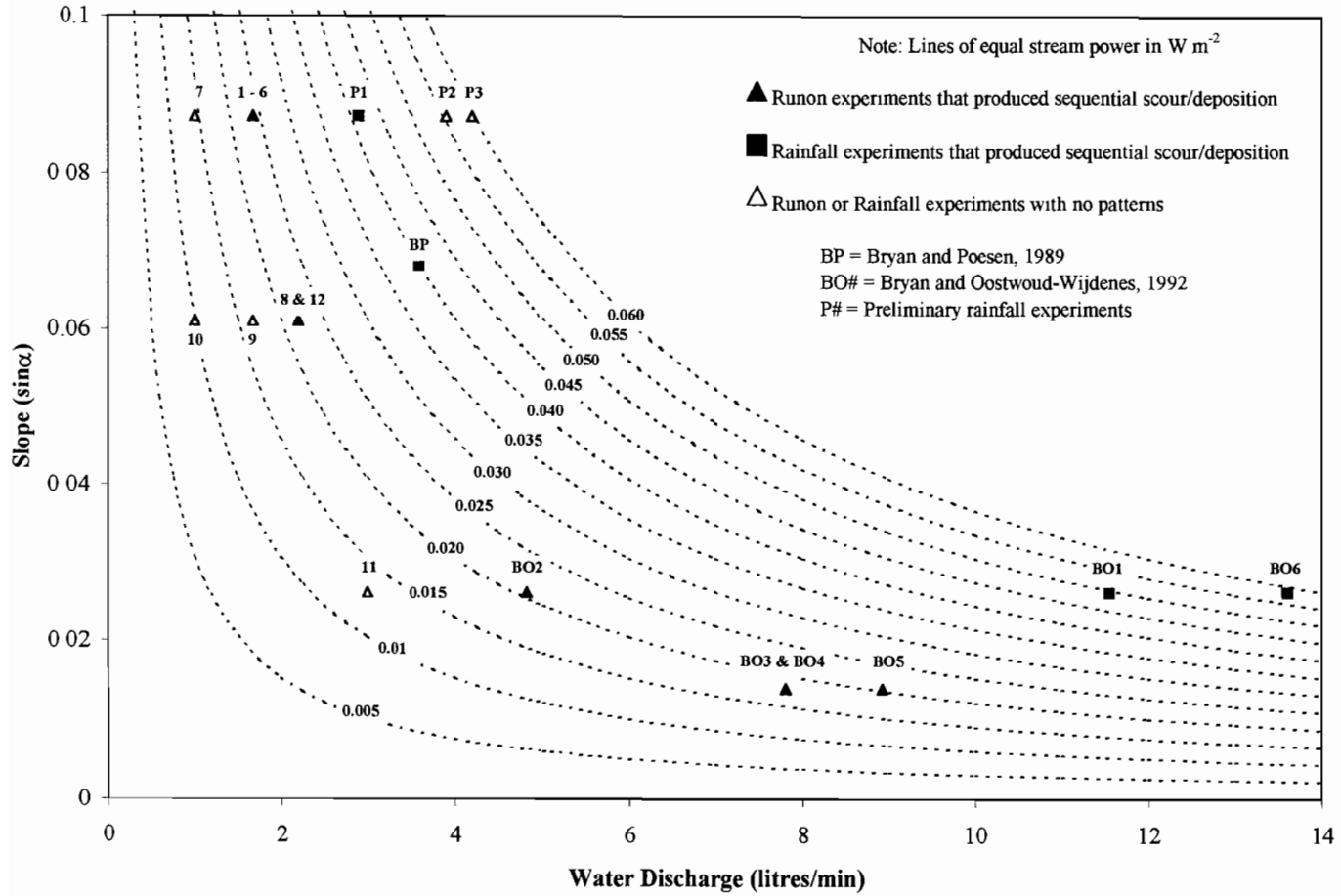
Fig. 6. Slope, water discharge, stream power relationships for simulated rainfall and runon experiments.

In addition to the mean data for each experiment shown in Table 2, the hydraulic conditions at the precise location and time at which initial scour developed during the most of the runon experiments have been isolated. The mean values for u^*, τ, Fr, and w (unit stream power) for experiments 1–6 (scouring) are 0.48 m s^{-1}, 2.35 Pa, 1.34 and 0.52 W m^{-2}, compared with values for experiments 7–10 (non-scouring) of 0.039 m s^{-1}, 1.53 Pa, 1.47 and 0.34 W m^{-2}, respectively. Values for u^* and w for scour and deposition agree closely with the values for rill initiation cited by Rose (1985) and Slattery and Bryan (1992).

Stream power is an index of the conditions necessary for initial selective transport, in this case flow with a strong velocity gradient, just sufficiently deep to immerse and destabilize protruding particles. The precise threshold value should reflect soil surface conditions and the height to which individual large particles protrude above the general surface. Clearly a sufficient proportion of particles must protrude, become destabilized and move, to produce a significant deposition zone, with associated feedback effects on surface roughness and hydraulic roughness. From this, it would appear that soils with strongly bimodal particle size distribution would be particularly suitable, though not necessarily essential, for sequential scour and deposition. The process will be enhanced if the large particles are aggregates with low particulate density and resistance to rolling.

Data from the runon experiments of Bryan and Oostwoud Wijdenes (1992) at Baringo plot (Fig. 6; BO2–BO5) almost exactly on the same threshold Ω value as the experiments in which sequential scouring developed in this project. It should be noted, however, that sequential scour steps already existed before the Baringo runon experiments. These were presumably formed by rain-impacted sheetflow or rainflow during a series of rainstorms. The laboratory simulated rainfall experiments (P1) show that sequential scour and deposition can form in such conditions, if the stream power is not too high. In these experiments, the upper threshold stream power (Ω) value which separates sequential scour from continuous rill incision appears to be about 0.05 W m^{-2}. In Bryan and Oostwoud Wijdenes' comparable laboratory experiments, sequential scouring developed with Ω values of 0.05 and 0.058 W m^{-2}. The difference between these results probably reflects the fact that in the latter experiment, the flume bed was not shaped to form a central thalweg, and so higher threshold stream power values were required before continuous rill development could occur.

The data from all these simulated rainfall experiments, together with those of Bryan and Poesen (1989) (Fig. 6) indicate that raindrop impact increases the threshold stream power necessary for selective transport. One effect of rainsplash is to disrupt the laminar sub-layer in sheetwash, reducing the flow velocity gradient, and limiting the tendency for protruding aggregates to roll. Some of the aggregates will breakdown under raindrop impact, so the net effect will be reduced selective transport of aggregates. Large sand grains will become more significant in selective transport, which because of higher density will require higher threshold stream power. Rainsplash is selective in both entrainment and transportation (Savat and Poesen, 1981), but is strongly affected by the runoff depth, diminishing swiftly once depth exceeds the median drop diameter. Splash intensity also generally diminishes rapidly after the first 10 min of rainfall, particularly on soils sensitive to sealing (Slattery and Bryan, 1992). It seems likely that the dominant process in both the initial laboratory experiments (P1–P3) and in the field at Baringo,

was rainflow (entrainment by splash with transport by flow (Moss and Walker, 1978)) rather than rainsplash. Rather few precisely controlled observations of rainflow entrainment are available, but the data of Moss and Walker (1978) suggest reduced selectivity and higher suspended load concentrations than in sheetwash.

It is difficult to identify precisely the relative importance of rainflow and sheetwash selectivity in generating scour/deposition patterns. In the initial laboratory experiments and those of Bryan and Oostwoud Wijdenes (1992), rainfall was produced by spray units with 5.5–6 m fall-height and mean intensity of 43 mm h^{-1}, but the median drop size was only 1.3 mm, so the kinetic energy produced was only about 70% of the level of natural rainfall of similar intensity. Flow depths greater than this median drop size covered most parts of the flume very soon after runoff commenced, so rainsplash or rainflow must have been minimal. Storms of similar intensity with durations around 40 min at least once a year at Baringo (Oostwoud Wijdenes, 1992). Field observations show that runoff generation on the lake flats is rapid in such rainfall, but the median drop size would be significantly larger (2–2.4 mm; Hudson, 1963), so rainsplash and rainflow would be more significant in such storms at Baringo. These processes would also, of course, be active in the more frequent storms of lower intensity or duration. While the scour/deposition patterns at Baringo may originate in single rainstorms, it seems certain that most, if not all result from the cumulative effects of a number of storms. One result is that deposition zones at Baringo are considerably thicker (up to 5 cm) than those produced during the short laboratory experiments.

In summary, it appears that threshold stream power values of 0.043 to 0.055 W m^{-2} are likely to be required to produce the scour/deposition sequences observed at Baringo, and that rainsplash and rainflow are more significant agents in their formation than in the laboratory. Lower stream powers would not produce the necessary selective transport, while higher stream powers would result in continuous rill scour. The occurrence of these features on the lake flats at Baringo therefore represents a fortuitous congruence of appropriate slope angles with characteristic rainstorm patterns. Because the water stability of large aggregates at Baringo was very low, protrusion of aggregates into the flow and selective aggregate transport is probably less important than in the laboratory runon tests. The incidence of surface crusting, the lower roughness of surfaces and the slightly finer texture would all contribute to explanation of the somewhat greater typical step length at Baringo. On the other hand, the spatial and temporal variability of natural rainstorms, together with slight variations in surface roughness and inclination would also explain the variability of step lengths observed.

Field observations clearly show that the cyclic deposition zones on the Baringo lake flats are preferred locations for growth of the low herbaceous plants of which the small-scale vegetation bands are comprised. Nothing is known of the precise moisture requirements of these plants, or how swiftly they can colonize deposition zones. The infiltration capacity of crusted scour zones is near zero, so water delivery to deposition zones can be approximately doubled. The moisture storage capacity of deposition zones obviously varies, but calculations with typical dimensions and bulk densities indicate capacity of dry soils to store all the water input from rainstorms up to about 30 mm, which recur several times per year. In reality, the figure will be lower as antecedent soil moisture content at the start of rainfall is usually between 5–10% (gravimetric), between

field capacity and wilting point, but this is counterbalanced by the effect of root development and enhanced activity of microorganisms on percolation into underlying soil. Although the vegetation bands wither during dry weather, the rapidity of response after rainfall suggests that many plants remain viable for prolonged periods. In theory, prolonged proliferation of these low herbaceous plants in should provide a preferred location for colonization by grasses and higher plants. There is, in fact, little evidence of further development, suggesting that grazing pressures on the Baringo lake flats are too high to allow colonization by anything other than unpalatable plants, or perhaps that the herbaceous plants are allelopathic.

5. Conclusion

Most banded vegetation is attributed in literature reports to vegetation degradation by overgrazing, trampling and drought. While such degradation certainly causes plant stress and can produce patches of bare soil, typically these are initially rather random in organization. Some further process is necessary to organize these patches into the regular alternating bands typically described in the literature. In most cases this process is probably selective soil erosion and deposition, supported by feedback effects on water infiltration and plant growth. Most reported occurrences of banded vegetation are at quite large scales, but small scale examples also occur on lake flats in northern Kenya, where low herbaceous plants preferentially colonize, or survive on, small alluvial deposits which provide enhanced moisture storage capacity. In some cases these small vegetation bands may represent a first stage in the recolonization of severely degraded surfaces, rather than a late stage in vegetation deterioration.

Laboratory experiments show that regular sequential scour/deposition patterns can develop on bare, homogeneous soil surfaces at scales similar to those in the field in Kenya. The key process in laboratory runon experiments is selective rolling of large aggregates which protrude across a steep velocity gradient in sheetflow. These are transported for varied step lengths, but are soon deposited as small alluvial fans in diverging shallower flow. The critical environmental condition is irregular shallow flow with a combination of slope inclination and runoff discharge which causes stream power to fluctuate above and below values of about $0.020–0.025$ W m^{-2}. Flows of higher stream power prevent significant deposition and lead to continuous rill scour.

Most of the laboratory features are produced by runon while those in the field in Kenya develop in rain-impacted flow, and are probably in part due to rainsplash and rainflow erosion. Simulated rainfall experiments in this project and previous studies show that the critical stream power values for formation of scour/deposition features in rain-impacted flow vary between about 0.043 and 0.055 W m^{-2}, depending on the degree of flow concentration caused by surface microtopography. It appears that the significance of aggregate selective transport is reduced under rainfall. Because of very low water-stable aggregation, finer soil textures and smoother slopes, step lengths between successive deposition zones are typically longer in the field at Baringo than in the laboratory.

The laboratory conditions clearly differed from those in the field, with somewhat steeper slopes and clearly defined thalwegs with relatively steep 'interrill' slopes. Nevertheless the experiments show that transverse deposition zones can evolve from primarily linear flow patterns. This evolution will be more pronounced in the field in Baringo, where 'interrill' slopes approach zero, and will probably also be enhanced by the surface roughness of colonizing vegetation.

The study shows that vegetation bands at this scale can develop as a result of sequential scour/deposition processes in runon and rain-impacted sheetflow, where deposit zones establish suitable conditions for colonization by some plants. These small scale vegetation bands may evolve into large-scale features with shrub and tree components, though this is apparently currently precluded at Baringo by intense grazing pressures or allelopathy. Nevertheless it does appear that these small scale vegetation bands can represent a stage in recovery of degraded surfaces rather that unequivocal evidence of advancing degradation.

Acknowledgements

References

Audrey, P., Rossetti, Ch., 1962. Observations sur les Sols et la Vegetation en Mauritanie du Sud-Est et sur la Bordure adjacent du Mali, FAO, Rome.

Boaler, S.B., Hodge, C.A.H., 1964. Observations on vegetation arcs in the northern region, Somali Republic. J. Ecol. 52, 511–544.

Bryan, R.B., 1990. Knickpoint evolution in rillwash. In: Bryan, R.B. (Ed.), Soil Erosion: Experiments and Models, Catena, Supp. Bd., 17, pp. 111–132.

Bryan, R.B., Oostwoud Wijdenes, D., 1992. Field and laboratory experiments on the evolution of microsteps and scour channels on low-angle slopes. In: Schmidt, K.H., De Ploey, J. (Eds.), Functional Geomorphology: Landform Analysis and Models, Catena, Supp. Bd., 23, pp. 1–29.

Bryan, R.B., Poesen, J.W.A., 1989 Laboratory experiments on the influence of slope length on runoff, percolation, and rill development. Earth Surface Processes and Landforms 12, 211–231.

Clos-Arceduc, M., 1956 Etude sur photographhies aeriennes d'une formation vegetale sahelienne: la brousse tigree. Bull. de l'IFAN, Ser A 7 (3), 677–684, Cited by Thiery et al., 1995.

Cornet, A., Delhoume, J.P , Montana, C., 1988. Dynamics of striped vegetation patterns and water balance in the Chihuahuan Desert. In. During, H.J., Werger, M.J.A., Willems, J.H. (Eds.), Diversity and Pattern in Plant Communities, SPB Academic Publishing, The Hague, The Netherlands, pp. 221–231.

Cornet, A., Montana, C., Delhoume, J P , Lopez-Portillo, J., 1992. Water flows and the dynamics of desert vegetation stripes. In: Hansen, A J., De Castri, F. (Eds.), Landscape Boundaries Consequences for Biotic Diversity and Ecological Flows, Ecological Studies, 92, Springer Verlag, New York, pp. 327–345.

Govers, G., 1985. Selectivity and transport capacity of thin flows in relation to rill erosion. Catena 12, 35–50.

Hemming, C.F., 1965. Vegetation arcs in Somaliland. J. Ecol. 53, 57–68.

Holwill, C J , 1997. Soil evaporation from tiger-brush in south-west Niger. J. Hydrol 189, 426–442.

Hudson, N.W., 1963. Raindrop size distribution in high intensity storms. Rhodesian J. Agric. Res. 1, 6–11

Ives, R., 1946. Desert ripples. Am. J. Sci. 244, 492–501.

Leprun, J.C., 1992. Etude de quelques brousses tigrees saheliennes:structure, dynamique, ecologie In: Le Floc'h, E., Grouzis, M., Cornet, A., Bille, J.C. (Eds.), L'Aridite, Une Contrainte au Developpement, ORSTOM Coll. Didactiques, Paris, pp. 221–244.

Litchfield, W.D., Mabbutt, J.A., 1962. Hardpan soil of semiarid southwestern Australia. J. Soil Sci. 13, 148–159.

Mabbutt, J.A., Fanning, P.C., 1987. Vegetation banding in arid western Australia. J. Arid Environ. 12, 41–59.

Moss, A.J., Walker, P H , 1978. Particle transport by continental water flows in relation to erosion, deposition, soils and human activities. Sedimentary Geol. 20, 81–139.

Oostwoud Wijdenes, D.J., 1992. The dynamics of gully-head erosion on a semi-arid piedmont plain, Baringo District, Kenya. Unpublished PhD thesis, University of Toronto, 212 pp

Rapp, A., 1974. A review of desertization in Africa. Water, vegetation and man SIES Report, 1, Secretariat for International Ecology, Stockholm, 77 pp.

Rose, C.W., 1985. Developments in soil erosional and depositional models. Adv. Soil Sci. 2, 1–63

Savat, J., De Ploey, J., 1982. Sheetwash and rill development by surface flow. In: Bryan, R.B., Yair, A. (Eds.), Badland Geomorphology and Piping. Geobooks, Norwich, pp. 113–126.

Savat, J., Poesen, J W A., 1981 Detachment and transportation of loose sediments by raindrop splash: I. The calculation of absolute data on detachability and transportability. Catena 8, 1–17.

Slattery, M.C., Bryan, R.B., 1992. Hydraulic conditions for rill incision under simulated rainfall: a laboratory experiment Earth Surface Processes and Landforms 17, 127–146

Snelder, D.J.R.M., 1993. Methods of rangeland improvement and revegetation for denuded, semi-arid savanna areas in the Baringo District, Kenya. Unpublished PhD thesis, University of Toronto, 208 pp.

Sutherland, R.A., Bryan, R.B., Oostwoud Wijdenes, D., 1991. Analysis of the monthly and annual rainfall climate in a semi-arid environment, Kenya. J. Arid Environ. 20, 257–275.

Thiery, J.M., D'Herbes, J.-M., Valentin, C., 1995. A model simulating the genesis of banded vegetation patterns in Niger. J. Ecol. 83, 497–507.

Torri, D., Sfalanga., Chisci, G., 1987. Threshold conditions for incipient rilling. In: Bryan, R.B. (Ed.), Rill Erosion: Processes and Significance, Catena, Supp Bd., 8, pp. 97–105

White, L P., 1969. Vegetation arcs in Jordan. J. Ecol 57, 461–464.

White, L.P., 1970. 'Brousse tigree' patterns in southern Niger. J. Ecol. 58, 549–553.

White, L.P., 1971 Vegetation stripes on sheet wash surface. J. Ecol. 59, 615–622

Worrall, G.A., 1959. The Butana grass patterns. J. Soil Sci. 10, 34–53.

The soil surface characteristics of vegetation stripes in Northern Mexico and their influences on the system hydrodynamics An experimental approach

Jean Louis Janeau [a,*], André Mauchamp [b,1], Gerardo Tarin [c]

[a] *Instituto de Ecologia, A.P. 632, 34000 Durango, Dgo, Mexico*
[b] *Instituto de Ecología, A.P. 63, 91000 Xalapa, Ver., Mexico*
[c] *Cenid-Raspa, A.P. 225 B, 35078 Gomez Palacio, Dgo, Mexico*

Abstract

Vegetation stripes were described in arid areas of Africa, Australia and México. They depend on the local concentration of rain water after runoff. In México, we described the soil surface characteristics of vegetation stripes and performed rainfall simulations to analyze its hydrodynamic behaviour. Simulations were performed on plots characterized by the four soil surface features represented in the stripes. Four types of surface crusts were found in the stripes, erosion, sedimentation, and two types of structural crusts. The less vegetated plots had relatively impervious crusts with low preponding rains and high constant runoff rates. On the contrary, the highly vegetated plot had a thin crust and abundant litter which allowed a high infiltration rate. Runoff rates were positively related to rainfall intensity. Those relationships between surface characteristics and runoff determine the fate of rain water and may allow the prediction of the amount of runoff for a specific rain on a given plot. © 1999 Published by Elsevier Science B.V. All rights reserved.

Keywords: Chihuahuan desert; Soil surface features; Vegetation stripes; Rainfall simulation; Hydrodynamics; Mexico

[*] Corresponding author. Orstom, A P. 17116596, Quito, Ecuador.
[1] Present address: Station Biologique de la Tour du Valat, Le Sambuc, 13200 Arles, France.

1. Introduction

The vegetation stripes, called 'mogotes' in Northern México, correspond to a very similar formation known as the 'brousse tigrée' described in Sahelian Africa (Clos Arceduc, 1956; Hemming, 1965; White, 1971) or the 'mulga groves' in Australia (Litchfield and Mabbut, 1962; Tongway and Ludwig, 1990). In Northern México, it is an important source of forage for the cattle and a source of fire wood. It is a succession of densely vegetated stripes and bare soil areas (Cornet et al., 1988; Montaña and Breimer, 1988; Delhoume, 1988). The vegetation stripes are approximately 50 m wide per 200 to 300 m long and are separated by bare soil stripes of about 250 m wide. They are found on slopes less than 1% and are parallel to the contour lines. The climatic and topographic conditions in which such striped patterns are found in Africa are similar to those of Northern México (Gallais, 1967; in Mauritania, Audry and Rossetti, 1962; in Mali, Leprun, unpublished; [2] in Niger, Ambouta, 1984; in Burkina Faso, Serpantie et al., 1992). In Mapimí, average annual rainfall is 264 mm and slope 0.9 to 1.1%. A very gentle upslope movement of the stripes is evidenced by the structure of the vegetation and the presence of remnants of trees and shrubs in the bare zone just downslope of a stripe (Mauchamp et al., 1993). This dynamics is due to a preferential establishment of seedlings at the upper edge which receives more water from runoff, and on the contrary, an increased mortality at the lower edge (Cornet et al., 1988; Montaña, 1992; Mauchamp et al., 1993). Several authors suggested that a progressive modification of the 11 soil surface features was responsible for the dynamics. These modifications would lead to changes in the infiltration rates and the water storage capacity of the soil, and would further affect the vegetation dynamics (Boaler and Hodge, 1964; White, 1971; Yeaton et al., 1977; Cornet et al., 1988; Montaña, 1992; Mauchamp, 1992). Soil surface features are characterised by the vegetation itself, the superficial pedological structure and result from complex interactions between flora, fauna, meteorological and possibly anthropological factors (Casenave and Valentin, 1992).

To characterise the spatial variability of the soil surface features and their role in the hydrodynamics of the vegetation stripes, we first described them along a transect perpendicular to the main axis of a stripe together with the detailed topography. The transect (Fig. 1) crossed a bare zone (Plot 1) and the pioneer (Plot 2), central (Plot 3) and senescence (Plot 4 in limit) zones of a stripe. Rainfall simulations were then used to analyse the relationship between these soil surface features and infiltration and runoff.

2. Site description and methods

The study was conducted in the Mapimi Biosphere Reserve (Chihuahuan desert, México, 26°N, 103°W). Mean annual rainfall is 264 mm (Standard deviation 65 mm, from 12 yr observation at the Reserve Station) and mean annual temperature is 20.8°C

---

[2] Leprun, J.C., 1978. Etude de l'évolution d'un système d'exploitation Sahélien au Mali. Unpub. report, Orstom, D.G.R.S.T., Paris, France.
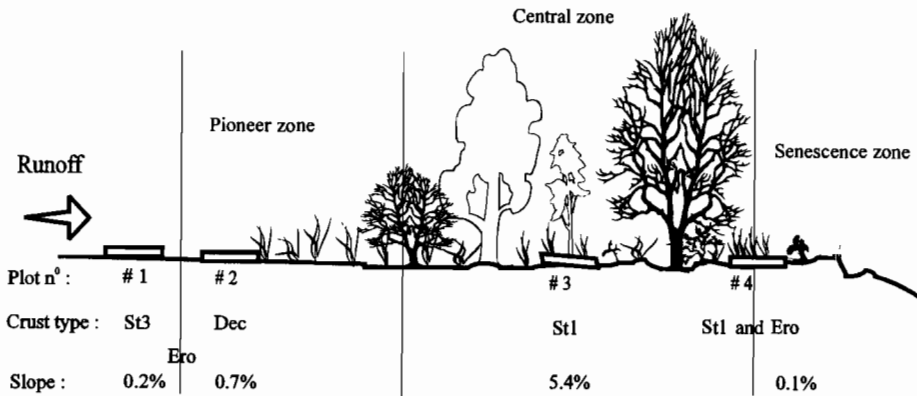
Fig. 1. Cross-section of a vegetation stripe along the main slope. The figure shows the plots 1–4 for the rainfall simulation experiments with their slope and their dominant crust characteristics.

with strong seasonal amplitudes. Most of the rain occurs as heavy showers from July to October. The soil is a luvic yermosol with less than 1% organic matter, on fine and medium alluviums resting on siltstones. The vegetation striped patterns cover 32% of the Reserve area, 25% of which are densely vegetated stripes (Montaña and Breimer, 1988).

A transect across the stripe was carefully described for soil and vegetation cover. Four plots corresponding to the main four zones of the vegetation stripes were set for rainfall simulations. On each 1 × 1 m plot, the soil surface features and the microtopography were measured on a regular grid of 380 points. Vertical needles maintained by a metallic frame were used to measure the topography. The soil surface features were characterised according to the typology of Casenave and Valentin (1992) on each of the 380 points. Structural crusts with one layer (st1), are formed by the splash effect at the first rainfall, they are fragile and about 1 mm thick. Structural crusts with three layers (st3), are formed by a vertical granulometric selection with a leaching of the fine elements under the rainfall effect (Valentin and Bresson, 1992). They can be up to 5 mm thick according to the amount of sand. The erosion crusts (ero), result from water and wind erosion of structural crusts, are about 1 mm thick and hardened. Sedimentation crusts (dec), result from the deposition of fine particles transported by runoff, are 2 cm thick with small 1 cm deep cracks and are composed of several microlayers which tend to curl up.

The rainfall simulator developed by Asseline and Valentin (1978) is a sprinkling device on top of a 4 m high tower enclosed in a large canvas to avoid wind. A calibrated nozzle fed by a constant waterflow oscillates with a controlled angle which allows the modification of the frequency with which the sprinkler passes over the plot. Rainfall intensity ranges between 15 to 130 mm/h. The size and kinetic energy of the raindrops are similar to those of natural rainfall of same intensities. Each plot was limited by a metallic frame inserted approximately 5 cm into the soil. The lower side of the frame had a gutter and the water running from the plot could be collected and measured. Each plot was submitted to five rains of constant intensity (12, 25, 50, 75 and 100 mm/h) with 10 days drying between two intensities. The 40 min rains were applied to initially

dry soil, and repeated 30 min later on wet soil. We registered the time when runoff started. Runoff water was then collected during 1 min periods with 2 min intervals at the beginning and with 5 min intervals as soon as the constant runoff rate was reached. The data allowed the calculation of (1) the preponding rain, that is the amount of water infiltrated before the runoff started including surface storage, (2) the coefficient of infiltration K_1 which is the proportion of the rain that infiltrated at the end of the simulation, and (3) Rx, the runoff intensity once a constant rate is reached. The simulations were performed from September 1989 to February 1990, during the cold and dry season.

3. Results

In Fig. 1, a schematic presentation is given of the experimental plots 1–4. The bare area, upslope from the stripe, had a 'st3' structural crust (plot 1, Table 1), with a discontinuous cover of coarse elements. Locally, it presented thin and hardened erosion crusts where runoff had removed the sand and coarse elements. Plot 1 had an average slope of 0.2% and a maximum micro relief of 5 mm. Within the stripes, plots 2, 3 and 4 corresponded to the three zones identified by Cornet et al. (1988), respectively the pioneer, central and senescence zones, plot 4 being in fact at the limit of the central and senescence zones. Plot 2 was characterised by an accumulation of silt with sand and a few coarser elements. It had a typical decantation crust (Plot 2, dec, Table 1) (Janeau and Ruiz de Esparza Villareal, 1992). It had an average slope of 0.7%. Curled up plates present a 1.5 cm micro relief. In the central zone, we observed two different situations. Where the vegetation was dense, there was no crust or a fragile drying crust (st1, plot 3) because of the absence of splash effect and the important faunal activity (Table 1). The main species were a tree, *Prosopis glandulosa* Torr. var. *torreyana* (Benson) M.C. Johnst., 'honey mesquite', two shrub species, *Flourensia cernua* DC., 'tarbush', and *Lippia graveolens* and a grass, *Hilaria mutica* (Buckl.) Benth., 'tobosa grass'. Where there were openings in the vegetation cover, particularly due to trampling by cattle, an erosion crust appeared locally and infiltration was much lower than on vegetated areas.

Table 1
Characteristics of the four rainfall simulations plots

	Vegetation cover		Crust composition			Type of crust
	Standing vegetation	Dry litter	Coarse elements	Sand	Crust (loam and clays)	
Plot 1, bare zone between stripes	–	–	16.4	59.4	24.2	st3 75%, ero 25%
Plot 2, pioneer zone	1.1	2.2	–	–	96.7	ero 15%, dec 85%
Plot 3, central with tree	83.8	13.1	–	–	3.1	st1 100%
Plot 4, central with grass cover	27.1	65.7	–	–	7.2	st1 90%, ero 10%

The proportion for each type of cover is given as a percentage of the plot surface (one m^2). 'St1' and 'st3' are structural crusts with 1 and 3 microlayers, respectively. 'ero' is an erosion crust. 'dec' is a depositional crust; as referred to the classification of Valentin and Bresson (1992).

Table 2
Preponding rainfall (mm) as influenced by the rain intensity and the initial condition of the plot, dry or wet

Intensity mm/h	Initial condition	Plot 1	Plot 2	Plot 3	Plot 4
12	dry	3 4	2.7	8.0	8.0
	wet	1.0	0.9	8.0	8.0
25	dry	2.9	2.9	4.8	16 7
	wet	1.4	1.2	1.8	2.4
50	dry	2.1	3.0	3.7	11.3
	wet	1.2	1.6	2.3	3.6
75	dry	2 5	2.6	5.5	11.1
	wet	1.7	2 0	3.0	3 2
100	dry	2.1	3.0	7.9	14 1
	wet	1.5	2.2	2.7	3.3

Plot 3 had a steeper slope (5.4%) and had a strong micro relief, up to five cm, due to the bunch grass *Hilaria mutica* and trampling by cattle. Vegetation and litter were abundant and the soil had a high porosity. Plot 4 was almost flat (slope 0.1%) with more than 65% of its surface covered by litter and had a 2.5 cm micro relief. Our plots did not include an area with major trampling effect. Finally, the senescence zone was characterised by a sharp erosion step of 5 to 10 cm due to running water during heavy rains. It had an erosion crust composed of one micro-layer. The vegetation was scarce, with dead trunks and a few degraded grass clumps. No plot was established in the senescence zone.

Under dry and wet conditions, the preponding rain ranged from 1 to 16.7 mm and was not clearly related to the rain intensities (Table 2). On average for the five intensities, it increased from the plots located in the upper, less vegetated zones to the more densely vegetated areas. For the simulation on dry soil, plots 1 and 2 had the lowest average values (2.6 and 2.8 mm, respectively, S.E. 0.2 and 0.07, $n = 5$), plot 3 had 6 (S.E. 0.7, $n = 5$) and plot 4 had the highest (12.2 mm, S.E. 1.3, $n = 5$). For the 12

Table 3
Infiltration coefficient K_i (% of the total rain applied) and final infiltration rates FIR (mm/h) as influenced by initial soil moisture and rainfall intensity Ip (mm/h)

Initial	Ip	Plot 1 FIR	K_i	Plot 2 FIR	K_i	Plot 3 FIR	K_i	Plot 4 FIR	K_i
dry	12	3.6	65 2	2.8	61.9	> 12	100	> 12	100
wet		3.4	43.0	1.3	34.5	> 12	100	> 12	100
dry	25	5.1	42.9	7.1	48.1	21.6	94 7	> 25	100
wet		3.1	23.2	4.6	25.5	16.4	73.6	19.9	89.8
dry	50	7	17.7	6.2	25.4	30.4	81.5	10	59 8
wet		7.3	13 4	6.5	16.8	22.1	52.5	8.5	31.9
dry	75	5	16.7	13.2	22.5	31	56.0	25.7	66.4
wet		4.1	8.9	16.9	24.0	20.5	35.4	17.7	29.8
dry	100	6.6	13.0	9.5	18.7	43	57.9	23.6	48.5
wet		6.8	9.3	8.4	8.3	35.6	39.5	24	31.6

Rainfall simulations were performed on 1 m² plots and lasted 40 min.
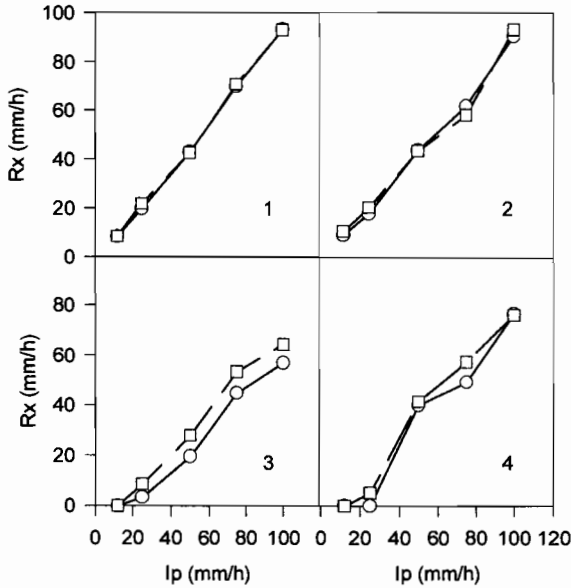
Fig 2. Relationship between the constant runoff rate Rx and the rainfall intensity for the plots 1 to 4 for dry (circles) and wet (squares) initial conditions

and 25 mm/h intensities, 100% of the rain infiltrated and hence, the preponding rain was limited by the total amount of rain rather than the soil characteristics. Preponding rain was lower under wet initial conditions and averaged 1.5 mm for the plots 1 and 2, 3.8 mm for plots 3 and 4 (Table 2). The infiltration coefficients K_1 ranged from 8–10% of the rain for non-vegetated plots and high rainfall intensities, to 100% for vegetated plots with the lowest rainfall intensity (Table 3). They were different depending on the initial conditions, always higher for dry soil, even when there was no clear difference of the constant runoff rate Rx. They were also systematically higher for vegetated plots than bare soils. The constant runoff rates were similar for plots 1 and 2, reaching more than 90% of the rain for the highest intensity, and lower for plots 3 and 4 (Fig. 2). On plot 3, Rx was positively related with rainfall intensity but the slope was lower. On that plot, the final infiltration rate reached a maximum of 43 mm/h for the 100 mm/h rain (Table 3).

4. Discussion and conclusions

The variations we observed of the total infiltration coefficient K_1 show the relationship between the infiltration capacity of soils and their surface features. K_1 was always higher for plots with vegetation than for bare soil plots 1 and 2. Aggregate breakdown may occur under vegetation cover due to air entrapment compression under fast wetting. It is not the case in our study where dense vegetation and litter limit the impact of raindrops and prevent splash effects, as also found elsewhere (e.g., Casenave and

Valentin, 1992). Moreover, biological activity, litter and roots favour superficial porosity and a better infiltration capacity. Our experiment was performed at the beginning of the dry season, with very few annual plants and a relatively low grass cover. During the rainy season, the effects of the vegetation on plots 3 and 4 would be even stronger than in the dry season and an annual plant cover may modify the infiltration capacity in the pioneer zone (Plot 2). The constant runoff rate Rx is reached when the infiltration stabilised at its minimum level for a fixed rainfall intensity. It depends on the soil surface features and is clearly reduced by the presence of vegetation (Fig. 2, plot 3–4). The similarity of Rx for non-vegetated plots, for both dry and humid initial conditions, shows that the crusts, although having a different structure, have the same hydraulic characteristics. Rx relates to the increase in rainfall intensity and the soil moisture conditions for the vegetated plots. The effect of micro-relief could be observed on plot 3 where it caused the formation of small puddles and thus changed the conditions of infiltration which took place under a water layer. The formation of small puddles during the experiment forced infiltration and the increase of Rx with intensity was limited.

The vegetation interacts with the crust type to determine its hydrodynamic characteristics. Plots 1 and 2, without vegetation, had different crust types but similar infiltration parameters. On the other hand, plots 3 and 4 had the same crust types, also had similar infiltration parameters, although they had different vegetation. Moreover, at the scale of a single shrub, we could show, in a previous study (Mauchamp and Janeau, 1993), the existence of an additional interaction between the vegetation and rainfall and infiltration. The canopy of the main shrub species of the stripes, *F. cernua* DC. ('tarbush'), Asteraceae, intercepts the rain and funnels it down to the basis of the plant where infiltration can be very high. We recorded infiltrations as high as 445 mm in a four h period on a $0.1 \ m^2$ surface surrounding the base of the shrub (Mauchamp and Janeau, 1993). The very high infiltration rates at the shrub basis was due to the presence of litter, an important faunal activity and the axis splitting phenomenon which was observed frequently for this species. Under the rest of the crown, there was a relatively more impervious crust with two superficial microlayers.

As underlined by most authors, the existence and maintenance of this type of pattern is due to the concentration effect of rainfall in 30 to 25% of the landscape, which thus benefits from a more favourable water balance. The characteristics of surface crusts, which have strong feedback relationships with the vegetation, determine the local runoff patterns. Low porosity crusts from the inter-stripe areas give birth to runoff as high as 95%, which then infiltrates in the following stripe. There, a higher porosity due to biological activity and the absence of a splash effect promotes infiltration and allows the maintenance of a dense vegetation cover. As observed during our simulations, surface characteristics influence preponding rain and runoff rates. They greatly influence rainfall that causes significant runoff and hence the maintenance of the stripped pattern. In the Mapimi area, winter rains of low intensity do not cause runoff and, although important for certain species of the formation, they play no role in the maintenance of the striped pattern.

When compared for infiltration parameters, our data coincided well with the estimations provided by Casenave and Valentin (1992) for similar soil surface features (Table 4). Our data, combined with a careful evaluation of the proportions of surface crusts in

Table 4

Comparison of the infiltration coefficients K_1 (%) predicted in Sahelian Africa by Casenave and Valentin (1992) (Estimated) and the coefficients observed during this study (Observed) in Northern Mexico for an intensity of 50 mm/h

Dry soil		Wet soil	
Estimated	Observed	Estimated	Observed
ero: 15–30; st3: 25–40	Plot 1: 17.7	ero: 20–30; st3:10–25	Plot 1. 13.4
st3· 25–40; dec: 35–55	Plot 2: 25.4	st3· 10–25, dec 25–45	Plot 2: 16 8
st1: 80–90	Plot 3: 81.5	st1. 75–85	Plot 3: 59.8
st1 + V < 50%: 60–70; ero: 15–30	Plot 4: 59.8	st1 + V < 50%: 50–60; ero: 20–30	Plot 4: 31 9

V < 50% = less than 50% vegetation cover.

the stripes and interstripe areas might allow the evaluation of the amounts of runoff to be included in a simulation model of the stripes hydrodynamics (Mauchamp et al., 1994). Moreover, our results allow the prediction of the fate of a stripe after a disturbance that would replace a type of crust by another, for example trampling. Trampling causes the destruction of the vegetation, the formation of impervious crusts and a preferential area for water flow where it acquires a sufficient velocity to cause erosion. These small gullies then drain the water from the stripe and locally leads to vegetation death, disturbing the pattern. For the same reasons, trails created by human activities have to be, when possible, parallel to the main axis of the stripes.

Acknowledgements

References

Ambouta, K , 1984. Contribution à l'édaphologie de la brousse tigrée de l'Ouest Nigérien. Thèse doctorale, Université de Nancy I, 116 pp.

Asseline, J., Valentin, C , 1978 Construction et mise au point d'un infiltromētre à aspersion. Cah. Orstom, sér Hydrol. XV (4), 321–349.

Audry, P., Rossetti, Ch , 1962. Observations sur les sols et la végétation en Mauritanie du Sud-Est et sur la bordure adjacente du Mali (1959 et 1961). Prospection écologique. Etudes en Afrique Occidentale. Projet du fonds spécial des Nations-Unies relatif au criquet pélerin. F.A.O., Rome, 267 pp., multigr., 33 Figs., 70 Réfs., 26 photos, 1 carte h.t. à 1/200 000e.

Boaler, S.B., Hodge, C.A.H., 1964. Observations of vegetation arcs in the Northern region, Somali Republic. J. Ecol. 52, 511–544.

Casenave, A., Valentin, C., 1992. A runoff capability classification system based on surface features criteria in the arid and semi-arid areas of West Africa. J. Hydrol. 130, 231–249.

Clos Arceduc, M , 1956. Etude sur photographies aériennes d'une formation végétale sahélienne: la brousse
tigrée Bulletin de l'Institut Francais d'Afrique Noire A-18, 677–684.

Cornet, A., Delhoume, J.P., Montaña, C., 1988. Dynamics of striped vegetation patterns and water balance in
the Chihuahuan Desert In: During, H.J., Werger, M J.A , Willems, J.H (Eds.), Diversity and Pattern in
Plant Communities pp. 221–231 The Hague SPB Academic Publishing, 278 pp.

Delhoume, J.P , 1988 Distribution spatiale des sols le long d'une toposéquence représentative In: Montaña,
C. (Ed.), Estudio integrado de los recursos vegetación, suelo y agua en la reserva de la biosfera de Mapimí
Ambiente natural y humano Instituto de Ecología, México, Publ. 23, pp 135–165.

Gallais, J., 1967 Le delta intérieur du Niger et ses bordures. Etude morphologiques. CNRS, Centre de
Recherches et Documentation Cartographiques et Géographiques. Mém. et Doc., Nouvelle série, Vol 3,
153 pp , 30 Figs., 16 pl photos, +1 carte h.t. à 1/2000 000e

Hemming, C.F., 1965. Vegetation arcs in Somaliland. J. Ecol. 53, 57–68.

Janeau, J.L , Ruiz de Esparza Villareal, R., 1992. Cartographie des états de surface d'une toposéquence
représentative du bassin versant de San Ignacio In: Actas del seminario de Mapimí. Instituto de ecología,
México , pp. 161–175.

Litchfield, W.H., Mabbut, J.A., 1962. Hardpan in soils of semi arid Western Australia. J. Soil Sci 13,
148–159.

Mauchamp, A., 1992. L'hétérogénité spatiale, sa dynamique et ses implications dans une mosaïque de
végétation en zone aride. Thèse de doctorat, Université de Montpellier II, France.

Mauchamp, A , Janeau, J.L., 1993. Water funneling by the crown of *Flourensia cernua*, a Chihuahuan Desert
shrub. J. Arid Environ. 25, 299–306.

Mauchamp, A., Montaña, C., Lepart, J., Rambal, S., 1993. Ecotone dependent recruitment of a desert shrub
(*Flourensia cernua*) in vegetation stripes. Oikos 68, 107–116.

Mauchamp, A., Rambal, S., Lepart, J., 1994. Simulating the dynamics of a vegetation mosaic: a spatialized
functional model. Ecol Modelling 71, 107–130.

Montaña, C , 1992. The colonization of bare areas in two phase mosaics of an arid ecosystem. J. Ecol. 80,
315–327

Montaña, C., Breimer, R.F , 1988 Major vegetation and environment units. In: Montaña, C. (Ed.), Estudio
integrado de los recursos vegetación, suelo y agua en la reserva de la biósfera de Mapimí. Ambiente
natural y humano. Instituto de ecología, México, Publ. 23, pp. 99–114.

Serpantie, G., Tezenas du Moncel, L., Valentin, C., 1992. La dynamique des états de surface d'un territoire
agropastoral soudano-sahélien sous aridification climatique: conséquences et propositions. In: L'aridité:
une contrainte pour le dévelopement. Orstom, collection Didactiques, pp. 419–447.

Tongway, D.J , Ludwig, J.A., 1990. Vegetation and soil patterning in semi arid mulga lands of Eastern
Australia. Aust. J. Ecol. 15, 23–34.

Valentin, C., Bresson, L.M., 1992. Morphology, genesis and classification of soils crusts in loamy and sandy
soils. Geoderma 55, 225–245.

White, L.P., 1971. Vegetation stripes on sheet wash surfaces. J. Ecol. 57, 549–553.

Yeaton, R.I , Travis, J., Gilinsky, E , 1977. Competition and spacing in plant communities: the Arizona upland
association. J. Ecol. 65, 587–595.

ELSEVIER

Morphology and microstructure of microbiotic soil crusts on a tiger bush sequence (Niger, Sahel)

O. Malam Issa [a,*], J. Trichet [a], C. Défarge [a], A. Couté [b], C. Valentin [c]

[a] *Institut des Sciences de la Terre d'Orléans, C.N.R.S.-Université d'Orléans, B.P 6759, 45067 Orleans cedex 2, France*
[b] *Muséum National d'Histoire Naturelle, Laboratoire de Cryptogamie, 12, rue Buffon, 75005 Paris, France*
[c] *ORSTOM, RED, 209-213, rue La Fayette, 75480 Paris, France*

Abstract

Microbiotic crusts resulting from the colonization of soil surfaces by communities of micro-organisms dominated by cyanobacteria, eucaryotic algae or lichens are widespread in arid and semi-arid regions. In the 'tiger bush' of Niger (Sahel) microbiotic crusts occur in bare bands between densely vegetated bands. The tiger bush soils are sandy loams with pH 4.7–6.5. Three different microbiotic crusts are recognised, forming strips parallel to the vegetation banding. They are all formed mainly by filamentous cyanobacteria dominated by *Schizothrix*. Other important genera are *Scytonema, Lyngbya, Microcoleus, Nostoc* and *Phormidium*. The filamentous micro-organisms trap sand particles and finer particles stick on the filament surfaces. These effects enhance soil cohesion and resistance to erosion. Soil porosity is also increased by the microbial cover, with additional pores delineated by filaments on the surfaces of crusts and porous organic bodies derived from microbial remains at depth. The microbiotic crusts are essential components of the tiger bush ecosystem. Water leaving the lower sides of vegetated bands results in plant decay, and on the upslope sides vegetation grows because of increased water supply. Microbial covers help resist erosion, and increase water and nutrient retention, thus providing substrates for the expansion of plants from adjacent vegetated bands. © 1999 Elsevier Science B.V. All rights reserved.

Keywords: Cyanobacteria; Microbiotic crusts; Sahel; Soil micromorphology; Soil stabilisation; Tiger bush

---

* Corresponding author. Fax· + 33-238-41-73-08; E-mail. oumarou.malam_issa@mailhost.univ-orleans.fr

1. Introduction

Biological and physical crusts are the main types of soil crust in arid and semi-arid regions. Physical crusts are formed by the action of water and, to a lesser extent, wind on soil particles at the surface of bare areas. Biological crusts, also called microbiotic crusts, result from the development of communities of micro-organisms (comprising generally cyanobacteria, eucaryotic algae, and lichens, but also bacteria, mosses, liverworts or fungi) on the surface of physical crusts.

Microbiotic crusts occur in arid and semi-arid regions of USA (Rychert and Skujins, 1974; Klubek and Skujins, 1980; Cole, 1990; Beymer and Klopatek, 1991; Belnap and Gardner, 1993), in steppe environments of Australia (Eldridge, 1993a,b), China (Reynaud and Lumpkin, 1988), in Israel (Verrecchia et al., 1995), and Sahelian Africa (Barbey and Couté, 1976; Dulieu et al., 1977; Isichei, 1980). They play major roles in soil stabilisation against both water and wind erosion (Campbell et al., 1989; Belnap and Gardner, 1993), and in water infiltration and generation of runoff (Eldridge and Greene, 1994). Loope and Gifford (1972) report that microbiotic crusts enhance water infiltration and prevent runoff, whereas Brotherson and Rushforth (1983) and Verrecchia et al. (1995) suggest the opposite. Microbiotic crusts also enhance moisture content (Belnap and Gardner, 1993; Verrecchia et al., 1995) and increase available nutrients by concen-
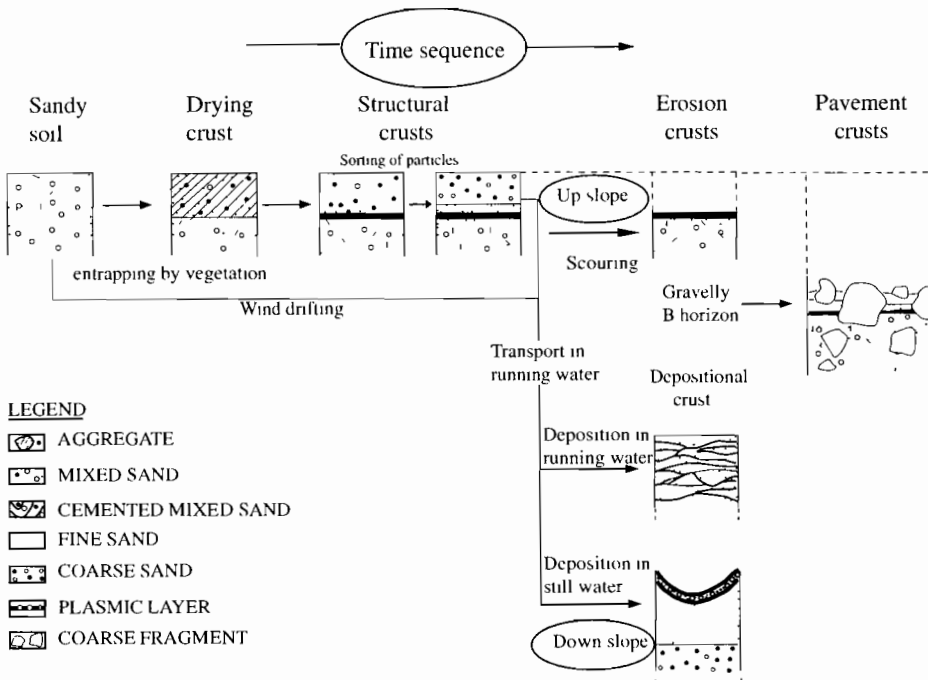

Fig. 1 Diagrammatic representation of the time sequence of soil crust formation (modified from Bresson and Valentin, 1990)

trating essential elements, such as nitrogen, which is fixed by cyanobacteria (Harper and Pendleton, 1993).

Microbiotic soil crusts commonly occur in association with physical soil crusts, which can be divided into three main groups on the basis of their mechanisms of formation: (i) structural crusts (Fig. 1), formed in situ by water drop impact; (ii) depositional crusts (Fig. 1), formed by deposition of particles transported by water from their original location; and (iii) erosion crusts (Fig. 1), formed by water or wind erosion of the two former crusts.

In the Sahelian zone of Niger, physical crusts comprise mainly sieving crusts, runoff crusts, still water depositional crusts and erosion crusts. Sieving crusts are structural crusts formed from two or three layers of sorted material (Fig. 1). The two-layered type is composed of a superficial layer of loose, coarse to medium sand overlying a plasmic (silt and clay) layer. The three-layered type comprises a top layer of loose coarse sand, a middle layer of fine sand, and a thin plasmic bottom layer. Pavement crusts (Fig. 1) are sieving crusts containing pebbles and gravels. Runoff crusts (Fig. 1) are very compact depositional crusts formed by deposition of particles transported by water. They exhibit submillimetric micro-layers, which are alternately coarse and fine. Still water depositional crusts (Fig. 1), also named sedimentation crusts, are formed by the deposition of particles in still water. They consist of densely packed and well-sorted particles, the size of which gradually increases with depth. The superficial layer is usually clay-rich and breaks into curled-up plates during periods of desiccation. Erosion crusts (Fig. 1) consist of a thin, smooth, clay-rich surface layer left after erosion of an overlying sand layer.

In this paper, we report detailed micromorphological observations on microbiotic crusts in the 'tiger bush' landscape near the village of Banizoumbou, in western Niger, in the Sahelian region of west Africa. The roles of these crusts in soil stabilisation and the water regime of the Sahelian environment are discussed.

2. Site descriptions, materials and methods

2.1. Site descriptions

Banizoumbou is about 70 km north-east of Niamey, the capital city of Niger. The study site lies between 13°32′N and 2°42″E, on a plateau formed by Tertiary fluvio-lacustrine deposits ('Continental terminal'; Greigert, 1966). The plateau, which is dissected in several parts by erosion, exhibits a slight slope of a maximum of 1% (Ambouta, 1997). A thick ferruginous duricrust caps the summit of the plateau (Fig. 2a), and underlies a 35–60 cm thick soil.

The climate is typical of the southern Sahel, with an annual rainfall of about 560 mm, occurring from mid-May to mid-September. Mean minimum and maximum temperatures are 22° and 34°C, respectively.

The vegetation of the plateau shows a characteristic pattern consisting of alternating densely vegetated bands comprising small trees and shrubs (Fig. 2a, arrows) and bare soil bands. From the air the resulting landscape resembles a tiger's fur (Fig. 2a), and is called 'tiger bush'. Examination of the vegetation banding reveals two distinct regions in
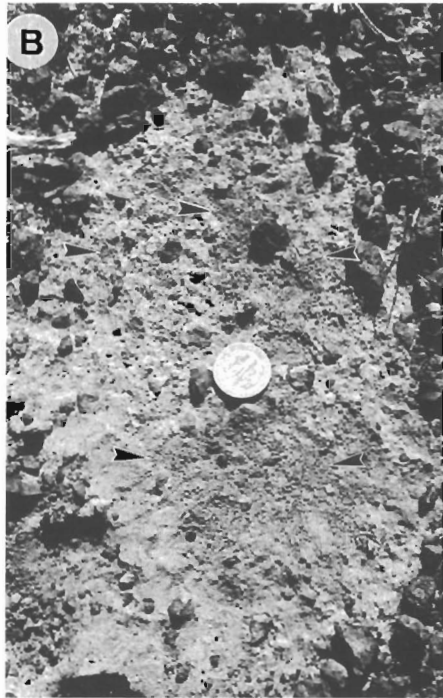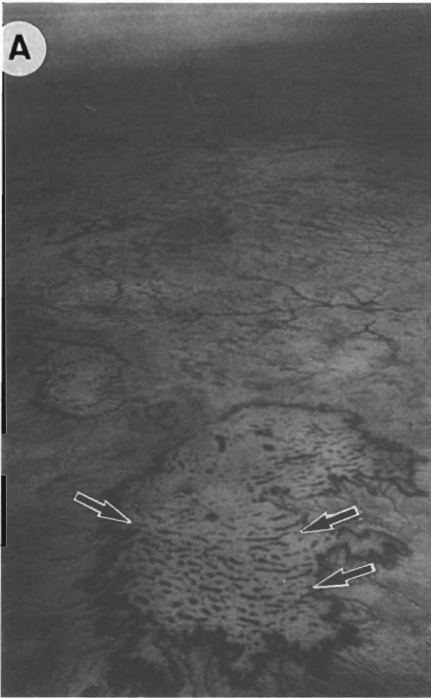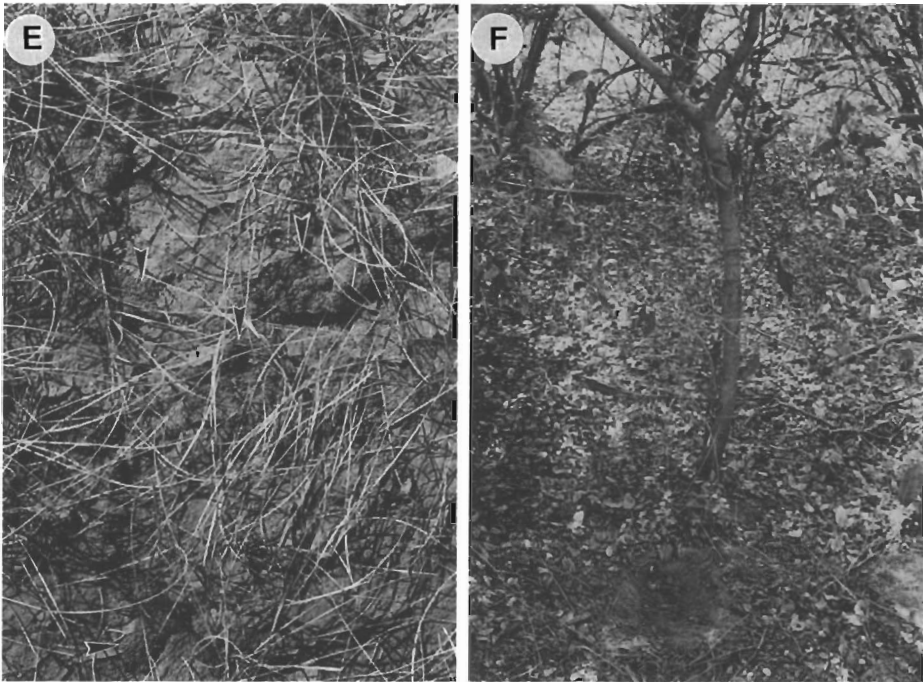
Fig. 2. Views of the sites studied. (a) Aerial view of the tiger bush landscape in western Niger on the top of a dissected plateau. Note the subparallel vegetation bands (arrowed), and the dark section of the ferruginous duricrust at the top of the cliff, approximately 15–20 m high, delimiting part of the plateau. (b–f) Views of the soil surface in the sites studied. (b) Site 1: The coarse superficial material was swept away to show the underlying fine sand layer, and vesicular pores (arrowed) at the surface of the third, plasmic layer. The superficial coarse material is visible at the top, the right, and the bottom right corner of the photograph. (c) Site 2: Darker areas correspond to patches of microbiotic crust. Lighter parts are erosion crusts. (d) Site 3: Polygonal cracking of microbiotic crust on sedimentation crust, and rare herbaceous plants. (e) Site 4: Polygonal cracking of microbiotic crust on a sedimentation crust, showing the dense herbaceous cover, and soil reworked by termites (arrowed). Scale bar is 7.5 cm. (f) Site 5: The soil is covered by a continuous litter layer.

each band (Fig. 3): a decaying section on the lower side, and a flourishing part on its upper side. This pattern is thought to be controlled by the downward movement of water (Ambouta, 1984; Cornet et al., 1992). The lower side of a band loses water, which is trapped by the upper section of the adjacent downslope band. This results in a gradual movement of the vegetated bands in an upslope direction at a rate of about 25 cm yr^{-1} (Thiéry et al., 1995; d'Herbès et al., 1997).

2.2. Crust sampling

Samples of soil crust approximately 7 cm thick were collected from each site (Fig. 3) in November 1994, at the beginning of the dry season. Five types of soil surface were
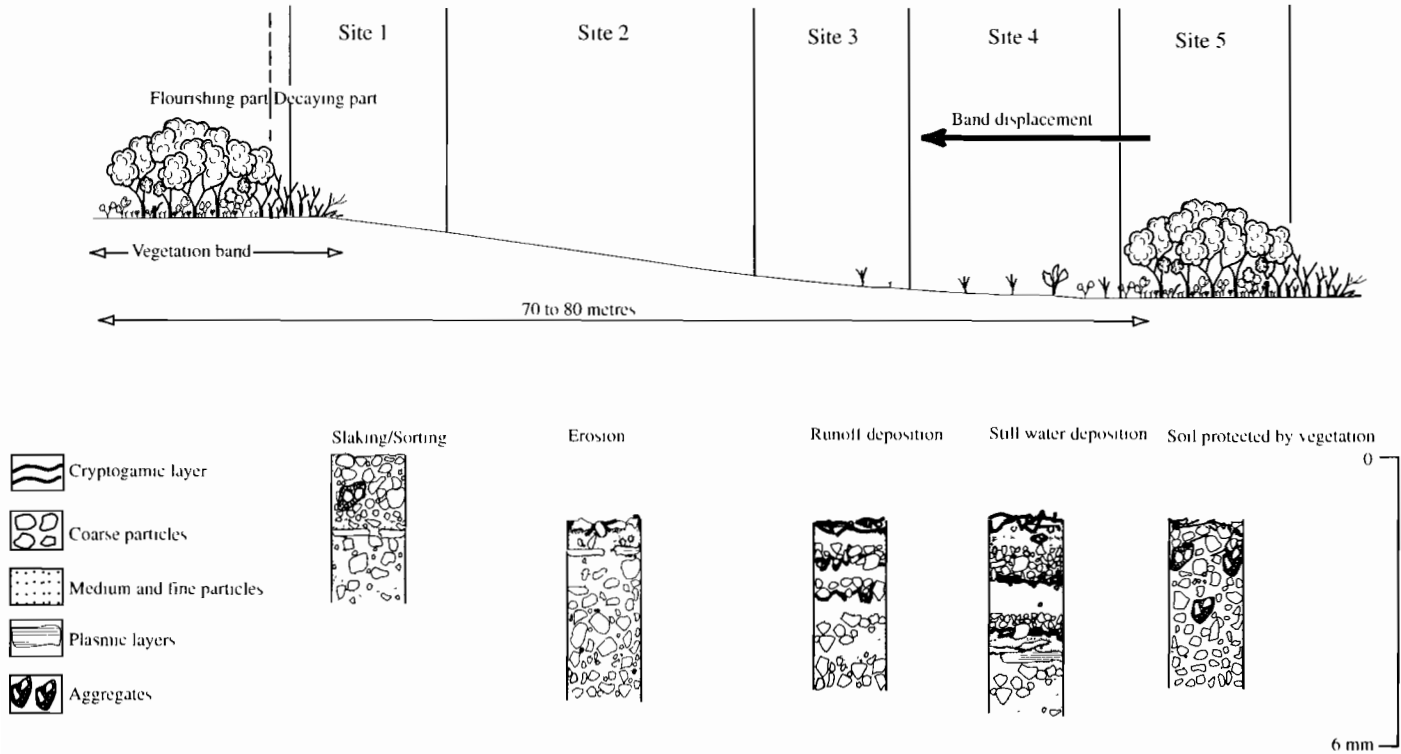
Fig. 3. Lateral and vertical patterns of a tiger bush soil sequence.

distinguished along the slope, from the decaying part of a vegetative band to the flourishing part of the next lower vegetative band (Fig. 3).

(1) Site 1 (Fig. 2b): close to the decaying section of the band, the soil surface was a sieving crust devoid of any microbial cover. Vesicular pores formed as air bubbles were recognisable when unconsolidated coarse superficial material was swept out.

(2) Site 2 (Fig. 2c): the soil surface was an erosion crust partly capped by microbiotic crust patches.

(3) Site 3 (Fig. 2d): the soil surface was a microbiotic crust capping a still water deposition crust. Scattered herbaceous plants were present at this site.

(4) Site 4 (Fig. 2e): the soil surface was similar to that at site 3, but the grass vegetation was denser. Emerging holes of termite galleries were frequently observed.

(5) Site 5 (Fig. 2f): the soil surface under the flourishing part of the lower band was covered by a permanent litter of dead tree leaves and herbaceous plants. Scattered mosses were observed.

One sample was collected from each of the five sites. Those from sites 2 to 5 were divided into four subsamples for particle size distribution and chemical analyses. The first subsamples were the superficial organo-mineral layers, ca. 2 mm thick, which comprised most the living micro-organisms of the crusts. The other three subsamples were taken at 10–20 mm intervals according to visible soil layering.

Table 1

Particle-size distribution, pH and total organic carbon content of the soils studied (values other than pH are dry weight percentages)

Sites	Physical crust type	Depth (mm)	Particle size distribution			pH	Total organic carbon (%)
			Sand (%)	Silt (%)	Clay (%)		
Site 1	Sieving	0–10	–	–	–		0.5
		10–15	71.0	21.0	13.5	6.4	0 6
Site 2	Erosion	0–2	57.2	34.1	12 2	6.3	0.9
		2–35	59.1	30.0	11.3	6.5	0.3
		35–55	62.7	27.7	12 2	6.5	0.3
		55–75	53.0	26.1	12.2	6.4	0.4
Site 3	Runoff deposition	0–2	54 2	29.4	13.8	5.9	1.8
		2–10	64.3	20.3	10.7	5 4	0.4
		10–20	64.5	24.8	10.0	5.0	0.3
		20–30	64.0	18.4	14.1	5.0	0 3
Site 4	Still water deposition	0–2	70.4	24.0	4.9	6.1	1.9
		2–12	59.5	34.3	7.2	5.8	0.7
		12–22	51.6	32.8	13.3	6.1	0.5
		22–42	54.9	31.8	13.4	6.1	0.4
Site 5	No crust	0–2	60.5	37.4	3.8	5.8	1.4
		2–17	64.6	20.6	11.5	5.5	0.7
		17–37	70.2	18.9	13.1	4.7	0 7
		37–57	72.6	17.5	13.5	5.5	0.7

Table 2
Micro-organisms observed in the sites studied (no micro-organism was observed at site 1)

	Taxons	Site 2: erosion crust	Site 3: runoff deposition crust	Site 4: still water deposition crust	Site 5: no crust
Cyanobacteria	*Chroococcus limneticus* Lemm.	+	−	−	−
	Lyngbya aerugineo-coerulea (Kütz.) Gomont	−	−	+	−
	L. aestuarii Liebman	−	−	−	+
	L. epiphytica Hieron	−	−	−	+
	Microcoleus sociatus W and G.S. West	−	+	−	+
	Nostoc Vaucher sp.	−	+	−	−
	Phormidium mucosum Gardner	−	+	−	−
	Schizothrix friesii (Ag.) Gomont	+	+	+	+
	S. penicillata (Kütz.) Gomont	+	+	+	−
	Scytonema javanicum Bornet	−	+	−	−
	Scy. stuposum (Kütz.) Bornet	−	+	−	−
Chlorophyta	*Desmococcus olivaceus* (Pers. ex Arch.) Laundon	+	−	−	−
	Actinotaenium cucurbita fo. rotundatum (Krieg.) Teiling	−	−	−	+

+ = Presence.
* = Heterocystous species.

2.3. Methods

Observations of soil surfaces were made at two scales, on a Nachet NS 50 stereomicroscope and on a JEOL JSM 6400 Scanning Electron Microscope (SEM). For SEM observations samples were coated with gold–palladium. Vertical thin sections were examined on a Zeiss Universal light microscope and on SEM. For SEM observations the sections were coated with carbon. Micro-organisms were collected from remoistened samples with a pipette under the stereomicroscope. Particle-size distributions were determined by dry sieving of sand particles and sedimentation of finer particles (pipette method). pH was measured with a 691 Metrohm pH meter on samples dispersed in water for 24 h. Total organic carbon (TOC) was measured with a CNS-2000 Leco analyser.

Fig. 4. Views of the soil surface under a stereomicroscope. (a) Site 1: Note the absence of any living organism or organic material, and the pore probably resulting from insect activity (arrowed) (scale bar is 0.5 mm). (b) Site 2: Small globular colonies of cyanobacteria (*C. limneticus* Näg.; G), larger, cupular chlorophyta (*Desmococcus* Brand; C), and filamentous cyanobacteria (*Schizothrix* Kütz.; F) (scale bar is 0.5 mm). (c) Site 4: Note the network of cyanobacterial filaments (F) (scale bar is 0.1 mm). (d) Site 5: Mosses on the surface of litter. Scale bar is 0.5 mm.
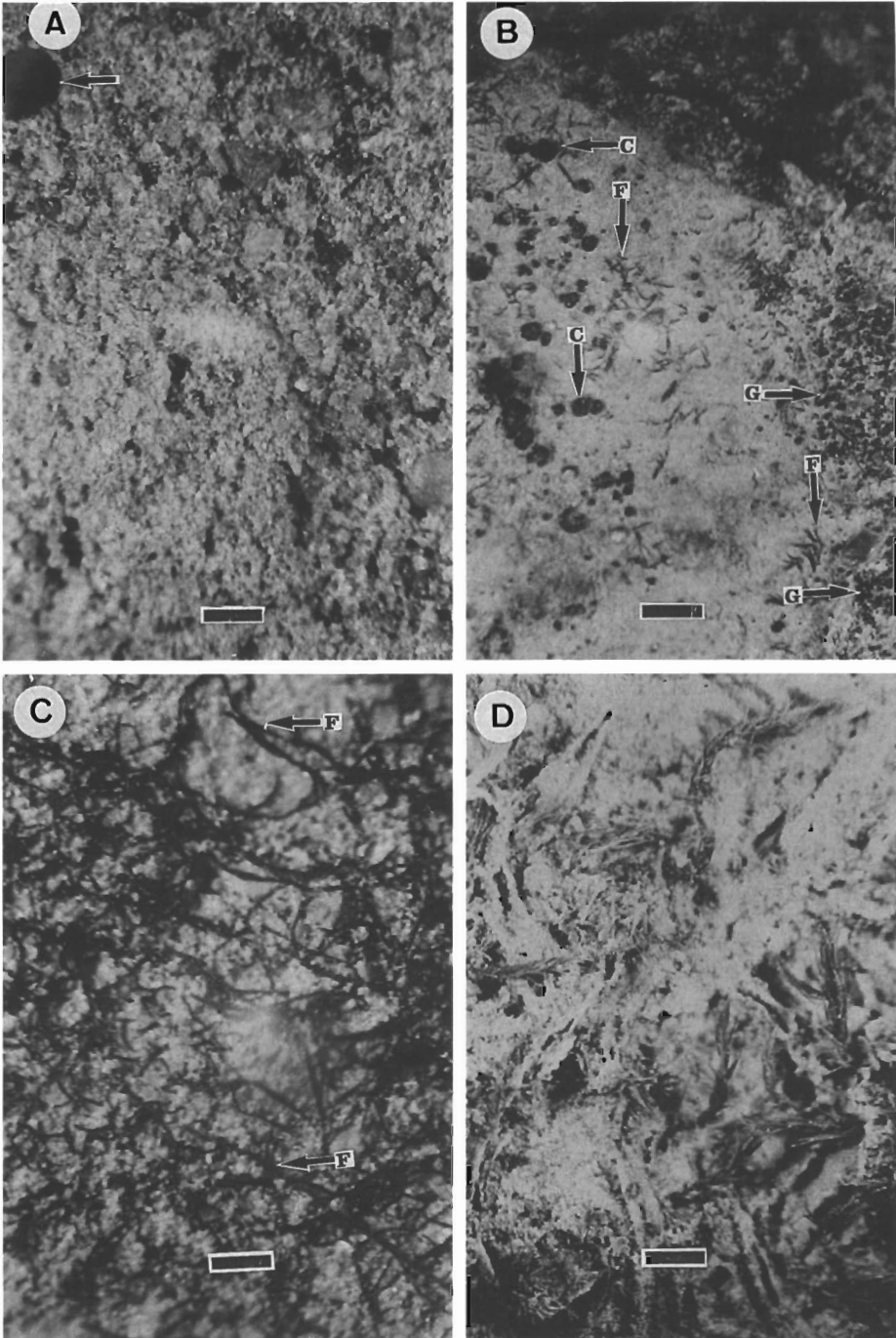
3. Results

3.1. Physical and chemical analyses

All sites had similar textures (sandy loam) and pH (4.7 to 6.5) values (Table 1). TOC content shows differences between sites, in particular in the superficial layers (Table 1). Superficial samples with a microbial cover (sites 2–4) were richer in TOC (0.9 to 1.9% dry weight) than the bare sample (0.5% at site 1). Densely microbially-covered samples (sites 3 and 4) were richer in TOC (1.8–1.9%) than the litter-covered sample (1.4% in site 5). Except for the sieving crust (site 1), the TOC content of deep samples was less than the superficial layers (Table 1). At depth, microbially-covered soils (sites 2–4) had less TOC (0.3 to 0.7%) than the litter-covered soil (site 5: 0.7%) or the sieving crust (site 1: 0.6%). Among microbially-covered soils, site 4, which supported a dense herbaceous cover, was richer in TOC (0.4–0.7%) at depth than sites 2 and 3 (0.3–0.4%).

3.2. Determination of micro-organisms

Micro-organisms present in the tiger bush samples belonged to two taxonomical groups: cyanobacteria and chlorophyta (Table 2). Cyanobacteria were dominant at all sites, but Chlorophyta (two species) were present only in two sites. Eleven species of cyanobacteria were identified (Table 2). All are filamentous except *C. limneticus*. Three species are heterocystous. *Schizothrix* is the most abundant genus at all sites. The communities forming microbiotic crusts (sites 2–4) were not fundamentally different from those present in the vegetated band of the tiger bush (site 5 in Table 2). The maximum diversity of species was observed at site 3.

3.3. Surface micromorphology

3.3.1. Site 1

Microscopic observations confirmed the absence of micro-organisms at this site. The material is composed essentially of rounded quartz grains, ca. 500 μm in mean diameter, accompanied by rare coarser sand grains (Fig. 4a). Pores probably resulting from insect activity were observed (Fig. 4a).

3.3.2. Site 2

Stereomicroscopic observations of microbiotic crust patches revealed the presence of three different microbial colonies.

(1) Black, globular organisms, approximately 10 μm in diameter when isolated, and 250 μm when associated (Fig. 4b). These were identified as cyanobacteria of the species *C. limneticus* (Table 2).

Fig. 5. SEM micrographs of the soil surface. (a) Site 2: Intertwining of filaments, which trap sand grains. Fine mineral particles stick onto the surfaces of filaments (arrowed). (b) Site 3: Network of filaments enmeshing sand grains and finer mineral particles. (c) Site 4: Contact between a filament and a sand grain. Note the filament print on the grain surface. Fine particles (arrowed) adhere to the filament surface. (d) Site 4: Filaments delineating superficial pores. Fine mineral particles adhere to the surfaces of filaments (arrowed) Bar is 10 μm
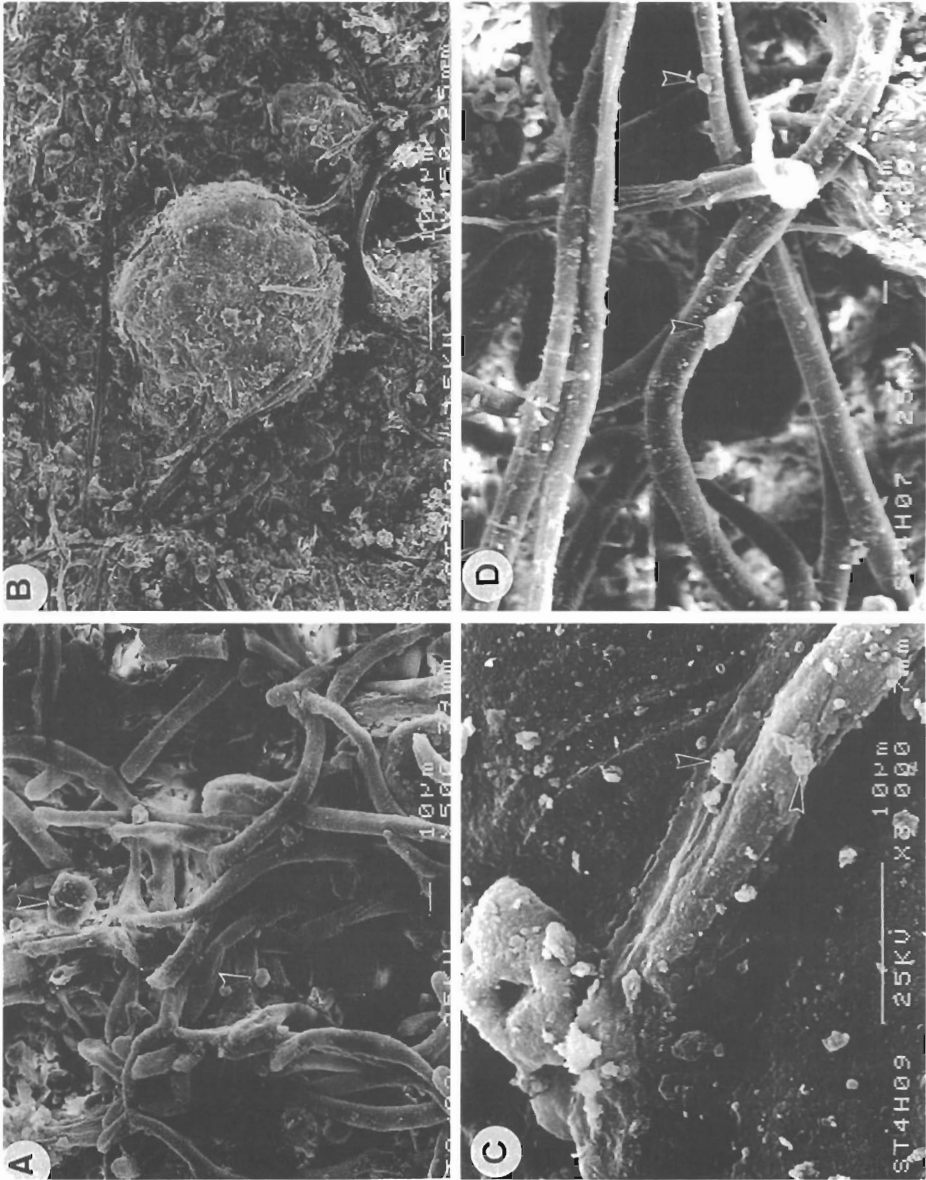
(2) Black or reddish, filamentous organisms, 10 to 25 μm in diameter (Fig. 4b), belonging to two species of the cyanobacterial genus *Schizothrix* (Table 2).

(3) Greenish, cupular-shaped organisms, 250 to 400 μm in diameter (Fig. 4b), identified as chlorophyta belonging to the genus *Desmococcus* (Table 2).

Under SEM the *Schizothrix* filaments appeared to form a superficial network delineating pores, several tens of micrometres in diameter (Fig. 5a). Sand particles were trapped in this network, whereas finer mineral particles adhered to the surface of filaments (Fig. 5a).

3.3.3. Sites 3 and 4

Under the stereomicroscope there was no significant micromorphological difference between sites 3 and 4, except that the density of micro-organisms was greater at site 4. The surface of crusts appeared to be formed by a network of black or reddish filaments, 10 to 25 μm in diameter (Fig. 4c). Some filaments formed pinnacles rising above the flat surface of the crust. Under SEM the filaments appeared, as at site 2, to trap sand particles and to have finer (< 5 μm) mineral particles adhering (Fig. 5b–c). The filaments delineated characteristic superficial pores, several tens of micrometres in diameter (Fig. 5d). Filament prints were observed on the surface of sand grains (Fig. 5c). Scattered liverworts were present at site 4.

3.3.4. Site 5

At the stereomicroscope scale, the soil surface appeared to be covered by debris of higher plants, mainly tree leaves. Mosses were especially abundant (Fig. 4d) and liverworts were also present. Rare very thin, colourless filamentous micro to organisms were observed in association with rare globular micro-organisms, 100–150 μm in diameter. SEM observations indicated the presence of two species of diatoms.

3.4. Vertical cross-section observations

3.4.1. Site 1

Two different layers were distinguished at this site (Fig. 6a): a superficial layer, 0.5–1.5 mm thick, which contained sand with rare disrupted soil aggregates, and an underlying layer, > 4 cm thick, which contained consolidated clay-rich material with

Fig. 6. Photomicrographs of vertical thin sections of soils. Scale bars are 160 μm. (a) Site 1. Sieving crust. Superficial layer of fine sand with disrupted aggregates (A) and clogged pores (arrowed), on a clay rich layer with laminated void coatings (L). The soil surface (upper right) is devoid of organisms. (b) Site 2: Erosion crust. The superficial plasmic layer exhibits laminated clay coatings (L) and rounded to vesicular pores (V). The underlying layer is formed by mixed material and exhibits polyconcave pores (V). (c) Site 2: Area covered with a discontinuous layer of living organisms (arrowed). The plasmic layer is thinner than in bare areas of the same site (b). (d) Site 3: Runoff deposition crust capped by a continuous superficial layer of living filamentous micro-organisms (F). The profile shows alternation of submillimetric sand and clay layers, and non-connected vesicular pores (V). Ancient microbiotic crusts (C) can be recognised at depth. (e) Site 4: Still water deposition crust capped by a continuous layer of living filamentous micro-organisms (F). The profile shows alternating clay and sand layers, which are thicker and better sorted than at site 3. Superficial layers include disrupted aggregates (A). Ancient microbiotic crusts (C) are seen at depth. (f) Site 4: Polygonal cracking (arrowed) of the superficial microbiotic crust. (g) Site 5: Superficial litter layer on non-layered mixed soil material.
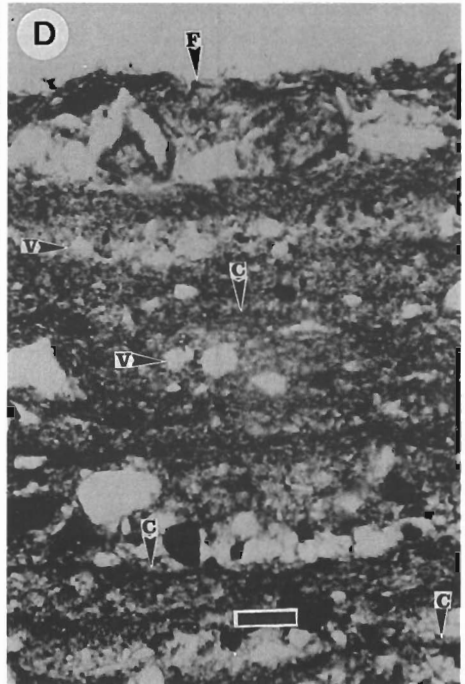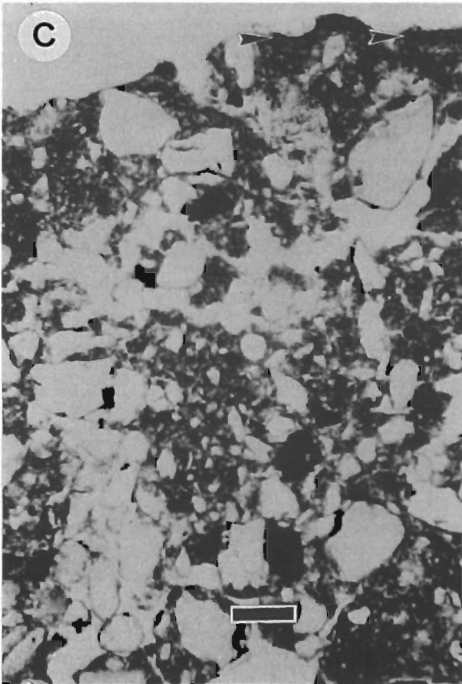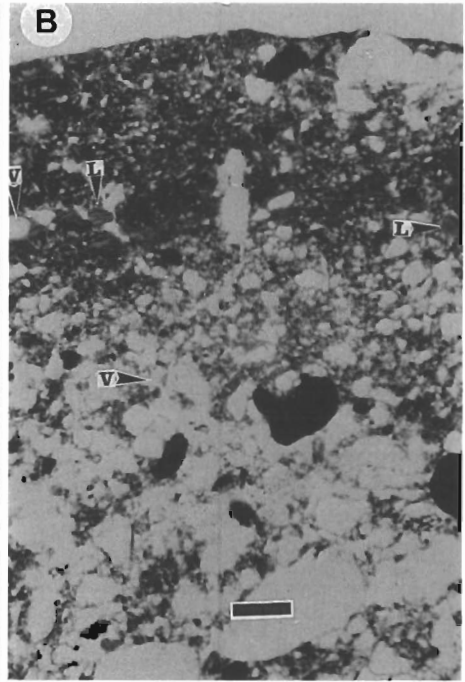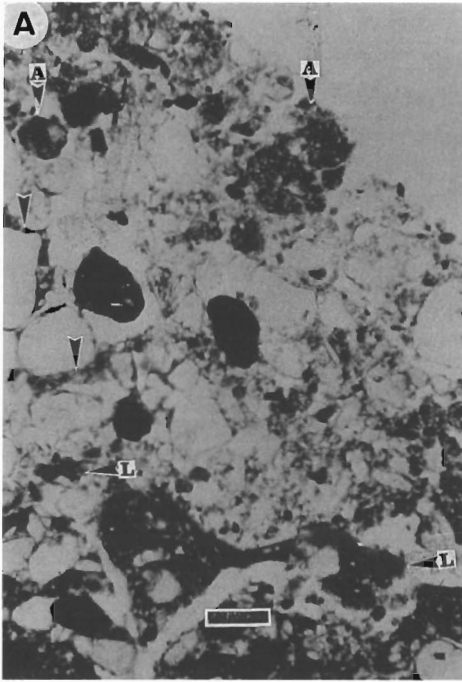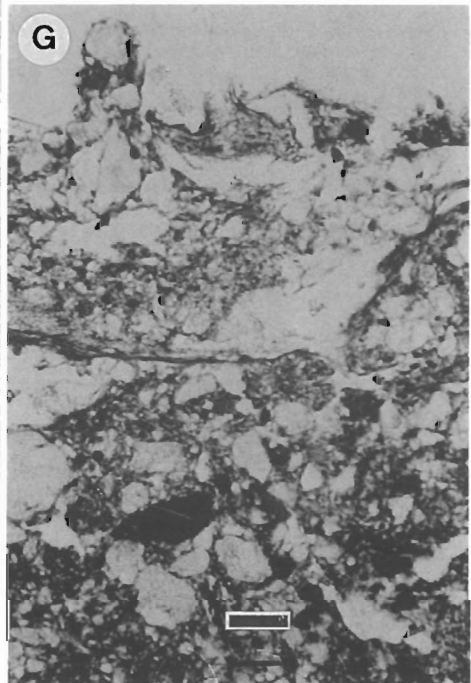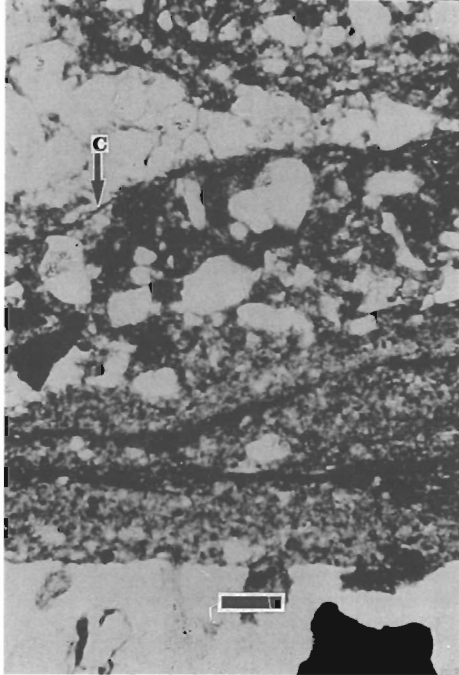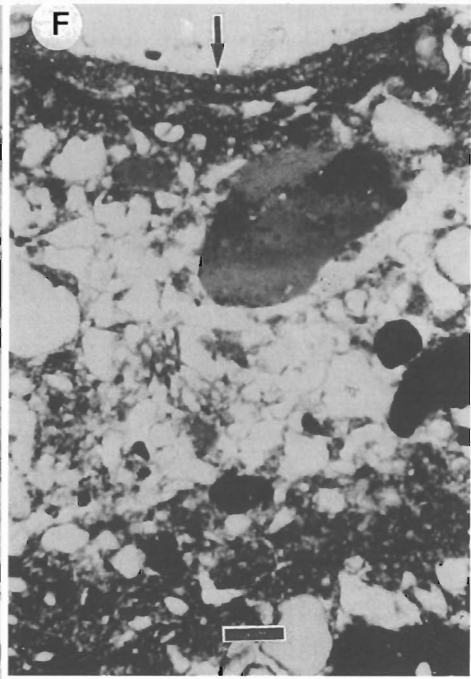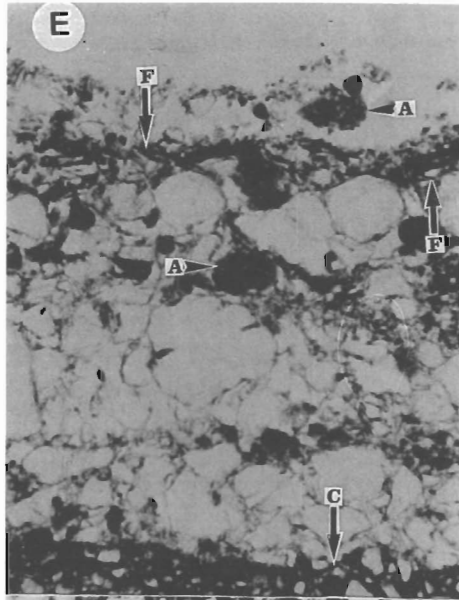
rare sand grains. The porosities of the two layers were different (Fig. 6a): pores in the top layer were partially clogged by plasmic material, but in the underlying layer they exhibited laminated clay coatings, probably resulting from illuviation. The two layers correspond, respectively, to the medium layer of fine sand and the bottom layer of fine particles of a sieving crust (Fig. 1).

3.4.2. Site 2

In the areas devoid of microbial cover, two layers were distinguished (Fig. 6b): a superficial layer, 0.8–1.5 mm thick, formed from plasmic material with rare sand grains, and an underlying layer, several centimetres thick, formed from mixed material. The plasmic layer was smooth and rigid and resulted from clay illuviation, as indicated by the abundance of laminated coatings (Fig. 6b). Pores were rounded to vesicular because of compaction, and partially clogged by clay washed from the soil surface. These features are characteristic of erosion crusts (Fig. 1). The lower layer contained mixed, non-sorted material, which consisted mostly of mixed sand, clay in intergrain spaces and non-living organic material (Fig. 6b).

In the areas covered with a microbiotic crust (Fig. 6c), the plasmic layer was thinner (0.1–0.2 mm thick), more structured, and contained more sand grains and non-living organic material than in bare areas (Fig. 6b). The boundary with the underlying layer of mixed material was diffuse. Pores were tubular and interconnected. Under SEM, the organic constituents of this layer, in particular the filaments, appeared to surround and bind soil particles into a coherent network (Fig. 7a,b). Organic bodies with a porous structure and comprising micron-sized spheres were frequently observed (Fig. 7a,c). X-ray microanalysis of the organic constituents revealed detectable amounts of Cl, K and Na, in addition to C.

3.4.3. Site 3

The soil profile exhibited alternating clay- and sand-rich layers (Fig. 6d) characteristic of runoff deposition crusts (Fig. 1). The soil can be subdivided into rhythmic units of variable thickness (0.2–0.4 mm), composed of a layer of sand overlying a thin layer of clay (Fig. 6d). Pores were rounded to vesicular because of compaction (Fig. 6d). The superficial microbiotic crust comprising filamentous cyanobacteria was formed at the surface of a clay layer (Fig. 6d). Ancient microbiotic crusts were recognised at depth as black organic laminae overlying clay layers (Fig. 6d). Filaments and porous organic bodies similar to those at site 2 (Fig. 7a,c) were also observed by SEM in this site, below the superficial layer of living cyanobacteria. X-ray microanalysis again indicated detectable amounts of Cl, K and Na in the organic material.

3.4.4. Site 4

As at site 3, the soil exhibited alternating layers of clay and sand (Fig. 6e). The microbiotic crust, 0.7 mm thick and made of filamentous cyanobacteria, was formed at the surface of a clay layer ca. 0.1 mm thick (Fig. 6e). Superficial polygonal cracking was observed with the light microscope (Fig. 6f). Filaments and porous organic bodies, similar to those present at sites 2 (Fig. 7a,c) and 3, were observed at depth, also with the same enrichment in Cl, K and Na.
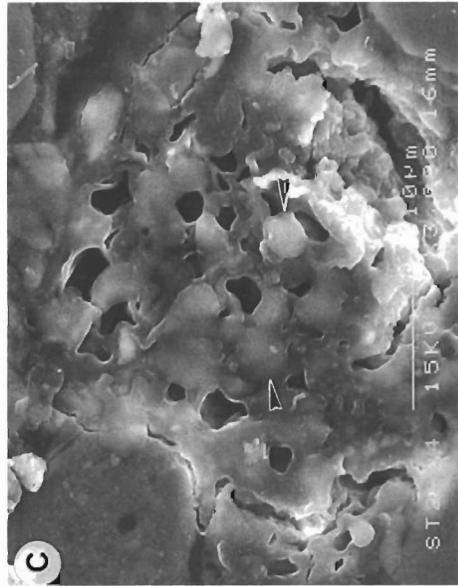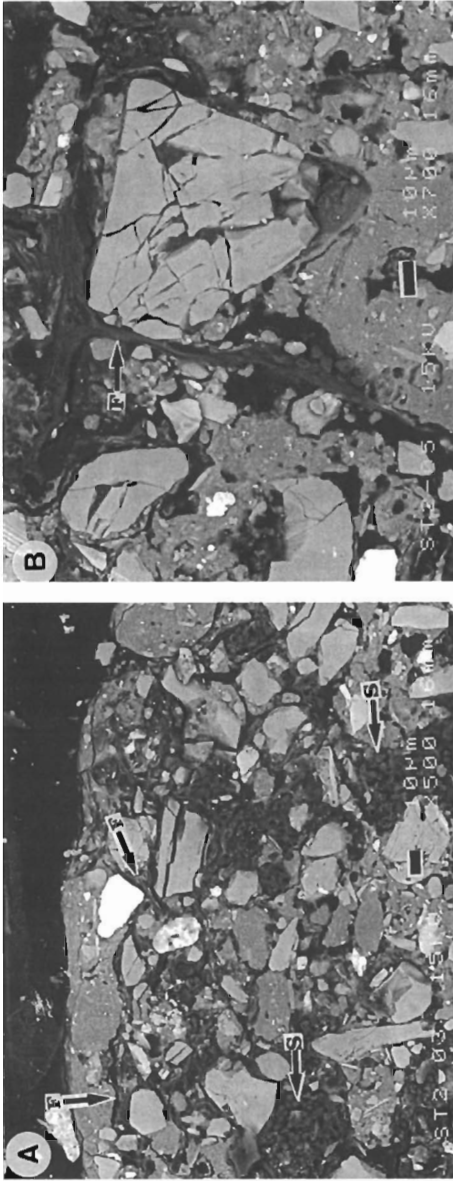
Below the microbiotic crust, the soil profile was composed of two successive units (Fig. 6e): in the upper unit ca. 3 mm thick, the clay and sand layers were thicker (0.6–1 mm) and better sorted than at site 3, whereas the microstructure of the lower unit was closer to that at site 3. In the clay layers of the upper unit the clay was usually associated with non-living organic matter at the top, but was mixed with silt and sand particles at the bottom (Fig. 6e). The features of the upper unit are characteristic of a still water deposition crust. As at site 3, ancient microbiotic crusts were recognised at depth (Fig. 6e).

3.4.5. Site 5

Two different layers were distinguished at this site (Fig. 6g): a superficial, discontinuous layer, ca. 1 mm thick consisting of mixed higher plant debris, sand grains, and finer mineral particles and an underlying layer consisting of material of various sizes disturbed by vegetation growth.

4. Discussion

4.1. Biological composition

As observed by others, the microbiotic crusts we studied were formed by microbial communities dominated by cyanobacteria. However, they differed from most other crusts in that the prevalent genus was *Schizothrix* (Table 2). Other microbiotic crusts are dominated by *Scytonema* sp. in the N'Djamena region, Tchad (Dulieu et al., 1977) and in savanna zones of Nigeria (Isichei, 1980), by *M. sociatus* in the western Negev Desert, Israel (Lange et al., 1992) and by *Microcoleus* spp. in desert soil crusts in Idaho, Utah and Colorado (Brock, 1975; Campbell, 1979). In semi-arid and arid lands of North America, the most widespread species of cyanobacteria is *M. vaginatus*. (Vauch.) Gom. Only in hot desert regions have microbiotic crusts been hitherto reported to consist mainly of *Schizothrix* (Johansen, 1993). Chlorophyta and liverworts are also common components of the microbiotic crusts in the tiger bush.

4.2. Soil stabilisation

Micro-organisms and mineral grains are closely associated at the surface of the tiger bush microbiotic crusts. The network of filamentous cyanobacteria traps sand grains, and clay and silt sized particles adhere to the surfaces of filaments (Figs. 4c and 5a,b,d). This has already been noted in other microbiotic crusts by Cameron and Devaney (1970) and Belnap and Gardner (1993). The ability of cyanobacterial filaments to cement

---

Fig. 7. SEM micrographs (backscattered electron mode) of a vertical thin section at site 2. (a) Cyanobacterial filaments (F) and dark organic bodies enmesh mineral grains. Some organic bodies appear to be micron-sized spheres (S). (b) Enlarged view of an area in (a), showing cyanobacterial filaments (F) surrounding mineral grains. (c) Enlarged view of a dark organic body in (a). Note the porous structure of the organic matter and the presence of microspheres (arrowed).

mineral particles to the surface of their polysaccharide envelopes is well known (Pentecost and Riding, 1986). Filament prints on the surface of mineral grains (Fig. 5c) suggest slight dissolution of the mineral at the contact with the filament.

Below the superficial layer of living cyanobacteria intermingled with mineral grains, filaments and organic bodies also appear to enmesh soil mineral particles (Figs. 6d,e and 7a,b). The porous organic bodies presumably derive from extracellular polymer secretions (EPS) of micro-organisms. Cyanobacteria and other bacteria commonly produce polysaccharide EPS which reorganize into three-dimensional networks (Défarge et al., 1996). The role of EPS in soil aggregate stabilisation has already been mentioned by Tisdall and Oades (1982). In the tiger bush soils this organic matter could be produced by the filamentous cyanobacteria or the microspheres (bacteria?) associated with the porous bodies (Fig. 7a,c).

The micro-organisms which form tiger bush microbiotic crusts thus provide cohesion to the soil through the trapping and binding effects of superficial living filaments and of microbial organic material present at depth. This cohesion enhances soil stabilisation against water and wind erosion, as was confirmed by placing bare soil samples from site 1 in water; they were completely dispersed after two days, whereas microbiotic crust samples from sites 2 to 4 remained intact after several months of immersion. In situ measurements made at other sites near Banizoumbou have shown that fewer mineral particles are removed from microbially-covered soils compared with bare soils (Malam Issa et al., 1998). These results agree with other studies, which have shown less erosion of soils covered by microbiotic crusts (Eldridge and Greene, 1994; McKenna Neuman et al., 1996; Eldridge and Kinnell, 1997).

At sites 3 and 4, the depositional crusts were interlayered at depth with ancient microbiotic crusts (Fig. 6d,e). In addition to their role in stabilisation of underlying soil, microbiotic crusts are thus probably involved in mineral particle retention and deposition on their surface, and therefore in soil accretion. Cyanobacterial mats, including *Schizothrix*-dominated mats, have been shown to control underwater particle sedimentation in shallow subtidal and intertidal marine areas (Neumann et al., 1970). In the depositional sites of the tiger bush, soil accretion occurs through a rhythmic aggradation of layers, alternately organic and mineral. The resulting structure is sedimentary rather than pedogenetic, and may be considered as a terrestrial stromatolite. Similarities between certain microbiotic soil crusts and stromatolites were noted by Campbell (1979).

4.3. Soil–water interactions

Microscopic observations of tiger bush samples revealed two features which may influence the water regime of the soil: (1) intertwining of the filamentous organisms at the soil surface delineates pores of significant sizes (Fig. 5a,d), which could favour water infiltration; (2) the presence of porous organic bodies at depth (Fig. 7a,c), which enhances the water retention capacity of the soil.

When wetted, two possible kinds of behaviour can be expected from the polysaccharide constituents of cyanobacterial envelopes and of spongy organic bodies: (1) swelling resulting from absorption of water by the polysaccharide constituents is limited and the

pore field allows water circulation, or (2) swelling reduces the pore size and enhances water retention by capillary forces. According to Verrecchia et al. (1995), the absorption of water by biological material and the retention of water by strong capillary forces are the ways in which microbiotic crusts limit water infiltration and promote runoff when rain starts.

The influence on the water regime of other organisms such as termites, which were conspicuous at site 4 (Fig. 2e), should also be considered. The foraging activity of these organisms has been shown to enhance water infiltration (Ouedraogo, 1997).

Further studies are necessary to determine the interactions of tiger bush microbiotic crusts and water. Laboratory measurements have indicated that microbial crusts enhance the water retention capacity of Sahelian soils similar to those of the tiger bush. At pF 2.5, water retention was 6.8–36% for microbially-covered samples but only 2.1–3.8% for bare samples (Malam Issa, unpubl. data).

4.4. Chemical composition

The presence of photosynthetic micro-organisms may account for the organic C enrichment of the surface layer of microbiotic crusts compared with bare and litter-covered soils (Table 1). The phototrophs fix atmospheric CO_2 at rates estimated by Beymer and Klopatek (1991) for microbiotic crusts in Pinyon-Juniper woodlands (Northern Arizona, USA) to range from 43 (grazed soil) to 350 kg C ha^{-1} yr^{-1} (ungrazed soil). A sample from site 4 of Banizoumbou tiger bush has been shown to fix 4.3–5.3 mg C m^{-2} mn^{-1} under laboratory conditions (Malam Issa, unpubl. data).

The supply of nitrogen in microbiotic crusts is mainly from cyanobacteria and lichens (Mayland et al., 1966; Jeffries et al., 1992). Nitrogen fixation in crusts can vary from 1 to 100 kg N_2 ha^{-1} yr^{-1} (Jeffries et al., 1992). In the tiger bush soils, which do not support lichens, nitrogen should be fixed mainly by the heterocystous cyanobacterial species *Nostoc* sp., *Scy. javanicum* and *Scy. stuposum* (Table 2). Some other species of cyanobacteria devoid of heterocysts are also able to fix nitrogen (Stal, 1995; Bergman et al., 1997).

4.5. Microbiotic crusts in tiger bush dynamics

The microscopic features of the tiger bush sequence revealed a specific organization of the soil between successive vegetated bands (Fig. 3). From the decaying part of the upper band down to the flourishing part of the lower band, the soil surface consists successively of a sieving crust (site 1), an erosion crust (site 2), a runoff sedimentation crust (site 3) and a still water deposition crust (site 4). In site 4, the still water deposition crust caps an ancient runoff deposition crust analogous to that at site 3 (Fig. 3). The superficial layer of the crust at site 2 corresponds to the lower, plasmic layer of the sieving crust at site 1 (compare Fig. 6a and b). The erosion crust at site 2 probably results from the evolution of a sieving crust (Fig. 3). Deposition of particles translocated from sites 1 and 2 induces the formation of depositional crusts at sites 3 and 4 (Fig. 3). These observations confirm the dynamic model of Bresson and Valentin (1990). The

downward movement of water which controls the formation of the tiger bush landscape is also responsible for the organisation of soil between the vegetated bands.

The cyclic evolution which results from the upslope migration of vegetated bands also affects the soil crusts. Vegetation decay at site 5 creates a bare soil which will evolve into a structural crust (site 1 type). The structural crust will be replaced by an erosion crust (site 2 type), then by a depositional crust (site 3 and site 4 types) supplied by particles translocated from structural and erosion crusts formed above. The depositional crust will be progressively invaded by the upslope migrating vegetation and thus become a site 5 type soil.

The microbiotic crusts are essential components of the tiger bush ecosystem. The zonation of microbiotic crusts is parallel to the tiger bush banding (Fig. 3). Site 1 is devoid of any microbial cover. The density of microbial cover increases from site 2 to site 4, and the microbial communities present at site 5 are close to those forming microbiotic crusts at sites 2 to 4 (Table 2). The most extensive development of microbiotic crusts is associated with temporary accumulations of water at site 4. The microbial cover enhances stabilisation of depositional crusts and promotes retention of sand and clay particles on their surface. The continuous aggradation of mineral layers, whose surface is recolonised by micro-organisms after deposition, results in soil accretion at this site. The resulting soil provides a stabilised, well-moistened and nutrient-enriched substrate for the upslope migration of plants from the adjacent vegetated band (site 5). The microbiotic crusts are then destroyed by root and faunal bioturbation which follows the establishment of higher plants.

5. Conclusions

This study has documented further occurrences of microbiotic crusts formed by cyanobacteria, chlorophyta and liverworts on the surface of soils in semi-arid tiger bush woodlands. The results confirm the role of a microbial cover and derived organic matter in microstructure development and stabilisation of the soils.

The microbiotic crusts are essential components of the tiger bush ecosystem. The downward movement of water, which controls the dynamics of the tiger bush landscape, also controls the lateral and vertical successions of crusts in the tiger bush sequence studied. The formation of microbiotic crusts in the lower parts of bare bands helps retain water, resist erosion and accumulate soil. Microbial activity also results in C and N enrichment of superficial soil. The upslope development of trees and shrubs of the vegetated bands takes place on this substrate. The development of microbiotic crusts between the zones with higher plants appears to be a biological adaptation favourable to the preservation of the structure and nutrient level of the soil during periods of denudation.

Microbiotic crusts may thus play a specific role in the conservation and improvement of soil properties in Sahelian regions. Through increase of resistance to erosion, enrichment in essential nutrients, and control on water uptake, they can favour the establishment of farm crops.

Acknowledgements

References

Ambouta, K., 1984. Contribution à l'édaphologie de la brousse tigrée de l'Ouest nigérien. Thèse de Docteur-Ingénieur, Université Nancy I, France, 116 pp.

Ambouta, J.M.K , 1997. Définition et caractérisation des structures de végétation contractée au Sahel: cas de la brousse tigrée de l'ouest nigérien. In: d'Herbès, J.M., Ambouta, J.M.K., Peltier, R. (Eds.), Fonctionnement et Gestion des Écosystèmes Forestiers Contractés Sahéliens. John Libbey Eurotext, Paris, pp. 41–57.

Barbey, C., Couté, A , 1976. Croûtes à cyanophycées sur les dunes du Sahel mauritanien. Bulletin de l'I.F.A.N. 38, sér. A, 732–736.

Belnap, J., Gardner, J.S., 1993. Soil microstructure in soils of the Colorado Plateau: the role of the cyanobacterium *Microcoleus vaginatus*. Great Basin Naturalist 53, 40–47.

Bergman, B., Gallon, J.R., Rai, A.N., Stal, L.J., 1997. N_2 fixation by non-heterocystous cyanobacteria. FEMS Microbiol. Rev. 19, 139–185.

Beymer, R.J., Klopatek, J.M., 1991. Potential contribution of carbon by microphytic crusts in Pinyon-Juniper woodlands. Arid Soil Res. Rehab. 5, 187–198.

Bresson, L.M., Valentin, C., 1990. Comparative micromorphological study of soil crusting in temperate and arid environments. Trans. 14th Int. Congr. Soil Sci., Kyoto, Japan, VII, pp. 238–243.

Brock, T D., 1975. Effect of water potential on a *Microcoleus* (Cyanophyceae) from a desert crust. J. Phycol. 11, 316–320.

Brotherson, J.D., Rushforth, S.R., 1983. Influence of cryptogamic crusts on moisture relationships of soils in Navajo National Monument, Arizona. Great Basin Naturalist 43, 73–78.

Cameron, R.E., Devaney, J.R., 1970. Antarctic soil algal crusts: scanning electron and optical microscope study. Trans. Am. Microsc. Soc. 89, 264–273.

Campbell, S.E., 1979. Soil stabilisation by a prokaryotic desert crust: implications for Precambrian land biota. Origins of Life 9, 335–348.

Campbell, S.E., Seeler, J.S., Golubic, S., 1989. Desert crust formation and soil stabilisation. Arid Soil Res. Rehab 3, 217–228.

Cole, D.N., 1990. Trampling disturbance and recovery of cryptogamic soil crusts in Grand Canyon National Park. Great Basin Naturalist 50, 321–325.

Cornet, A.F., Montana, C., Delhoume, J P, Lopez-Portillo, J., 1992. Water flows and the dynamics of desert vegetation stripes. In: Hansen, A.J., Di Castri, F. (Eds.), Landscape Boundaries. Consequences for Biotic Diversity and Ecological Flows Springer-Verlag, New York, pp. 327–345.

d'Herbès, J.M., Valentin, C., Thiéry, J.M., 1997. Synthèse des connaissances acquises sur la brousse tigrée nigérienne: hypothèse sur la genèse et les facteurs déterminant les différentes structures contractées. In: d'Herbès, J.M., Ambouta, J.M.K., Peltier, R. (Eds.), Fonctionnement et Gestion des Écosystèmes Forestiers Contractés Sahéliens. John Libbey Eurotext, Paris, pp. 131–152.

Défarge, C., Trichet, J., Jaunet, A.M., Robert, M., Tribble, J., Sansone, F.J., 1996. Texture of microbial sediments revealed by cryo-scanning electron microscopy. J. Sedimentary Res. 66, 935–947.

Dulieu, D., Gaston, A., Darley, J., 1977. La dégradation des pâturages de la région de N'Djamena (Rép. du Tchad) en relation avec la présence de cyanophycées psammophiles: étude préliminaire Revue d'Elevage et de Médécine Vétérinaire des Pays Tropicaux 30, 181–190.

Eldridge, D.J., 1993a. Cryptogams, vascular plants, and soil hydrological relations: some preliminary results from the semiarid woodlands of eastern Australia. Great Basin Naturalist 53, 48–58.

Eldridge, D.J., 1993b. Cryptogam cover and soil surface condition: effects on hydrology on a semiarid woodland soil. Arid Soil Res. Rehab. 7, 207–217.

Eldridge, D.J., Greene, R.S.B., 1994. Assessment of sediment yield by splash erosion on a semi-arid soil with varying cryptogam cover. J. Arid Environ. 26, 221–232.

Eldridge, D.J., Kinnell, P.I.A., 1997. Assessment of erosion rates from microphyte-dominated calcareous soils under rain-impacted flow. Aust. J. Soil Res. 35, 475–489.

Greigert, J., 1966. Description des formations crétacés et tertiaires du bassin des Iullemmeden (Afrique occidentale) Publications de la Direction Mines et Géologie, Niger, 2. Bureau de Recherches Géologiques et Minières, Niamey, Niger, 234 pp.

Harper, K.T., Pendleton, R., 1993. Cyanobacteria and cyanolichens: can they enhance availability of essential minerals for higher plants?. Great Basin Naturalist 53, 59–72.

Isichei, A.O., 1980. Nitrogen fixation by blue-green algal soil crusts in Nigerian savannah. In: Rosswall, T. (Ed.), Nitrogen Cycling in West African Ecosystems. SCOPE-UNEP International Nitrogen Unit, Royal Swedish Academy of Sciences, Stockholm, pp. 191–198.

Jeffries, D.L., Klopatek, J M., Link, S.O., Bolton, H Jr., 1992. Acetylene reduction by cryptogamic crusts from a blackbrush community as related to resaturation and dehydration. Soil Biol. Biochem. 24, 1101–1105.

Johansen, J.R., 1993. Cryptogamic crusts of semiarid and arid lands of North America. J. Phycol. 29, 140–147.

Klubek, B., Skujins, J., 1980. Heterotrophic N_2-fixation in arid soil crusts. Soil Biol. Biochem 12, 229–236.

Lange, O.L., Kidron, G.J., Büdel, B., Meyer, A., Kilian, E., Abeliovich, A., 1992. Taxonomic composition and photosynthetic characteristics of the 'biological soil crusts' covering sand dunes in the western Negev Desert. Functional Ecology 6, 519–527.

Loope, W.L., Gifford, G.F., 1972. Influence of a soil microfloral crust on select properties of soils under Pinyon-Juniper in southeastern Utah. J. Soil Water Conserv. 27, 164–167.

Malam Issa, O., Trichet, J., Défarge, C., Valentin, C., Rajot, J.L., 1998. Micromorphology of microbiotic crusts from Niger soils. Influence on soil–water dynamics. Trans 16th Int. Congr. Soil Sci., Montpellier, France, Symp. 30, 961, 7 pp.

Mayland, H.F., McIntosh, H.T., Fuller, W.H., 1966. Fixation of isotopic nitrogen on a semiarid soil by algal crust organisms. Soil Sci Soc. Am. Proc 30, 56–60.

McKenna Neuman, C.M., Maxwell, C., Boulton, J W., 1996. Wind transport of sand surfaces crusted with photoautotrophic microorganisms. Catena 27, 229–247

Neumann, A.C., Gebelein, C.D., Scoffin, T.P., 1970. The composition, structure and erodability of subtidal mats, Abaco, Bahamas. J. Sedimentary Petrol. 40, 274–297.

Ouedraogo, P., 1997. Rôle des termites dans la structure et la dynamique d'une brousse tigrée soudano-sahélienne. Thèse de doctorat, Université Paris VI, France, 282 pp.

Pentecost, A., Riding, R., 1986. Calcification in cyanobacteria. In: Leadbeater, B.S.C., Riding, R. (Eds.), Biomineralization in Lower Plants and Animals. Clarendon Press, Oxford, pp. 73–90.

Reynaud, P.A., Lumpkin, T A., 1988. Microalgae of the Lanzhou (China) cryptogamic crust. Arid Soil Res. Rehab. 2, 145–155.

Rychert, R.C., Skujins, J., 1974 Nitrogen fixation by blue-green algae-lichen crusts in the Great Basin Desert. Soil Sci. Soc. Am. Proc. 38, 768–771.

Stal, L J., 1995. Physiological ecology of cyanobacteria in microbial mats and other communities. New Phytol. 131, 1–32.

Thiéry, J.M., d'Herbès, J M., Valentin, C., 1995. A model simulating the genesis of banded patterns in Niger. J. Ecology 83, 497–507.

Tisdall, J.M., Oades, J.M., 1982. Organic matter and water-stable aggregates in soils. J Soil Sci. 33, 141–163.

Verrecchia, E., Yair, A., Kidron, G.J., Verrecchia, K., 1995. Physical properties of the psammophile cryptogamic crust and their consequences of the water regime of sandy soils, North-western Negev Desert, Israel. J. Arid Environ. 29, 427–437.

Water balance in a banded vegetation pattern A case study of tiger bush in western Niger

S. Galle [a,*], M. Ehrmann [b], C. Peugeot [c]

[a] LTHE, BP 53, 38041 Grenoble, Cedex 9, France
[b] ORSTOM, Niamey, Niger
[c] ORSTOM, Montpellier, France

Abstract

The tiger bush is a patterned woodland with alternating bare area and vegetated stripes. In Niger, it covers one third of the Sahelian zone. These natural forests are of considerable economical interest since they are the main source of livestock forage and domestic energy. Its sustainable exploitation needs improved understanding of its dynamics. The redistribution of water between thicket and intervening bare areas is decisive for the water supply of the vegetation. Tiger bush patterning replicates an elementary unit composed of a bare area, the upslope border, the core and the downslope margin of the thicket. (Each zone of tiger bush is characterised by specific soil crusting associated with vegetation). Both water storage and runoff have been monitored after each rain, over a period of 4 yr, including contrasting rainy seasons, on the different zones composing the tiger bush. On the three crusted zones, runoff has a piecewise linear relationship with rain: on closed plots, runoff yield vs. annual rainfall ratio reaches 54% on bare soil, 2% on upslope border and 18% on downslope border. The measured infiltration confirms these rates on independent plots. In the core of the thicket, measured infiltration corresponds with the sum of the contributions of upslope zones, weighted by their relative lengths. This model predicts that bare area contributes up to 62% of the thicket supply, while direct rain is 27%, the senescence zone is 10% and the upslope border contribution is negligible (1%). The average water infiltration in the thicket is equal to $4 \times$ the incident rainfall, but water redistribution is not homogeneous within the core of the thicket. By the most favourable location, infiltration depth is measured to be about $8 \times$ the rainfall. The important runoff, mainly generated on the impervious bare area crosses the upslope border of the thicket without infiltrating, and entirely benefit to the core. Nothing is left to

* Corresponding author. Tel.: + 33-4-76-82-70-12; fax: + 33-4-76-82-52-86; e-mail: sylvie.galle@hmg.inpg.fr.

the downslope border, only rainfed. The upslope border, often described as favourable location for young plants is only rainfed most part of the year. By the end of the season, its increasing porosity, due to vegetation and termite activity let it benefit of the last rains. The simple water balance model based on runoff measurement is satisfactorily validated by independent observed infiltration. © 1999 Elsevier Science B.V. All rights reserved.

1. Introduction

In Niger, tiger bush woodlands supply the major part of domestic energy (Peltier et al., 1995) and contribute to livestock forage. As the anthropogen pressure increases, so too does the risk of damage to the ecosystem. The need for sustainable exploitation implies an understanding of tiger bush dynamics. Tiger bush is a patterned woodland made up of alternating bare areas and vegetated stripes. It occurs in arid or semi-arid climates, where water availability is limited, relative to vegetation needs. Similar patterned vegetation has been reported in many parts of the world: in Sahelian Africa (from Mauritania to Somali), in Australia, Mexico, and in the USA. Since the first description in Niger by Clos-Arceduc (1956), Boaler and Hodges (1964) postulated the importance of the superficial water dynamics in the maintenance of the spatial structure: sheet runoff is generated on the bare ground area which benefits the downslope vegetation stripe. Although numerous studies have been undertaken describing similar ecosystems all over the world, very few of them have actually measured runoff or soil moisture distribution over bare and vegetated areas to validate water dynamics hypotheses. Moreover, these studies concern different continents: Slatyer (1961) and Greene (1992) worked in Australia; Cornet et al. (1992) and Mauchamp et al. (1994) in Mexico. Since 1992, hydrological and ecological studies related to tiger bush functioning have been undertaken in Niger as part of two international experiments HAPEX-Sahel [1] (Goutorbe et al., 1994) and GCTE-SALT [2] (Menaut et al., 1993).

Peugeot et al. (1997) measured high runoff generation on tiger bush bare surface. But at the plateau scale, the contribution to the foothill runoff is limited to the bare border of the plateau. This difference must be due to the sink role of the vegetated stripes. Seghieri et al. (1997) studied the relationship between surface soil water dynamics and herbaceous plant development on the upslope part of the thicket. The present paper aims to calculate water balance of an entire tiger bush unit, including bare and vegetated areas, to validate a rain redistribution hypothesis. We monitored measurements of runoff and soil moisture content in each zone composing a tiger bush unit in Niger during a period of 4 yr, including contrasting rainy seasons. The data were monitored at a rain dependent time step.

---

[1] HAPEX-Sahel: Hydrological and Atmospheric Pilot Experiment in the Sahel.

[2] GCTE-SALT: Global Change Terrestrial Ecosystems-Savane à Long Terme core project.

2. The study area

Tiger bush covers $22\,000$ km^2, or one-third of the Sahelian Niger, between 13° and 15°N (Ambouta, 1984). The year is divided into two seasons, 90% of the annual rain fall in three months (from July to September), the remaining part of the year is a dry season. Within these latitudes, rainstorms are mostly convective, and annual rainfall varies from 400 mm in the north to 700 mm in the south. Tiger bush forest occurs exclusively on plateau, capped with a thick Pliocene iron pan (Gavaud, 1966). The shallow gravelly soils (25 to 85 cm) have very low nutrient reserves (Ambouta, 1984) and are poorly developed.

The tiger bush study site is located on a plateau near the Banizoumbou village, 70 km northeast from Niamey (13°32′N, 2°42′E). Its elevation is 250 m, and the general slope of the plateau is about 0.2%, ranging from 0.06% to 0.5%. Mean annual rainfall for that region is 560 mm for the period of 1905 to 1989 (Lebel and Le Barbé, 1997). The study site presents typical tiger bush facies with trees covering 25% of the area shown on the aerial photograph (Fig. 1).

Seghieri (pers. comm.) has studied the vegetation of this plateau on a 700 m long transect crossing eight vegetated stripes. She found that the average width of the perennial vegetation stripes was 10 m (± 7 SD), and 50 m (± 28 SD) for the bare areas. The high standard deviation is due to the undulating border of the thickets. The main woody species are *Combretum micranthum* G. Don and *Guiera senegalensis* J.F. Gmel. averaging 2.40 m in height. Vegetation zonation is observed, based on slope orientation.

On another site nearby, Thiéry et al. (1995) observed that soils in and between vegetation bands showed few morphological differences, apart from those which can be directly accounted for by the influence of the vegetation itself (i.e., higher porosity and rooting within the band). These observations are consistent with other soil surveys of Nigerien tiger bush (Ambouta, 1984, and Barker, 1992). Though soil textural properties show few differences, the soil surface, on the contrary, presents various types of crusts organised in a typical succession as described on our site by Seghieri et al. (1997).

These observations led us to divide the tiger bush into four discrete zones based on vegetation and soil crust type. The crustal type and characteristics presented here refer to the Sahelian surface crust classification proposed by Casenave and Valentin (1992). The runoff ratio, K_r, is defined by the ratio of the runoff depth to the rainfall depth for a given rainstorm. Casenave and Valentin (1992) measured K_r for each crust type with a rainfall simulator. The four zones of the tiger bush are described from upslope to downslope, starting with the runoff generating areas: (1) The downslope border of the thicket, often called 'senescence' zone considering it contains a majority of dead stumps with a few mature trees. It is covered mainly by structural crusts indicating intensive sheet flow ($K_r = 75$–85%). Structural crusts are composed of different layers (coarse sandy layer at the top, finer particles at the bottom) and result from a granulometric sieving impacted by rain drops. (2) The bare area covered by erosion and gravel crusts, with the highest runoff potential ($K_r = 80$–90%). Erosion crusts consist of a smooth surface made up of a single seal of fine cemented particles more or less colonised by algae, while gravel crusts are composed of fine particles including coarse fragments. (3) The upslope border zone with predominant sedimentation crusts resulting from sedi-
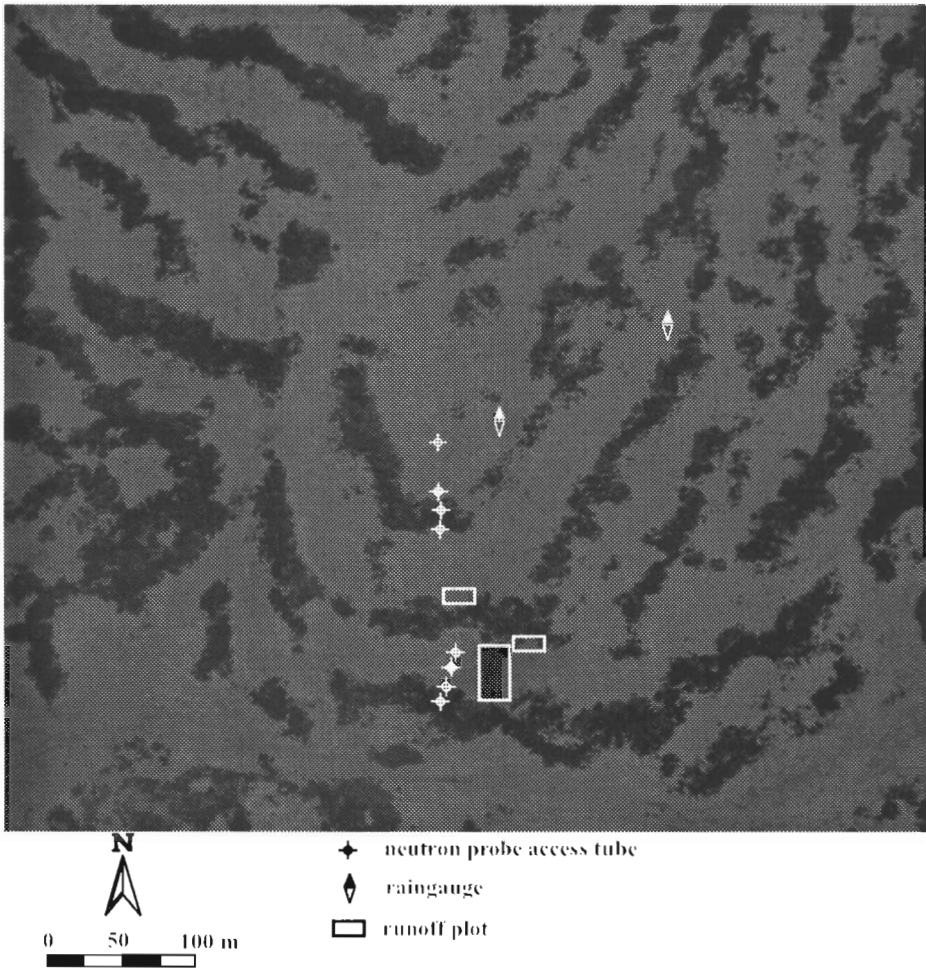
Fig. 1. Aerial photograph of the Banizoumbou plateau.

ments deposits, evidence of ponding processes ($K_r = 45$–55%). Its vegetation is composed of annual species, woody seedlings, and a few mature trees. (4) The body of the thicket contains mature trees which prevent an herbaceous layer developing. Here the soil is covered by litter and dead branches characterising high biological activity, high root density, high permeability, and the absence of surface crusting.

This simplified description of variability along the axis of maximum slope does not take into account lateral variation of the thicket showing bays and capes (Fig. 1). Given the field observations of plant species and crustal types, the following hypothesis proposed by Thiéry et al. (1995) describing functioning of the system can be assessed. This hypothesis states that the bare area, with a high runoff capability, feeds the downslope vegetation strip which in turn benefits from the water supply. Pioneer species

at the front and dead trees at the rear of the thicket suggest that the pioneer front is always favoured with respect to water feeding.

3. Methods

The study area, including three vegetation arcs, covers an area of 200×200 m^2 and is shown in Fig. 1. The hydrological fieldwork was carried out from January, 1992 to December, 1995 including four rainy seasons and three dry seasons. Rainfall amount and intensity were measured at the event time step using raingauge recorders forming part of the EPSAT-Niger [3] rainfall monitoring network described in Lebel et al. (1992).

3.1. Runoff

Three runoff plots were set up to provide discharge measurements on bare zone, upslope border and downslope border. As it is closed, a runoff plot is designed to measure runoff generated on a selected area. The total runoff crossing an open area will be higher if it receives water from the upward zone. This plot arrangement did not measure runoff generated on the body of the thicket, as it is assumed to be null. This assumption is based on observation of both absence of soil crusting and high macroporosity due to termite activity.

A runoff plot consists of a rectangular area of natural soil surrounded by an iron border driven 10 cm into the soil and equipped downstream with a collector feeding a 1 m^3 tank for water volume measurements. A by-ten divider is mounted on the bare zone plot to supply excess volume to a second tank. Water volume in the tanks were measured after each rainstorm. Each plot is assumed to be representative of the hydrologic behaviour of the surface crust enclosed. The three plots have the same width, but their length varies to include the total length of each zone of tiger bush. The plot areas are 26×5 m^2, 13×5 m^2, and 12.4×5 m^2, for bare, pioneer and downslope borders, respectively. The bare soil plot has been monitored from early July, 1992 to the end of the 1993 rainy season, whereas only the 1995 rainy season data set is available for the two other plots.

3.2. Soil water content

Soil moisture profiles were measured in two lines of neutron probe access tubes. Each line, installed perpendicularly to a different vegetation strip, included at least one access tube in each of the four zones of the tiger bush. On this lateritic plateau, the access tubes were installed using a motorised hammer drill. The drilling rod and the access tubes had the same diameter to ensure tight contact with the surrounding soil. A narrow 5-cm diameter seal of cement was settled around the tube on the soil surface, to prevent downward leakage of water. On the first line, four access tubes were placed to a

---

[3] EPSAT: Estimating Precipitation using SATellite.

depth ranging from 0.90 m to 1.20 m. On the second line, eight access tubes were placed to a depth of 3.40 m, and one, in the center of the thicket, to a depth of 5.40 m. Soil water measurements were made using a Solo25s neutron probe (Nardeux, France). For calibration, two soil samples of 500 g were used. The first consists of sandy clay loam (56% sand, 26% clay) from the 0–250 cm soil layer. The second, taken from the 250–550 cm layer, was more loamy and homogeneous. These samples were analysed using the nuclear absorption desorption technique described by Couchat et al. (1975). The resulting calibration equation is a function of the dry bulk density. It was measured with a gamma-ray probe (Nardeux Solo40), with values ranging from 1.65 g cm^{-3} in the 0–20 cm top layer, to 1.8 g cm^{-3} at deeper layers. Further details on the calibration technique used on tiger bush can be found in Cuenca et al. (1997).

Soil moisture profiles were monitored at a rain-dependent time step. Measurements of soil water content were made as soon as possible after each rainstorm. Typically, rainfall occurred during the night, and measurements were made 12 h later. Measurements were taken 1, 2 and 4 days later if no rain occurred. After that, the frequency was progressively decreased to once weekly during the rainy season or to once monthly during the dry season.

4. Results

4.1. Rainfall

The four observed years correspond to different amounts and temporal distributions of rainfall. The average (530 mm) was close to the climatic mean (560 mm, Lebel and Le Barbé, 1997) but a wide range of variation was observed (250 mm). During the driest year (425 mm in 1992), once the rains started, no gap occurred in the distribution of the 10-days rainfalls (Fig. 2). In 1993, the total amount was greater (490 mm) but a dry period covering 20 days occurred at the beginning of the season. This long dry period
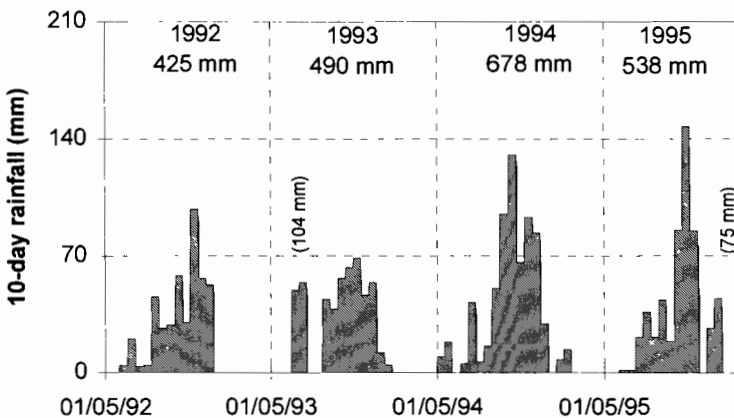
Fig 2. 10-days rainfall distribution on tiger bush site (Banizoumbou) for the four studied years and annual total.

dried out the soil. The following year, 1994, had both a high total (678 mm) and a continuous distribution, except for 25 mm before and after the season. The last year showed a 10-days period without rain before the last rains of the season. The total amount (538 mm) was close to the long term average.

4.2. Runoff

For each one of the three plots, the relationship between rainfall depth and runoff depth showed the same behaviour (Fig. 3). Whenever rain is lower than a threshold (P_T), no runoff occurs, and for higher rainfall, runoff increases linearly with the amount precipitated (P) within the observed range of rain. The resulting broken line is a particular piecewise linear model where the origin and slope of the first line are null. The only parameters to determine are the precipitation threshold and the slope of the second line. They are estimated by simple linear regression, the fitting quality being characterised by the determination coefficient (r^2). The model is formulated:

$$\text{Roff} = 0 \qquad\qquad \text{if } P < P_T \qquad\qquad\qquad (1a)$$

$$\text{Roff} = \alpha(P - P_T) \qquad \text{if } P \geq P_T \qquad\qquad\qquad (1b)$$

where P_T is the rainfall threshold and α the slope. The parameters of the model for the three plots, summarised in Table 1, were computed from the 1992 to 1993 data set for the bare soil plot, and from the 1995 data set for the two other plots. The 95% confidence interval is shown on Fig. 3. Due to tanks overflowing, some data are missing in these data sets. Except for upslope border, no data are available for rain higher than 45 mm.

The slope α, or runoff ratio, increases from the upslope border (15%), to the senescence zone (42%), and the bare zone (70%) which is enhanced by the decrease of the associated rain threshold (from 30 to 5 mm). This order agrees with those of Casenave and Valentin (1992), but the slope (α) is lower than K_r on upper and lower border of the thicket, and similar on bare soil.

These three piecewise linear models were applied to simulate runoff at the event time step, on each plot, for the four rainy seasons. Cumulative runoff yield over one season on one plot, given in Table 2 together with the ratio of annual runoff yield over annual rainfall depth, allow the inter-annual comparison of the behaviour of the plots. The averaged total amount of estimated runoff is about 270 mm (or 51% of annual rain) in the bare zone, three times lower (16% of rain) for the senescence zone, and very low (2% of rain) for the upslope border. These ratios are lower than the slope of the model because of the threshold effect. The percentage varies with year according to the proportion of low-rain events to the annual amount of rainfall.

4.3. Soil water content

The minimum soil water content, corresponding to the driest moisture profile, measured by the end of the dry season (May) depends on the location but remains steady over years (Fig. 4). Whatever the previous rainy season, the dry profile remained the same. During the prolonged 7 months of dry season, drainage and evapotranspiration
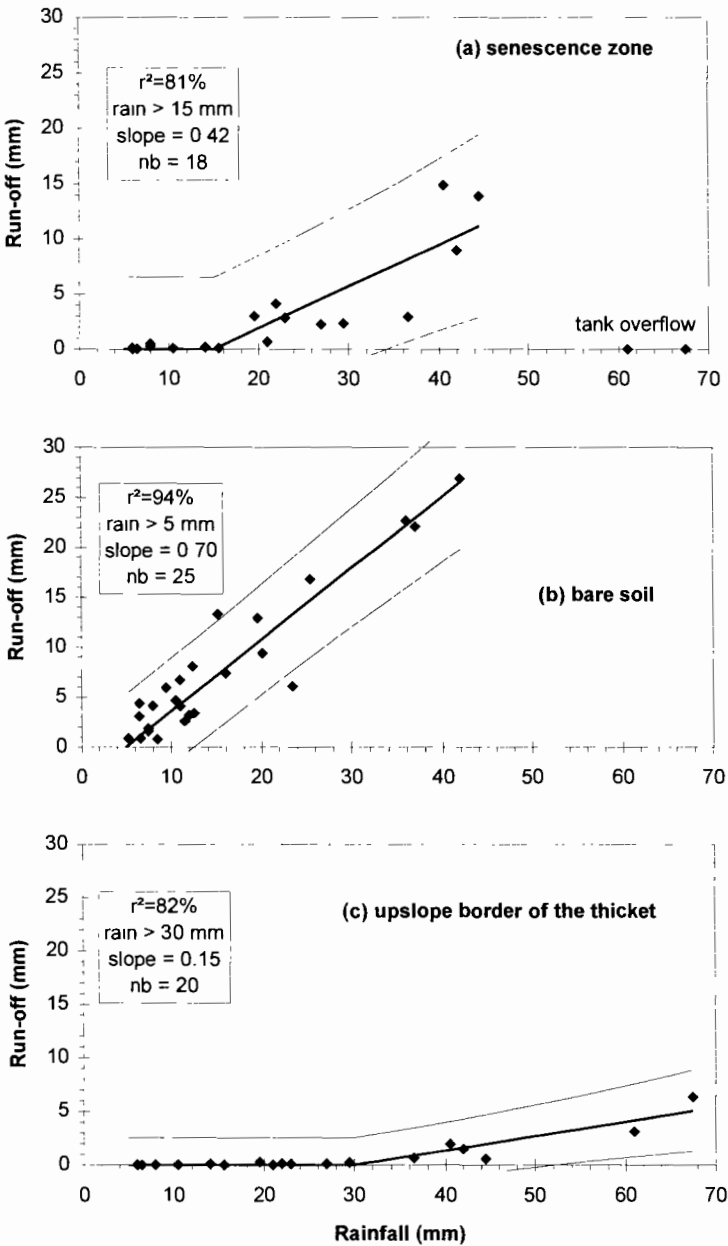
Fig 3. Observed and fitted runoff vs. rainfall. (a) Senescence zone, (b) bare zone, (c) upslope border.

exhaust the profile. The remaining water is tightly bound to the soil and becomes unavailable for plants or redistribution. Besides, the maximum water profile depends on

Table 1
Regression parameters (and associated error) between runoff and rainfall

	Senescence zone	Bare zone	Upslope border
r^2	81%	94%	82%
Rain limit (mm)	15 (4)	5 (1)	30 (10)
Slope	0.42 (0.06)	0.70 (0.04)	0.15 (0.03)
Sample	18	25	20

the rainy season. The annual range of variation of soil water content characterises the infiltration processes of each year and each zone (Fig. 4).

From upslope to downslope we find: (1) the senescence zone with low available water, but higher than in the bare zone, that is significantly increased during 1992 and 1994; (2) the bare zone with a low available soil water where the infiltration front does not progress deeper than 50 cm, whatever the year. The high rainfall in 1994 generated deeper infiltration compared with other seasons, with still a weak storage, however; (3) the upslope border of the thicket had a higher storage than the two upslope zones. The total volume of stored water varies considerably with annual rain: the wet front reached 80 cm in 1993, and down to 2.40 m in 1994; (4) the body of the thicket stores a huge amount of water. Whatever the year, the maximum measured profile remained the same, i.e., close to field capacity, in the 0–5.40 m layer of soil (not seen on graph because of the scale). Despite its depth (5.40 m), the infiltration front crosses the bottom of the access tube and deep drainage occurs. The annual amount of infiltrated water cannot be measured in this zone.

These results are summarised in Table 3, where the maximum available water is the difference between maximum and minimum profile of each year. A high infiltration corresponds to a rainy year showing a high rainfall amount, but also a regular distribution of rain. Although 1993 and 1995 had higher rainfall than 1992, the dry periods occurring during these years were unfavourable for deep infiltration.

Taking duration into consideration, the noticeable difference in soil water content among the four zones composing the tiger bush is further strengthened. For example, one can observe the monthly evolution of soil water storage during the 1994 rainy season (Fig. 5). The body of the thicket rapidly increased its water storage to reach a maximum on the 6th August, maintaining this level for the ensuing 2 months. On the other hand, the upslope border had to wait until the 2nd September to skip to a higher water content corresponding to one less month of high water storage. The same

Table 2
Estimated runoff using the fitted piecewise linear model

	Senescence zone		Bare zone		Upslope border	
	(mm)	(% Rain)	(mm)	(% Rain)	(mm)	(% Rain)
1992	56	13%	204	48%	7	2%
1993	77	16%	254	52%	9	2%
1994	111	16%	345	51%	15	2%
1995	102	19%	286	53%	17	3%
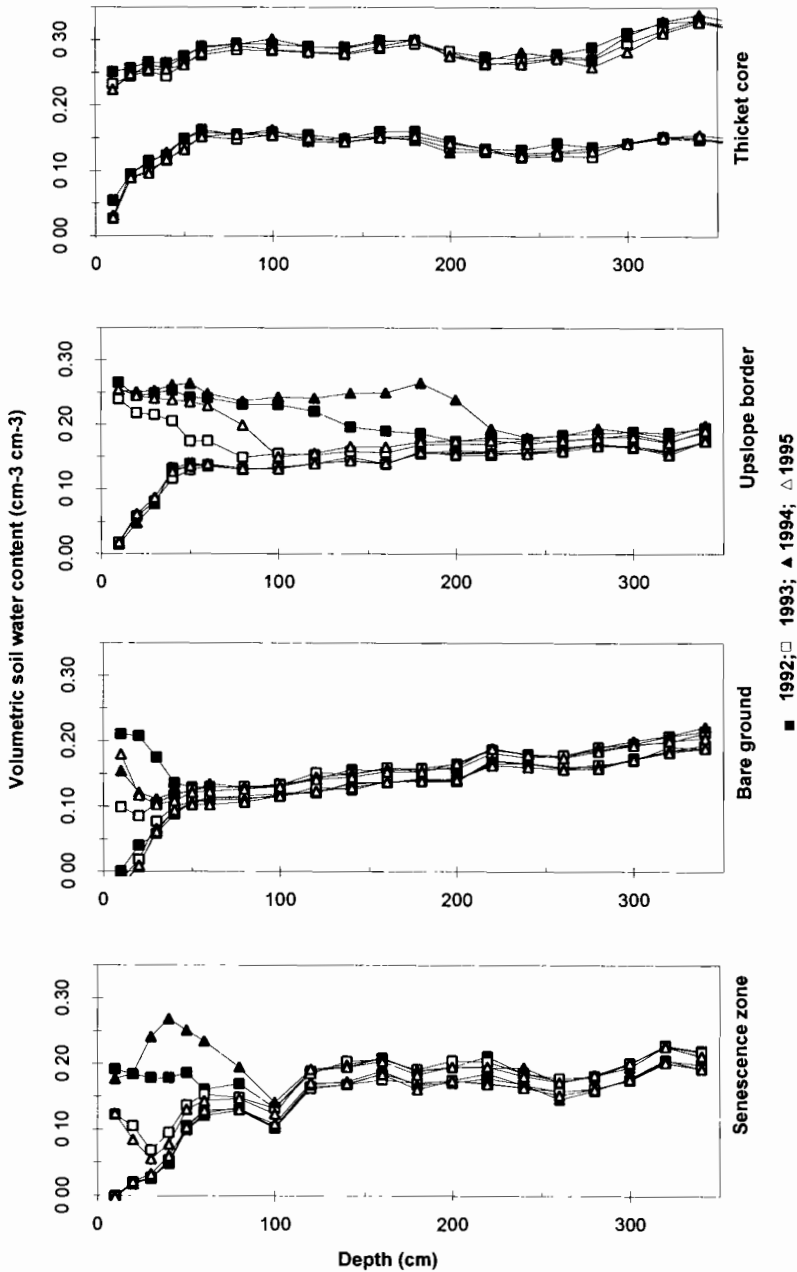
Fig. 4. Annual range of soil moisture content (1 May–1 November) for the four zones and the four monitored years.

noticeable increase was observed by the end of the rainy season (10th October, or 6 days before the last rain), for the upslope border of this zone, and never in the bare area. A

Table 3
Observed infiltration in the four zones of the tiger bush: maximum available water in 0–3.40 m soil layer, and maximum depth of the wetting front

	Senescence zone		Bare zone		Upslope border		Thicket core	
	water (mm)	depth (m)	water (mm)	depth (m)	water (mm)	depth (m)	water (mm)	depth (m)
1992	140	1.00	111	0.50	221	2.00	503(*)	> 5.40
1993	108	0.40	81	0.40	113	0.80	498(*)	> 5.40
1994	176	1.00	97	0.40	279	2.20	510(*)	> 5.40
1995	86	0.40	94	0.40	147	1.00	485(*)	> 5.40

(*): Drainage is observed.

lower increase in soil water content was also observed for the senescence zone. A delay in fully charging the upslope border of the thicket, compared to its core was also observed during the three other years (1992, 1993 and 1995).

4.4. Water balance

Establishing the soil water balance on each tiger bush area allows the functioning hypothesis detailed earlier to be validated. Considering a rain event, soil water balance can be expressed as follows:

$$\text{Infiltration} = \text{Rain} + \text{Runon} - \text{Runoff} \tag{2}$$

Where Runon and runoff respectively refer to water volumes reaching and leaving a given area, by surface movement.
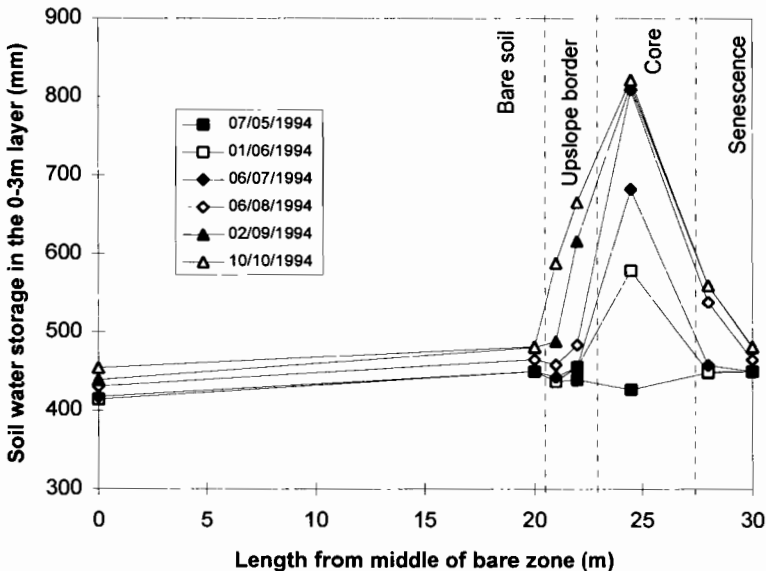
Fig. 5. Increase in soil water storage (0–3 m) on a transect perpendicular to a tiger bush elementary unit, during 1994 rainy season.

Two elements of the soil water balance equation (Eq. (2)) were directly measured on the site (rain and runoff). The infiltration occurring during a rain event equals the change in soil water storage before and after the event plus deep drainage and evapotranspiration (Eq. (3)).

$$\text{Infiltration} = \Delta S + D + \text{ETR} \qquad\qquad (3)$$

where ΔS is the change in soil water storage in the monitored soil layer, D is the deep drainage beyond this level, ETR is the real evapotranspiration.

The change in soil water storage is measured using neutron probe. As soil physical properties of the soil are not known, drainage flux cannot be assessed. So we consider only those events when no deep drainage occurs ($D = 0$), i.e., the wetting front has not crossed the bottom of the tube. This limit does not affect bare soil, upslope and downslope border of the thicket as seen on Fig. 4. Furthermore, infiltration in the thicket core is only accessible during the beginning of the season. As soil water measurements are not exactly synchronised with rain, evapotranspiration occurring in the meantime has to be assessed and added to the measured change in water storage to obtain the actual amount infiltrated during a rainstorm.

Evapotranspiration is estimated using methodology developed by Monteny et al. (1997). They worked on the evaporation of a savannah located nearby (1 km), mainly covered by the same woody species *G. senegalensis*. They showed that soil moisture depletion affects the evapotranspiration rate through an increase in the local large-scale surface resistance. When nearly 40% of the total soil water is depleted in the root zone, soil water content controls the evaporative regime of the Sahelian land surface. This relation can be expressed as follows:

$$\text{ETR}/\text{ETP} = (1/0.6) * S/S_{\max} \qquad \text{if } 0 < S/S_{\max} \leq 0.6 \qquad (4)$$

$$\text{ETR}/\text{ETP} = 1 \qquad\qquad\qquad \text{if } 0.6 < S/S_{\max} \leq 1$$

where *ETR* is the real evapotranspiration, *ETP* is the potential evapotranspiration, $S/S_{\max}$ is the fraction of available water in the considered depth of soil.

Potential evapotranspiration was measured at the Banizoumbou weather station situated 2 km from our plateau. Estimated evaporation agreed with that recorded by Culf et al. (1993), and also by Wallace and Holwill (1997) on another tiger bush site in Niger. They found evaporation from bare areas decreased from 4 mm day^{-1} on the day following a rainstorm to 0.5 mm day^{-1} 3 days later.

The remaining unknown in Eq. (2) was runon. Three assumptions were made from our understanding of the water dynamics suggested by experimental data: (i) all generated runoff is transmitted to the downward zone, i.e., no lateral flux of water exists; (ii) runoff from the thicket body is negligible; and (iii) all generated runoff benefits the core of the thicket. The third assumption is the strongest but it highly simplifies the functioning by considering that upslope generated runon simply crosses bare soil and upslope border of the thicket without infiltration benefit. Given the amount of runoff generated on upslope zones, a particular attention must be given to the water balance of the upslope border of the thicket. All assumptions were tested by comparing estimated and actual infiltration.

Following assumption (i), the contribution of each upslope zone (z) to runon in the thicket core is proportional to its relative area. For a transect of unit width, only the length (L_z) of each zone is required. These lengths were measured on our tiger bush site (Table 4). A simple infiltration model derived from Eq. (2) can then be developed using two different expressions for source or sink area.

For source areas (senescence zone, bare soil and upslope border):

$$\text{Infiltration}(z) = \text{Rain} - \text{Runoff}(z) \tag{2.1}$$

where runoff in the z zone is estimated using the piecewise linear models.

For sink area (core of the thicket):

$$
\begin{aligned}
\text{Infiltration} \quad &= \quad \text{Rain} + \text{Runon} \\
&= \quad \text{Rain} + \sum_z \left(L_z / L_{\text{core}} \times \text{Runoff}(z) \right)
\end{aligned} \tag{2.2}
$$

where L_z is the length of the zth source area.

Using this model, infiltration can be estimated for any incident rainfall on each of the four zones of our tiger bush. In Fig. 6, the infiltration model based on rainfall (thick line) and its 95% confidence interval (dotted lines) is compared with the measured change in water storage corrected by the evapotranspiration (Eq. (3)). The 95% confidence interval of the model equal to the confidence interval of the piecewise runoff model. If the model satisfactorily represents reality, most of observed infiltration depths should remain in the 95% interval. The error associated with change in soil moisture is the sum of instrumental error, calibration error and integration error. Vandervaere et al. (1994) presented an error analysis for estimating the variance of volumetric water content and soil water storage. The error increases with the soil storage. On our site, maximum limits of error on change in soil moisture are 2.3 mm, 1.7 mm, 5.6 mm and 12.3 mm for senescence, bare soil, upslope and core of the thicket, respectively. The error associated with rainfall measurements is about 2 mm (Lebel pers. comm., 1996).

In the senescence zone (Fig. 6a), the model overestimates the infiltration for high rainfalls. This should not be the case if additional runon feeds this zone. Hypothesis (ii) implies that no water runs off the core of the thicket is fulfilled. When rain exceeds 45 mm (highest runoff measurement), the linear extension of the model should overestimate the infiltration. It is likely that the runoff is no longer a linear response to rain. To

Table 4
Length of each zone comprising the tiger bush study site

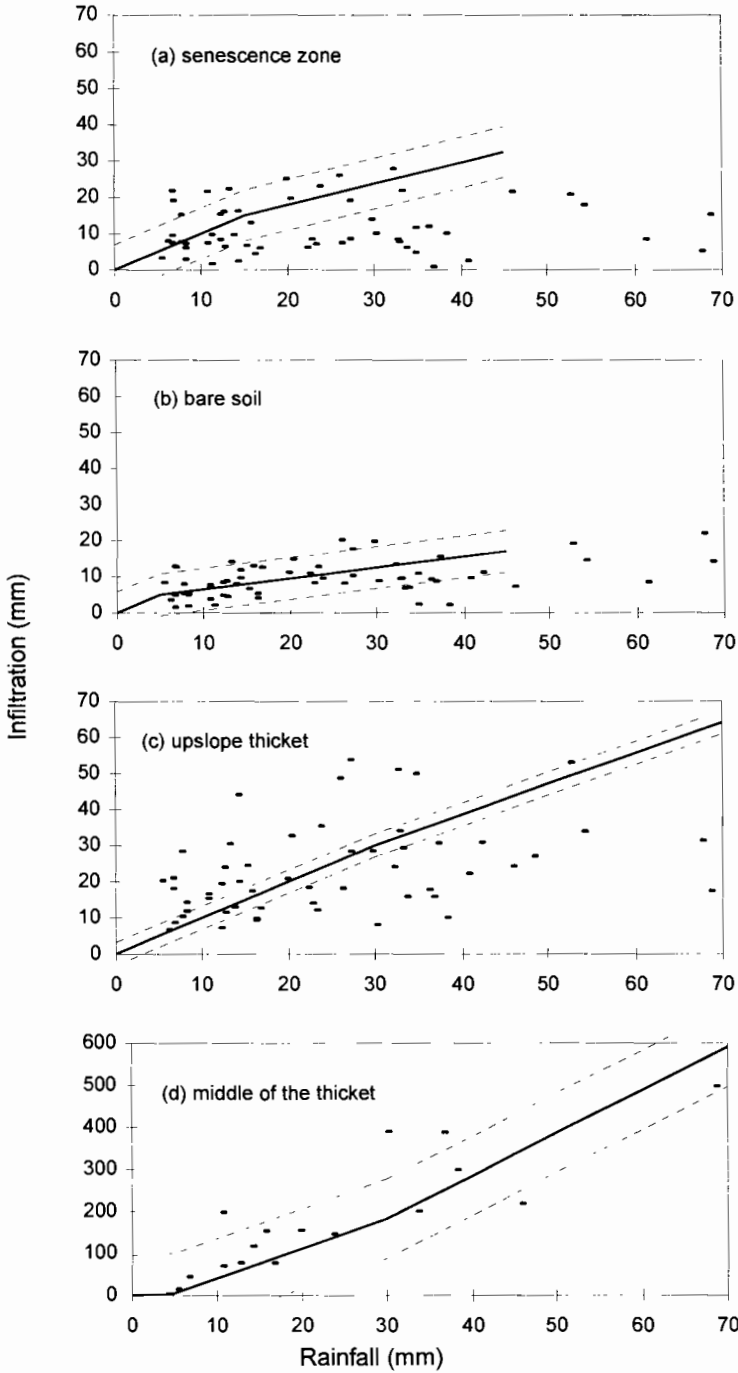|	Length	
	(m)	(%)
Downslope border	12	22
Bare soil	23	43
Pioneer front	13	24
Thicket body	6	11
Total	54	100

Fig. 6. Observed and modelled change in soil water storage (infiltration) vs. rainfall: (a) senescence zone, (b) bare zone, (c) upslope border, (d) middle of the thicket.

understand the difference between estimated and actual infiltration for lower rainfalls, one must remember that the neutron probe access tubes are not located in the runoff plots and that the soil crusts are spatially variable. Our access tubes are surrounded by erosion crusts, while the senescence runoff plot is mainly covered by structural crusts with a lower runoff coefficient (Peugeot et al., 1997). The overestimation of infiltration in our access tubes may be partially explained by variations of soil properties encountered when generalising from a point measurement to the areal estimate.

For the bare soil zone (Fig. 6b), model estimates fit satisfactorily with actual measurements. This result is important as it is the main source area of runoff, due both to its high runoff coefficient and also its area (43% of a tiger bush unit).

For the upslope border of the thicket (Fig. 6c), the model does not globally over- or under-estimate infiltration. Yet the scattering of the points implies that not only rainfall amount are involved in the determination of infiltration depth in this zone. For instance, initial soil moisture, rain intensity or vegetation development may play a role.

In the core of the thicket, the weighted sum of the upslope runoff (Eq. (2.2)) is compared with the measured infiltration. In this particular area, huge water content variations are observed from border to center, and location of the tube within the thicket must be taken into account. In Mexico, Mauchamp et al. (1994) showed that infiltration is higher in the upslope part of the thicket and then decreases to senescence zone. In Niger, an asymmetric triangle has been used to roughly approximate distribution shape (Fig. 5). Our two access tubes are located in the upper part of the thicket, corresponding to the maximum infiltration potential, or to the summit of the triangle. Given the geometry, the observed water in this location is equal to twice the average core water content. Model output fits fairly well with observed data, the infiltrated water is about $8 \times$ the rainfall volume when rain exceeds 5 mm (Fig. 6). A maximum infiltration of 500 mm (about the annual rainfall depth) has been recorded for a single rainy event 70 mm rain. Globally, the core of the thicket infiltrates about $4 \times$ the rain corresponding to direct rainfall plus incoming runon. The relative contributions of the upslope areas are 10% for senescence, 62% for bare soil and only 1% for upslope border in the beginning of the rainy season (Table 5).

For each source area, error terms (modelled minus observed infiltration) have been correlated with antecedent soil moisture. The stored water has been considered for the

Table 5
Water balance of an elementary tiger bush unit over a period of 4 yr

	Estimated runoff (% of rain)	Contribution of each component to thicket supply (%)
Rain	–	27%
Downslope border	18%	10%
Bare soil	54%	62%
Pioneer front	2%	1%
Thicket body	−277%(*)	–

(*): Negative runoff is infiltration.
Only rains exceeding 5 mm are considered.
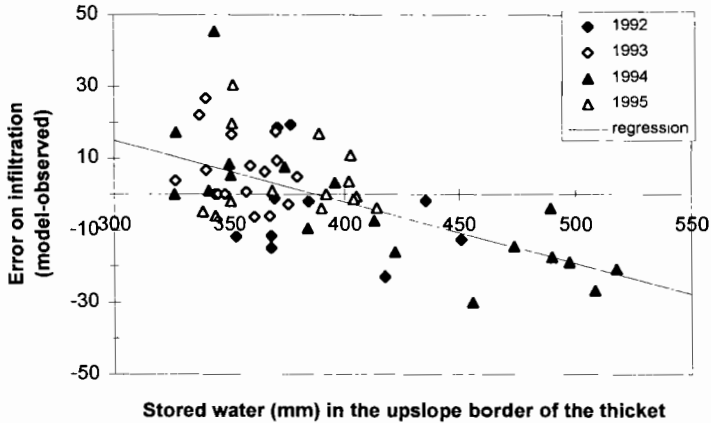
Fig. 7. Error on infiltration in the upslope border of the thicket vs. total stored water in this zone.

0–30 cm surface soil layer and the 0–340 cm total storage. As the determination coefficients between superficial soil water and error of the model are lower than 11% on every zone, they are not significant for our sample. It is the same for the 0–340 cm layer, except for the upslope border. In this case, $r^2 = 34\%$ and the error terms are inversely proportional to soil moisture (Fig. 7). Higher measured water content implies underestimation of the infiltration by the model.

5. Discussion

The data set from the tiger bush study site allowed us to verify a simple water balance model at rain event time step. The results of the water balance confirm and quantify the hypothesis on water redistribution among the different zones constituting a tiger bush unit, first developed by Clos-Arceduc (1956). Yet some process must be further identified.

The runoff potential of a tiger bush zone can be described as a function of its surface soil crusts (Thiéry et al., 1995). Our results show good agreement in relative classification but measured runoff ratio is systematically lower than the reference data of Casenave and Valentin (1992). These differences could be explained by the difference in scale of the study areas. We work on large runoff plots (about 80 m²) when they simulate runoff on 1 m² closed plots. Additionally, natural rainfall intensities may be different than simulated ones.

The bare zone, covered by erosion and gravel crusts, generate large amount of runoff; more than half of annual rain becomes runoff. The infiltration measurements confirm these values, and wetting fronts were never observed to pass 50 cm. The thicket zone, including core and border, receive this runon and redistribute it in a heterogeneous manner.

The upslope border, hardly benefit from this extra supply of water. As a low runoff coefficient was measured on closed runoff plot (only 2% of annual rain produces

runoff), a good infiltration potential should be expected. Measured infiltration on open area where all upslope runon arrives is not higher than rain height. The model expresses it by considering runon equal to zero. This result may seem paradoxical, it is due to infiltration dynamics. Vandervaere et al. (1997) measured a saturated hydraulic conductivity of 5.2 E-04 mm s^{-1} for sedimentation crusts of the upslope border, lower than for structural crusts covering downslope border (8.3 E-04 mm s^{-1}), yet the latter produce higher runoff. The low runoff height measured in the upslope border of the thicket is not due to high hydraulic conductivity but to the microtopography. The natural obstacles (roots, leaves) create local zones where water is temporarily stored (up to 30 mm) allowing longer time for surface storage infiltration. However, the major part goes through and reaches the body of the thicket. There, the macroporosity (due to microfauna) allows rapid infiltration under the ponded conditions found after rain. Chase and Boudouresque (1989) have shown that a single 0.8 cm diameter termite channel had sufficient capacity to drain 0.6 l min^{-1} during a 30 min test. Therefore, despite receiving important runon, only water stored in the ripples appears to infiltrate in the upslope thicket.

In the upslope border of the thicket, the mean infiltration rate is reproduced, however, our simple piecewise linear model shows a wide scattering when compared with actual measurements. Error analysis shows a correlation between total stored water and error. Whether this relation was due to hydrodynamic properties, i.e., an increase in infiltration capacity with soil water content, the correlation should also be significant with surface soil water. As stored water increase with time, the measured correlation may be due to the joint progress of the rainy season and annual plant development. Moreover, the correlation with stored water is not significant on the other tiger bush zones where very little annual vegetation develops. By the end of the season, annual plants have finished their growth and cover upslope zone of tiger bush (Seghieri et al., 1997). The stems slow down the runon from upslope areas, and the roots brake surface soil crusts. Saturated hydraulic conductivity increases in the subsoil 6-fold compared with the sedimentation crust (Vandervaere et al., 1997). Thus, the plant roots reduce the impeding effect of the sedimentation crusts, allowing more infiltration in the upslope zone compared with the beginning of the season. Termite activity linked to vegetation development should reinforce this trend, as they generate macropores for their harvesting activity. As seen in Fig. 7, the highest values of soil water storage, implying noticeable correction of the modelled infiltration (up to 30 mm) is mainly observed by the end of two long rainy years (1992 and 1994). In 1995, when the model is calibrated with the runoff data, the rainy season did not last long enough for water storage to reach high values. Because of the high variability of Sahelian rainy season (total amount and temporal distribution), a single year monitoring may lead to miss some behaviour pattern. Although limited, this seasonal increase in infiltration potential may be important for vegetation dynamics (wetting front progress from 80 cm to 2 m deep).

The core of the vegetation receives all upslope generated runon, except by the very end of rainy season as discussed above. Our model has not been tested during the end of the season due to lack of measurements. However by this time, infiltration in the core should be reduced due to higher infiltration in the upslope border. Since the observed maximum increase during the four monitored years is about 30 mm in the upslope

border, the relative length of the two zones implies a maximum 70 mm decrease of infiltration in the thicket core. This correction is low compared with measured amounts, and close to the model confidence interval (100 mm) at this location. During the first part of the rainy season, the measured infiltration height is indeed striking, reaching 8 × the incident rain recorded in the most favoured location of the thicket and an average of 4 × the rain received over its total length. These significant amounts of available water in the thicket core explain why two Sudanian woody species (*Gardenia sokotensis* and *Combretum nigricans*: Seghieri et al., 1997) are observed there, beyond their climatic optimum. The concentration ratio is high compared to other studied sites: Cornet et al. (1992) measured a concentration ratio of 3.5 at Mapimi (Mexico) and Tongway and Ludwig (1990) report a ratio of 2 for one rain event at Lake Mere (Australia). The concentration ratio varies with surface ratio (bare plus thicket area divided by thicket area) equal to 5 in our site, 4.5 in Mapimi and 2 in Lake Mere. In Niger, surface ratio is shown to be also related to annual rain (Valentin and d'Herbes, 1998).

Macroporosity is a key factor regulating rainfall redistribution among tiger bush. The rapidity of water infiltration in the core of the thicket explains the significant gradient between the core and its borders. All incoming runon is infiltrated in the core, leaving nothing for the downslope border. The downstream zone has an infiltration ratio much lower than one, equal or slightly lower than the modelled infiltration considering runon equal to zero. This observation confirms the conclusion of Galle et al. (1997) which compared two thickets with and without runon contribution. They found that the bare zone contributed mainly to total infiltration in the core, a lesser extent to the upslope border, and a negligible amount in the downslope area. The water deficit in that area, strengthened when annual rainfall is low, explains why most trees are dead in this «senescence» zone. However, water can cross the thicket on special occasions or by some temporary gullies created by human or animal paths. Though rare, these occasions may be important for Sahelian vegetation which is able to benefit from episodic water supply.

6. Conclusion

Tiger bush patterning replicates an elementary unit composed of a bare area, the upslope border of a thicket, the body or core of the thicket and its downslope margin or senescence zone. These terms refer to vegetation dynamics, and they reflect different water storage capacities induced by rain redistribution. By measuring both runoff and infiltration, hypotheses on water redistribution can be validated by comparing model estimates with actual measurements. Water balance determined at rain time steps confirms the generally supposed redistribution of rain: three zones generate runoff, with runon benefiting the thicket. However, the results show that despite its favourable location, the crusted upslope part of the thicket does not benefit much from additional water supply. The thicket comprises three zones possessing large differences in available water over a short distance (about 10 m). This sharp gradient is due mainly to changes in macroporosity that allow for extremely rapid infiltration in some zones under ponded conditions. The core of the thicket acts as a sink.

Locally, a tiger bush unit act as source–sink system (Ludwig et al., 1998) but at the plateau scale, the connections of intervening bare areas allow runoff circulation. Numerous gullies rise in the plateau covered by tiger bush, and Peugeot et al. (1997) show that the plateau contributes runoff to the foothills. Obviously, total wood exploitation would lead to very high runoff generation (70% of rain exceeding 5 mm), through destruction of the sink areas leading in term to disastrous erosion in the foothills, as seen on the Filingué region where road allows easy access for wood exploitation. Conversely, some intervening bare areas are essential to the development of the woody vegetation as they bring 62% of the thicket water supply. Planting them with trees must be avoided.

Acknowledgements

References

Ambouta, K., 1984. Contribution à l'édaphologie de la brousse tigrée de l'Ouest Nigérien. Thèse Docteur Ingénieur. Univ. Nancy I, 1–116 pp.

Barker T., 1992. Vegetation pattern in the Nigerien tiger bush. Mémoire, Bachelor of Science Dept. Geography, Coventry Polytechnic, 91 pp.

Boaler, S.B., Hodges, C.A.H., 1964. Observations on vegetation arcs in the northern region Somali Republic. J. Ecol. 52, 511–544.

Casenave, A., Valentin, C., 1992. A runoff capability classification system based on surface features criteria in semi-arid areas of West Africa. J. Hydrol. 130, 231–249.

Chase, R.G., Boudouresque, E., 1989. A study of method for revegetation of barren crusted Sahelian forest soils. ICRISAT proceeding of workshop, pp. 125–135.

Clos-Arceduc, M., 1956. Etude sur photographies aériennes d'une formation végétale sahélienne: la brousse tigrée. Bull IFAN, XVIII, Sér. A (3), 677–684.

Cornet, A., Montana, C., Delhoume, J.-P., Lopez-Portillo, J., 1992. Water flows and the dynamics of desert vegetation stripes. In Hansen, A.J., di Castri, F. (Eds.), Springer-Verlag, Coll. Ecological studies, pp. 327–345.

Couchat, P., Carre, C., Marcesse, J., Ho, J., 1975. The measurement of thermal neutron constants of the soil: application to the calibration of neutron moisture gauges and to the pedological study of the soilo. In: Schrack, R.A., Bowman, C.D. (Eds.), Nuclear cross sections and technology. US Dept. of Congress, pp. 516–579.

Cuenca, R.H., Brouwer, J., Chanzy, A., Droogers, P., Galle, S., Gaze, S.R., Sicot, M., Stricker, H., Angulo-Jaramillo, R., Boyle, S.A., Bromley, J., Chebhouni, A.G., Cooper, J.D., Dixon, A.J., Fies, J.-C., Gandah, M., Gaudu, J.-C., Laguerre, L., Soet, M., Steward, H.J., Vandervaere, J.-P., Vauclin, M., 1997. Variability of profile and surface soil moisture content and physical property measurement during HAPEX-Sahel intensive observation period. J. Hydrol. HAPEX-Sahel Special Issue 188–189, 226–268.

Culf, A.D., Allen, S.J., Gash, J.H.C, Lloyd, C.R., Wallace, J.S., 1993. Energy and water budgets of an area of patterned woodland in the Sahel. Agric For. Meteorol. 66, 65–80.

Galle, S., Seghieri, J., Mounkaila, H., 1997. Fonctionnement hydrologique et biologique à l'échelle locale. Cas d'une brousse tigrée au Niger. In: d'Herbès, J.-M., Ambouta, J.M K., Peltier, R. (Eds.), Fonctionnement et gestion des écosystèmes forestiers contractés Sahéliens. Ed. John Libbey, Paris, pp. 105–118

Gavaud, M.,1966. Etude pédologique du Niger occidental ORSTOM ed , Paris, pp. 109–116.

Goutorbe, J.-P., Lebel, T , Tinga, A., Bessemoulin, P., Brouwer, J., Dolman, A.J., Engman, E.T., Gash, J.H.C., Hoepffner, M., Kabat, P., Kerr, Y.H., Monteny, B.A., Prince, S., Saïd, F., Sellers, P., Wallace, J.S , 1994. HAPEX-Sahel: a large scale study of land–atmosphere interactions in the semi-arid tropics. Ann. Geophys. 12, 53–64.

Greene, R.S.B., 1992. Soil physical properties of three geomorphologic zones in a semi-arid mulga woodland. Aust. J. Soil Res. 30, 55–69.

Lebel, T., Le Barbé, L , 1997. Rainfall climatology of the central Sahel during the years 1950–1990. J. Hydrol HAPEX-Sahel Special Issue 188–189, 44–74.

Lebel, T., Sauvageot, H , Hoepffner, M., Desbois, M., Guillot, M., Hubert, P., 1992. Rainfall estimation in the Sahel: the EPSAT-Niger experiment. Hydrol. Sci. J. 37 (3), 201–215

Ludwig, J , Tongway, DE., 1998. Mardsen S. Stripes, strands or stripples: modelling the influence of three landscape banding patterns on resource capture and productivity in semi-arid woodlands, Australia. Catena, this issue.

Mauchamp, A., Rambal, S., Lepart, J., 1994 Simulating the dynamics of a vegetation mosaic a spatialised functional model. Ecol Modelling 71, 107–130.

Menaut, J.-C., Saint, G., Valentin, C., 1993. SALT, les Savanes à Long Terme. Analyse de la dynamique des savanes d'Afrique de l'Ouest: mécanismes sous-jacents et spatialisation des processus. Lettre du Programme Environnement, CNRS 10, 34–36.

Monteny, B.A., Lhomme, J.-P., Chehbouni, A., Troufleau, D , Amadou, M., Sicot, M , Verhoef, A., Galle, S., Said, F., Lloyd, C.R., 1997. The role of the Sahelian biosphere on the water and the CO_2 cycle during the HAPEX-Sahel Experiment J. Hydrol. HAPEX-Sahel Special Issue 188–189, 507–525.

Peltier, R., Bertrand, A., Lawali, M., Madon, G., Montagne, P , 1995. Marchés ruraux de bois-énergie au Sahel Bois forêts tropiques 245, 75–89.

Peugeot, C., Esteves, M., Rajot, J.-L., Vandervaere, J -P., Galle, S , 1997 Runoff generation processes: results and analysis of field data collected at the East Central Supersite of the HAPEX-Sahel experiment. J. Hydrol. HAPEX-Sahel Special Issue 188–189, 181–204

Seghieri, J., Galle, S., Rajot, J.-L., Ehrmann, M , 1997 Relationships between the soil moisture regime and the growth of the herbaceous plants in a natural vegetation mosaic in Niger. J. Arid Environ. 36, 87–102.

Slatyer, R.O., 1961. Methodology of a water balance study conducted on a desert woodland (*Acacia aneura* F. Muell.) community in central Australia. UNESCO, Paris, Coll. Arid Zone Research, pp 15–25.

Thiéry, J M., Valentin, C., d'Herbès, J.M., 1995. A model simulating the genesis of banding patterns in Niger. J. Ecol. 83, 497–507.

Tongway, D.J., Ludwig, J.A., 1990. Vegetation and soil patterning in semi-arid mulga lands of Eastern Australia Aust J. Ecol. 15, 23–34.

Valentin, C., d'Herbes, J.M., 1998 The Nigerien tiger bush as a natural water harvesting system. Catena, this issue.

Vandervaere, J.-P., Vauclin, M., Haverkamp, R., Cuenca, R.H., 1994. Error analysis in estimating the soil water balance of irrigated fields during the EFEDA experiment: 1. Local standpoint J Hydrol. 156, 351–370.

Vandervaere, J.-P , Peugeot, C., Vauclin, M., Angulo-Jaramillo, R., Lebel, T., 1997. Estimating hydraulic conductivity of crusted soils using disc infiltrometers and minitensiometers J. Hydrol. Hapex-Sahel Special Issue 188–189, 205–225.

Wallace, J.S , Holwill, C.J., 1997. Soil evaporation from tiger bush in southwest Niger. J. Hydrol 188–189, 415–431.

Testing the validity of upslope migration in banded vegetation from south-west Niger

A. Chappell [a,b,*], C. Valentin [c], A. Warren [b], P. Noon [b],
M. Charlton [d], J.M. d'Herbes [c]

[a] *Department of Physical Geography, University of Lund, Box 118 S-221 00 Lund, Sweden*
[b] *Department of Geography, University College London, 26 Bedford Way, London WC1H 0AP, UK*
[c] *ORSTOM, B P 11416, Niamey, Niger*
[d] *Department of Physics and Astronomy, University College London, Gower Street, London WC1E 6BT, UK*

Abstract

Recent studies of banded vegetation have suggested a successional model, in which bare bands are colonised in a pioneer front on the upslope side of a vegetation band. Vegetation patterns in south-west Niger have been interpreted to suggest that spatial transitions reflect this form of temporal succession, and in these patterns there is corroborating evidence for slow up-slope migration. However, given the inherent difficulties of long-term field experiments there are few data to judge the validity of this model. The use of the artificial radionuclide caesium-137 (^{137}Cs) to provide information on net soil flux over the past ca. 30 years offers potential in this regard. Furthermore, the identification of various types of soil crust, which can induce different types of hydrological behaviour, provides valuable information for predicting soil evolution. To test the hypothesis that banded vegetation migrates upslope, a 70-m transect encompassing two vegetation bands and a single bare lane was sampled in south-west Niger. The transect was aligned orthogonal to the bands and approximately parallel to the direction of water, soil and nutrient flow. Soil samples for gamma-ray spectrometry and particle-size analysis were collected along the transect at 21 locations with 1-m intervals in the lower part and three samples were obtained on the upper part. Prior to collection, the soil surface characteristics were examined to distinguish between crust types and to identify the presence of termite activity. The results demonstrate the utility of these techniques for examining the net redistribution of soil over a period of three decades and its relations to vegetation succession. The amount of soil eroded was found generally to decrease downslope, whilst the proportion of fine silt in the soil generally increased downslope. These patterns correspond with the location of the erosion and sedimentation crusts identified

---

[*] Corresponding author

using a standardised classification. The relations between microtopography and net soil flux may also explain some of the spatial variation in soil redistribution processes. The intensity of crust and ^{137}Cs measurements on the upslope edge of the lower vegetation band enabled the calculation of the upslope migration rate (ca. 0.19–0.27 m yr^{-1}) which coincided with independent studies in the same region. However, because considerable spatial variations in topography and soil flux were found to occur over very small distances, further detailed studies over larger areas will be needed. © 1999 Elsevier Science B.V. All rights reserved.

1. Introduction

Stripes of vegetation and bare ground have been noted on aerial photographs at many places worldwide and several hypotheses have been proposed to explain their origin. The perpendicular alignment of vegetation arcs in Jordan and in Mali to the dominant wind has been interpreted as evidence for their association with aeolian transport (White, 1969; Leprun, 1992). However, detailed studies of the dynamics of vegetation bands in northern Mexico (Cornet et al., 1992; Montaña, 1992) were taken to suggest that their formation was related to surface wash. The second hypothesis is now widely accepted where low-frequency, high magnitude rainfall events produce runoff on slightly inclined slopes on which the soils have low permeability resulting from an abundance of fine particles (Cornet et al., 1992). In this environment, surface wash is generated in the bare patches between the bands but accumulates and infiltrates at their upslope edges, where the resulting soil moisture promotes plant colonisation. Furthermore, it is hypothesised that when plants colonise this zone, they gradually cut off the supply of water and nutrients to the rest of the band. Consequently, the whole band should move upslope (Thiery et al., 1995).

The runoff hypothesis is now also generally accepted as an explanation for the 'brousse tigrée' banded vegetation patterns of south-west Niger. Support for the hypothesis in this area has been provided by Thiery et al. (1995), who also showed a temporal succession of different crusts across the band and interband. These authors developed a model to simulate formation of the bands, which could generate a variety of patterns depending on varying rainfall and surface wash conditions. However, the dynamic operation of this model cannot be verified without difficult long-term studies. Early field evidence of band shifts mainly due to aeolian activity has been provided by Leprun (1992), working in Mali, where a bench-mark in 1955 was located within a band and 21 years later was found to be in a barren lane. The migration distance was apparently 15.8 m, resulting in a mean annual velocity of 0.75 m yr^{-1}. Other bench-marks in the same region indicated annual velocities ranging between 0.20 m yr^{-1} and 0.25 m yr^{-1} (Leprun, 1992).

Since soil redistribution is essential for the operation of the plant successional model, it is reasonable to assume that long-term monitoring of soil erosion would provide an indicator of band migration. Unfortunately, studies of contemporary soil erosion cannot give accurate estimates for periods long enough to cover the rate of band migration (Higgitt, 1991) especially in semi-arid environments with high spatial and temporal

variability in rainfall. However, many of the problems with long-term monitoring of soil redistribution can be overcome by using the artificial radionuclide caesium-137 (^{137}Cs) to trace soil movement (Sutherland and de Jong, 1990). The ^{137}Cs technique provides accurate net soil flux measurements aggregated over the last ca. 30 years (Martz and de Jong, 1991) and has been used successfully in many environments throughout the world (Walling and Quine, 1992).

Thus, the aim here is to measure net soil flux in south-west Niger using ^{137}Cs and to relate it to surface features and transitions in the structure of the brousse tigrée in an attempt to validate the model and quantify the rate of upslope band migration.

2. Materials and methods

2.1. Study area

The study area is 70 km east of Niamey in south-west Niger. The climate is semi-arid with a monomodal rainfall distribution. The average rainfall at Niamey for the period 1905–1989 was about 560 mm (Lebel et al., 1992), but for the past 25 years the rainfall has been persistently below-average with a mean of about 495 mm. Potential evapotranspiration is approximately 2000 mm (Sivakumar, 1989).

During the summer, south-westerly winds are replaced periodically by easterly squalls with short-duration, high-intensity rainfall. The intense rainfall can cause crusting, clay eluviation and rapid removal of unconsolidated material from the surface (Casenave and Valentin, 1989). Strong winds precede many of the squalls, and these raise large quantities of dust. During the dry winter months, north-easterly winds of the Harmattan dominate, bringing dust from southern Sahara (McTainsh and Walker, 1982). Drees et al. (1993) reported a highly seasonal occurrence of dust deposition in Niger. They suggested that the frontal storms were responsible for more dust infall than was the Harmattan.

2.2. Banded vegetation structure, soil and hydrological processes

The brousse tigrée in this region occurs only on broad ironstone-capped plateaux with slopes generally lower than 0.3°. The parent material of soil on the plateaux is highly weathered, humus-poor and sesquioxide-rich. Clays are mostly kaolinitic. The soil is gravely loam over cemented ironstone gravel (Manu et al., 1991). It is acid (pH < 5), of low nutrient status and has little water storage capacity because of its shallow depth and large content of coarse fragments. The surface has bare patches interspersed with bands of vegetation of varying sizes, oriented with their long axis parallel to the contour (Thiery et al., 1995). The soil within the vegetation bands is different from that between the bands; pH is 5 to 6 and it is humus-rich, and approximately 20 cm thick above the ferricrete cobbles.

The brousse tigrée (band and interband) has been divided into five typical zones (Thiery et al., 1995), shown in Fig. 1. The central zone (C) in the figure has a dense (60–100%) canopy, small shrubs in the understorey and sparse grass cover. The soil has
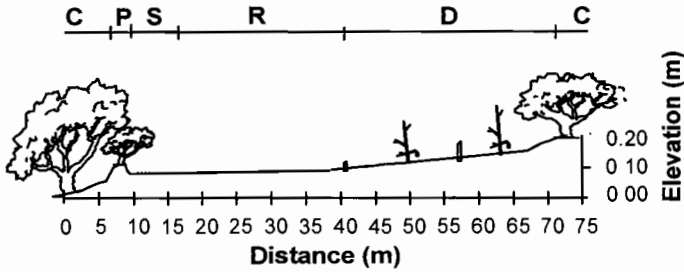
Fig. 1. Schematic cross-section of 'brousse tigrée' showing the typical zones, topography and the soil sample locations.

high porosity related mainly to termite activity. Surface crusts are virtually absent apart from a few remnants of 'sedimentary' crusts and 'erosion' crusts which are restricted to the vicinity of active termite mounds. The degraded zone (D) has low shrub cover (40–0%) and is dominated by 'structural sieving' crusts indicative of intensive impact of rainfall and sheetflow (Valentin and Bresson, 1992). The runoff zone (R) has no plant cover, but includes erosion and gravel crusts which produce intensive runoff. The sedimentation zone (S) is also devoid of vegetation with the exception of annual grasses in the lowest zones and is characterised by sedimentary crusts which spread over nearly the whole surface and cover old erosion and gravel crusts. The pioneer zone (P) comprises either a 'bay' or 'cape' structure in which the former has nearly total cover of annual grasses whilst the latter is predominantly colonised by *Guiera senegalensis*. In both situations the sedimentary crusts are almost entirely destroyed by plant emergence and termite activity.

2.3. Sampling and laboratory analyses

Soil samples and in situ soil crust observations were collected at 24 sites in March, 1995 along a transect aligned orthogonal to the orientation of the vegetated bands (Fig. 1). In the lower part of the transect samples were collected at 21 locations with 1 m intervals because variation in sedimentation rates were thought to be more variable here, whilst only three samples were obtained on the upper part. Samples were taken from small pits (0.01 m^2) to a depth which varied with contact to ironstone cobbles. Each sample was weighed, homogenised and subsampled to provide a representative sample of the soil profile and then re-weighed.

The particle-size distribution was determined by a Malvern 2600 laser sizer on subsamples with the organic matter removed prior to ultrasonic disaggregation. The threshold values for percentage clay, silt and sand content used in subsequent analyses are 2 μm, 60 μm and 1128 μm.

The ^{137}Cs activity was measured by gamma-ray energy spectrometry. The soil samples were prepared by air-drying and grinding with mortar and pestle to pass a 1-mm sieve. The samples were placed in a standard Marinelli (re-entrant) beaker which was then located on a horizontally-oriented 20% relative efficiency hyper-pure germanium (HpGe) gamma-ray detector. The detector was coupled to spectroscopy-grade amplifiers

and a PC-based data collection system. Calibration samples were used to derive the absolute ^{137}Cs activities in each sample.

2.4. Calculation of net soil flux from ^{137}Cs

The ^{137}Cs concentration in the soil of the plateau is ten times greater than at other locations in this region (Chappell, 1995). It is thought that the preferential accumulation of ^{137}Cs-enriched dust beneath vegetation on the plateau is responsible, thus making it difficult to identify a 'stable' ^{137}Cs reference site (Chappell, 1995). Because of this the site chosen as the reference was devoid of vegetation except for a layer of annual grasses, close to the study area, where there has been no cultivation or wood cutting for at least ca. 30 years, and where only limited erosion is likely to have taken place. A mass-specific exponential model was fitted to the ^{137}Cs profile for the soil at this site ($r^2 = 0.97$). The model is:

$$\log_{10} C_i = 0.933 - 0.034 D_i \tag{1}$$

where C is the mass specific ^{137}Cs concentration (Bq kg^{-1}), D is the soil depth (cm) and i is the sample depth increment. The values of 0.034 and 0.933 represent the terms S and E in Eq. (2) below but are not appropriate for the Plateau region. The ^{137}Cs inventory predicted by the model for this site (2066 ± 125 Bq m^{-2}) is the best approximation of the reference ^{137}Cs inventory for an 'undisturbed' site in the study area (Chappell, 1995). It is acknowledged that a more precise estimate of the fallout inventory would require many samples (Sutherland, 1994), but these are unavailable in the present case.

To calculate the net soil flux a relation between the movement of ^{137}Cs and the redistribution of soil must be established (Walling and Quine, 1990). The model developed by Zhang et al. (1990) for rangeland areas was used here to estimate surface lowering at erosional sites, although it cannot be used for depositional sites. It utilises the widely reported exponential depth distribution of ^{137}Cs in rangeland areas to estimate the depth of soil removed from a site from the difference between the ^{137}Cs remaining in the profile and the ^{137}Cs reference level:

$$Y = 100\ln(1 - X_1)/ - SPE \tag{2}$$

$$X_1 = (R - A)/R$$

where Y is mean annual soil loss (t ha^{-1} yr^{-1}), S is the depth distribution shape coefficient, P is the number of years since 1963 and X_1 is the reduction ratio of the total ^{137}Cs activity per unit area (A), at each site, relative to the reference inventory (R) in the same units (Bq m^{-2}). A value of 0.144 was used for S to represent the shape coefficient of ^{137}Cs profile on the Plateau soils. Since the thin soil on the Plateau was known to be approximately 20 cm in depth before the soil matrix was dominated by ferricrete cobbles, an additional term (E) with a value of 1.5 was used in the net soil flux model (2) to offset the total depth of soil removed. It was derived from empirical model fitting using existing soil ^{137}Cs profiles in this region (Chappell, 1995).

An additional model is needed to define the relation between ^{137}Cs and net soil gain. It is reasonable to assume that sites of accumulation are the result of deposition either

from surface wash or the wind, and that both are more likely to occur beneath vegetation. Surface wash deposits are likely to have a uniform ^{137}Cs profile with depth. By assuming further that the ^{137}Cs concentration of the mobile aeolian material accumulated beneath vegetation is approximately constant, its ^{137}Cs depth-distribution should also be uniform. Thus, the modified proportional model suitable for establishing the mean annual net soil gain for sites along the transect which have ^{137}Cs activity greater than the reference level is:

$$Y = 10(DBX_2 F)/T \tag{3}$$

$$X_2 = (A - R)/A$$

where Y is the mean annual net soil gain (t ha^{-1} y^{-1}), D is the sample depth (m), B, the bulk density of soil (kg m^{-3}), X_2 (the reduction ratio of the total ^{137}Cs activity per unit area at each site as defined above), F is the adjustment which accounts for the preferential accumulation of [137]Cs (0.1) and T is the time elapsed since 1963 (years) to enable comparison with the equation for net soil erosion (Eq. (2)). No adjustment has been made for the preferential accumulation of dust in the samples.

3. Results and discussion

The particle size distributions of samples along the transect selected from within and between the vegetation bands (Fig. 2) show large amounts (60–80%) of silt and small amounts of sand and clay. The silt mode dominates all samples. At sites protected from wind erosion by a vegetated canopy, this is probably due to the accumulation of aeolian dust (McTainsh and Walker, 1982). At unprotected sites between the vegetation bands the accumulation of aeolian material is unlikely. Here the dominance of silt suggests that the silt-rich aeolian accumulations in the vegetation bands have been redistributed to the interband by surface wash. This may occur when intense rainfall reaches a soil where vegetation has died out, for example in the degraded zone of the band (Thiery et al., 1995). It is hypothesised that a decrease in the vigour of plants in the lower part of a band is caused by a reduction in moisture and nutrients which results from the capture of moisture and nutrients by plants colonising the upper part of the band (Thiery et al., 1995). This process is reflected in a temporal succession of different soil crusts (Valentin and Bresson, 1992). The decline in vegetation cover on the lower edge of the band exposes soil to intensive rainfall causing the development of structural crusts which maximise runoff and which remain unaltered because of reduced termite activity. The acceleration of runoff in this zone increases erosion, removes the structural crusts and exposes the gravely layer. This in turn produces gravel crusts which generate even more intense runoff, but protect at the same time the soil from further degradation. The accumulation of wash deposits in the sedimentation zone reduces the slope gradient allowing the formation of sedimentation crusts.

The proportion of the clay and silt fraction (Fig. 2) in the soils of the degraded zone is very similar to that found in those of the central zone. The proportion of clay and silt in soils decreases across the degraded and runoff zones whilst that of sand increases.
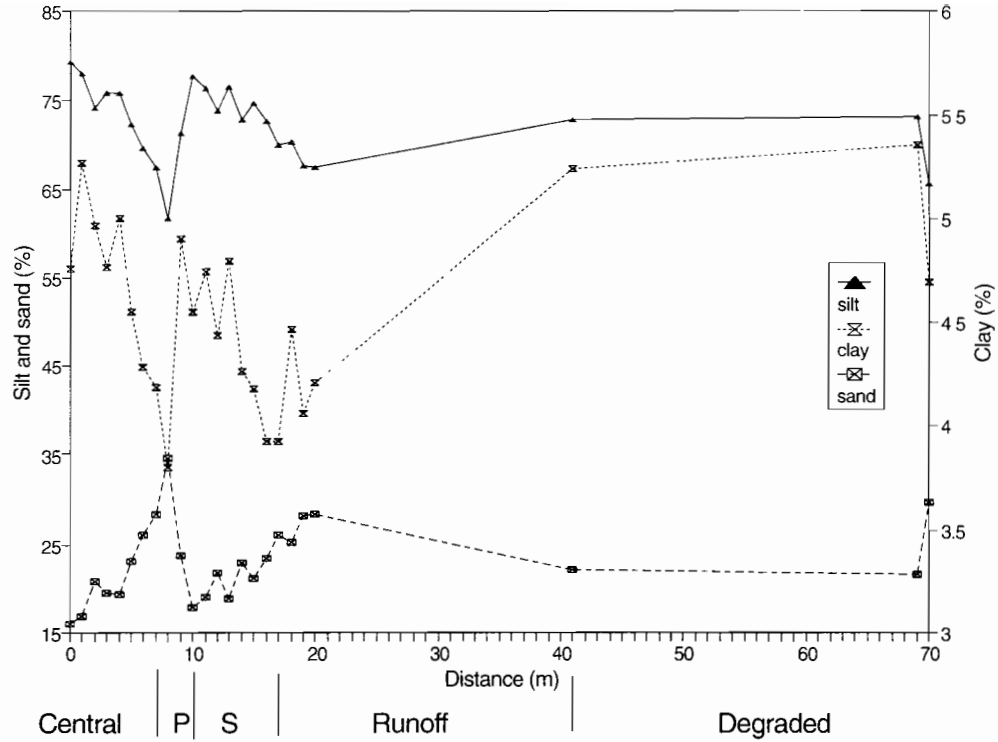
Fig. 2. Proportion of sand (> 1128 μm), silt (> 60 μm) and clay (< 2 μm) fractions in the soil along the soil sampling transect.

Structural and gravel crusts were identified in these zones (Table 1). There is a remarkable similarity in the distributions of silt and ^{137}Cs along the sample transect (Fig. 3): both generally decrease downslope from the degraded zone across the runoff zone and both increase in the sedimentation zone. There is also a strong relationship between crust types and brousse tigrée zones (Table 1). In general, the distribution of the mobile silt and clay fractions, of ^{137}Cs and of soil crusts suggest that soil is eroded in the degraded zone, transported across the runoff zone and deposited in the sedimentation zone.

The distribution of ^{137}Cs-derived net soil flux along the transect (Fig. 4) varies between -63 t ha^{-1} yr^{-1} and $+14$ t ha^{-1} yr^{-1}. The average net soil flux for each of these zones (Table 1) reveal a general pattern of decreasing net soil flux and show a strong relationship with crust type. The equivalent total soil loss depth is shown (Table 1). Sites in the degraded and runoff zones have the largest net soil loss amounting to an average total soil depth loss of 14.7 cm. In general, the levels of ^{137}Cs in the soils of the central and pioneer zones are slightly lower than the reference level (2066 ± 125 Bq m^{-2}) and hence these soils must have suffered net soil loss. Single net soil flux measurements from other interbands in the region (Chappell, 1995) have shown similar values for net soil flux (between -90 t ha^{-1} yr^{-1} and $+5$ t ha^{-1} yr^{-1}).

The only site of net soil gain in the present transect exhibits a rate considerably greater than that of the average annual dust accumulation (4 t ha^{-1} yr^{-1}), measured using the ^{137}Cs technique (Chappell, 1995). The large difference between these results suggests that the soil gain at this site is probably due not only to the accumulation of material redistributed by surface wash but also to the accumulation of dust. Adjacent to this site of net soil gain there is a micromound (Fig. 4) which coincides with the localised net soil loss probably as a result of surface wash from this point. This process probably accounts for the structural crusts in the pioneer zone (Table 1), the increased proportion of silt (Fig. 2), the decreased proportion of sand and the large net soil gain (Fig. 4). It is reasonable to suppose that similar processes are operating to remove soil

Table 1

Spatial extent along the sampling transect of brousse tigrée zones, soil crust classes and the average net soil flux per zone

Brousse tigrée zones						
	Central	Pioneer	Sedimentation	Runoff	Degraded	Central
Sample labels	A–G	H–J	K–Q	R–U	V–X	
Distance (m)	0–7	7–10	10–17	17–41	41–72	72–73
Soil crust location (m)						
Sieving, erosion and gravel		8.3–9.4	11–17	17–41	41–67	
Sedimentation		9	10–17			
Net soil flux (t ha^{-1} yr^{-1})	-5.10 ± 0.4	-16.67 ± 3.58	-7.61 ± 1.10	-43.17 ± 16.60	-25.74 ± 3.0	
Total soil depth (cm)	-1.6	-5.3	-2.4	-14.7	-8.8	
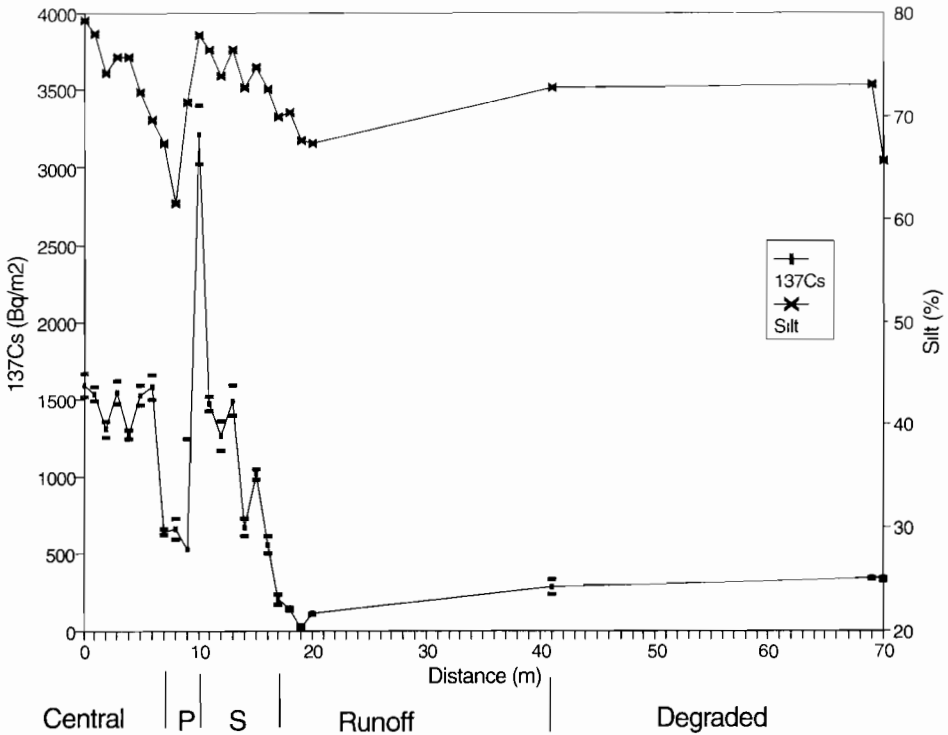
Fig. 3. Spatial distribution of ^{137}Cs (Bq m^{-2}) and silt content along the soil sampling transect.

from beneath the vegetated canopy and that they result in the general net soil loss in the central zone of the vegetated band.

A more plausible explanation for net soil loss in this central zone might be thought to be that when intense rainfall causes flooding in the upslope bare lane and the soil in the band is already nearly saturated, flood-water passes into and through the vegetated band (Thiery et al., 1995; p. 501). However, in the bands surrounding the present transect moisture levels were found (with neutron probes) to be large (Galle et al., this issue) and porosity is also thought to be large at these sites because of termite activity (Thiery et al., 1995). This suggests that the flood-water processes invoked to explain the net soil loss in the vegetated band sampled in this study do not take place in other vegetated bands. The difference between this transect and others may be the relatively steep gradient in the central and degraded zones downslope of the micromound (Fig. 4) which probably accelerates drainage and surface wash causing localised net soil loss.

Upslope of the micromound along the present sampling transect there has, in general, been net soil loss for the last three decades (Fig. 4). Nonetheless, the presence of sedimentation crusts (Table 1), the increasing silt content (Fig. 2) and the decreasing rate of soil loss (Fig. 4) in the sedimentation zone, all suggest that recent deposition has occurred on a previously eroded surface. This accumulation has occurred at least in the last 19 years, on the evidence of the dendrochronology date for a tree (*G. senegalensis*)
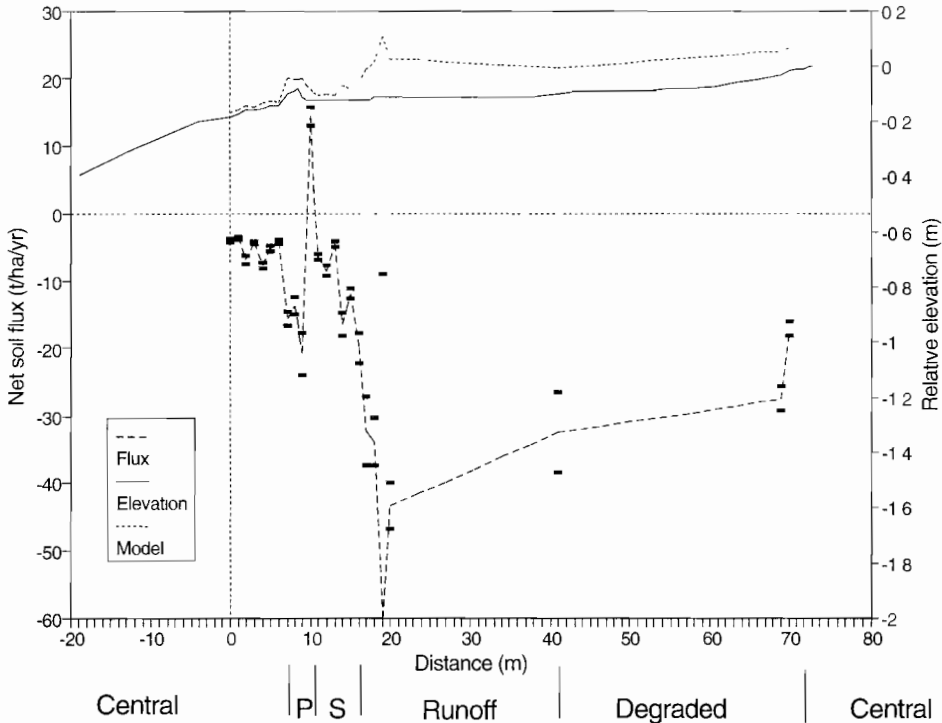
Fig. 4. Spatial distribution of net soil flux, measured relative elevation and modelled original relative elevation along the sampling transect.

located in the pioneer zone, adjacent to the site of net soil gain. The micromound probably creates a barrier for low intensity surface wash events and promotes sediment deposition, seedling emergence and, since deposition tends to decrease the slope gradient (Fig. 4), the upslope migration of the band. Thus, the accumulation rate in the sedimentation zone is a function of net soil flux and distance and it is tenable to propose that the distance of upslope migration of the vegetation band is the same as the distance between the centre of the micromound and the upslope edge of the sedimentation zone. This edge appears to be between the sedimentation and runoff crusts located respectively at 7 m and 8 m from the micromound centre. Thus, a first approximation to the upslope migration rate, provided by dividing the extent of the sedimentation zone by the approximate minimum duration of deposition (19 years, as indicated by the tree date), is 0.37 m yr^{-1} and 0.42 m yr^{-1}.

 Assuming that the upslope migration rate is constant, a more rigorous estimate of the distance of upslope migration can be predicted from a measurement of total soil loss at the edge of the sedimentation zone using the regression equation:

$$M = -0.0618F + 2.1902 \tag{4}$$

where M is the upslope distance from the centre of the micromound; and F is total soil loss (kg m^{-2}). The regression procedure minimises the least squares variation ($r^2 = 0.83$)

of the distance from the centre of the micromound and total soil flux for samples between the site of maximum net soil gain and minimum net soil loss (Fig. 5). The inclusion of an intercept term significantly improves the least squares fit. Although the site of net soil gain is included in the sedimentation zone, it was not included in the calculation of the regression equation because it was thought that the soil had accumulated from aeolian deposition and soil erosion from the micromound. Samples associated with runoff crusts in the runoff zone were included in the analysis because they improved the fit of the regression line. The total soil losses for sites bordering the sedimentation and runoff zones (-63.82 kg m^{-2} and -103.03 kg m^{-2}, respectively) were derived by multiplying the net soil loss at these locations (-1.99 kg m^{-2} yr^{-1} and -3.21 kg m^{-2} yr^{-1}, respectively) by 32, the total number of years. These total soil losses were substituted into Eq. (4) and provided a distance from the micromound of 6.1 m and 8.6 m, respectively, which resulted in a mean annual upslope migration rate of 0.19 m yr^{-1} and 0.27 m yr^{-1} for the last 32 years. This migration rate is consistent with detailed observations of digitised aerial photographs from 1950, 1975 and 1992 (Mougenot et al., in preparation) which produced a mean annual migration rate of between 0.2 m and 0.8 m from 1950 to 1975, and between 0.12 m and 0.48 m from 1950 to 1992.
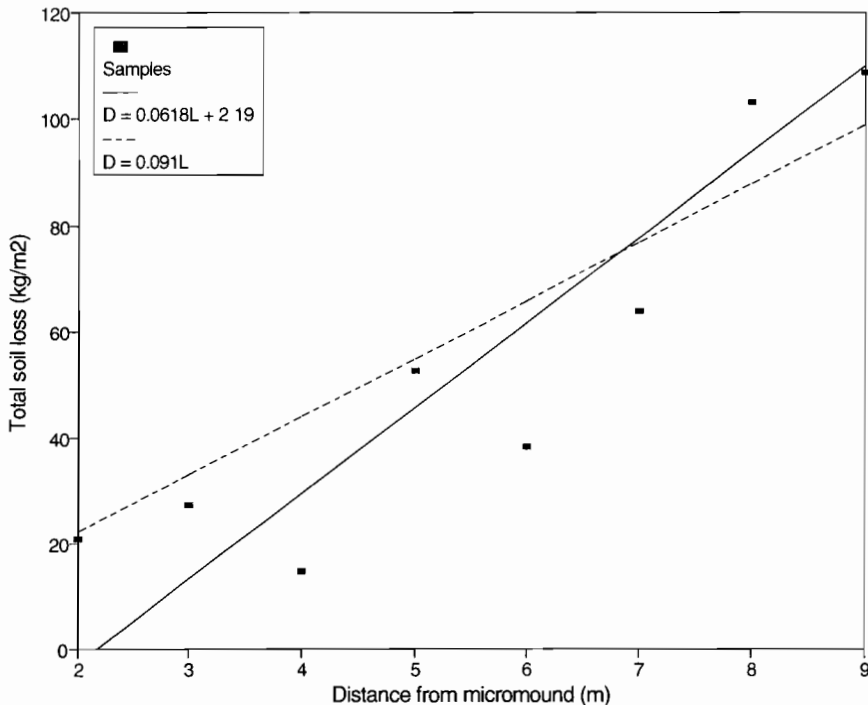

Fig. 5. Scatter plot of net soil loss and distance from micromound with fitted least squares linear regression lines.

4. Summary and conclusions

The ^{137}Cs technique for measuring net soil flux identified the vegetation band and the interband as zones of net soil loss. However, the soil texture, crust type and the ^{137}Cs content of samples obtained along the transect show that there is a decrease in net soil loss, resulting from recent accumulation, in the sedimentation zone of the downslope vegetation band. These apparently contradictory results are probably due to the particular band of this sample having a relatively steep topographic gradient that produces good drainage, which in turn results in localised surface wash and erosion processes beneath the vegetation. The accumulation on the upslope side of the vegetation band is probably caused by the presence of a micromound, which has reduced surface wash and enhanced deposition. There is corroboration of such accumulation in the evidence of the sedimentation crusts and in the model predictions for the upslope migration of the vegetation band (Thiery et al., 1995). The rate of accumulation in the sedimentation zone was considered to be representative of the upslope migration rate which was calculated to be approximately 0.19–0.27 m yr^{-1}.

These results show that the average annual migration rate of the banded vegetation can be calculated from accurate measurement of net soil flux for the last 32 years using the ^{137}Cs technique. The spatial variability along the transect (across the band) was anticipated but the variation along the vegetation band was not. It is necessary to ensure that a single transect is representative of the pattern of soil redistribution. This should be done either by detailed topographic sampling prior to soil sampling or by improved soil sampling which encompasses the spatial variation across and along the vegetation bands. Both approaches must account for the observed occurrence of the bay and headland pattern in the pioneer zone of the vegetation bands as this may be caused by differences in micro-topography and lateral flow between the vegetation bands.

In order to develop the ^{137}Cs technique for measuring soil redistribution in this environment many samples would be required which would be very time-consuming. A viable alternative might be to develop the relationship established here between different types of crust and their ^{137}Cs content to produce a calibration curve for rapid calculation of net soil flux from different crust types.

References

Casenave, A., Valentin, C., 1989. Les Etats De Surface De La Zone Sahelienne: Influence sur l'infiltration. Editions de l'ORSTOM, Paris.

Chappell, A. 1995. Geostatistical mapping and ordination analyses of ^{137}Cs-derived net soil flux in south-west Niger. Unpublished doctoral thesis, University of London.

Cornet, A , Montaña, C., Delhoume, J.P., Lopez-Portillo, J., 1992. Water flows and the dynamics of desert vegetation stripes In: Hansen, A.J., di Castri, F. (Eds.), Landscape Boundaries Consequences for Biotic Diversity and Ecological Flows. Ecological Studies, 92. Springer Verlag, New York, pp. 327–345.

Drees, L.R , Manu, A., Wilding, L.P., 1993. Characteristics of aeolian dusts in Niger, West Africa. Geoderma 59, 213–233

Higgitt, D.L., 1991. Soil erosion and soil problems. Prog. in Phys Geog. 15 (1), 91–100.

Lebel, T., Sauvegeot, H., Koepffner, M., Desbois, M., Guillot, B., Hubert, P., 1992. Rainfall estimation in the Sahel: the EPSAT-Niger experiment. Hydrol. Sci. J. 37, 201–215.

Leprun, J.C., 1992. Etude de quelques brousses tigrées sahéliennes: structure, dynamique, écologie. L'aridité, une contrainte au développement. In: Le Floc'h, E., Grouzis, M., Cornet, A., Billie, J.C. (Eds.), ORSTOM, Coll. Didactiques, Paris, pp. 221–244.

Manu, A., Geiger, S.C., Pfordresher, A., Taylor-Powell, E., Mahamane, S., Ouattara, M., Isaaka, M., Salou, M., Juo, A.S.R., Puentes, R., Wilding, L.P., 1991. Integrated management of agricultural watersheds (IMAW): Characterisation of a research site near Hamdallaye, Niger. TropSoils Bulletin No. 91-03. Soil Management CRSP North Carolina State University, USA/S and CSD Texas A&M University, USA/IN-RAN Niamey, Niger/USAID Niamey, Niger.

Martz, L.W., de Jong, E., 1991. Using caesium-137 and landform classification to develop a net soil erosion budget for a small Canadian Prairie watershed. Catena 18, 289–308.

Montaña, C., 1992. The colonization of bare areas in two-phase mosaics of an arid ecosystem. J. Ecol. 78, 789–798.

Mougenot, B., d'Herbes, J.M., Ichaou, A., in preparation. How do vegetated arcs move upwards in Niger. Submitted to Acta Oecologica.

McTainsh, G.H., Walker, P.H., 1982. Nature and distribution of Harmattan dust. Z Geomorph., N.F. 26, 417–435.

Sivakumar, M.V.K., 1989. Agroclimatic aspects of rainfed agriculture in the SSZ. In: Soil Crop and Water Management Systems for Rainfed Agriculture in the SSZ. Proceedings of an International Workshop, Jan. 1987, ICRISAT Sahelian Centre, Niamey, Niger, 17–38 ICRISAT, Patancheru, AP 502 234, India.

Sutherland, R.A., 1994. Spatial variability of ^{137}Cs and the influence of sampling on estimates of sediment redistribution. Catena 21, 57–71.

Sutherland, R.A., de Jong, E., 1990. Estimation of sediment redistribution within agricultural fields using caesium-137 Crystal Springs, Saskatchewan, Canada. Applied Geography 10, 205–221.

Thiery, J., d'Herbes, J.M., Valentin, C., 1995. A model simulating the genesis of banded vegetation pattern in Niger. J. Ecology 83, 497–507.

Valentin, C., Bresson, L.M., 1992. Morphology, genesis and classification of surface crusts in loamy and sandy soils. Geoderma 55, 225–245.

Walling, D.E., Quine, T.A., 1990. Calibration of caesium-137 measurements to provide quantitative erosion rate data. Land Degradation and Rehabilitation 2, 161–175.

Walling, D.E., Quine, T.A., 1992. The use of caesium-137 measurements in soil erosion surveys. Proc. IAHS Symposium on Erosion and Sediment Transport Measurement Programs in River Basins, Oslo, August, 1992.

White, L.P., 1969. Vegetation arcs in Jordan. J. Ecol. 57, 461–464.

Zhang, X., Higgitt, D.L., Walling, D.E., 1990. A preliminary assessment of the potential for using caesium-137 to estimate rates of soil erosion in the Loess Plateau of China. Hydrol. Sci. J. 35, 267–276.

Niger tiger bush as a natural water harvesting system

C. Valentin [a,*], J.M. d'Herbès [b]

[a] ORSTOM, 213, rue La Fayette, 75480 Paris Cedex 10, France
[b] ORSTOM, B.P. 5045, 34032, Montpellier Cedex 1, France

Abstract

Tiger bush in Niger has been often hypothesised to act as a natural water-harvesting system. The interband:band ratio (IBR) and the related efficiency of the system in terms of water concentration and woody biomass production appeared as crucial questions to be addressed and documented. This study focused on the role of annual rainfall upon the structure and the functioning of the tiger bush system. A regional transect, totalling approximately 200 km in length was established north/south across the rainfall gradient. It included 10 local transects each spanning five interbands and bands. Along the local transects, surface features were carefully recorded as well as woody biovolume. One of these local transects was completely harvested so that biovolume could be related to biomass. Annual woodcutting was estimated after a detailed regional study. In addition to field measurements performed in 1995, the IBR was measured on sequential aerial photographs (1950, 1955, 1962, 1975, 1992), using a $16 \times$ binocular magnifier combined with a stage micrometer with 0.1 mm division. A simple model of rainwater redistribution was designed based on surface conditions properties. The best correlation of IBR was obtained with annual rainfall averaged over the last 15 yr (Ra_{15}). This ratio was dramatically increased where Ra_{15} declined below a threshold of approximately 350 mm. The ratio between the water shedding zone (RZ) and the infiltration zone (IZ), RZ:IZ, based on field crust type survey, was a better predictor for the water-harvesting efficiency of the system than was IBR. The water harvesting model could be used as a satisfactory predictor for woody biomass ($R^2 = 0.83$). Best simulations were obtained when wood cutting during the last 8 yr was accounted for. The water harvesting and concentration enables wood production which equals that of the forest in much more humid southern zones. The thicket production in the banded patterned systems succeeds in over-compensating the barrenness of the interbands, even exceeding woody biomass of industrial plantations in the same region. Due to the gradual thickening of the infiltration zone, the water-harvesting system becomes no longer effective at the wetter southern end of the tiger bush

---

* Corresponding author.

domain ($Ra_{15} = 685$ mm). Conversely, the decreasing favourable conditions to infiltration should lead to a dry limit of ($Ra_{15} = 155$ mm). Therefore, woody biomass production of the tiger bush is controlled by two opposing trends linked to mean rainfall. The result is that the production of these structures reaches a maximum at 550 mm mean annual rainfall. The sustainable use of tiger bush in the longer term requires the careful maintenance of this natural water harvesting system, with no attempts of afforestation in the interbands, no agriculture, and only moderate wood harvesting in the vegetation bands. Rehabilitation strategies which mimic the natural tiger bush ecosystem are the most appropriate under these climatic circumstances. © 1999 Elsevier Science B.V. All rights reserved.

1. Introduction

Under arid and semi-arid conditions, the concentration of resources into patches results in a higher plant productivity (Noy-Meir, 1973). Such patches occur frequently in the form of dense vegetation bands aligned perpendicular to slope, interspersed with bare soil. These banded vegetation patterns, which support distinctive communities of grasses, shrubs and trees, have been reported throughout the Sahelian zone from Mauritania (Audry and Rossetti, 1962) to Somalia (MacFayden, 1950), in East African (Belsky, 1989) and South African semi-arid regions (Van der Meulen and Morris, 1979) as well as in the Middle East (Vezey-FitzGerald, 1957; White, 1969); Mexico (Cornet et al., 1988) and Australia (Slatyer, 1961). Many authors considered overland flow as an essential factor in the formation and the maintenance of these banded systems (e.g., Ambouta, 1984; Mabbut and Fanning, 1987; Tongway and Ludwig, 1990; Greene, 1992; Dunkerley and Brown, 1995; Thiéry et al., 1995).

In these environments, often referred to as 'tiger bush' in West Africa (in French 'brousse tigrée', Clos-Arceduc, 1956), the capture and storage of limited water resource appeared to be optimized through a spatial partitioning between run-off, run-on and infiltration, the bare interband acting as a source, and the vegetation band as a sink (Noy-Meir, 1973; Ludwig et al., 1998). In support of this natural water harvesting theory, infiltration input in the bands was found to exceed 1.5–2.5 times the local precipitation (Hemming, 1965; Cornet et al., 1988; Bromley et al., 1997).

In a given site, the amount of run-on to the vegetation bands is generally assumed to be controlled by the surface conditions of the interband. Hydrologic characters of the two main system components, often broken into subzones, have been assessed using rings method (Slatyer, 1961; Ambouta, 1984), rainfall simulation tests (Tongway and Ludwig, 1990; Delhoume, 1996) and disk infiltrometers (Greene, 1992; Vandervaere et al., 1997; Bromley et al., 1997). However, relatively little is known about factors controlling water shedding and trapping efficiencies and run-off models are still needed to predict redistribution within the system.

If the vegetated run-on band requires a certain area of interband to shed run-off water, the relative dimensions of these two components must be an essential factor to the maintenance of the system. It has been thus postulated that the width of the interbands

should increase relative to that of the bands as rainfall decreases. (Gavaud and Boulet, 1967; Ambouta, 1984). The interband intervals can range from one to four times as wide as the bands (Gavaud and Boulet, 1967; Mabbut and Fanning, 1987). However, no factor has been clearly shown to influence the width of the vegetation area as compared to the run-off contributing area (Dunkerley and Brown, 1998).

Even less documented is the plant biomass production within the band. Because water inflow is the first critical factor for production under these climatic conditions (Noy-Meir, 1973), it seems reasonable to speculate that productivity should be affected by the factors controlling run-off from the bare band and infiltration into the vegetation band.

The objectives of this study were (1) to investigate the factors influencing the interband width:band width ratio, (2) to design a simple predictive model of rainwater redistribution based upon surface conditions, (3) to relate woody phytomass to the efficiency of the tiger bush regarded as a water-harvesting system.

2. Methods

2.1. The tiger bush domain in Niger

In south western Niger, the plateaux where tiger bush patterns may occur covers an area estimated at 22 000 km^2 (Ambouta, 1984) and located between 13°N and 15°N (Gavaud and Boulet, 1967). This region shares many characteristics of sites where vegetation banding has been reported. The annual rainfall is characterized by a strong temporal and spatial variability. This is due to periodic regional droughts and the randomness of local convective storms. However, in the long-term, annual rainfall clearly decreases from approximately 750 mm in the south to 400 mm in the north (Gavaud and Boulet, 1967). Rainfall distribution is monomodal, starting usually in June and lasting until mid-September. Intensive dry spells occur from late September until the subsequent rainy season in June. In Niamey, most rainfall occurs in storm events. The median rainfall intensity being 35 mm h^{-1} and 35% of the total rainfall falling with an intensity exceeding 50 mm h^{-1} (Lebel et al., 1997). Mean monthly maximum and minimum air temperatures are 36.0°C and 22.2°C, respectively with the maximum in April (40.9°C) and the minimum in January (15.9°C). Mean annual potential evapotranspiration is 2294 mm (Sivakumar et al., 1993).

The region is underlain by the Birrimian crystalline basement complex, part of the Precambrian pan-African shield. The overlying rocks consist of a complex formation of loamy sandstone of Miocene deposits called the Continental Terminal. These highly weathered materials are covered with sand deposits of late Quaternary age which tend to plug the dry valley systems and in the north form dunes oriented ENE–WSW (Gavaud and Boulet, 1967; Wilding and Daniels, 1989; d'Herbès and Valentin, 1997). The gentle undulating landscape is disrupted by broad, nearly flat-topped, ironstone-capped plateaux of the Continental Terminal. The tiger bush patterns occur only on these plateaux. However, where thin, discontinuous aeolian sands survive on the plateaux, there is typically no vegetation banding probably due to an insufficient surface for production of

run-off. In the tiger bush systems, the bare interbands are generally steeper (slope gradient = 1.3%) than the vegetated bands (0.8%; Ambouta, 1984).

In this region, the differences in the topsoils of the interbands and bands have been ascribed to the influence of the vegetation itself through accumulation of litter and rooting (White, 1971; Ambouta, 1984; Barker, 1992). In general, these soils exhibit between 0.1 and 0.9 m of gravely loam (35–60% silt and clay) over ubiquitous ironstone gravel and more or less cemented sesquioxyde sheets. Mineral reserves in these acidic soils (pH < 5.0) are low. Due to the iron pan and the gravel, these soils offer a low water-holding capacity. According to the reference base of the International Society of Soil Science et al. (1994), most of these soils have been classified as Skeletic Leptosols (d'Herbès and Valentin, 1997). Detailed physical and pedologic descriptions have been given by Ambouta (1984), Wilding and Daniels (1989), Barker (1992) and Legger and van der Aa (1994).

Typically, the thickets of the Nigerien tiger bush are contour-aligned and arranged in more or less concentric rings surrounding the slightly convex tops of the plateaux, forming more parallel arcs than straight bands. The downslope distance between arcs ranges from 35 to 150 m, and the width of the thickets from 10 m to 40 m (Gavaud and Boulet, 1967; White, 1970; Bromley et al., 1997). These arcs may extend up to 100–300 m. The wavelength, i.e., interband width plus band width, is mainly controlled by slope (d'Herbès and Valentin, 1998; Eddy et al., 1998).

The interbands are completely devoid of vegetation. Starting from the bare area, a sequence of three zones is more or less systematically encountered in a downslope direction through the arc (Ambouta, 1984; Thiéry et al., 1995; Bromley et al., 1997): (1) a grassy open bush consisting of a nearly total grass cover of annual plants, such as *Microchloa indica* (Linn. f.) (Seghieri et al., in press), associated with the shrub *Guiera senegalensis* J.F. Gmel; (2) a closed bush with a canopy cover between 60 and 100% of tall shrubs and trees, up to 8 m, dominated by *Combretum* spp., with an understorey of small shrubs, such as *Gardenia sokotoensis* Stapf et Hutch, and a very sparse grass cover (< 5%); (3) a bare open bush with a cover declining from 40 to 0% contributed mainly by *Combretum micranthum* and small shrubs as *Boscia angustifolia* A. Rich. and *B. senegalensis* (Pers.) Lam.

2.2. Regional transect and field measurements

To investigate the effect of rainfall upon the geometry and the woody biomass production of the tiger bush pattern, a regional transect, was established north/south across the rainfall gradient (Fig. 1). Nearly 200 km long, it included nine study sites at intervals as regular as possible depending on tiger bush occurrence and accessibility for a four-wheel drive vehicle. Zoukouara was the southernmost plateau with tiger bush that could be recognized on the panchromatic SPOT images of February 1991 (field resolution 10 m). Only one selected site, located north of Farantara, our northernmost site, was not sampled due to safety reasons, the region north of the 14° parallel being out of governmental control. Each site consisted of a local line transect spanning five wavelengths of the banding. One site, Dingazi, encompassed two transects, one with typically patterned and one with large bands and interbands.
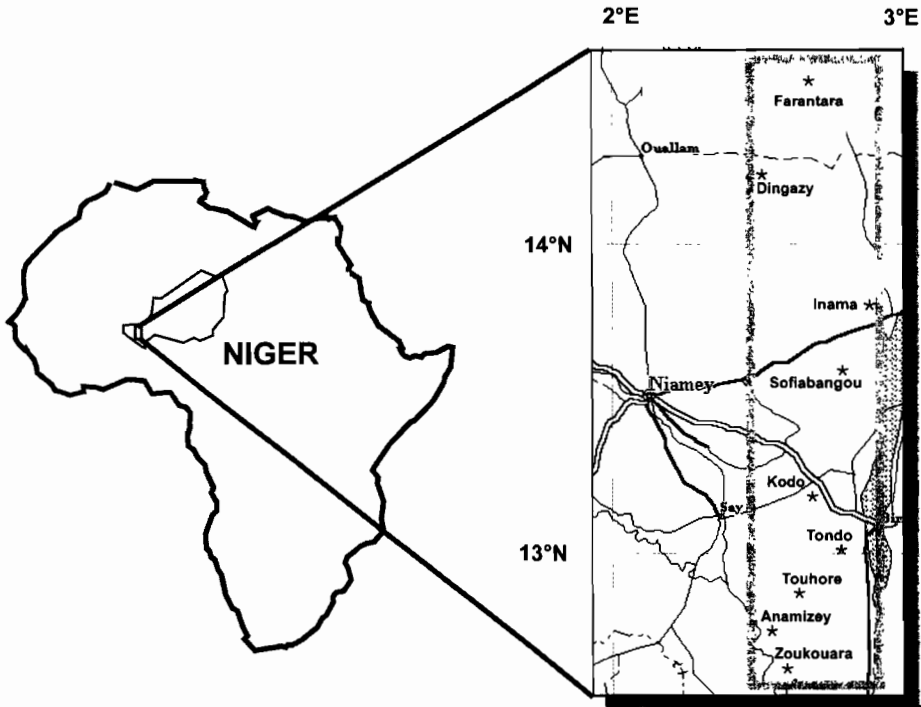
Fig. 1. Location map of the regional transect including the nine selected sites.

The location of each local transect was assessed using a Global Position System and recorded on aerial photographs at 1:50 000. The transect started in the down-slope portion of the uppermost band, a degraded zone (D, Fig. 2), crossed the bare run-off area (R), into the leading edge of the next band, a sedimentation zone (S) and a pioneer zone (P) and the core of this band (C), crossed the same sections in the second, third and fourth bands and stopped at the boundary of the down-slope portion of the fifth band (D). Detailed topographic profiles along these transects were derived from careful survey with an optical theodolite. Steel measuring tapes were laid on the ground to demarcate the boundaries of the tiger bush elements as characterized by vegetation cover and soil surface features using the method presented by Thiéry et al. (1995).

Along the line transects, surface features were carefully recorded after the crust typology of Valentin and Bresson (1992) and the run-off capability classification of Casenave and Valentin (1992). The portions of areas of the surface covered by these classes (%) were visually assessed at intervals varying from 0.5 m to 15 m depending on the heterogeneity of the soil surface. The main features of the different classes of surface conditions identified in the tiger bush transects are presented in Table 1.

In tandem with the topographical survey, the woody vegetation was visually assessed along the line transect, in terms of soil cover (Sc, %), mean shrub height (Msh, m) and dominant species. The combination of vegetation and surface features survey resulted in the definition of the five typical zones presented in Fig. 2 and in Table 2.
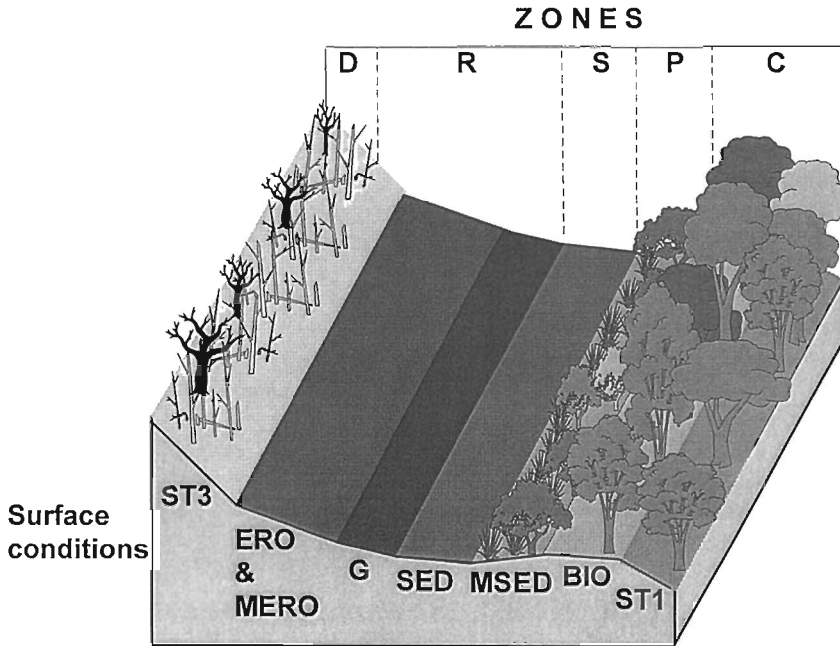
ZONES

Fig. 2. Schematic cross-section across a tiger bush wavelength showing the different zones (see Tables 1 and 2 for definitions of zones and surface conditions).

The phytovolume (Pv_z, m^3) was computed for any given zone z, as

$$Pv_z = sl_z Sc_z Msh_z \qquad (1)$$

where s is the width of the transect (1 m), l_z (m) is the length of the zone z along the transect, Sc_z (%) is the soil cover and Msh_z the mean height of woody vegetation (m) in zone z.

2.3. Estimation of aboveground woody phytomass

To assess the aboveground woody phytomass, woody plants were exhaustively harvested along a 20-m wide transect spanning six thickets in Sofiabangou, the most central site of the regional transect (Fig. 1). The dry woody phytomass (WM) was then assessed including leaves, branches and timbers for the six thickets (Ichaou, 1995). Since the phytovolume (PV) of these thickets had been assessed, a relation with WM could be established, enabling the conversion of PV (m^3) into WM (kg) through the multiplicative coefficient of 1.64 (kg m^{-3}). Assuming that this relation was valid for similar plant communities, it was applied to the ten transects.

In the view of relating WM to water supply, one must distinguish woody phytomass per hectare of thicket core (WMt) from the woody phytomass per hectare of patterned plateau (WMp = WMt Iz, where Iz is the percentage of the transects occupied by thicket cores). WMp had to be broken into two categories: WMo that was observed in situ and

Table 1

Main features and properties of the different surface conditions in the Nigerien tiger bush (adapted from Valentin and Bresson, 1992; Casenave and Valentin, 1992)

Type	Structure	Thickness (mm)	Infiltrability (mm ha^{-1})	Mean run-off coefficient[a] (Rc, %)	Zone[b]
Structural crusts					
Slaking (ST1)	rough surface, weak textural differentiation, weak void interconnection	1–3	5–8	35	C
Sieving (ST3)	coarse sandy layer at the top, vesicular fine sandy layer, seal of fine particles at the bottom	2–10	0–5	50	R
Coarse pavement (G)	similar to the sieving crust including coarse fragments and much pronounced vesicular porosity	2–30	0–2	90	R
Erosion crusts (ERO)	smooth exposed seal made of fine cemented particles, possible vesicles	< 1	0–2	85	R
Microphytic erosion (MERO)	similar to ERO but colonised by microphytes as algae	< 1	0–2	85	R
Depositional crusts					
Run-off (ROF)	interbedding of sandy layers and seals of finer particles, possible vesicles	2–20	1–5	50	R
Sedimentary (SED)	larger particles at the top, finer particles at the bottom, possible vesicles, frequent curled-up plates	2–50	0–2	72.5	S
Microphytic sedimentary (MSED)	similar to S but more platy in structure and colonised by microphytes as algae and mosses	2–50	4–7	50	P
No crust (BIO)	continuous and evolved forest litter, high termitic porosity	–	25–40	7 5	C

[a]Rc: mean cumulative run-off/rainfall ratio, as assessed through rainfall simulation tests.

[b]Main zone of occurrence, D: degraded, R. run-off, S: sedimentation, P: pioneer, C: central (after Thiéry et al., 1995).

Table 2
Main characteristics of the zones across the Nigerien tiger bush (see Fig. 2)

Zone	Shrubs/trees cover	Main surface features	Slope gradient	Microtopographic features
Degraded	low	ST3	moderate	common microsteps
Run-off	nil	ERO, MERO, G, ROF	low	
Sedimentation	nil	SED	nil–very low	
Pioneer	low	MSED	very low	frequent micro-counterslopes
Central	high	BIO, ST1	very low	

WMc that had been cut for fuelwood over a certain period of time. We have therefore WMp = WMo + WMc.

The estimation of woodcutting has been carried out within a circle centred in Niamey with a 150-km radius (Project Energie II, 1991). During the year 1990, every day, 24 h a day, every wood transport entering Niamey was enquired about the wood amounts and its origin. The whole area was divided into squares of 3240 ha. Considering that local wood cutting on the plateaux is insignificant compared to the export to Niamey, the annual wood cutting was assessed for each of these squares. This annual rate of wood cutting was then categorized into five gross classes from < 500 tons to > 6000 tons. The original data from the squares encompassing our nine sites were provided by one of the investigators of the woodcutting study (Montagne, personal communication). However, the proportion of each square occupied by tiger bush was unknown. Therefore, we have held constant the proportion of dense vegetation on the plateaux to equal 5.2% which is the mean value for this soil cover as assessed through satellite image analysis of the square degree of Niamey (lat.: 2–3°E; long.: 13–14°N; d'Herbès and Valentin, 1997). Because we had no indication of the long term response of woody biomass to wood cutting, we used different levels of wood cutting intensity from 5 to 15 yr to evaluate WMc.

2.4. Estimation of interband:band ratio from sequential aerial photographs

To investigate the possible effect of rainfall upon the interband:band ratio (IBR) of the banded patterns, we studied sequential aerial photographs at approximately 1:50 000-scale taken in 1950, 1955, 1962, 1975 and 1992 (Table 3). For each photograph, we pinpointed the transect sampled in the field, and measured the total length of the transect and the width of the thickets using a 16 × binocular magnifier combined with a stage micrometer with 0.1 mm divisions. We estimated the error to be < 10%, given the marked contrast between thicket and bare interband.

2.5. Estimation of annual rainfall in space and in time

A simple model had to be designed to estimate the annual rainfall over a given period at a given location along the regional transect. In Niamey, rainfall data are available for

Table 3
Aerial photography specifications (see Fig. 1 for site location)

| Date | Nov. 1950 | Nov.–Dec. 1955 | Sept.–Nov. 1962 | Jan–Apr. 1975 | Sept. 1992 | Oct.–Nov. 1992 |
| Mission | IGN-AOF | IGN-ND-31-II | IGN, ND, 31-XV | IGN, 75 NIG 40/600 | NASA, Hapex–Sahel | DG-DA/IGNN-JICA |
Approx. scale	1:50 000	1:50 000	1:50 000	1:50 000	1:50 000	1:60 000
Farantara	011–318		230	3297		1–21
Dingazi	011–153		352	3143		4–19
Inama	016–163		255	2635		9–21
Banizoumbou	016–338		337	2767	88	
Kodo	016–596		603	2961		
Tondo	016–723	506	698	3090		
Touhore		485		4846		
Anamizey		416		4892		
Zoukouara		353		4943		

the period 1905–1995. However we limited ourselves to a period of 20 yr preceding the oldest aerial photograph, i.e., 1930. Long-term annual rainfall patterns were plotted using n-years moving averages, n being varied from 5 to 20 yr. Relating the dates of the aerial photographs to the annual rainfall in Niamey averaged over the period 1930–1995 (556 mm), and to the 10-yr and the 20-yr moving averages, it appeared that photographs of 1950, 1955 and 1975 were taken after a period of about average rainfall, 1962 of above average rainfall, and 1992 of pronounced below average rainfall.

As shown by many authors (e.g., Lebel et al., 1992; Sivakumar et al., 1993), the Niamey region is characterized by strong latitudinal variation of annual rainfall. Over the period 1950–1989, Lebel et al. (1992) estimated the increasing north-to-south gradient as approximately constant and equal to 100 mm per degree of latitude. Using the data set of Sivakumar et al. (1993) over the period 1931–1990, including five locations along the gradient, the mean annual rainfall (Ra) could be regressed onto latitude (L) through the equation

$$Ra = 2930.8 - 179.12\,L \tag{2}$$

where Ra is mm and L is degrees (Fig. 3; $R^2 = 0.96$).

Because large scale averages retain this general climatic gradient (Lebel et al., 1992), we assumed that this latitudinal relation held constant over time. Considering the mean annual rainfall in Niamey Ran (Latitude 13.5°, Fig. 4) over a given period we had:

$$Ra_{sp} = Ra_{np} - 179.12(Ls - 13.5) \tag{3}$$

where Ra_{sp} (mm) was the mean annual rainfall at the latitude Ls (in degrees), over the time-period p.
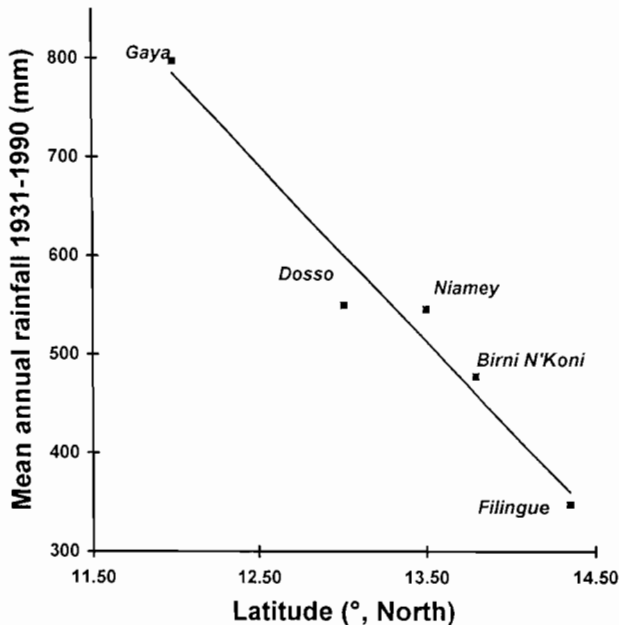

Fig. 3 Influence of latitude upon annual rainfall averaged over the period 1931–1990 (after Sivakumar et al., 1993) for five Nigerien cities as affected by latitude ($R^2 = 0.96$).
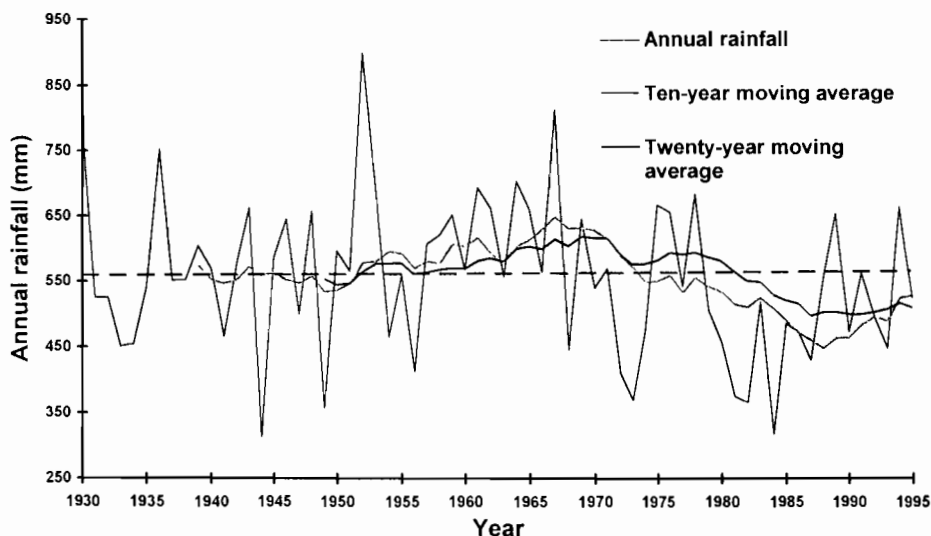
Fig. 4. Annual rainfall in Niamey (1930–1995).

Due to the high temporal and spatial variability of rainfall in the region, such a rough model was unable to estimate annual rainfall, but was postulated to reflect the shifts of the isohyets commonly observed over a long period in the region (Sivakumar et al., 1993).

2.6. The water harvesting model

Three simplifications and assumptions were made.

1. The five wavelengths of each local transect were broken into ten distinct parts including five identical run-off zones (RZ) and five identical infiltration zones (IZ). The run-off zones were characterized by the percentages of surface types ST3, ERO, G, SED and MSED (Table 1) averaged over the five wavelengths. Due to their similarities, the ST3 and ROF (Table 1) types were merged into a single category. Similarly, no distinction has been made between surfaces ERO and MERO. The infiltration zone was defined by the percentages of ST1 and BIO surface types.

2. For each of these ten zones, the amounts of run-off (Off), run-on (On), and infiltration (In) was calculated using the model proposed by Casenave and Valentin (1992), and recently validated at similar scales in the region (Peugeot, 1995; d'Herbès and Valentin, 1997). Water flows were assumed to be additive which means that flows in one zone were the sums of flows for each type of surface identified in the zone (Valentin and Casenave, 1992). For each type of surface, the values of the run-off coefficient (Rc) and hence of its infiltration coefficient (Ic = 1 − Rc) are presented in Table 1.

3. The first run-off zone was assumed to receive no run-on from upslope, in other words to be the uppermost of the whole hillslope.

Table 4
Main characteristics of the ten local transects along the regional transects

Site	Latitude	Longitude	SG(%)	MWL(m)	$VC_{50}(\%)$	$VC_{55}(\%)$	$VC_{62}(\%)$	$VC_{75}(\%)$	$VC_{92}(\%)$	$VC_{95}(\%)$	$Ra_{15-1995}$
Farantara	14°28.87'	2°38.61'	0.40	55.3	0.44		0.47	0.39	0.31	0.30	310
Dingazi1	14°13.18'	2°30.20'	0.18	131.5	0.45		0.51	0.46	0.36	0.44	360
Dingazi2	14°11.71'	2°30.87'	0.21	64.4	0.89		0.52	0.53	0 44	0.39	363
Inama	13°44.97'	2°49.12'	0.25	66.2	0.46		0.50	0.47	0 37	0.38	441
Sofiabangou	13°33.04'	2°46.44'	0.41	89.7	0.44		0.51	0.53	0.45	0.47	476
Kodo	13°12.52'	2°40.88'	0.41	86.1	0.51		0.57	0.47		0.45	537
Tondo	13°01.60'	2°43.19'	0.30	77.8	0.57	0.58	0.56	0.54		0.46	570
Touhore	12°53.56'	2°39.12'	0.28	71.3		0.60		0.60		0.58	594
Anamizey	12°46.83'	2°34.92'	0.71	55.5		0.64		0.56		0.51	614
Zoukouara	12°38.25'	2°40.20'	0.48	55.0		0.66		0.66		0.64	641
Mean	13°47.50'	2°64.69'	0.36	75.3				0.53		0.46	491

SG: slope gradient; MWL: mean length of a cycle including bare interband and vegetated band (1995); Vc_n: vegetation cover in the year n as assessed from aerial photographs and in the field in 1995; Ra_{15-95}: estimated annual rainfall averaged over the 15 yr prior to 1995.

Based on these simplifications and assumptions, the basic equations for Off, On, and In could be written as

$$Off_z = Ra \sum_{s=1}^{s=n} Rc_s C_s \tag{4}$$

$$On_z = Off_{z-1}(1_{z-1}/1_z) \tag{5}$$

$$In_z = Ic_z(Ra + On_z) \tag{6}$$

where Off_z (mm) is the run-off production of the length percentage l_z (%) along the local transect occupied by the zone z, Ra is annual rainfall (mm), Rc_s (%) is the run-off coefficient of the surface type s and C_s (%) the percentage of surface occupied by the surface type s.

The component $\sum_{s=1}^{s=n} Rc_s C_s$ is the mean run-off coefficient of the zone z (Rc_z)

On_z (mm) is the run-on received by the zone z from the upstream adjacent zone $z - 1$.
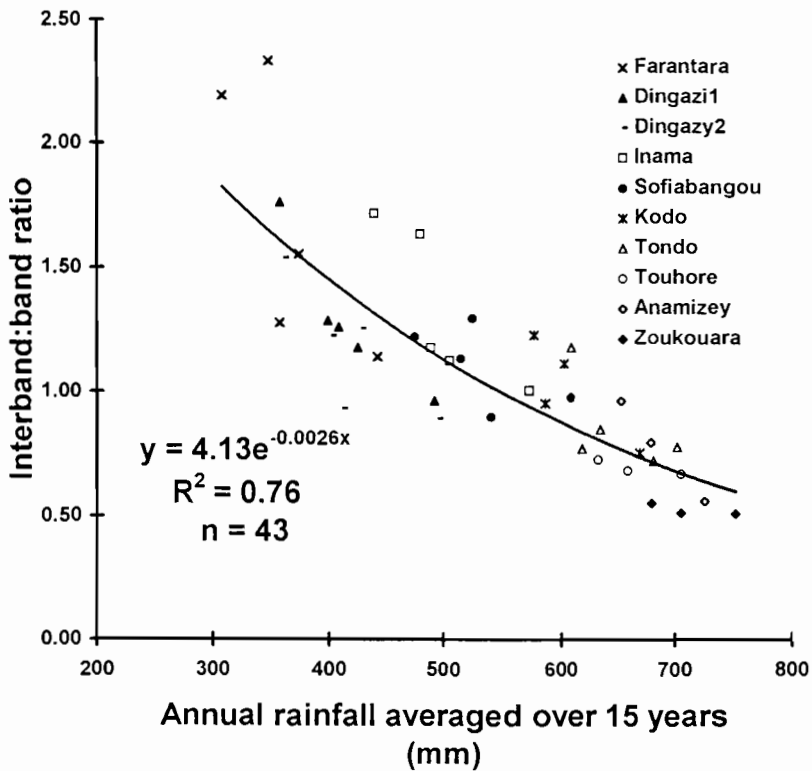
Fig. 5. The influence of annual rainfall averaged over 15 yr upon interband·band ratio after field measurements (1995) and aerial photographs of 1950, 1955, 1962, 1975, and 1992 from ten local transects across a regional transect in Niger

Ic_z (%) is the infiltration coefficient of the zone z.

The water harvesting efficiency (WHE) of the system is assessed by the ratio In/Ra calculated for the infiltration zone, combining Eqs. (5) and (6):

$$WHE = Ic_{iz}(1 + Rc_{rz}Rz/Iz) \qquad (7)$$

where Ic_{iz} (%) is the infiltration coefficient of the infiltration zone, Rc_{rz} (%) the run-off coefficient of the run-off zone, Rz (%) the length of the run-off zone and Iz (%) the length of the infiltration zone.

3. Results

3.1. The impact of rainfall upon interband:band ratio

The main characters of the ten local transects are presented in Table 4. We combined the data on interband:band ratio (IBR) measured on the sequential aerial photographs over the period 1950–1992 and the field observations of 1995. IBR ranged from 0.51 to 2.33 depending on climatic conditions. Best correlation of IBR with Ra_p ($R^2 = 0.76$) was found for a time period of $p = 15$ ($R^2 = 0.60$, 0.64 and 0.68 for $p = 5$, 10 and 20, respectively). Fig. 5 clearly portrays the impact of temporal and spatial variations of Ra_{15} upon IBR. This figure suggests that IBR was dramatically increased where Ra_{15}

Farantara 1962   **Farantara 1992**

Fig. 6. Aerial photographs from Farantara site. The interband:band ratio was increased from 1.13 in 1962 ($Ra_{15} = 426$ mm) to 2.3 in 1992 ($Ra_{15} = 315$ mm).

Table 5

Main surface characteristics and run-off properties of each site
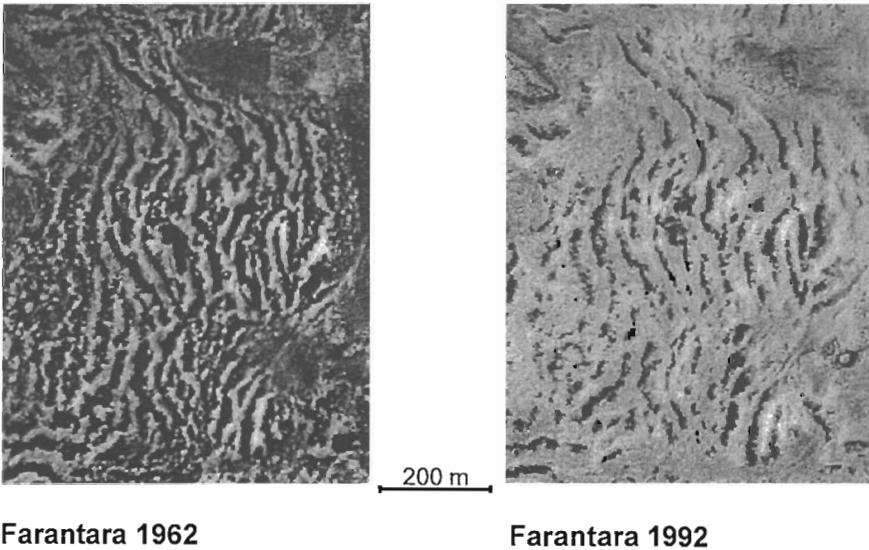
Site	ST3(%)	ERO(%)	MERO(%)	G(%)	SED(%)	MSED(%)	BIO(%)	ST1(%)	RZ(%)	IZ(%)	RZ:IZ	Rc_{rz}(%)	Ic_{iz}(%)
Farantara	0 15	0.44	0.00	0.00	0.15	0.12	0.10	0.03	0.87	0.13	6.83	0.52	0.87
DingaziY	0.23	0.23	0.00	0.11	0.09	0.15	0.06	0.13	0.81	0.19	4.18	0.55	0.73
DingaziL	0.25	0.10	0.00	0.08	0.14	0.24	0.13	0.06	0.81	0.19	4.37	0.46	0.84
Inama	0.21	0.18	0.07	0.02	0.21	0.15	0.10	0.06	0.84	0.16	5.32	0.42	0.82
Sofiabangou	0.22	0.11	0.03	0.09	0.13	0.11	0.15	0.15	0.70	0.30	2.37	0.44	0.78
Kodo	0.18	0.11	0.08	0.18	0.09	0.06	0.16	0.14	0.70	0.30	2.38	0.58	0.80
Tondo	0.06	0.08	0.13	0.06	0.18	0.16	0.18	0.16	0.67	0.33	2.00	0.38	0.80
Touhore	0.31	0.06	0.04	0.07	0.12	0.07	0.17	0.15	0.68	0.32	2.13	0.40	0.80
Anamizey	0.19	0.08	0.02	0.24	0.06	0.11	0.18	0.11	0.70	0.30	2.37	0.62	0.82
Zoukouara	0.19	0.15	0.07	0.00	0 06	0.02	0.22	0.28	0.50	0.50	0.99	0.30	0.77
Mean	0.21	0.15	0.05	0.08	0.12	0.12	0.15	0.13	0.72	0.27	3.29	0.47	0.80

The surface types are listed in Table 1.

RZ is the proportion of surface occupied by the run-off zones, IZ by the infiltration zones; Rc_{rz} is the run-off coefficient of the run-off zones, Ic_{iz} the infiltration coefficient of the infiltration zones.

Table 6
Results from five iterations of the rainwater redistribution model, including run-off amount (Off$_n$, mm) in the run-off zone and infiltration amount (In$_n$, mm) in the core of the thicket for the wavelength n; mean infiltration amount (MIn, mm) and water-harvesting efficiency (WHE = MIn/Ra15)

Transect	Off$_1$	In$_1$	Roff$_2$	In$_2$	Roff$_3$	In$_3$	Roff$_4$	In$_4$	Roff$_5$	In$_5$	MIn	WHE
Farantara	160	1218	173	1299	174	1305	174	1305	174	1305	1287	4.15
Dingazi1	197	862	239	990	245	1009	246	1012	246	1012	977	2.71
Dingazi2	168	925	186	992	187	997	187	997	187	997	982	2.70
Inama	186	1171	206	1260	208	1267	208	1267	208	1267	1246	2.83
Sofiabangou	210	765	250	838	253	845	254	846	254	846	828	1.74
Kodo	309	1016	372	1134	379	1148	380	1150	380	1150	1119	2.08
Tondo	216	797	254	859	257	864	258	864	258	864	850	1.49
Touhore	239	882	281	953	284	959	284	960	284	960	943	1.59
Anamizey	383	1250	455	1389	463	1405	464	1407	464	1407	1371	2.23
Zoukouara	195	644	253	689	257	692	257	692	257	692	682	1.06
Mean	226	953	267	1040	271	1049	271	1050	271	1050	1028	2.26

declined below a threshold of approximately 350 mm. For example, in Farantara (Fig. 6) IBR was twice as large in 1992 than in 1962 whilst it remained virtually unchanged in Zoukouara since 1955 (Table 4).

3.2. Surface properties and hydrologic simulations

Aerial photographs alone could not provide accurate data on the areal proportion of run-off and infiltration zones along the local transects since some sections of the vegetated bands contribute significantly to run-off, (Fig. 2; Table 1). Specific data on soil surface conditions are thus necessary. Table 5 lists the areal proportion occupied by each surface type along the local transects. No clear climatic influence was shown for run-off coefficients of the run-off zones (Rc$_{rz}$) or for the infiltration coefficient of the

Table 7
Woody phytomass per hectare of thicket core (WMt) and per hectare of patterned plateau (WMp) as the sum of the biomass evaluated in the field (WMo) and the biomass cut over a period of 8 yr (WMc)

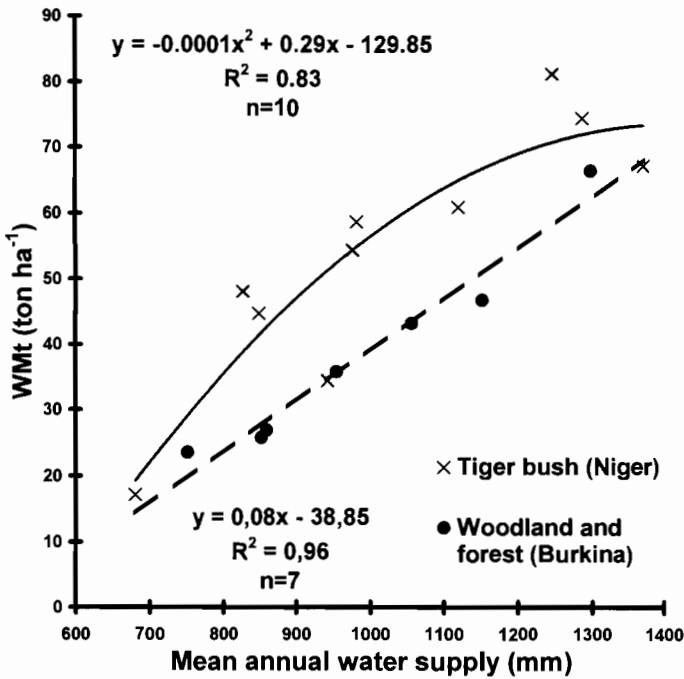| Site	WMt (ton ha^{-1})	WMp (ton ha^{-1})	WMo (ton ha^{-1})	WMc (ton ha^{-1})
Farantara	74.35	9.49	9.49	0.00
Dingazi1	54.26	10.47	6.65	3.83
Dingazi2	58.64	10.91	7.09	3.83
Inama	81.20	12.85	4.82	8.02
Sofiabangou	48.05	14.26	14.26	0.00
Kodo	60.78	17.98	6.21	11.77
Tondo	44.75	14.93	11.05	3.88
Touhore	34.40	10.98	9.03	1.95
Anamizey	67.08	19.90	12.20	7.70
Zoukouara	17.12	8.59	8.59	0.00
Mean	54.06	13.04	8.94	4.10

Fig. 7. Influence of mean annual water infiltrated in the thicket core upon the woody above-ground phytomass (WMt) of tiger bush in Niger ($R^2 = 0.83$) compared to the influence of mean annual rainfall upon the woody above-ground phytomass of unpatterned woodland and forest of southern Burkina (after Guinaudeau, 1984).

infiltration zones. More conspicuous was the favourable influence of Ra_{15} upon the thickening of the thicket core (STI + BIO, $R^2 = 0.75$) resulting more from increasing BIO ($R^2 = 0.78$) than STI ($R^2 = 0.53$). The ratio between the water shedding zone (RZ) and the infiltration zone (IZ), RZ:IZ decreased linearly with Ra_{15} ($R^2 = 0.79$), within a much wider range (0.99–6.83) than the interband:band ratio (0.51–2.33). These two ratios are strongly correlated ($R^2 = 0.84$).

Simulated run-off amount (Off_n) in the run-off zone, infiltration amount (In_n) in the core of the thicket for the wavelength n, mean infiltration amount (MIn) and water harvesting efficiency (WHE = MIn/Ra_{15}) are shown in Table 6 for the five wavelengths of each local transect. These data suggest that even though run-off from the first thicket can attain the second run-off zone, its effect upon the run-off and infiltration of the next zones remains very limited. Consequently, water uptake in the fifth thicket did not largely differ from the water intake in the first thicket due to the very effective trapping effect of the infiltration zone. Results from five iterations of the rainwater redistribution model are shown by WHE values (Table 6). The infiltration in the thicket core was found higher than precipitation, especially in the most arid sites. WHE decreased linearly with increasing Ra_{15} ($R^2 = 0.72$).

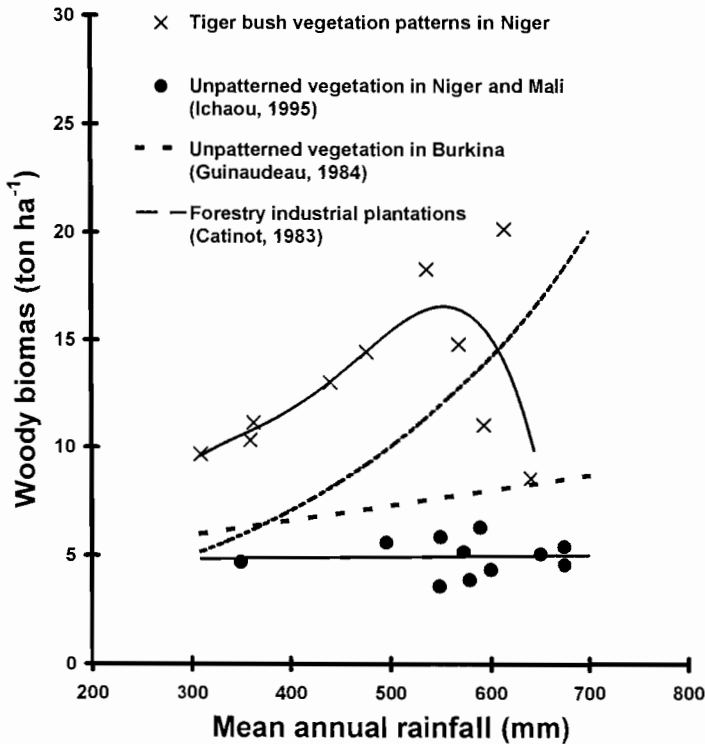$$WHE = -0.0064Ra_{15} + 5.386 \qquad (8)$$

Fig. 8. Influence of mean annual rainfall upon the tiger bush woody above-ground phytomass per hectare of plateau in Niger (WMp), compared to unpatterned vegetation in Niger, Mali and Burkina and forestry industrial plantations in the Sahelian and Sahelo-Sudanian regions.

3.3. Woody phytomass as influenced by mean annual rainfall and water intake

The best fit ($R^2 = 0.83$) between WMt and MIn was obtained when 8 yr of wood cutting was considered (Table 7; Fig. 7):

$$WMt = -0.0001MIn^2 + 0.29MIn - 129.85 \tag{9}$$

R^2 was respectively 0.71, 0.81, 0.82 and 0.73 for 5, 7, 10 and 15 yr of wood cutting, respectively.

Wood cutting was the most severe in the two sites located next to tarred roads (Inama and Kodo, Fig. 1) where WMc exceeded WMo. According to this curve fitting, a maximum of WMt = 80.4 ton ha^{-1} should be obtained for MIn = 1450 mm which was very similar to the MIn value calculated for Farantara, the northernmost site with WHE = 4.15.

The ratio Rz:Iz appears to be crucial for prediction of WMt and Wmp. Because this ratio may be tedious and difficult to evaluate in the field, it may be more attractive (especially for foresters) to predict Rz:Iz from rainfall data, using the regression equation ($R^2 = 0.79$):

$$Rz:Iz = -0.0136Ra_{15} + 9.96 \tag{10}$$

The percentage area covered with thicket cores (Iz) increased with rainfall ($R^2 = 0.75$):

$$Iz = 0.0008Ra_{15} - 0.1237 \tag{11}$$

This equation suggested that $Iz = 0$ for $Ra_{15} = 155$ mm.

Combining Eqs. (6), (7), (9) and (10) demonstrates that the influence of Ra_{15} on the production of the thicket cores (WMt) is complex but can be fit with a fourth order polynomial function of Ra_{15}. Eq. (8) suggested that the water harvesting system should not be efficient (WHE < 1) for $Ra_{15} > 685$ mm.

Since WMp = WMt Iz, the tiger bush domain should fall within the rainfall range defined by the two minima of Iz (155 mm) and WHE (685 mm). As shown in Fig. 8, WMp had a tendency to increase with rainfall up to threshold and then to plummet dramatically and to become as low as for unpatterned vegetation. This reflected the fact that WMp was controlled by two opposing trends (WMt Iz) linked to mean rainfall. The result was that WMp reaches a maximum for 550 mm mean annual rainfall as indicated by the adjusted polynomial function of Ra_{15} of the fifth order (Fig. 9). Best fits were obtained for the increasing section of the curve ($R^2 = 0.99$). Predictions are less robust for the plummeting section of the curve.
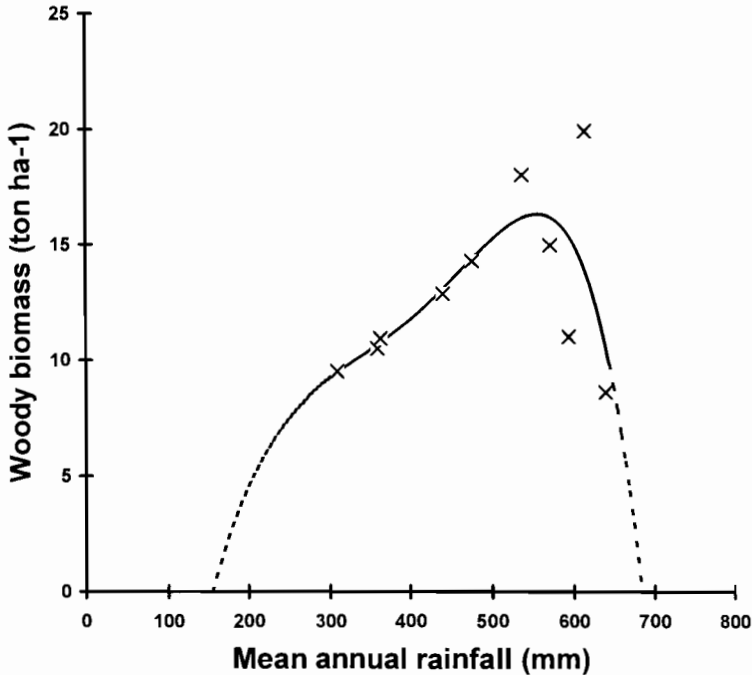

Fig. 9. Climatic tiger bush domain as inferred from the observed (squares) and adjusted (dotted line) influence of mean annual rainfall upon the tiger bush woody above-ground phytomass per hectare of plateau in Niger (WMp) Note that the mean annual rainfall has been averaged over the period 1980–1994.

4. Discussion

4.1. The efficiency of the natural water harvesting system for woody biomass production

As might intuitively be anticipated, vegetated bands in more humid regions require smaller catchment areas to shed run-off water, hence a marked decline of the interband:band ratio with increasing rainfall. Our results are consistent with the observations of Ambouta (1984) in the same region (IBR = 2.1 for 400–450 mm, 1.2 for 450–600 mm and 0.9 for 600–800 mm). IBR values as high as 5 to 20 have been reported by White (1969) in the very arid region of Jordan (Ra = 50–100 mm). In fact, comparisons with other regions are made difficult due to the different nature of the interband areas. For example, under an annual rainfall of 250 mm in Australia, IBR was found to range from 3 to 5 (Slatyer, 1961) but the water-shedding efficiency of the interbands was presumably hampered by the presence of perennial grass, annual forbs and even isolated trees. In our case, the clearness of the relationship between IBR and Ra_{15} was favoured by the fact that the bare interband zones exhibited invariably the same succession of crust types associated with a high run-off coefficients.

Our results suggest that the run-off zone:infiltration zone ratio based on field crust type survey was a better predictor for the water-harvesting efficiency (WHE) of the system than was IBR. A part of the vegetated surface, especially in the most arid region, generates significant run-off. Only the thicket core can therefore be considered as a sink for overland flow. As a result WHE showed a wider range than IBR and a more pronounced decline with rainfall increase. The simulated values of WHE are consistent with the few data available in the literature (1.5–2.5 in northern Mexico, Cornet et al., 1988; 1.38 in eastern Australia, Greene, 1992). In Niger these simulated values of WHE agree well with the data obtained from field measurements which fall in the range 1–2 for the thicket core in a region south of Niamey (Bromley et al., 1997). However, this redistribution model of rainwater along the transects across the banded patterns may suffer some exception due to local heterogeneity. This variability can be associated with local landscape concavities and salients of the pioneer zone (Thiéry et al., 1995). Slight counterslopes may force run-off to accumulate and to preferably infiltrate in these zones. This may explain why a higher water storage (WHE = 3.2, compared to 1.6 in the thicket core) could be locally simulated and corroborated by field measurements in this pioneer zone (Bromley et al., 1997). Heterogeneity in local microroughness may also result in higher run-off concentration into the thicket core (Peugeot, 1995; Galle et al., 1998).

Due to the prevailing role of crusts in hampering infiltration, field survey of surface crusts appears to be a useful tool for predicting the spatial variation in soil moisture as shown by the consistency between simulations and field measurements. The very simple model derived from the hydrological characters of these crusts (Casenave and Valentin, 1992) has proven to also be efficient to predict water redistribution along cultivated hillslope in the region (Rockström and Valentin, 1997).

As pointed by our many authors (e.g., Noy-Meir, 1973; Schreiber et al., 1995), understanding run-off offers a key to biotic processes in arid and semi-arid regions. A satisfactory relation could be obtained between the simulated water intake in the thicket

core and woody biomass despite the numerous coarse simplifications and assumptions on the amount of cut wood. The very high values of simulated WMt ($17-81$ ton ha^{-1}) were consistent with field data from tiger bush in West Africa ($21-88$ ton ha^{-1}, Hiernaux and Gérard, submitted). As illustrated in Fig. 7, the mean annual water infiltrating into the thicket cores to produce such biomass under Sahelian conditions are very similar to the mean annual rainfall required to support woodland and forest in the Sudanian zone. Thus this water concentration enables wood production which equals that of a forest in much more humid southern zones. This implies that local high production is made possible but not that the tiger bush system would be invariably more effective that vegetation with no tiger bush patterns under the same climatic conditions. To tackle this issue, we need to compare woody biomass per hectare not of thicket but of plateau (WMp) with unpatterned vegetation in the same region. WMp of the patterned plateau was found three times higher than plateau in Niger and Mali with no tiger bush patterns (Fig. 8; Ichaou, 1995). However these latter values have not been corrected by the amount of cut wood (WMc). Even though the mean value of WMc considered for the tiger bush (5.1 ton ha^{-1}) is systematically added to WMp, the woody biomass of unpatterned vegetation remains approximately half of that of the tiger bush. The thicket production in the banded patterned systems succeeds therefore in overcompensating the barrenness of the interbands, as much as even exceeding woody biomass of industrial plantations in the same region (Fig. 8). This is corroborated by the WMp values available for Burkina Faso (Fig. 8). Similarly, banded vegetation systems in Australia have a net primary production about double that of landscape systems with no patterns (Ludwig et al., 1998).

4.2. The climatic domain of the tiger bush

This regional transect also gives some insight on the climatic domain of tiger bush. In addition to slope conditions (d'Herbès and Valentin, 1998), this domain appears to be limited in the south by the water-harvesting efficiency of the system (WHE $= 1$ for $Ra_{15} = 685$ mm). In the most arid zone, the decline in rainfall is over-compensated by an increase of the run-off zone:infiltration zone ratio. However, such a system requires the existence of an infiltration zone Iz which tends to disappear below $Ra_{15} = 155$ mm (Eq. (11)). This may explain why similar formations may occur under $200-250$ mm in Mali, north of the 15°N parallel (Leprun, 1998; Hiernaux and Gérard, submitted) and under $150-200$ mm north of the 17°N parallel in Mauritania (Audry and Rossetti, 1962). The disappearance of tiger bush in Niger, north of the 15°N parallel seems therefore more related to a change in geomorphic than to rainfall conditions. No lateritic plateaux covered with shallow gravely soils occur north of this limit. The climatic optimum ($Ra_{15} = 550$ mm) for woody biomass production from banded vegetation patterns is comparable to the rainfall optimum for run-off production under natural conditions at the scale of West Africa (Valentin, 1996). Along a regional transect from the Sahara to the tropical forest, run-off coefficient was found to decline regularly whilst rainfall increases. The result of these two opposed trends is a maximum of mean annual run-off amount for an annual rainfall of approximately 600 mm. Such a consistency among the

two optima tend to confirm the strong relation between the tiger bush patterns and run-off. Because of the frequent shift of the isohyets in the region, the rainfall figures (Ra_{15}) should be taken for their relative and not absolute values. In particular, Ra_{15} may overemphasize the drought of the 1980's.

4.3. Maintenance and rehabilitation of the tiger bush system

Lack of understanding of this system has led to poor management in the past. Foresters considered the bare interbands to be a sign of degradation, and reafforestation attempts were initiated. In Niger, the main technology was the construction of half-moon shaped furrows in the interbands. The reafforestation attempts were spectacular failures. Not only did the seedlings in the interbands receive insufficient rainfall to survive, the furrows and seedlings trapped overland flow necessary for the maintenance of the downslope vegetation, which consequently began to decay. With further disturbance, such as intensive fuelwood harvesting or ephemeral cropping of sorghum or millet, the spatial pattern of water redistribution was altered, run-off increased, and serious gully erosion resulted (Hiernaux and Gérard, submitted). Our simulations suggest that the tiger bush is a nearly hydrologically closed system, acting as a very effective buffer; overland flow was only very slightly incremented from the first to the fifth wavelength (Table 6). Moreover, the vegetated bands form natural benches which enhance soil conservation (d'Herbès and Valentin, 1998). Therefore breakdown of the banded patterns of woody vegetation caused a marked degradation of the landscape.

As emphasized by many authors (Thiéry et al., 1995; Orr, 1995; Ludwig et al., 1998), rehabilitation strategies which mimic the natural tiger bush ecosystem are the best appropriate. Tree planting alone is not expected to be sufficient without restoring surface conditions. As suggested by our results, the restoration of the BIO surface type is essential for improving infiltration, and thus the chance of success for vegetation regrowth. BIO is characterized by decomposed litter and intensive bioturbation, i.e., by the absence of crusts and of crusting hazards. Therefore branch mulching, which protects soil surface from erosion and attract termites, has great promise in terms of acceptance and cost effectiveness as shown in the Nigerien tiger bush by Chase and Boudouresque (1987).

4.4. Climatic variations

As shown in Fig. 5, the synchronic study of a regional transect provides information on diachronic evolution. Our observations indicated that shifts in rainfall isohyets have been associated with a shift in the interband:band ratio. Better correlations were found for a rainfall averaging period of 15 yr, suggesting that such a period was necessary for the vegetation to response to rainfall changes. It is noteworthy that a 10 to 15-yr cycle is used by foresters in the region to enable woody plant regrowth between two successive harvests (Orr, 1995).

Ambouta (1984) described the process of thinning of bands subjected to drought. A drought period should accelerate the decay of the downslope edge of the band, while the

pioneering process of the upslope edge should be seriously reduced if not stopped. As a result the IBR increases, still enabling sufficient water to be shed from the bare interband and trapped into the thicket core. The contrast between band and interband is enhanced resulting in a thinned thicket, and an even thinner thicket core. In years of return to normal, or above average, the bottom edge of the band should receive enough water from the overland flow to develop again whilst the pioneer zone should extend. However this process is limited by the water-harvesting efficiency of the system which tends to decrease with the IBR.

As simulated by Thiéry et al. (1995), these alternating periods should result in a net migration of the vegetation bands. After caesium-137 measurements (Chappell et al., 1998) this upslope migration rate should be of few 0.1 m per year. These results have been obtained near the Sofiabangou site, i.e., in the central part of the regional transect. Because rainfall and associated IBR are subject to more pronounced variations in the northern part of the transect, slightly higher rates are speculated in the most arid zone. However, even on scanned and enlarged aerial photographs, such migrations are very difficult to perceive (Fig. 6).

Despite major rainfall variations, especially in the north, no transformation of pattern type was observed on the aerial photographs. This suggests that the limits between the banded vegetation pattern (tiger bush) and other patterns in the region (spotted, diffuse, etc., Ambouta, 1984) are mainly topographic in nature (d'Herbès and Valentin, 1998).

5. Conclusion

Based on a detailed survey of surface conditions on ten sites along a regional transect, simulation modelling indicated that the tiger bush in Niger functions as a natural water-harvesting system. The major critical factor for the efficiency of this system is the ratio between the run-off zone, which includes a part of the vegetated band, and the infiltration zone, limited to the thicket core. The soil surface acts as a regulator controlling the partitioning of rainwater between run-off, run-on, infiltration and runout. Due to the very effective buffering effect of the bands for the overland flow, the banded systems on the plateaux, albeit not utterly hydrologically closed, limits considerably the risks of degradation of the adjoining hillslopes and valleys. The tiger bush system has a very effective buffer for overland flow not only at the interband–band scale but also at the landscape scale. Although this natural water-harvesting system has proved to be robust and productive, its sustainable management requires some care. In particular it is essential to maintain high run-off production in the run-off zone (afforestation of the bare interbands are meaningless) and high infiltration rate in the infiltration zone (no-cultivation, no complete clearing, but perhaps some selective wood-cutting).

The observation of sequential aerial photographs from 1950 to 1992 highlighted the great plasticity of the tiger bush system which adjusted its geometry (IBR) to the fluctuating mean annual rainfall averaged over the last 15 yr. In the face of drought conditions, IBR was dramatically increased, enlarging therefore the catchment area to

shed run-off to maintain the remaining vegetation. Upon the return of more favourable conditions, the initial geometry recovered. Such variations in time were validated in space along the regional transect. The possible adjustment of geometry to rainfall conditions confer a great robustness to the system even under arid conditions.

The concentration of run-on into thicket cores favours high local woody biomass production $(20-80$ tons ha$^{-1})$ similar to that of woodland and forest in the wet savannah zone, reflecting the infiltration depth in the thicket (as high as 1450 mm in the northernmost site). Even converted into value per hectare of plateau, namely accounting for the run-off zone, the woody biomass production was found to exceed that of forestry industrial plantations under the same climatic conditions.

References

Ambouta, K.J.M., 1984. Contribution à l'édaphologie de la brousse tigrée de l'Ouest nigérien. Doctor-Engineer thesis, University of Nancy, 116 pp

Audry, P., Rossetti, C., 1962. Observations sur les sols et la végétation en Mauritanie du Sud-Est et sur la bordure adjacente du Mali (1959 et 1961). Prospection écologique. Etudes en Afrique Occidentale. Projet du fonds spécial des Nations-Unies relatif au criquet pélerin. F.A.O. Rome, 267 pp

Barker, T., 1992. Vegetation pattern in the Nigerien tiger bush. Department of Geography, Coventry Polytehnic, B.S. dissertation, 92 pp.

Belsky, A.J., 1989. Landscape patterns in a semi-arid ecosystem in East Africa. J. Arid Environ. 17, 265–270.

Bromley, J., Brouwer, J., Barker, A P., Gaze, S.R., Valentin, C., 1997. The role of surface water redistribution in an area of patterned vegetation in Southwest Niger. J. Hydrol. 198, 1–29.

Casenave, A., Valentin, C., 1992. A run-off capability classification system based on surface features criteria in semi-arid areas of West Africa. J. Hydrol. 130, 231–249.

Chappell, A., Valentin, C., Warre, A., Charlton, M., d'Herbès, J.M., 1998 Testing the validity of upslope migration in banded vegetation from southwest Niger. Catena, this issue.

Chase, R., Boudouresque, E., 1987. Methods to stimulated plant regrowth on bare Sahelian forest soils in the region of Niamey, Niger. Agric. Ecosyst. Environ. 18, 211–221.

Clos-Arceduc, M., 1956. Etude sur photographies aériennes d'une formation végétale sahélienne: la brousse tigrée. Bulletin de l'IFAN, série A 7, 677–684.

Cornet, A.F., Delhoume, J.P., Montaña, C., 1988. Dynamics of striped vegetation patterns and water balance in the Chihuahuan desert. In: During, H.J., Wergner, M.J.A., Willems, J.H. (Eds.), Diversity and Pattern in Land Communities. SPB Academic, The Hague, Netherlands, pp. 221–231.

d'Herbès, J.-M., Valentin, C., 1997 Land surface conditions of the Niamey region: ecological and hydrological implications. J. Hydrol. 188–189, 18–42.

d'Herbès, J.-M., Valentin, C., 1998. Slope gradient control of banded woodland patterns in Niger. Catena, this issue.

Delhoume, J.P., 1996 Fonctionnement hydro-pédologique d'une toposéquence de sols en milieu aride (Réserve de la Biosphère de Mapimi, Nord-Mexique). PhD, University of Poitiers, 295 pp.

Dunkerley, D.L., Brown, K.J., 1995. Run-off and run-on areas in a patterned chenopod shrubland, arid western New South Wales, Australia: characteristics and origin. J. Arid Environ. 30, 41–55.

Dunkerley, D.L., Brown, K.J., 1998. Banded vegetation near Broken Hill, Australia: Significance of surface roughness and soil physical properties. Catena, this issue.

Eddy, J., Humphreys, G S., Hart, D.M., Mitchell, P.B., Fanning, P.C., 1998 Vegetation arcs and litter dams: similarities and differences. Catena, this issue.

Galle, S., Ehrmann, M., Peugeot, C., 1998. Water balance on a banded vegetation pattern. The case of the tiger bush in western Niger. Catena, this issue.

Gavaud, M., Boulet, R., 1967 Carte pédologique de reconnaissance de la République du Niger. Feuille de Niamey à 1/500000, ORSTOM, Dakar, Vol. 3, 1120 pp

Greene, R.S.B., 1992. Soil physical properties of three geomorphic zones in a semi-arid mulga woodland. Aust. J. Soil Res. 30, 55–69.

Guinaudeau, F , 1984. Estimation des volumes et de la productivité des formations forestières sèches. Revue des méthodes et des résultats. E.N.I.T.E.F., Nogent sur Vernisson, 83 pp

Hemming, C.F., 1965. Vegetation arcs in Somaliland. J. Ecol. 53, 157–167.

Hiernaux, P , Gérard, B., submitted. Does patchiness increase vegetation productivity, diversity and stability? The case of 'brousse tigrée' in the Sahel. Acta Oecologica.

Ichaou, B., 1995. Etude de la productivité des formations forestières de brousse tigrée et de brousse diffuse: conséquences pour la gestion et la régénération de ces formations. I.P.R. de Katibougou, Mali, 161 pp.

International Society of Soil Science (ISSS), International Soil Reference and Information Centre (ISRIC), Food and Agriculture Organization of the United Nations (FAO), 1994. World Reference Base for Soil Resources. Wageningen/Rome, 161 pp.

Lebel, T., Sauvageot, H., Hoepffner, M., Desbois, M., Guillot, B., Hubert, P., 1992. Rainfall estimation in the Sahel: The EPSAT–Niger experiment. Hydrol. Sci. J. 37 (3), 201–215.

Lebel, T., Taupin, J.-D., d'Amato, N., 1997. Rainfall monitoring during Hapex-Sahel: I. General rainfall conditions and climatology. J. Hydrol. 188–189 (74), 96.

Legger, D., van der Aa, M., 1994. Soils of the 'West central site' Niger, Hapex–Sahel 1992. Department of Soil Science and Geology, Wageningen Agricultural University, 31 pp.

Leprun, J.C., 1998. The influences of ecological factors on the tiger bush along a gradient from Mali to northern Burkina Faso. Catena, this issue.

Ludwig, J.A., Tongway, D.J., Marsden, S.G., 1998. Stripes, strands or stipples: Modelling the influences of three landscape banding patterns on resource capture and productivity in semi-arid woodlands, Australia. Catena, this issue.

Mabbut, J.A., Fanning, P.C., 1987. Vegetation banding in arid Western Australia. J. Arid Environ. 12, 41–59.

MacFayden, W.A., 1950. Vegetation patterns in the semi-desert plains of British Somaliland. Geog. J. 115, 199–211.

Noy-Meir, I., 1973. Desert ecosystems: environment and producers. Annu. Rev. Ecol. Systematics 4, 25–51.

Orr, B., 1995. Natural forest management in Sahelian ecosystem of southern Niger. J. Arid Environ. 30, 129–142.

Peugeot, C., 1995. Influence de l'encroûtement superficiel du sol sur le fonctionnement hydrologique d'un versant sahélien (Niger). Expérimentations in situ et modélisation. PhD, University of Grenoble, 356 pp.

Project Energie II, 1991. Schéma directeur d'approvisionnement en bois-énergie de Niamey. République du Niger/Seed/CTFT, Niamey, 128 pp.

Rockström, M., Valentin, C., 1997. Hillslope dynamics of on-farm generation of surface water flows: the case of rainfed cultivation of pearl millet on sandy soil in the Sahel Agric. Water Manage. 33, 183–210.

Schreiber, K.F., Yair, A., Schachak, M., 1995. Ecological gradients along slopes of the northern Negev highlands, Israel. Adv. GeoEcol. 28, 209–229.

Seghieri, J., Galle, S , Rajot, J.L., Ehrmann, M., in press. Relationships between the soil moisture regime and the growth of the herbaceous plants in a natural vegetation mosaic in Niger. J. Arid Environ.

Sivakumar, M.V.K., Maidoukia, A., Stern, R.D., 1993. Agroclimatology of West Africa: Niger. ICRISAT, Patancheru, Andra Pradesh, India, Information Bulletin no. 5, 2nd edn., 48 pp. +append.

Slatyer, R.O., 1961 Methodology of a water balance study conducted on a desert woodland (Acacia aneura F. Muell) community in central Australia. Plant–water relationships in arid and semi-arid conditions. UNESCO Arid Zone Research, 16, Proceeding of Madrid Symposium, pp. 15–26.

Thiéry, J., d'Herbès, J.-M., Valentin, C., 1995. A model for simulating the genesis of banded patterns in Niger. J. Ecol. 83, 497–507.

Tongway, D.J., Ludwig, J A., 1990. Vegetation and soil patterning in semi-arid mulga lands of Eastern Australia. Aust J. Ecol. 15, 23–34.

Valentin, C., 1996. Soil erosion under global change. In: Walker, B.H., Steffen, W.L. (Eds.), Global Change and Terrestrial Ecosystems, Cambridge Univ. Press, IGBP Book Series, no. 2

Valentin, C., Bresson, L.-M., 1992. Morphology, genesis and classification of soil crusts in loamy and sandy soils Geoderma 55, 225–245.

Valentin, C., Casenave, A , 1992. Infiltration into sealed soils as influenced by gravel cover. Soil Sci. Soc. Am. J. 56, 1167–1673.

Van der Meulen, F., Morris, J.W., 1979. Striped vegetation patterns in a transvaal savanna (South Africa). Geo-Eco-Trop 3, 253–266.

Vandervaere, J.-P., Peugeot, C., Angulo Jaramillo, R., Vauclin, M., Lebel, T., 1997. Estimating hydraulic conductivity of crusted soils by using disc infiltrometers and micro-tensiometers. J. Hydrol. 188–189, 203–223.

Vezey-FitzGerald, D.F., 1957. The vegetation of the Red Sea coast north of Jedda, Saudi Arabia. J. Ecol. 45, 547–562.

White, L.P., 1969. Vegetation arcs in Jordan. J. Ecol. 57, 461–464.

White, L.P., 1970. Brousse tigrée patterns in southern Niger. J. Ecol. 58, 549–553.

White, L.P., 1971. Vegetation stripes on sheet wash surfaces. J. Ecol 59, 612–615.

Wilding, L.P., Daniels, R., 1989 Soil-geomorphic relationships in the vicinity of Niamey, Niger. Tropsoils Bull., pp. 89–101.

Stripes, strands or stipples: modelling the influence of three landscape banding patterns on resource capture and productivity in semi-arid woodlands, Australia

John A. Ludwig *, David J. Tongway, Stephen G. Marsden

CSIRO Wildlife and Ecology, GPO Box 284, Canberra, ACT 2601, Australia

Abstract

In the semi-arid open woodlands or savannas of eastern Australia banded vegetation is a common form of landscape patchiness. This banding can form relatively long strands or shorter stripes across the landscape, or small patches can occur in a stippled pattern. In degraded areas these patches can be completely removed from the landscape. This study addresses two related questions: does the type of patchiness (strands, stripes, or stipples) significantly influence how efficiently these semi-arid landscapes capture and store scarce soil resources; and how does this efficiency compare with landscapes that have lost all their patches? Results from a landscape simulation model, validated for a semi-arid woodland study site, demonstrated that the loss of landscape patchiness had the greatest influence on the capacity of the landscape to capture rainfall as soil water—reduced by about 25% compared to banded landscapes. This 25% loss of soil water reduced annual net primary productivity in these systems by about 40%. Banded patterns (stripes or strands) captured about 8% more rainfall as soil water than a stippled pattern; this increased their plant production by about 10%. However, these differences between banding patterns were relatively small compared to the impact of totally eliminating patchiness, which can occur with severe land degradation. This implies that preventing the loss of landscape patchiness is very important for managing savannas for production and conservation goals. © 1999 Elsevier Science B.V. All rights reserved.

Keywords: Stripes; Strands; Stipples

* Corresponding author. CSIRO Wildlife and Ecology, PMB 44, Winnellie, Darwin, NT 0822, Australia; Tel.: +61-8-9844-8423; Fax +61-8-8944-8444; E-mail: john.ludwig@terc.csiro au

1. Introduction

In many arid and semi-arid environments around the world, limited rainfall and runoff–runon processes have lead to vegetation patchiness on many types of landscapes. Different terms have been used to described this phenomenon. For example, Archer (1990) has described patchy savanna parkland sites in southern Texas as 'two-phase mosaics'. Belsky (1995) used this term to describe patchiness in some of the Serengeti grasslands of East Africa. Montaña (1992) described vegetation patches on the Mapimí Reserve in the southern Chihuahuan Desert, Mexico, as two-phase mosaics. This patchiness on Mapimí has also been described as 'stripes' (Cornet et al., 1992). Similar vegetation stripes in West Africa have been termed 'brousse tigrée' (Thiery et al., 1995), or 'tiger bush' in the more English-speaking East Africa. Vegetation 'banding' has been used to describe *Acacia aneura* grove–intergrove patterns in parts of arid Western Australia (Mabbutt and Fanning, 1987), Central Australia (Slatyer, 1961) and Eastern Australia (Boyland, 1973).

Vegetation banding can be of different forms even within a relatively small landscape area. For example, on a 200 ha study site in the semi-arid *Acacia* woodlands of Eastern Australia (Fig. 1), ribbon-like 'strands' of vegetation occur along minor, low-relief drainages (Fig. 2). In higher areas of the landscape, these more continuous strands are broken into shorter 'stripes', which are oriented along contours. Along low ridges, small patches or groves of *A. aneura* are 'stippled' across the landscape. These three banding patterns are related to soil-depth and fertility catenas, from shallower, poorer soils along
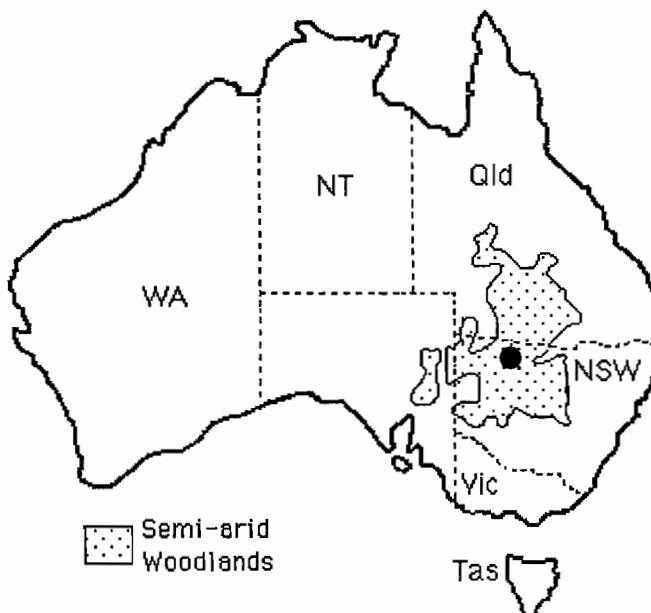

Fig. 1. Location of the landscape study site (●) within the semi-arid woodlands of Eastern Australia (after Harrington et al., 1984; Ludwig et al., 1994).
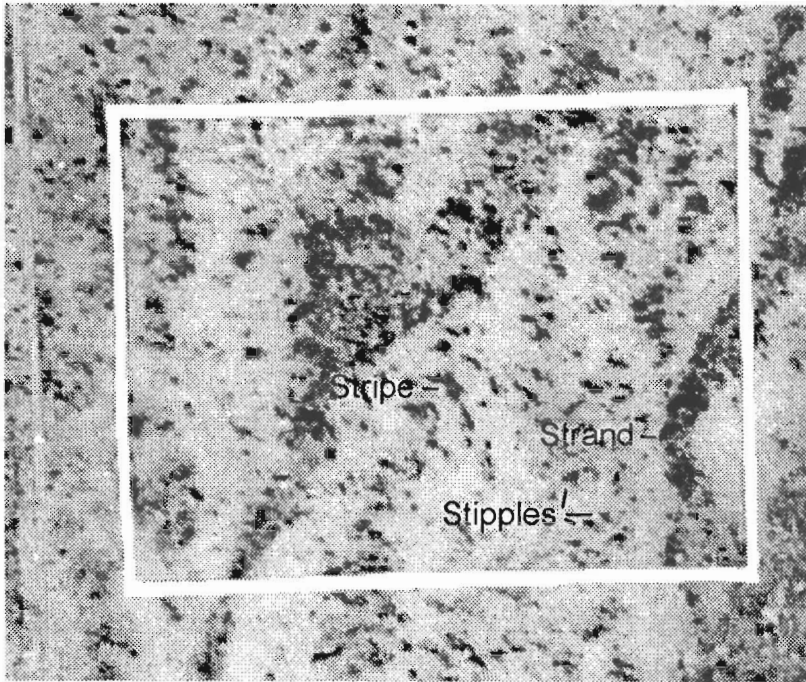
Fig. 2. A scanned aerial-photo of the 200 ha study site (within rectangle) showing *A. aneura* vegetation (dark areas) in different banding patterns (see text). A detailed description of the study site, including the direction of overland water flows, are given in Tongway and Ludwig (1990).

ridges to deeper, richer soils in the drainage bottoms (Tongway and Ludwig, 1990; Ludwig and Tongway, 1995).

Although vegetation banding has been extensively described and reviewed in reference to theory (e.g., Wiens, 1995), causes (e.g., Belsky, 1995), genesis (e.g., Thiery et al., 1995) and dynamics (e.g., Mauchamp et al., 1994), less attention has been paid to the function that patchiness plays in arid and semi-arid landscapes. One hypothesis is that patchiness functions to optimise the capture and storage of limited water and nutrients within these landscapes, and hence tends to maximise plant productivity within the system (Ludwig and Tongway, 1995). This hypothesis is based on the theory that many arid lands are source–sink or runoff–runon systems (Noy-Meir, 1973). This theory predicts that in environments with limited rainfall, plant productivity will be higher if rainwater is concentrated into patches rather than being uniformly dispersed over the landscape. This landscape function hypothesis has been confirmed by field data (Ludwig and Tongway, 1995, 1997) and simulation studies (Ludwig et al., 1994; Ludwig and Marsden, 1995).

In this study we extend these simulation studies to address two related questions. Firstly, compared to a landscape with no patchiness, how strongly does the presence of patches influence resource capture, and hence productivity? Secondly, in terms of

resources and productivity, is it important whether patches are small and scattered over the landscape (stippled), or occur in short bands (stripes) or as long bands (strands)?

2. Methods

2.1. Semi-arid savanna landscape simulations

This simulation study was based on a semi-arid *A. aneura* open woodland or savanna landscape located in eastern Australia (Fig. 1). The banded *Acacia* groves, forming strands, stripes or stipples, are interspersed with open intergroves (Fig. 2). All three of these forms can be identified by focusing on different areas of the scanned aerial-photo. For the simulations, we assumed four areas, each 1 ha in size and with a uniform 1% slope. Three had patches dispersed as stipples, stripes or strands, occupying 25% of the 1 ha area, and one had no patches (Fig. 3). Each landscape area was gridded into 100 equal-sized units, and each unit was designated as being either a patch (black cell) or an interpatch (white cell) to form the desired patterns.
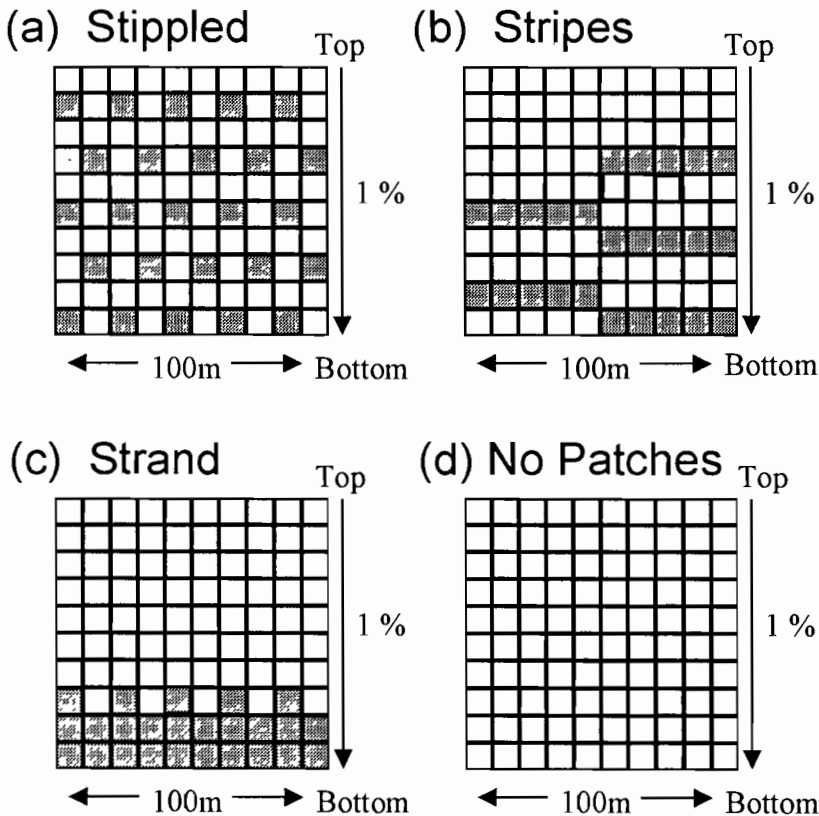

Fig. 3. Top-view schematics of patches (solid grid cells) and interpatches (open grid cells) for the four landscape patchiness patterns simulated in this study: (a) stippled—dispersed patches; (b) stripes—larger, elongated patches; (c) strands—long linear, basal patches; and (d) no patches.

Simulations were used to describe how water, as the primary limiting resource, flows down the landscape, through the units, and possibly out the bottom of the system (Fig. 3). If the amount of rainfall (R), and its intensity, exceeds the water storage capacity (SC) or the infiltration rate (IR) of the soil within an interpatch area then runoff (ROff) occurs (Fig. 4). This ROff can be captured by down-slope patches, or run out (ROut) of the landscape system. If the IR or SC of a patch is exceeded then ROff occurs from the patch, to the next down-slope interpatch, patch or out of the system. Computation details are provided in Appendix A.

ROut from the 1 ha landscape following a rainfall event at time (t) in functional form was:

$$ROut_t = f(R, IR, SC)_t \tag{1}$$

Rainfall (R) amounts and intensities, and temperatures, used in the simulations were taken from a 31.5 year record obtained from a Class A weather station located at Cobar, New South Wales, in the centre of the semi-arid woodlands. Total ROut from the bottom of each of the four landscape systems, averaged over the 31.5 years, was taken as the measure of resource loss.

Based on data from soil studies on the study site (Greene, 1992; Greene and Ringrose-Voase, 1992), soil infiltration rates (IR) for patches and interpatches were set at 60 and 10 mm/h. Soil depths are about 100 and 45 cm for patches and interpatches, respectively. Total soil water storage capacities (SC) for patches and interpatches are dependent on their soil depths and the water holding capacities of their soils, which are 42% and 35%, respectively. The soils on the site are Xerollic Haplargids.

2.2. Landscape simulation model

A 'flow-filter' landscape model has been developed to quantify how semi-arid open woodlands or savannas function to 'filter-out' resources 'flowing' about these land-
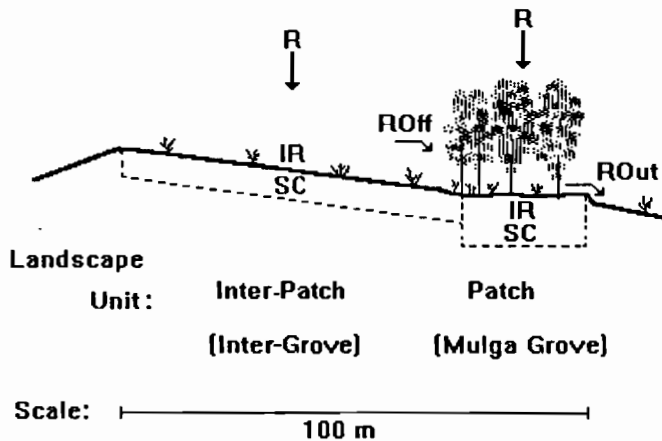

Fig. 4. Side-view schematic of a semi-arid landscape showing how water from rainfall (R) may runoff (ROff) when amounts and intensities exceed the infiltration rate (IR) or water storage capacity (SC) of the soil in the interpatch. Runoff not captured and stored by patches will run out (ROut) of the landscape system (after Ludwig et al., 1994).

scapes (Ludwig et al., 1994). Annual net plant production (NPP) for the four landscape systems with different banding patterns was estimated by using a simulation model, called SEESAW (a simulation of the ecology and economics of semi-arid woodlands; Ludwig et al., 1992, 1994). This model has a modular structure, going from climatic inputs to financial outputs (Fig. 5). For the purposes of this landscape simulation, which focuses on ROut and NPP, outputs from the sheep production (SHEEPSAW) and financial (ECONOSAW) modules were not required.

Each module of SEESAW is deterministic, and mechanistic. For example, the WATDYN module, adapted from Walker and Langridge (1996), uses a modified Penman–Monteith equation to estimate daily transpiration and evaporation soil water losses (Raupach, 1991). It also estimates a number of resistances to soil water losses, such as plant canopy aerodynamic drag, and soil surface sealing or crusting (details in Walker and Langridge, 1996). For our purposes, WATDYN was used to compute total ROut as a yearly average from each of the four landscape systems based on the soil water dynamics in each landscape unit across each system.

The FORSAW module of SEESAW computes net primary production (NPP) of forage through time (t) as a function of plant available moisture (PAM), available nitrogen (AN) in the soil, air temperatures (TEMPS), incoming solar radiation (SOLRAD) and atmospheric carbon dioxide concentrations (CO_2):

$$NPP_t = f(PAM, AN, TEMPS, SOLRAD, CO_2)_t \qquad (2)$$

PAM was estimated from soil water dynamics (i.e., WATDYN). Soil available nitrogen (AN) dynamics was based on nutrient relationships in arid lands (Charley and
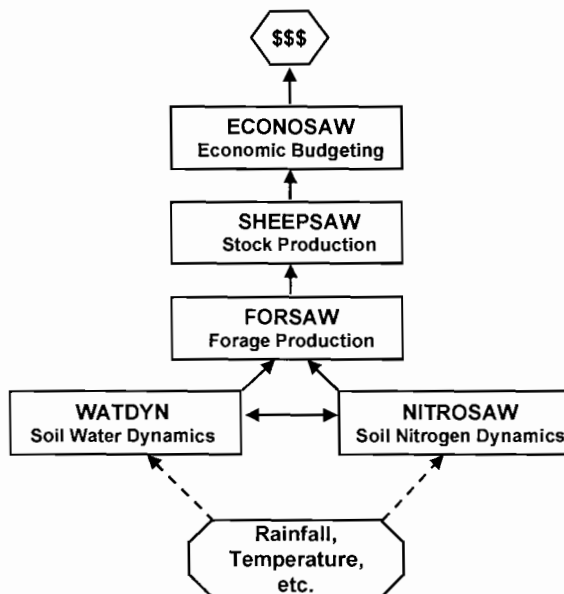

Fig 5. The modular and flow structure of the SEESAW simulation model, from environmental inputs to financial outputs (after Ludwig and Marsden, 1995).

Cowling, 1968), where pools of mineralizable nitrogen tend to build-up during droughts, then produce 'flushes' of available nitrogen with drought-breaking rains.

Forage production by seven plant guilds (ephemeral forbs, perennial forbs, ephemeral grasses, palatable C3 perennial grasses, palatable C4 perennial grasses, fibrous C4 perennial grasses and palatable shrubs) was simulated. Given initial biomass of leaves, stems and roots for each guild, the daily rate of fixation of new photosynthetic biomass was calculated using a scheme in wide usage by plant growth modellers (e.g., Hanson et al., 1988). First a maximum photosynthetic fixation rate per day (dependent on the genetic potential of the plants in each guild) is computed based on available radiant energy (SOLRAD). Then this maximum rate is adjusted by rate enhancing or limiting factors (PAM, AN, TEMPS and CO_2), resulting in a daily rate. The impact of these factors differs between the guilds.

The concentration of CO_2 has been increasing at a rate of about 1.5 ppmv (0.4%) per year (Pearman, 1988). Increased CO_2 is known to enhance the yield of C3 crops due to increased net photosynthesis, but not in C4 crops (Gifford, 1988). This production enhancement due to increasing CO_2 appears to be linear up to about 700 ppmv. In FORSAW, maximum photosynthetic rates for each guild were adjusted by increasing CO_2 concentration changes over the 31.5 year simulated, the C3 plant guilds being enhanced while C4s were unaffected.

For each plant guild, maximum photosynthetic rate occurs at a temperature optimum, with 'bell-shaped' functions limiting this rate at temperatures lower or higher than this optimum. The minimum and maximum temperatures at which net photosynthesis becomes negative (i.e., daily respiration losses exceed photosynthetic gains) also differs among plant guilds (e.g., C4s have higher optimums, minimums and maximums than C3s).

Plant available moisture (PAM) is that factor that most strongly limits the maximum photosynthetic rate. For example, under the warm and windy conditions of spring and summer, soil water in soil surface layers can quickly become limiting, particularly to those plant guilds with shallow roots systems (e.g., ephemeral forbs and grasses). As soils dry, PAM can quickly drop below a threshold, below which soil water is limiting. The function relating the limitation of maximum photosynthetic rate to PAM, expressed as volumetric soil water contents (e.g., cm^3 H_2O/cm^3 soil) can be taken as sigmoidal, with asymptotes at zero when contents are low and at one when contents are high. A similar function can be used for the rate limitation due to available nitrogen (AN) in the soil, as derived from the NITROSAW module, but the threshold below which the rate drops off is generally quite low. In other words, the plant guilds in these semi-arid woodlands are well adapted to growing under conditions of low soil nutrients (Charley and Cowling, 1968).

In simulating the production of new plant biomass, or its decline, the FORSAW module of SEESAW estimates a number of other growth processes. The translocation and assimilation of new photosynthate to new leaf, stem and root biomass depends on the 'internal' demands for maintaining a 'balance' between these plant organs (i.e., a shoot to root ratio). It assumes that these ratios remain relatively constant within a plant guild, but differ between guilds, depending on the life form of the guild (i.e., forb, grass, shrub, tree). For example, if the shoot to root ratio increases (i.e., above the constant),

then photosynthate will be translocated down from shoots to roots, thus re-establishing the balance. If shoot biomass is consumed by stock, lowering the shoot to root ratio, then photosynthate will be used to grow new shoots.

At certain temperatures and daylengths, depending on the plant guild, photosynthate may be translocated to flowers, fruits and seeds, or other types of propagules (e.g., new tillers or buds in plants that reproduce vegetatively). The processes of seed germination and senescence and death are also simulated in FORSAW. Seeds will germinate and seedlings will establish with favourable moisture and temperatures conditions. When conditions are unfavourable, senescence and death of plant parts, or entire plants, will occur. The drop of dead plants, or parts thereof, to litter, and the subsequent breakdown and decomposition of this litter, was also simulated. The consumption of plant parts is computed by the SHEEPSAW module. The details of these plant growth, death and consumption functions, as used in SEESAW, are beyond the scope of this paper, but this information is available from the authors.

3. Results

The SEESAW model was validated before running the simulations on the four artificial landscape systems (of fixed size, shape and slope) with different patch patterns
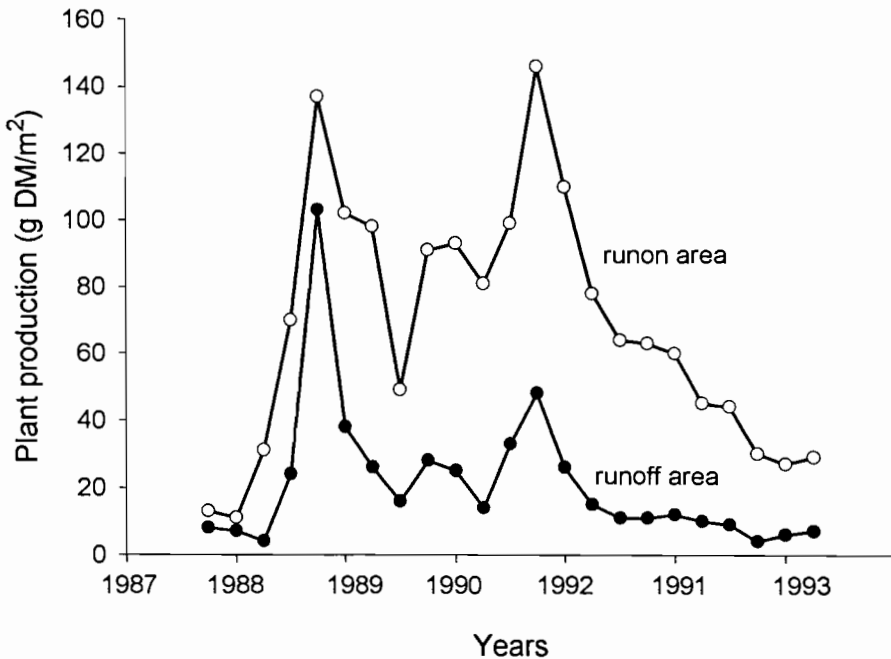

Fig. 6 Forage production (g/m^2) in landscape patches (runon areas) and interpatches (runoff slopes) over 6 years (1988 to 1993) on the semi-arid woodland study site (after Hodgkinson and Freudenberger, 1997).

(stippled, stripes, strands and no patches) over 31.5 years. Validation was based on 6 years of forage production and rainfall data from the study site (Hodgkinson and Freudenberger, 1997). The patches (runon areas or landscape sinks) consistently had higher plant production (all guilds combined) than interpatches (runoff areas or source zones) (Fig. 6). Clearly, spatial redistribution of water and nutrients across landscapes drives spatial heterogeneity in plant production (Noy-Meir, 1981). However, the temporal patterns of production over the 6 years were similar with high forage growth peaks during good years (e.g., 1988). On both runoff and runon areas total forage production steadily declined with the drought that started in 1991, but less so for the runon patches. Although not shown here for brevity, production data for each plant guild over the 6 years was used to validate the ability of SEESAW to simulate plant growth and death patterns.

The loss of runoff (ROut) from the simulated landscape systems with no patches was about 25% greater than for those with patches (Fig. 7). The stripe and strand banded patterns were about 8% more efficient at capturing runoff than the stippled pattern. Run-out from the stippled system maybe higher because runoff from rains probably flows between and around the smaller patches. As striped and strand patterns capture and conserve the most rainwater, these systems had an annual net primary production (NPP) of nearly 500 kg/ha (Fig. 8). The landscape system with no patches only had an NPP of about 280 kg/ha, about 40% lower than that for stripe and strand patterned
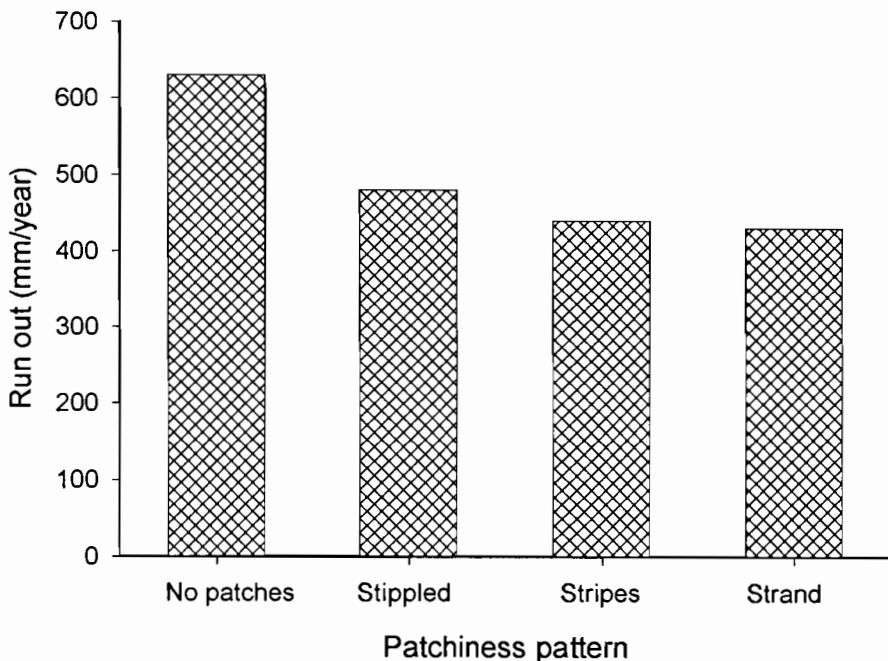

Fig. 7. Average losses of water as run out (mm/year) from the four simulated landscapes: no patches compared to stippled, stripped or strand patch patterns (see Fig. 3 for patterns).
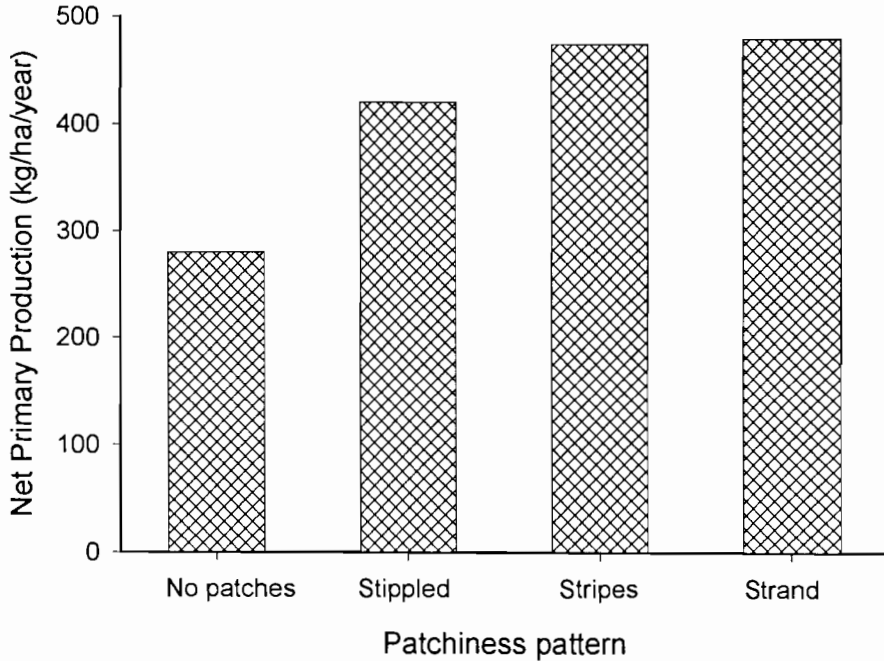
Fig. 8. Annual net primary production (kg/ha per year) from simulated landscapes for three patch-pattern types and no patches (see Fig. 3 for examples of these patterns).

landscapes. Because these banded patterns captured about 8% more soil water than the stippled pattern, their NPP was by about 10% higher.

4. Discussion

4.1. Impacts of patch loss

These simulations demonstrate that the loss of landscape patchiness can result in a dramatic reduction in a limited resource (soil water) and, hence, reduce productivity by 40%. This loss of landscape patches also impacts on soil fertility. Patches are known to be 'islands of fertility' (e.g., Garner and Steinberger, 1989). The concentration of nutrients within such patches, particularly in soil layers near the surface, are often many times those in the interpatch spaces (Tongway et al., 1989; Tongway and Ludwig, 1990, 1994). For example, areas of landscape with intact patches had significantly higher concentrations of soil nitrogen and organic carbon, water infiltration rates, and plant production, compared to landscapes with degraded patches (Table 1). Thus, the main message is that the loss of patches means the loss of the rich soils, and the plants, that constitute these patches.

Further, once a landscape has lost its patches, it significantly losses its ability to capture, store and recycle any *new* materials (e.g., soil sediments, litter, seeds) that are washed or blown into the system (Ludwig and Tongway, 1995). Such degraded

Table 1
Differences in nitrogen and organic carbon in the 0–1 cm soil layer, in water infiltration rates and plant production between two landscape areas, one with intact patches and the other with degraded patches. Data from areas of semi-arid woodland on 'Trafalgar' station, near Cobar, New South Wales (for details, and other examples, see Tongway and Smith, 1989; Tongway and Ludwig, 1997a,b)

Characteristic	Landscapes patches	
	Intact	Degraded
Soil nutrients		
Available nitrogen (ppm)	75.4[a]	22.4[b]
Organic carbon (%)	1 5[a]	0.8[b]
Infiltration rate (mm/h)	49.2[a]	7.8[b]
Plant production (g/m²)	231 2[a]	13.6[b]

Characteristics with different superscript letters are significantly different ($P = 0.05$), based on Tukey's HSD test

landscape systems can be termed dysfunctional (Tongway and Ludwig, 1997b). In other words, the system has become 'leaky'. Rainwater and nutrients are no longer efficiently captured and stored within the landscape—runoff becomes run-out, carrying away valuable rainwater, sediments and organic matter out of the system (e.g., into creeks, rivers, pans and lakes). This also means less plant production, or none at all, if levels of available water and nutrients remain below critical thresholds and plants fail to respond to rainfall because of loss of patches (Hodgkinson and Freudenberger, 1997). Thus, under degradation pressures, dysfunctional landscapes become poor in nutrients, lose water infiltration potential, and have significant declines in plant production.

The signs of decline or loss of landscape patchiness are often very obvious (Tongway and Ludwig, 1997b). For example, in some of the patchy woodlands near the study site, it is not uncommon to observe *Acacia* groves where every tree is dead and the ground is bare within the groves, and across the intergroves. Also, log-mounds, formed when dead trees fall over, show signs of breakdown and erosion, with logs exposed above an eroded surface. Typically, such logs are buried by a mound of fertile soil, which is covered with perennial plants (Tongway et al., 1989). Thus the signs are clear, but what about the causes?

Basically, the answer to this question is overgrazing. Although there are different types of overgrazing (Freudenberger et al., 1997), the loss of landscape patches is caused by an excessive consumption of the plants (e.g., perennial grasses) that form patches. Over time, and especially during droughts, excessive defoliation of plants can lead to their deaths (Hodgkinson, 1992), resulting in reduced patch size and density. Thus, overgrazing leads to landscape dysfunction, often within specific areas such as along fences and near watering points—a pattern observed around the world (Coughenour, 1991). Of course, other factors can contribute to loss of landscape patchiness. For example, high intensity fires in old, dense Mediterranean forest will completely consume the vegetation, producing smooth, homogeneous or non-patchy surfaces which have high rates of soil erosion after such fires (Lavee et al., 1995). They found that more open forest with more frequent, but cooler fires, have naturally patchy surfaces which do not erode.

Another question is why has overgrazing only occurred since pastoral settlement? In Australia's rangelands this was about 150 years ago (Noble and Tongway, 1986). The likely answer is that pastoralism brought more consumers, e.g., domestic sheep and cattle, and feral camels, horses, donkeys, rabbits, goats and pigs. All of these have been introduced to landscapes that since ancient time had only been grazed by macropodid marsupials (Freudenberger et al., 1997). Stock watering points were extensively developed, with the effect that kangaroo populations have greatly increased, especially in places where its natural predator, the dingo, has been controlled to protect stock. The net result is a 'total grazing pressure' that eventually destroys landscape patchiness. How can such degraded landscapes be fixed?

4.2. Landscape rehabilitation

The rehabilitation of dysfunctional landscapes can be achieved only by restoring landscape patches, that is, by rebuilding the structures that trap and store limited soil resources (Tongway and Ludwig, 1993). Experimental work has demonstrated that new patches can be restored on bare slopes by simply building piles of brush of about 10 m^2 (Tongway and Ludwig, 1996). It was found that these brush piles functioned to trap runoff, sediments and litter flowing or blowing around the landscape. After only 3 years, soil sediments and litter had significantly accumulated within the brush piles. Compared to controls, nitrogen and carbon levels were 30% higher, water infiltration rates increased 10-fold and the abundance of soil invertebrates increased four-fold. Perennial grasses and forbs re-established within the brush piles, but not in the controls, even though the experimental plots were being subject to moderately high grazing pressures by sheep and kangaroos (Ludwig and Tongway, 1996). The 'spiky' branches of the brush pile protected new plants from grazing.

Some rangeland managers in the semi-arid *Acacia* woodlands of eastern Australia already make brush piles when they cut branches from *Acacia* during droughts to 'emergency' feed their sheep (Harrington et al., 1984). However, rather than leaving branches next to the trees they are cut from, managers should be encouraged to build brush piles in places where rehabilitation is most needed, and with piles orientated along contours to increase their efficiency for trapping runoff.

Larger brush piles can be built by using bulldozers to 'thin' shrubs, where a chain is pulled between two bulldozers working parallel to the contours (Noble et al., 1997). At an appropriate spacing between strips, chaining creates large piles of uprooted trees (i.e., large patches) that are very efficient at trapping soil and litter. These strips or piles of brush and trees also provide refuge sites for fauna such as small mammals and lizards. Of course, landscape restoration using the chaining method must be very carefully planned (i.e., no chaining on steep landscapes).

4.3. Soil condition and biodiversity

Semi-arid landscapes used for grazing must be managed wisely to avoid the loss of patches. Land managers need to acknowledge the significance of patches and incorpo-

rate this knowledge into property management plans. This includes having an understanding of why overgrazing reduces patchiness, soil surface condition and productivity, thus leading to landscape dysfunction, desertification, and losses of biodiversity.

Maintaining landscape patchiness is vital for maintaining biodiversity, and vice versa, as the two are closely linked. For example, if biologically derived soil pores (i.e., those > 0.75 mm) are closed, then the infiltration of water virtually stops (Greene, 1992). These biopores are formed by soil fauna such as ants and termites burrowing within favourable patchy habitats (Noble and Tongway, 1988; Whitford et al., 1992; Eldridge, 1993a; Greenslade and Smith, 1994). The cover of plants and cryptogams on a landscape are also important for slowing runoff and erosion (Eldridge, 1993b; Greene et al., 1994); this cover also protects biopores from raindrop impacts that tends to collapse them (see Greene, 1992, for details). The type and nature of soil surface stone and rock cover can also greatly influence runoff (Lavee and Poesen, 1991). For example, they found that landscapes with small (3 cm) stones resting on top of the soil surface consistently produced less runoff than bare soil at stone covers ranging from 30 to 88%.

Thus, the management of soil surfaces and patches is of critical importance in maintaining landscape function; that is, the capturing and storing of limited soil resources and producing good plant growth (Tongway and Ludwig, 1997a,b), and therefore conserving soil biotic diversity. Grazing land management must integrate both production and conservation goals (Foran et al., 1990). Morton et al. (1995) and Stafford Smith (1994) provide some guidelines for assessing whether a pastoral property is being managed sustainably. Ludwig and Freudenberger (1997) provide a landscape perspective on semi-arid grazing land sustainability, which is not achieved by managing only for landscape patchiness, but involves responding to many social, economic, ecological and political factors. Therefore, a knowledge of how landscapes function, and the importance of patches in this function, whether in stripes, strands or stipples, can contribute to the formation of policies and programs to achieve a goal of sustainable integration of production and conservation activities and values in rangelands.

Acknowledgements

Appendix A. Algorithm for the computation of runoff (ROff) between landscape units and run out (ROut) of the landscape system

The aim of this landscape simulation study was to investigate how three patch patterns, stipples, stripes and strands, influence the amount of water flowing out of a

hypothetical landscape system and, hence, its potential productivity. Therefore, a number of other factors which could influence run out and productivity were held constant, and a number of simplifying assumptions were made. For this study of patch pattern slope, patch area and interpatch area were held constant at 1%, 25% and 75%, respectively. Patch size was set at 100×100 m, and stripe and strand patches were consistently located towards the bottom of the simulated hillslope (Fig. 3). For simplicity, it was assumed that lateral or reticulate flows were not significant in our simulations because the landscape was assumed to be a flat planar surface of uniform 1% slope.

Computations were spatial and temporal. Runoff and run out were computed temporally for each rainfall event over a 31.5 year record from Cobar, New South Wales, Australia, given:

1. If no rain occurs (the usual case), soil water balance for each landscape patch pattern unit (see Fig. 3) was computed using the WATDYN model (Walker and Langridge, 1996).
2. If rain occurs and if the amount of rainfall (R), and its intensity, exceeds the water infiltration rate (IR) or the water storage capacity (SC) of the soil within a landscape
   unit, then runoff (ROff) occurred from that unit (see Fig. 4).

The spatial computations were as follows:

1. Runoff, $ROff_z$, was first computed for each landscape unit (z) in the row at the top of the landscape (Fig. 3) as:

$$ROff_{1z} = R_{1z} - IR_{1z},$$

   that is, rainfall inputs, (R_{1z}), less infiltration, IR_{1z}, in mm/h, summed over the 24 h/day. Soil water storage for each unit was then computed given the amount of water infiltrated into the soil, balanced against other relationships within WATDYN.
2. Second, $ROff_{2z}$ was computed for the second row of landscape units, that is those immediately downslope of the first row. For the second row of landscape units, runoff was computed as:

$$ROff_{2z} = SR_{2z} - IR_{2z}$$

   where $SR_{2z} = R_{2z} + ROn_{2z}$, that is, the supply rate of water to unit z in row 2 is the sum of rainfall inputs and runon, ROn_{2z}, which equals the runoff from the unit above ($ROn_{2z} = ROff_{1z}$). Note that these calculations do not apply to the first row since it is at the top of the landscape and does not receive runon.
3. Third, the above computations were repeated for each of the rows in the landscape system—10 in our four different simulated landscape systems (Fig. 3).
4. Last, run out (ROut) from the landscape system was equal to the sum of the amount of runoff computed for the last row of landscape units (i.e., $ROut_z = ROff_{10z}$).

Finally, note that as computations proceed down the rows of landscape units, that some units are designated as 'runon patches' (Fig. 3), which have significantly higher infiltration rates than runoff units (3 vs. 25 mm/h). It is the effect of patterning of these patches that was investigated in this simulation study.

References

Archer, S., 1990. Development and stability of grass–woody mosaics in a subtropical savanna parkland, Texas, U.S.A. Journal of Biogeography 17, 453–462.

Belsky, A.J., 1995. Spatial and temporal landscape patterns in arid and semi-arid African savannas. In: Hansson, L., Fahrig, L., Meeriam, G. (Eds.), Mosaic Landscapes and Ecological Processes. Chapman and Hall, London, pp. 31–56.

Boyland, E.E., 1973. Vegetation of the mulga lands with special reference to south-western Queensland. Tropical Grasslands 7, 35–42.

Charley, J.L., Cowling, S.W., 1968 Changes in soil nutrient status resulting from overgrazing and their consequences in plant communities of semi-arid areas. Proceedings of the Ecological Society of Australia 3, 28–38.

Cornet, A.F., Montaña, C., Delhoume, J.P., Lopez-Portillo, J., 1992. Water flows and dynamics of desert vegetation stripes. In: Hansen, A.J., di Castri, F. (Eds.), Landscape Boundaries—Consequences for Biotic Diversity and Ecological Flows. Springer-Verlag, New York, pp. 327–345

Coughenour, M.B., 1991. Spatial components of plant–herbivore interactions in pastoral, ranching, and native ungulate ecosystems. Journal of Range Management 44, 530–542.

Eldridge, D.J., 1993a. Effects of ants on sandy soils in semi-arid eastern Australia: local distribution of nest entrances and their effect on infiltration of water. Australian Journal of Soil Research 31, 509–518.

Eldridge, D.J., 1993b. Cryptogam cover and soil surface condition: effects on hydrology on a semi-arid woodland soil. Arid Soil Research and Rehabilitation 7, 203–217.

Foran, B.D., Friedel, M., MacLeod, N.D., Stafford Smith, D.M., Wilson, A.D., 1990. The Future of Australia's Rangelands. Australian Government Publishing Service, Canberra.

Freudenberger, D.O., Hodgkinson, K.C., Noble, J.C., 1997. Causes and consequences of landscape dysfunction in Australian rangelands. In: Ludwig, J., Tongway, D., Freudenberger, D., Noble, J., Hodgkinson, K. (Eds.), Landscape Ecology, Function and Management: Principles from Australia's Rangelands, Chap. 6, CSIRO Publishing, Melbourne, pp. 63–77.

Garner, W., Steinberger, Y., 1989. A proposed mechanism for the formation of 'fertile islands' in the desert ecosystem. Journal of Arid Environments 16, 257–262.

Gifford, R.M., 1988. Direct effects of higher carbon dioxide concentrations on vegetation. In: Pearman, G.I. (Ed.), Greenhouse: Planning for Climate Change. E.J. Brill Publ., New York, pp. 506–519.

Greene, R.S.B., 1992. Soil physical properties of three geomorphic zones in a semi-arid mulga woodland. Australian Journal of Soil Research 30, 55–69.

Greene, R.S.B., Ringrose-Voase, A.J., 1992. Micromorphology and hydraulic properties of surface crusts formed on a red earth soil in the semi-arid rangelands of eastern Australia. In: Ringrose-Voase, A.J., Humphreys, G.S. (Eds.), Soil Micromorphology: Studies in Management and Genesis. Proc. IX Int. Working Meeting of Soil Micromorphology, Townsville, Australia, July 1992. Developments in Soil Science 22, Elsevier, Amsterdam, pp. 763–776.

Greene, R.S.B., Kinnell, P.I.A., Wood, J.T., 1994. Role of plant cover and stock trampling on runoff and soil erosion from semi-arid wooded rangelands. Australian Journal of Soil Research 32, 953–973.

Greenslade, P., Smith, D., 1994. Soil faunal responses to restoration by mulching of degraded semi-arid soils at Lake Mere, New South Wales. In: Pankhurst, C.E. (Ed.), Soil Biota: Management in Sustainable Farming Systems. CSIRO Publishing, Melbourne, pp. 67–69.

Hanson, J.D., Skiles, J.W., Parton, W.J., 1988. A multi-species model for rangeland plant communities. Ecological Modelling 44, 89–123.

Harrington, G.N., Mills, D.M.D., Pressland, A.J., Hodgkinson, K.C., 1984. Semi-arid woodlands. In: Harrington, G.N., Wilson A.D., Young, M.D. (Eds.), Management of Australia's Rangelands. CSIRO Publishing, Melbourne, pp. 189–207.

Hodgkinson, K.C., 1992. Elements of grazing strategies for perennial grass management in rangelands. In: Chapman, G.P. (Ed.), Desertified Grasslands: Their Biology and Management, Academic Press, London, pp. 77–94.

Hodgkinson, K.C., Freudenberger, D.O., 1997. Production pulses and flow-ons in rangeland landscapes. In: Ludwig, J., Tongway, D., Freudenberger, D., Noble, J., Hodgkinson, K. (Eds.), Landscape Ecology,

Function and Management: Principles from Australia's Rangelands, Chap. 3, CSIRO Publishing, Melbourne, pp. 23–34.

Lavee, H., Poesen, J.W.A., 1991. Overland flow generation and continuity on stone-covered soil surfaces. Hydrological Processes 5, 345–360.

Lavee, H., Kutiel, P., Sagev, M., Benyamini, Y., 1995. Effect of surface roughness on runoff and erosion in a Mediterranean ecosystem: the role of fire. Geomorphology 11, 227–234.

Ludwig, J.A., Freudenberger, D.O., 1997. Towards a sustainable future for rangelands In: Ludwig, J., Tongway, D., Freudenberger, D., Noble, J., Hodgkinson, K. (Eds.), Landscape Ecology, Function and Management: Principles from Australia's Rangelands, Chap. 10. CSIRO Publishing, Melbourne, pp. 121–131.

Ludwig, J.A., Marsden, S.G., 1995. A simulation of resource dynamics within degraded semi-arid landscapes. Mathematics and Computers in Simulation 39, 219–224.

Ludwig, J.A., Tongway, D.J., 1995. Spatial organisation of landscapes and its function in semi-arid woodlands, Australia Landscape Ecology 10, 51–63.

Ludwig, J.A., Tongway, D.J., 1996. Rehabilitation of semiarid landscapes in Australia: II. Restoring vegetation patches. Restoration Ecology 4, 398–406.

Ludwig, J.A., Tongway, D.J., 1997. A landscape approach to rangeland ecology In. Ludwig, J., Tongway, D., Freudenberger, D., Noble, J., Hodgkinson, K. (Eds.), Landscape Ecology, Function and Management: Principles from Australia's Rangelands, Chap. 1, CSIRO Publishing, Melbourne, pp. 1–12.

Ludwig, J.A., Sinclair, R.E., Noble, I.R., 1992. Embedding a rangeland simulation model within a decision support system. Mathematics and Computers in Simulation 33, 373–378.

Ludwig, J.A., Tongway, D.J., Marsden, S.G., 1994. A flow-filter model for simulating the conservation of limited resources in spatially heterogeneous, semi-arid landscapes. Pacific Conservation Biology 1, 209–215.

Mabbutt, J.A., Fanning, P.C., 1987. Vegetation banding in arid Western Australia. Journal of Arid Environments 12, 41–59.

Mauchamp, A., Rambal, S., Lepart, J., 1994 Simulating the dynamics of a vegetation mosaic: a spatialized functional model. Ecological Modelling 71, 107–130.

Montaña, C., 1992. The colonization of bare areas in two-phase mosaics of an arid ecosystem. Journal of Ecology 80, 315–327.

Morton, S.R., Stafford Smith, D.M., Friedel, M.H., Griffin, G.F., Pickup, G., 1995 The stewardship of arid Australia: ecology and landscape management. Journal of Environmental Management 43, 195–217

Noble, J.C., Tongway, D.J., 1986. Pastoral settlement in arid and semi-arid rangelands. In: Russell, J.S., Isbell, R.F. (Eds.), Australian Soils: The Human Impact. University of Queensland Press, St. Lucia, pp. 217–242.

Noble, J.C., Tongway, D.J., 1988. Termite feeding sites and their influence on soil fertility and herbage productivity in semi-arid *Acacia aneura* communities. In: Stehle, P.P (Ed.), Proceedings of 5th Australasian Conference on Grassland Invertebrate Ecology. D&D Printing, Melbourne, pp. 236–242.

Noble, J.C., MacLeod, N.D., Griffin, G.F., 1997. The rehabilitation of landscape function in rangelands. In: Ludwig, J., Tongway, D., Freudenberger, D., Noble, J., Hodgkinson, K. (Eds.), Landscape Ecology, Function and Management: Principles from Australia's Rangelands, Chap. 9, CSIRO Publishing, Melbourne, pp 107–120.

Noy-Meir, I., 1973. Desert ecosystems: environment and producers. Annual Review of Ecology and Systematics 4, 25–51.

Noy-Meir, I., 1981. Spatial effects in modelling arid ecosystems. In: Goodall, D.W., Perry, R.A. (Eds.), Arid-land Ecosystems: Structure, Functioning and Management, Vol. 2, Cambridge University Press, Sydney, pp. 411–432.

Pearman, G.I., 1988 Greenhouse gases: evidence for atmospheric changes and anthropogenic causes. In: Pearman, G.I. (Ed.), Greenhouse: Planning for Climate Change. E.J. Brill Publ., New York. pp. 3–21.

Raupach, M.R., 1991. Vegetation–atmosphere interaction in homogeneous terrain: some implications of mixed-layer dynamics. Vegetatio 91, 105–120.

Slatyer, R.O., 1961. Methodology of a water balance study conducted on a desert woodland (*Acacia aneura*) community. Arid Zone Research 16, 15–26.

Stafford Smith, M., 1994 Sustainable production systems and natural resource management in the rangelands.

Proceedings, Outlook 94, Vol. 2, Natural Resources. Australian Bureau of Agricultural and Resource Economics, Canberra, pp 148–159.

Thiery, J.M., D'Herbes, J.-M., Valentin, C, 1995. Journal of Ecology 83, 497–507.

Tongway, D J., Ludwig, J.A., 1990. Vegetation and soil patterning in semi-arid mulga lands of eastern Australia Australian Journal of Ecology 15, 23–34.

Tongway, D.J., Ludwig, J.A., 1993 Rehabilitation of minesite and pastoral land. the ecosystem function approach. In di Russo, M. (Ed). Proceedings, Goldfields International Conference on Arid Landcare Milena di Russo Publ., Hamilton Hill, Western Australia, pp. 51–57

Tongway, D.J., Ludwig, J A., 1994. Small-scale resource heterogeneity in semi-arid landscapes. Pacific Conservation Biology 1, 201–208

Tongway, D.J, Ludwig, J A, 1996 Rehabilitation of semiarid landscapes in Australia II. Restoring productive soil patches. Restoration Ecology 4, 388–397.

Tongway, D.J., Ludwig, J.A, 1997a. The conservation of water and nutrients within landscapes. In: Ludwig, J, Tongway, D., Freudenberger, D., Noble, J., Hodgkinson, K. (Eds), Landscape Ecology, Function and Management. Principles from Australia's Rangelands, Chap. 2. CSIRO Publishing, Melbourne, pp 13–22.

Tongway, D.J., Ludwig, J A., 1997b. The nature of landscape dysfunction in rangelands. In: Ludwig, J, Tongway, D, Freudenberger, D., Noble, J., Hodgkinson, K. (Eds), Landscape Ecology, Function and Management: Principles from Australia's Rangelands, Chap. 5. CSIRO Publishing, Melbourne, pp. 49–61

Tongway, D.J., Smith, E.L, 1989. Soil surface features as indicators of rangeland site productivity. Australian Rangeland Journal 11, 15–20.

Tongway, D J., Ludwig, J.A., Whitford, W.G., 1989. Mulga log mounds: fertile patches in the semi-arid woodlands of eastern Australia. Australian Journal of Ecology 14, 263–268.

Walker, B.H., Langridge, J.L., 1996. Modelling plant and soil water dynamics in semi-arid ecosystems with limited site data. Ecological Modelling 87, 153–167.

Whitford, W.G., Ludwig, J.A., Noble, J.C., 1992. The importance of subterranean termites in semi-arid ecosystems of south-eastern Australia. Journal of Arid Environments 22, 87–91.

Wiens, J.A, 1995. Landscape mosaics and ecological theory. In: Hansson, L, Fahrig, L., Merriam, G. (Eds.), Mosaic Landscapes and Ecological Processes. Chapman and Hall, London, pp. 1–26